

PEDOGENESIS & CARBON DYNAMICS ACROSS A LITHOSEQUENCE UNDER  
PONDEROSA PINE

by

Katherine Ann Heckman

---

A Dissertation Submitted to the Faculty of the  
DEPARTMENT OF SOIL, WATER & ENVIRONMENTAL SCIENCE

In Partial Fulfillment of the Requirements  
For the Degree of

DOCTOR OF PHILOSOPHY

In the Graduate College

THE UNIVERSITY OF ARIZONA

2010

UMI Number: 3427633

All rights reserved

INFORMATION TO ALL USERS

The quality of this reproduction is dependent upon the quality of the copy submitted.

In the unlikely event that the author did not send a complete manuscript and there are missing pages, these will be noted. Also, if material had to be removed, a note will indicate the deletion.



UMI 3427633

Copyright 2010 by ProQuest LLC.

All rights reserved. This edition of the work is protected against unauthorized copying under Title 17, United States Code.



ProQuest LLC  
789 East Eisenhower Parkway  
P.O. Box 1346  
Ann Arbor, MI 48106-1346

THE UNIVERSITY OF ARIZONA  
GRADUATE COLLEGE

As members of the Dissertation Committee, we certify that we have read the dissertation prepared by Katherine Ann Heckman entitled Pedogenesis & carbon dynamics across a lithosequence under ponderosa pine and recommend that it be accepted as fulfilling the dissertation requirement for the Degree of Doctor of Philosophy

\_\_\_\_\_ Date: 10/21/2010  
Craig Rasmussen

\_\_\_\_\_ Date: 10/21/2010  
Raina Maier

\_\_\_\_\_ Date: 10/21/2010  
Egbert Schwartz

\_\_\_\_\_ Date: 10/21/2010  
Jon Chorover

\_\_\_\_\_ Date: 10/21/2010  
Jeffrey Silvertooth

Final approval and acceptance of this dissertation is contingent upon the candidate's submission of the final copies of the dissertation to the Graduate College.

I hereby certify that I have read this dissertation prepared under my direction and recommend that it be accepted as fulfilling the dissertation requirement.

\_\_\_\_\_ Date: 10/21/2010  
Dissertation Director: Craig Rasmussen

## STATEMENT BY AUTHOR

This dissertation has been submitted in partial fulfillment of requirements for an advanced degree at the University of Arizona and is deposited in the University Library to be made available to borrowers under rules of the Library.

Brief quotations from this dissertation are allowable without special permission, provided that accurate acknowledgment of source is made. Requests for permission for extended quotation from or reproduction of this manuscript in whole or in part may be granted from the author.

SIGNED: Katherine Ann Heckman

## ACKNOWLEDGEMENTS

I would like to thank all the collaborators who made contributions to the research projects I pursued during my time in graduate school: Amy Welty-Bernard for the fantastic T-RFLP and pyrosequencing work, Angelica Vasquez-Ortega for assistance in processing DOM samples, Selene Hernandez Ruiz for the HPLC data, Xiaodong Gao for the peak decomposition work, Dr. Heike Knicker for the NMR training, and Dr. Francisco Gonzalez-Vila for the pyrolysis instruction.

Many thanks to Dr. Mary Kay Amistadi and Dr. Mercer Meding who ran and reran and reran samples for me and provided me with the instrumental training and data necessary to complete my research. Lab managers are the patron saints of all graduate students.

Thank you to my mother and brother, Kristy and Nick Heckman, for their patience, support, and encouragement.

Thank you to Pavel Polynkin for all the time he spent teaching me spectroscopy, physics, and Russian, among other things. I know I am responsible for more than a few of his gray hairs, but I never would have been able to graduate if it weren't for his expert tutelage.

I would also like to thank my committee members for their time and input: Dr. Jeffrey Silvertooth, Dr. Raina Maier, Dr. Egbert Schwartz, Dr. Jon Chorover, and Dr. Craig Rasmussen.

And of course, special thanks to my major advisor, Dr. Craig Rasmussen, whose patience apparently knows no bounds.

## DEDICATION

I would like to dedicate this dissertation to Dr. Wendy Anderson and Dr. D. Alexander

Wait who were always kind and generous to me, even when I didn't deserve it.

## TABLE OF CONTENTS

ABSTRACT .....	9
INTRODUCTION .....	11
Intellectual merit & research context .....	11
Literature review .....	12
Dissertation format and collaborative contributions .....	34
PRESENT STUDY .....	35
REFERENCES .....	40
 <b>APPENDIX A: LITHOLOGIC CONTROLS ON REGOLITH WEATHERING AND</b>	
<b>MASS FLUX IN FORESTED ECOSYSTEMS OF THE SOUTHWESTERN USA.....</b>	
Abstract .....	49
1. Introduction .....	50
2. Methods .....	52
3. Results & Discussion .....	65
4. Summary .....	82
5. Figures & Tables .....	85
6. References .....	98
 <b>APPENDIX B: GEOLOGIC CONTROLS OF SOIL CARBON CYCLING AND</b>	
<b>MICROBIAL DYNAMICS IN TEMPERATE CONIFER FORESTS .....</b>	
Abstract .....	107
1. Introduction .....	108
2. Methods .....	111

### TABLE OF CONTENTS -- Continued

3. Results .....	122
4. Discussion .....	129
5. Summary.....	134
6. Acknowledgements .....	135
7. Figures & Tables .....	136
8. References .....	147

#### **APPENDIX C: CHANGES IN DISSOLVED ORGANIC MATTER DURING BIOGEOCHEMICAL INCUBATION OF FOREST FLOOR MATERIAL IN THE PRESENCE OF QUARTZ, GOETHITE AND GIBBSITE SURFACES .....**

Abstract .....	155
1. Introduction .....	156
2. Methods .....	159
3. Results .....	165
4. Discussion .....	175
5. Summary .....	181
6. Acknowledgements .....	182
7. Figures & Tables .....	183
8. References .....	190

#### **APPENDIX D: EXPOSURE TO GOETHITE AND GIBBSITE SURFACES ALTERS DOM NUTRIENT DYNAMICS AND MICROBIAL COMMUNITY COMPOSITION .....**

198

**TABLE OF CONTENTS -- Continued**

Abstract .....	199
1. Introduction .....	200
2. Methods .....	202
3. Results .....	208
4. Discussion .....	212
5. Summary .....	220
6. Acknowledgements .....	221
7. Figures & Tables .....	222
8. References .....	229

## ABSTRACT

Three studies were completed to investigate the influence of mineral assemblage on soil organic carbon (SOC) cycling and pedogenesis in forest soils. Two studies utilized a lithosequence of four parent materials (rhyolite, granite, basalt, limestone/volcanic cinders) under *Pinus ponderosa*, to explicitly quantify the contribution of parent material mineral assemblage to the character of the resulting soil. The first study explored variation in pedogenesis and elemental mass loss as a product of parent material through a combination of quantitative X-ray diffraction and elemental mass balance. Results indicated significant differences in degree of soil development, profile characteristics, and mass flux according to parent material.

The second study utilized the same lithosequence of soils, but focused on organic C cycling. This study explored variation in SOC content among soils of differing mineralogy and correlations among soil physiochemical variables, SOC content, soil microbial community composition and respiration rates. Metal-humus complex and Fe-oxhydroxide content emerged as important predictors of SOC dynamics across all parent materials, showing significant correlation with both SOC content and bacterial community composition. Results indicated that within a specific ecosystem, SOC dynamics and microbial community vary predictably with soil physicochemical variables directly related to mineralogical differences among soil parent materials.

The third study focused specifically on the influence of goethite and gibbsite on dissolved organic matter characteristics and microbial communities which utilize DOM as a growth substrate. Iron and aluminum oxides were selected for this study due to their

wide spread occurrence in soils and their abundance of reactive surface area, qualities which enable them to have a significant effect on SOC transported through forest soils. Results indicated that exposure to goethite and gibbsite surfaces induces significant differences in DOM quality, including changes in thermal properties, molecular structure, and concentrations of P and N. Investigation of the decomposer communities indicated that exposure to goethite and gibbsite surfaces caused significant differences in microbial community structure.

These investigations emphasize the important role of mineral assemblage in shaping soil characteristics and regulating the cycling of C in soils, from the molecular scale to the pedon scale.

## INTRODUCTION

### **Intellectual merit & research context**

Organic C cycling in soils has been the subject of extensive research (cf. Oades, 1988; Sollins et al., 1996; Baldock & Skjemstad, 2000; v. Lützow et al., 2006), especially in recent years as concerns over global climate change have piqued interest in mechanisms of soil organic C stabilization. Soils, and their associated litter layers, contain approximately 1920 petagrams of carbon, or roughly 1.25 times that of atmospheric and aboveground biomass stores combined (Ver et al., 1999). Despite the amount of research that has gone into understanding soil C cycling, the mechanisms regulating the size and turnover rate of the soil C pool are not fully understood.

Interactions among the mineral matrix, soil microbial communities and organic matter are at the heart of soil C cycling. The mineral matrix of the soil accounts for the largest portion of the soil by mass and to a large degree determines the physiochemical environment of the soil. Differences in soil moisture and temperature regimes also have a strong effect on soil C cycling. However, within a specific ecosystem type, and therefore holding climactic variables fairly constant, soil mineral assemblage exerts a profound influence on soil physiochemical variables, which in turn influence soil microbial communities and organic C cycling.

In the soil environment, minerals can promote the preservation of organic C and increase its residence time. The mineral matrix stabilizes soil organic C against microbial degradation in many ways, including: i) bonding of organics to mineral surfaces (Kleber et al., 2007; Mikutta et al. 2007); ii) formation of metal-humus complexes (Baldock and

Skjemstad, 2000; Nierop et al., 2002; Scheel et al., 2007); iii) suppression of microbial respiration due to  $\text{Al}^{3+}$  toxicity (Illmer et al., 1995, 2003; Scheel et al., 2007); and iv) occlusion of organics within aggregate structures (Reicosky et al., 1997; Tebrügge and Düring, 1999; Six et al., 2002). Though a basic understanding of how these mechanisms operate in nature exists, the comprehension and prediction of soil organic matter dynamics is hampered by the simultaneous operation of several mechanisms (von Lützow et al., 2006) and a lack of molecular-scale understanding of the processes (Sollins et al., 1996).

This work seeks to advance the understanding of mechanisms of organic C stabilization in soils, with a specific focus on the influence of soil mineral assemblage on soil organic C characteristics and microbial communities.

## **Literature review**

### ***1. Global climate change & soil organic carbon cycling***

Globally, soils and their associated litter layers contain approximately 1920 petagrams of carbon (Batjes, 1996; Ver et al., 1999). Soils contain the largest terrestrial pool of organic C, roughly three times the amount of C in terrestrial vegetation and twice the amount of C in the atmosphere (IPCC, 2001; Denman et al., 2007). Given sufficient time and constant environmental conditions, soil C content reaches and maintains a steady level determined by the physiochemical characteristics of the soil and the surrounding environment (Jenny, 1941). In this steady-state, organic C inputs are approximately equal to organic C losses through soil respiration and leaching processes,

and the size of the soil C pool remains relatively constant. However, changes in land use as well as changes in soil moisture and temperature conditions can increase organic C losses from soils, resulting in a net efflux of C and decreasing the size of the soil C pool (Houghton et al., 1999). The rising concentration of CO<sub>2</sub> in the atmosphere has increased interest in reversing C losses from soils and increasing the overall size of the global C pool through better land management decisions or increasing net primary productivity. A detailed understanding of the processes regulating soil C stabilization is necessary both to predict changes in soil C stocks and guide land management decisions.

Approximately 40% of the world's soil C stock is contained in forest soils, and forest soils cover about 33% of the total land area in the United States alone (Kimble et al., 2003). Mechanisms of C stabilization in forest soils are especially important, both due to the size of the C pool involved and the large amount of forested land.

## ***2. Mechanisms of organic C stabilization in forest soils***

The mechanisms of organic C stabilization in forest soils have been extensively researched (cf. Oades, 1988; Sollins et al., 1996; Baldock & Skjemstad, 2000; Kalbitz et al., 2000; v. Lützow et al., 2006, Kögel-Knabner et al., 2008) and can be grouped into three broad categories: i) Sorption to mineral surfaces; ii) Formation of metal-humus, or organo-metal complexes; and iii) Occlusion, or physical isolation from microbial communities. These processes are not mutually exclusive, and stabilization of organics often involves the simultaneous operation of multiple mechanisms.

***2.1 Sorption:*** Sorption to mineral surfaces has long been recognized as an important factor controlling soil organic matter content (Greenland, 1971; Martin and

Haider, 1986; Theng and Tate, 1989). In addition to its strong effects on organic C cycling, sorption of organics to mineral surfaces has other important effects on the soil system. Coatings of organic matter on clays can increase particle surface area and reactivity, and interaction with dissolved organic matter increases the dissolution rates of minerals (Stevenson, 1994; Drever and Stillings, 1997). Both the amount and type of organic C bound to the mineral surface will vary based on mineralogy. The specific bonding mechanism, strength of bond, and OC functional groups involved may also vary based on the specific characteristics of the mineral surface (Mikutta et al., 2007; Wattel-Koekkoek et al., 2001).

Organics may be sorbed to the mineral surface by a variety of bonding mechanisms (Chorover, 2008; Essington, 2004): i) Cation exchange: This mechanism involves the adsorption of a quaternized N atom in an aliphatic chain or heterocyclic ring (R-NH<sub>2</sub>, ring NH, hetero-N) to a negatively charged mineral surface site (such as the adsorption of a protonated amino acid to a basal plane siloxane surface site); ii) Anion exchange: When mineral surface sites become protonated, this positive charge may be satisfied by anionic groups (R-OO<sup>-</sup>) of organics; iii) Water bridging: Weak H bonds can form between negatively-charged organic functional groups and hydrogens from water molecules hydrating a mineral surface; iv) Cation bridging: A negatively-charged functional group may displace a water of hydration from cations on the mineral exchange complex, and form a bond with the exchangeable cation. In this way the cation forms a “bridge” in between the mineral surface and the OC molecule; v) Ligand exchange: Ligand exchange is the strongest form of mineral-OM bonding. At low pH, when oxide

surface functional groups are protonated, carboxylate and phenolate groups can replace hydroxyls of the mineral and form strong bonds with the oxides ( $\text{FeOH}_2^+ (s) + \text{R-COO}^- (aq) \leftrightarrow \text{FeOOC-R} (s) + \text{H}_2\text{O} (l)$ ); vi) Hydrogen bonding: Though the bond is very weak, basal oxygens of silicate interlayers may interact with hydrogens of organic functional groups. vii) Van der Waals bonding: SOM and mineral surfaces may form bonds when the fluctuations of their polarizations are correlated; viii) hydrophobic interaction: Non-polar organic components (hydrophobic) may be excluded from the aqueous phase. These organic components are expelled from the solution and precipitate onto mineral surfaces.

The dominant type of interaction between organics and mineral surfaces in natural systems will necessarily depend on the specific structural characteristics of the mineral, but will also vary based on characteristics of the organic matter and the conditions of the soil system, i.e. soil moisture, precipitation amount and patterns, base saturation, soil pH, etc.

The stability of a given organo-mineral bond varies, thus the degree of protection against microbial degradation will vary. Moreover, the so-called recalcitrance or persistence of sorbed organic matter is more relative than absolute. Sorption to mineral surfaces does increase the mean residence time (MRT) of SOM in comparison to the free/light fraction, as evidenced by older radiocarbon ages (Eusterhues et al. 2003) and lower mineralization rates of mineral associated SOM (Kalbitz et al 2005). Persistence of mineral associated OM in soils is considered evidence that sorption to mineral surfaces does reduce the bioavailability and accessibility of OM (Sollins et al. 1996, von Lützow et al. 2006, Marschner et al. 2008). Also, during later stages of decomposition and with

depth in the profile, the importance of sorption to mineral surfaces increases (von Lützow et al. 2006).

The manner in which SOM is bound to the mineral surface plays a large role in its bioavailability (Mikutta et al. 2007). Organic matter bound to Al or Fe oxyhydroxides through ligand exchange may be difficult to displace. On the other hand, organic matter bound loosely to the mineral surface through water bridging or hydrogen bonding may be more easily detachable and biodegradable. Organics bound to mineral surfaces due to electrostatic forces are sensitive to pH changes, and may desorb from the mineral surface when pH increases (Stevenson, 1994).

The structure and size of the SOM particle is also an important determinant of how it will bond to mineral surfaces and how bioavailable it will be. Acidity or basicity of the organic compound is especially important, as well as hydrophobicity or solubility. Small molecules sorbed to mineral surfaces may not be immediately available to soil microbes, however microbes can produce secretions (i.e. enzymes, metal-binding proteins) that effectively desorb the OM so that it may be consumed (Chenu & Stotzky 2002). However, macromolecules may undergo conformational changes upon adsorption that significantly reduce their susceptibility to extracellular enzymes.

Nutrient levels in the soil also affect the bioavailability of sorbed OM.

Degradation of the heavy fraction of soil from density separation (SOM sorbed to mineral surfaces) can be accelerated through the addition of a labile substrate (Ohm et al. 2007). This priming effect indicates that sorbed SOM may be mineralized if conditions are made more favorable for the degrading microorganisms.

Recently, Kleber et al. (2007) introduced the concept of "zonal structures" to explain variations in the bioavailability of SOM sorbed to mineral surfaces. Several other authors (Kaiser & Guggenberger 2003, Hassink 1997, Six et al. 2002, and others) have put forth similar explanations involving C saturation thresholds and the limited capacity of mineral surfaces to protect SOM from degradation. The "zonal structure" model involves the self-assembly of DOM particles in solution into several zones varying in proximity and bond strength to the mineral surface. The *contact zone* or the layer of OM particles closest to the mineral surface, is bound strongly to the mineral surface through ligand exchange. SOM particles in the *hydrophobic zone* and *kinetic zone* are less directly in contact with the mineral surface. SOM in these zones are more weakly bound to the mineral surface and are therefore more susceptible to desorption and biodegradation. This conceptual model is attractive because it accounts for the movement of OM into and out of the heavy/mineral fraction of soils, but can also account for the longer MRT of the heavy/mineral pool of SOM.

In summary, SOM sorption to mineral surfaces is an important mechanism of organic C stabilization. However, many times sorption reactions are reversible and sorbed organics may become bioavailable depending on the specific conditions present, including the solution chemistry, the binding mechanisms in operation, and substrate availability.

**2.2 Metal-humus complexes:** In the aqueous phase, dissolved organics may form bonds with dissolved Fe and Al cations and their hydroxyl phases,  $\text{Al}(\text{OH})_x$  and  $\text{Fe}(\text{OH})_x$ . These metal-humus or organo-metal complexes may persist in the solution state, or may

precipitate onto mineral surfaces. These complexation reactions induce chemical and conformational changes in the organics which reduce their bioavailability (Baldock and Skjemstad, 2000; Nierop et al., 2002; Scheel et al., 2007).

The formation and precipitation of metal-humus complexes is mediated to a large degree by soil pH. Ion exchange, metal complexation, and adsorption to mineral surfaces all utilize the same exchange sites on organic matter, and which specific interaction takes place between the organics and the mineral matrix is strongly affected by pH. The solubility of dissolved organic matter (DOM) increases with increasing pH due to deprotonation of carboxylic groups (Kalbitz et al., 2000), but the abundance of metal cations tends to decrease with increasing pH. Metal-humus complex formation and precipitation processes occur at the high end of the solubility spectrum. This includes the solubility of the mineral/metal constituents as well as the solubility of the organic component. Metal cations in solution may preferably bind to mineral surfaces as solution pH is raised above an acid value, but after some time mineral adsorption sites become saturated. Following the saturation of exchange sites, metal ions may cluster into oxyhydroxides and precipitate onto mineral or organic surfaces. DOM may interact with the metal cations or mineral surfaces at any point in this process. Low molecular weight organic components such as sugars, organic acids and amino acids have high solubility and form both stable complexes with mineral surfaces and precipitates with metals in solution. Larger organics with lower solubility also readily form bonds with mineral surfaces and metals in solution, but the presence of charged functional groups may be necessary for the formation of metal-humus complexes.

Adsorption reactions can involve a wide variety of mineral phases, with bonding mechanisms and strength varying according to mineral and DOM composition.

Adsorption of organics on mineral surfaces occurs over a wide range of pH values and in almost all soil environments. Precipitation of metal-humus complexes in soils occurs in a more restricted set of circumstances, since both the organic and mineral constituents must be solubilized in order to combine and precipitate. Regardless, precipitation of DOM with metal cations or sesquioxides is still quite common in soils, especially in acid and sandy forest soils where complexation of organics with Fe and Al is involved in the process of podsolization.

Formation of either metal-DOM precipitates or mineral-OM complexes also necessarily depends on the availability of reactants. The balance between dissolution of metal cations from the solid mineral phase and the sorption of the dissolved metal cations onto solid phases controls the distribution of metal cations between aqueous and solid phases. Since metal cations and organics must be present in the aqueous phase for the formation of metal-humus complexes and their subsequent precipitation, metal to C ratios in solution are important in determining the rate of metal-humus complex formation. Scheel et al. (2007) studied the effects of Al to C ratios on the formation of Al-DOM complexes and found that increasing metal to C ratios increased the formation of Al-DOM complexes, but only to a certain point. At low Al to C ratios, Al-DOM complexes are soluble due to the low  $\text{Al}^{3+}$  concentrations in solution (Jansen et al., 2003). Further, the specific form of organic matter will also play a role in determining the formation of metal-humus precipitates. Scheel et al. (2007) also found that extensive precipitation of

DOM occurred at Al to C ratios exceeding 0.03. However, since only a certain fraction of DOM can be precipitated, further increases in Al to C ratios did not lead to increased DOM precipitation.

Formation of metal-DOM precipitates also depends on specific metal species and oxidation state. Fe (II) does not readily form metal-DOM precipitates, but Fe(III) does. Over the pH range of 3.5 to 4.5, formation of Al-DOM complexes was found to be highly pH dependent, whereas the formation of Fe(III)-DOM complexes was not (Nierop et al. 2002).

The balance between sorption of organics to mineral surfaces and precipitation of metal-humus complexes is governed by the concentration of metal cations and DOM in the soil and their partitioning among solid and aqueous phases. Inorganic reactants involved in metal-DOM precipitation include Fe and Al, present as free cations or mono and dihydroxide ions, and various other heavy metals. Inorganic reactants involved in adsorption reactions involve a wide range of mineral phases from primary minerals to secondary phyllosilicates to oxides. Both precipitated and sorbed organics may have a wide variety of molecular forms. Sorbed organics may be charged or uncharged and of varying sizes. Aliphatic and higher molecular weight organics may be preferentially precipitated by  $Al^{3+}$  in solution, but low molecular weight organic acids can form metal-DOM complexes as well. The presence of carboxyl groups or phenolic groups on organics may be necessary to their participation in the formation of metal-DOM complexes. Both sorption and complexation occur in many environments and are not

mutually exclusive. Precipitation may be of greater importance in acid and sandy soils, whereas sorption may be more important in soils with high clay contents.

**2.3 Occlusion within aggregates:** Organics may also be protected from degradation by occlusion within soil aggregate structures. Aggregate formation and persistence can involve both adsorption reactions and precipitation of metal-humus complexes, as well as the participation of the soil microbial community.

Aggregates of soil materials are held together through bonding of both biological and inorganic components. Biota and biological exudates (i.e. bacteria, plant roots, hyphae, earthworm casts) play an especially important role in the process of soil aggregate formation. Aggregates are typically studied in two ways: formation of aggregates in the laboratory, and separation of aggregates from soil through the application of different energy levels (i.e. wet sieving, shaking, sonication). Microaggregates (<250 $\mu\text{m}$  in diameter) are more stable than macroaggregates (>250 $\mu\text{m}$  in diameter). Under field conditions, macroaggregate persistence is mostly a function of land management technique, whereas microaggregates are usually dispersed only by very intense rainfall events (Tisdall, 1991).

Microaggregates of different sizes are held together by different mechanisms and/or materials. Bacteria secrete large amounts of polysaccharides which bind clays to the surface of bacterial cells. Adhesion of clays to the bacteria both act to preserve the bacterial biomass after death and to protect the bacterial cell from attack from protozoa and nematodes during its lifetime (Foster, 1988). Organic matter found in association with the fine clay fraction (<0.2  $\mu\text{m}$ ) and aggregates <2  $\mu\text{m}$  in diameter is typically

amorphous with low C:N ratio and is thought to originate from humified microbial cell walls, microbial cytoplasm, or microbial exudates. These microaggregates may form clusters up to 20  $\mu\text{m}$  in diameter.

Microaggregates 2-20  $\mu\text{m}$  in diameter may also be composed of silts, clays, cells and cell colonies encrusted with mineral material (Tisdall & Oades, 1982). Very little plant material is found within these aggregates. These aggregates are very stable and are thought to form through compaction induced by root and microbial cell growth. As the soil particles are compacted, they form bonds both through interactions between charged mineral surfaces and microbial exudates and dead microbial biomass.

Aggregates 20-250  $\mu\text{m}$  in diameter for the most part are made up of conglomerations of 20  $\mu\text{m}$  aggregates held together by plant and fungal debris and charge-bearing secondary minerals such as oxyhydroxides and disordered aluminosilicates. Aggregates of this size are intermediate in stability between smaller and larger aggregates. Organic matter isolated from these aggregates has a higher C:N ratio and is less decomposed than organic matter from smaller aggregates. However, recent research indicates that this so-called “occluded” organic matter may actually be older than the more decomposed organics found in direct association with mineral surfaces or in smaller aggregates.

Macroaggregates (>250  $\mu\text{m}$  in diameter) vary in their stability. Macroaggregates formed in soils rich in secondary charge-bearing minerals may be very stable, whereas other macroaggregates may disintegrate upon wetting. Some macroaggregates are bound

mainly through mineral interactions, whereas others are bound together by fungal hyphae and polysaccharides.

Organic materials may bind microaggregates into larger conglomerations and stabilize these larger aggregates by blocking large pores in the aggregates. Blocking of large aggregate pores by organic debris and fungal hyphae slows water infiltration into the aggregate and prevents aggregate break-up. Hyphae of vesicular arbuscular (VA) mycorrhizal fungi have been identified as the main stabilizers of macroaggregates, though saprophytic and ectomycorrhizal hyphae also stabilize aggregates in forest soils. Extracellular polysaccharides produced by roots and microbes also act to stabilize macroaggregates, especially outside the influence of the rhizosphere. However, these compounds are relatively labile and may not persist for long periods in the soil.

Soil microorganisms vary in their ability to stabilize aggregates. Especially for forested ecosystems, fungi play an especially important role. The contribution of microbes to improving aggregate stability increases in the following order: fungi > actinomycetes > bacteria (Lynch and Bragg, 1985). However, it should be noted that there is a large amount of variation within each group of microbes. Fungal hyphae create a net which entangles mineral and organic particles, bringing them close enough that bonds and microaggregates can form. At a larger scale, hyphae can also bind microaggregates together to form macroaggregates (Miller & Jastrow, 1990). In grassland and agricultural systems, roots and root exudates may be as important as fungi to aggregate formation. In a laboratory study, Thomas et al. (1993) found that

macroaggregate stability was nearly equivalent in soils exposed to just plant roots and just VAM fungi, indicating that both factors play a role in aggregate formation in soils.

Though organics play an important role in aggregate stabilization, clays may be the main contributors to aggregation processes in soils, with charge-bearing clays being of primary importance. In a laboratory setting, both speed of aggregate formation and macroaggregate strength were shown to increase with clay content (Wagner et al. 2007). Wagner et al. (2007) found that addition of organic residues to soils did promote aggregation in wholly disaggregated soils, but the influence of added organics diminished over time. Stevenson (1994) also reported a secondary role of organic matter to clays in aggregate formation. Stevenson (1994) also found that organic matter played a larger role in aggregation processes in kaolinitic soils than in smectitic soils, indicating that clay surface charge is an important factor determining the influence of clays on aggregate formation.

Occlusion within aggregates is thought to preserve C through physically limiting microbial access. Pore size is the limiting factor for penetration of microbes, enzymes, and water into aggregates (Killham et al., 1993). Pore-size exclusion prevents interactions between the substrate and the microbial community, thereby increasing the mean residence time of the C. These organics preserved within aggregate structures are often referred to as the “occluded” fraction of SOM. Typically, occluded organics account for 15-30% of total organic matter in surface horizons, but may reach values up to 50% in forest soils (Golchin et al., 1994b; Wander and Bidart, 2000; Rasmussen et al., 2005; Wagai et al., 2008). The literature may read as if the processes of aggregate formation are

well established. However, the characteristics of organics found within the occluded fraction are often inconsistent with the established aggregation processes, and the mechanisms governing the occlusion of organics in aggregates are not well known. Golchin et al. (1994b) proposed a model of soil C occlusion stating that occluded C is formed through the fractionation and biodegradation of particulate organic C and that these intermediate degradation products become associated with minerals and aggregates during the decomposition process. However, the concentration of specific organic materials such as fungal spores and pollen are sometimes higher in the occluded fraction than in the free/light fraction indicating that specific organic compounds may be selectively preserved in aggregates. Inherent structural recalcitrance may also explain the large concentrations of black C often found in the occluded fraction (Golchin et al., 1994; Rasmussen et al., 2005; Swanston et al., 2005; Brodowski et al., 2006). At the same time, relatively intact plant debris and labile compounds are also found in the occluded fraction (cf. Wagai et al., 2009).

The current paradigm of organic C stabilization in soils maintains that turnover of the stable pool of C (C with mean residence times of 1000 years or more) is controlled largely by sorption to mineral surfaces, while occlusion and structural recalcitrance play a role in stabilization of organic C with mean residence times of days to decades (Kögel-Knabner et al., 2008). However, recent studies have indicated that occluded organics can be as old or older than C sorbed to mineral surfaces (Baisden et al., 2002; John et al., 2005; Rasmussen et al., 2005; Rethemeyer et al., 2005; Swanston et al., 2005; Marin-

Spiotta et al., 2008; Paul et al., 2008), indicating that the role of aggregates in soil C cycling is not fully understood.

### **3. Dissolved organic matter**

Dissolved organic matter (DOM) can be generally defined as the water soluble fraction of soil organic matter which passes through a filter of 0.45  $\mu\text{m}$  pore size (Kalbitz et al., 2000). However, different pore sizes have been used in different studies. DOM is composed of a wide variety of organics derived from leaching of litter layers and soil humus, root exudates, and microbial metabolites. Though dissolved organic matter (DOM) comprises only ~1% of the total organic C in soils, DOM is the most mobile fraction of soil organic carbon (Zsolnay, 1996) and is the largest source of new C inputs to subsurface soils (Zech and Guggenberger, 1996). Previous research has also suggested that biodegradation of soil organic matter is mediated by the aqueous phase, (Kalbitz et al., 2003a) and that DOM may be the most important C source for soil microbes in general since C uptake mechanisms require an aqueous environment (Metting, 1993; Jandl and Sollins, 1997; Marschner & Kalbitz, 2003). Many studies suggest only a limited portion of DOM is degradable by autochthonous microbial communities. Estimates vary due to differences in DOM extraction techniques and incubation lengths and range from 10-44% (Jandl and Sletten, 1999; Kalbitz et al., 2000; Yano et al., 2000; Sachse et al., 2001). The biodegradable portion of DOM is termed the *labile* fraction, while the remaining portion is termed the *recalcitrant* portion. The recalcitrant portion of DOM is rich in aromatic compounds and is more humified than the labile pool (Kalbitz et al., 2003a).

DOM abundance and composition in soils is the product of many interacting factors. DOM concentrations decrease with increasing soil depth (Michalzik et al., 1999), and increase with increasing litter production (Currie and Aber, 1997; Tipping et al., 1999) and increasing microbial activity (Williams and Edwards, 1993; Whalen et al., 1999). Sorption to mineral surfaces, through the mechanisms described above, causes dramatic decreases in DOM concentrations and bioavailability in soils (cf. Sollins et al., 1996; Kaiser and Guggenberger, 2000). In addition, formation and flocculation of metal-humus complexes also reduces DOM bioavailability (Greenland, 1971; Tipping and Woof, 1990; McDowell and Wood, 1984).

#### ***4. Microbe-mineral interactions in soils***

The soil microbial community is a diverse mix of bacteria, actinomycetes, fungi, microalgae, and protozoa. Most soil microbes exist in biofilms attached to soil mineral surfaces rather than living freely in the soil solution. This is evident both from microscopic observations of soil particle surfaces, the electrokinetic properties of cells (Burns, 1989; Maier et al., 2000), and the molecular composition of organics intimately associated with mineral surfaces (Golchin et al., 1994).

Both the composition and activity of the community are heavily dependent on the physiochemical environment immediately surrounding them. A broad range of soil characteristics can influence microbial communities, some examples being redox potential, water potential, pH, substrate type and availability, temperature and cation exchange capacity among many others. As soil conditions change, microbial communities adapt and change as well. Predators may turn to prey, and microbial

biomass itself can become the best available nutritional source when substrate conditions are limiting (Metting, 1993; Maier et al., 2000).

Though relatively labile C substrates may be available in the rhizosphere (due to root exudates and sloughing) and in preferential flow paths (“hot spots”), the majority of the soil environment is oligotrophic (Grayston et al., 1997; Bundt et al., 2007). Even when C substrates are available, microbial growth and respiration may be limited by N or P availability. Bioavailability of C, N and P in soils is further limited by interaction with the mineral portion of soil according to the mechanisms outlined above (see section *Mechanisms of organic C stabilization in forest soils*). Limiting N and P availability have important effects on both microbial community composition and activity (Saggar et al. 1998; Güsewell et al. 2009).

Interactions among soil microbes and the mineral phase are numerous and complex. These interactions have consequences not only for the microbial communities involved, but also for organic C cycling in soils. Changes in microbial community structure and activity alter the rate at which organic C is consumed in soils as well as altering the character of the organic C itself.

**4.1 Acidity & Aluminum toxicity:** The mineral matrix also influences soil microbial communities through the release of dissolved aluminum. Al is the third most abundant element in crustal rock and is ubiquitous in soils. However, no metabolic role of Al is known (Fischer, 2002). Aluminum is present in most soils to varying degrees, but exerts the most influence in acidic soils which comprise approximately 30% of arable land. The adaptation of soil bacteria to Al is not a well-studied phenomenon. Studies that

exist vary in scope and focus, and definitive protocols for the study of bacterial Al resistance have not been firmly established. However, progress is being made and knowledge of the role of Al in soils and its effect on bacteria is expanding.

In general, aluminum is toxic to soil bacteria, though species differ in their sensitivity. In some species growth is inhibited by amounts as low as micromolar concentrations. However, some acidophilic species have been isolated that can tolerate 100-200 mM (Fischer, 2002). The exact mechanisms of Al toxicity are not clearly understood, but it has been shown that Al can penetrate the cell envelope and bind to DNA, indicating that it is a mutagen (Flis, 1993; Wood, 1995). Fischer et al. (2002) has shown that Al toxicity is also based on its substitution for magnesium in biological reactions, having a binding strength to ATP of  $10^7$  times greater than that of magnesium. Introduction of small amounts of Al to colonies extracted from acidic soils causes an increase in lag time and doubling time and a decrease in growth rate and cell concentration (Wood, 1995; Fischer et al., 2002). Cells are most sensitive to Al during division (log phase). Al interferes with cell division, leading to elongation of the bacterial cells.

Bacterial tolerance to Al is species specific (Illmer and Schinner, 1999), with even bacterial strains of the same species showing variability in their development of Al tolerance. Repeated exposure to Al does not confer tolerance, indicating that Al tolerance is a stable genetic character and does not occur by spontaneous genetic mutation (Flis et al., 1993; Campo et al., 2001). Fischer (2002) confirmed this by showing that there is an increase in lag phase when Al-tolerant cultures are transferred to media without Al,

indicating an inducible Al resistance in *A. cryptum* (an acidophilic soil bacteria), rather than resistance due to a mutation. Understanding the genetic trait that confers tolerance is important to researchers whose main objective is to develop bacterial strains with which to inoculate extremely acidic soils (Flis et al., 1993). *Rhizobium loti* has been shown to have a high level of tolerance, but does not have plasmids, indicating that the gene/s for Al tolerance must be contained in chromosomal DNA. Jo et al. (1997) isolated an Al-tolerant gene from *Arthro bacter viscosus*. This gene was also found in chromosomal DNA. The isolated gene was extracted and transferred to *E. coli* and successfully endowed *E. coli* with Al tolerance. The exact mechanisms by which these genes confer Al tolerance are not known, but it is thought that Al taken up into the cell is detoxified by binding proteins, tolerance enzymes, or the compartmentalization of Al into a vacuole.

Isolating the effects of Al on soil bacteria is complicated by the fact that acidity and Al in soils are irrevocably linked; therefore a bacterial species must have tolerance for both acidity and Al toxicity. The bioavailability and species of Al present in soil solution is heavily dependent on pH. At pH values less than 5, Al is present in its monomeric ( $\text{Al}^{3+}$ ) and most toxic form. Also, the relative proportion of the exchange complex dominated by aluminum is more important than total concentrations of exchangeable Al alone (Wood, 1995).

Interpreting the direct effects of Al toxicity is also complicated by the interaction between Al and phosphorous, as well as the influence of plant roots on conditions in the rhizosphere. Phosphorous readily forms stable complexes with Al in soil solution, thereby binding Al and decreasing its bioavailability (Illmer and Schinner, 1999). Other

nutrients to a lesser degree can also bond with monomeric Al and form insoluble precipitates. This causes confusion, because what may appear to be the effects of Al toxicity, may actually be the effects of nutrient limitations. Differences in P concentrations in growth media may be responsible for the often extremely contradictory results regarding the extent of Al-tolerance in bacteria (Illmer and Schinner, 1999). Plants also experience detrimental effects due to high Al concentrations. Plant roots excrete citrate, malate, and oxalate which chelate Al and reduce its toxicity. These root secretions coupled with the activities of nitrifying bacteria can raise soil pH in the rhizosphere, creating a reduced area of Al toxicity suitable for bacterial growth. For these reasons, Al stress levels experienced by microbial communities in soils are spatially heterogeneous and difficult to determine (Flis et al., 1993).

Al toxicity has broad impacts on the microbial ecology and C cycling of acidic soil systems. Concentrations of monomeric Al and soil organic matter are highly correlated in acidic soils (Mulder et al., 2001; Illmer et al., 2003). However the same correlations have been shown between pH and soil organic matter (Bottner et al., 1998), emphasizing the irrevocable link between acidity and Al toxicity. Illmer et al. (2003) also found negative correlations between levels of monomeric Al, microbial biomass, respiration rates and ATP production, but only in soils with pH values less than 4. Fungi may have a higher tolerance for monomeric Al than bacteria (Kanazawa and Kunito, 1996; Kawai et al., 2000), which is evidenced by higher fungal: bacterial ratios with increasing Al and acidity (Fierer and Jackson, 2006; Rousk et al., 2009).

**4.2 Microbes and mineral weathering rates:** Microbes are strongly influenced by mineral surfaces and dissolution products, but mineral dissolution rates are also influenced by microbial activity. Bacterial mineral weathering is ubiquitous in soils of all types, but is essential to maintain nutrient levels in acidic forest soils.

Microbial activity promotes mineral weathering in a variety of ways. Microbial metabolites or biodegradation products (i.e. low molecular weight organic acids such as citrate, oxalate, etc.), can degrade mineral surfaces through acid attack. Organic acids can also be very effective metal chelators. The formation of organo-metal complexes removes mineral weathering products from solution and drives weathering reactions forward (Tan, 1986; Stevenson, 1994). In studies of goethite and gibbsite specifically, the presence of 2-ketogluconate and citrate (common microbial byproducts) increased Fe and Al activities by several orders of magnitude (Essington, 2005). Formation of organo-metal complexes can also inhibit the crystallization of Fe and Al oxides in soils (Kodama and Schnitzer, 1977, 1980).

Most microbes live attached to mineral surfaces; estimates are as high as 90% of the soil microbial community living attached to either mineral or organic surfaces (Maier et al., 2000). Though the effects of microbes are difficult to separate from purely abiotic processes, colonization of mineral surfaces generally promotes mineral weathering. In fact, the transition from rock to soil begins with the colonization of the rock surface with lichens (Banfield et al., 1999). As mineral weathering progresses, the community structure at the rock surface grows in diversity and complexity. Communities in the newly formed soil are different than those at the rock/soil interface (Certini et al., 2004).

Furthermore, microbial communities shallowly embedded in the rock are different than those located at the rock surface (McNamara et al., 2006).

Microbes not only utilize mineral surfaces as anchoring points, but may also use minerals as a source of inorganic nutrients or as terminal electron acceptors in respiration. Microbes may promote mineral dissolution passively through the release of non-specific organic acids. Mineral-derived elements chelated by these organic acids may be taken up by microbes or converted to other forms which may then be bioavailable (Stevenson, 1994). However, some microorganisms produce element-specific complexing agents to improve bioavailability of low-solubility nutrients such as Fe (Hersman et al., 1996). Other microorganisms may utilize humic substances in soils as “electron shuttles” to assist in the use of Fe(III) and Mn(IV) as terminal electron acceptors (Lovely et al., 1996). Since different minerals necessarily vary in their elemental compositions, mineral type influences microbial community composition through differences in micronutrient availability (Gleeson et al., 2006). Therefore, specific mineral surfaces may be colonized by communities best suited to extract micronutrients from those minerals or utilize terminal electron acceptors such as Fe.

### **Dissertation format & collaborative contributions**

The research presented in this dissertation is discussed in detail in four appendices (A, B, C & D). A broad overview of the work is given in the chapter entitled “Present study”. The research reported in appendices B, C and D was collaborative in nature. All contributors to the research are listed on the title page of each appendix. In all cases, the majority of lab work and writing were performed by the author (Katherine Heckman). Dr. Craig Rasmussen made significant contributions to all studies in the form of text edits, data interpretation, intellectual guidance, and experimental design. Other collaborative contributions were as follows:

For appendix B: Amy Welty-Bernard performed the T-RFLP analysis and contributed the following sections of text: Methods section 2.3 and Results section 3.2.

For appendix C: Angelica Vazquez Ortega assisted with running samples on the Ion Chromatograph, the HPLC, and the ICP-MS. Dr. Xiaodong Gao performed peak decomposition analyses on the FTIR spectra. Dr. Jon Chorover assisted with experimental design, data interpretation and text edits.

For appendix D: Dr. Egbert Schwartz and Amy Welty-Bernard provided analysis of the pyrosequencing data and text associated with the pyrosequencing analysis. Angelica Vazquez Ortega assisted with running samples on the Ion Chromatograph, the HPLC, and the ICP-MS. Dr. Craig Rasmussen and Dr. Jon Chorover assisted with experimental design, data interpretation and text edits.

## PRESENT STUDY

The methods, results, and conclusions of this study are presented in the papers appended to this dissertation/thesis. The following is a summary of the most important findings in this document.

The overarching theme of this work is the influence of soil parent material type on pedogenesis and C cycling in soils. The work presented in this dissertation ranges in both scale and specificity. Two studies (Appendices A & B) examine pedogenesis and organic C cycling at the pedon scale. These studies both utilize a lithosequence to illustrate the importance of soil mineral assemblage to soil characteristics and C content. The third study (Appendices C & D) investigates organo-mineral interactions at the molecular level, and specifically examines interactions between oxide surfaces and dissolved organic matter derived from forest floor material.

The first study (Appendix A) explored variation in pedogenesis and elemental mass loss as a product of parent material through a combination of quantitative X-ray diffraction and elemental mass balance. Soils were taken from a lithosequence of four parent materials (rhyolite, granite, basalt, limestone/volcanic cinders) under *Pinus ponderosa*. Results indicated significant differences in profile characteristics, and chemical mass flux according to parent material. Calculations of mass flux were confounded by the addition of volcanic cinders in the limestone soils and addition of eolian materials in both the basalt and limestone soils. These variations in parent material were accounted for using a combination of refractory element indices, and x-ray diffraction in the case of quartz additions. Total mass flux from the basalt soils during

weathering of bedrock was balanced or exceeded by addition of eolian materials, leading to a total mass flux of  $+36 (\pm 97) \text{ kg m}^{-2}$  (parenthetical values are the standard error of three replicates). Elemental mass balance calculations for the limestone soils were made in reference to a mixed parent material, including both the underlying limestone bedrock and the volcanic cinders deposited throughout the formation of the soil. Total mass flux from the limestone soils during weathering of both cinder material and underlying bedrock was also balanced or exceeded by addition of eolian materials, leading to a very small and highly variable total mass flux of  $-3 (\pm 97) \text{ kg m}^{-2}$ . Rhyolite and granite soils exhibited large differences in degree of weathering and mass flux regardless of the nearly identical elemental and mineralogical compositions of the respective parent materials. Mass flux from granite soils was  $-203 (\pm 36) \text{ kg m}^{-2}$ , whereas mass flux from the rhyolite soils was much larger ( $-576 (\pm 39) \text{ kg m}^{-2}$ ), due differences in parent material grain size and bulk density. The data from this lithosequence demonstrates quantitatively the influence of parent material on inorganic C consumption during pedogenesis and that pedogenesis on different parent materials leads to the production of soils with significantly different physiochemical characteristics and abilities to sequester organic C.

The second study (Appendix B) examines the role of soil parent material in determining soil organic C (SOC) contents, and identifies key soil physiochemical characteristics associated with SOC content. Soils utilized for this study were taken from the same lithosequence of forest soils used in the first study. This study focused on the following specific questions: i) Within a specific ecosystem type, how do SOC contents vary among sites with differing mineralogy? ii) What physicochemical variables are most

highly correlated with SOC content, soil microbial community composition and soil respiration? and iii) What mechanisms account for the influence of these variables on SOC cycling? Soil physiochemical and microbiological properties were characterized and compared on the basis of mineral assemblage, pH, organic carbon content, bacterial community composition, respiration rate, microbial biomass, specific metabolic activity ( $q\text{CO}_2$ ), and  $\delta^{13}\text{C}$  of respired  $\text{CO}_2$ . The selected field sites spanned a physicochemical gradient, ranging from acid (pH of 5.2) to basic (pH of 7.1) from rhyolite to granite to basalt to limestone. The acidic rhyolite and granite soils had measureable amounts of exchangeable  $\text{Al}^{3+}$  (up to  $3 \text{ cmol}_+ \text{ kg}^{-1}$ ). SOC content varied significantly among sites, ranging from 3.5 to  $11 \text{ kg C m}^{-2}$  in limestone and rhyolite soils, respectively. Soil bacterial communities were also significantly different among all sites. Metal-humus complex and Fe-oxyhydroxide content emerged as important predictors of SOC dynamics across all sites, showing significant correlation with both SOC content (Al-humus:  $R^2=0.71$ ;  $P<0.01$ ; Fe-humus:  $R^2=0.75$ ;  $P<0.001$ ; crystalline FeOx:  $R^2=0.63$ ;  $P<0.01$ ) and bacterial community composition (Al-humus:  $R^2=0.35$ ;  $P<0.05$ ; Fe-humus:  $R^2=0.51$ ;  $P<0.01$ ; oxalate-extractable Fe:  $R^2=0.59$ ;  $P<0.01$ ). Moreover, soil pH was significantly correlated with exchangeable  $\text{Al}^{3+}$ , metal-humus complex content, bacterial community composition, and microbial biomass C/N ratios. Results indicated that within a specific ecosystem, SOC dynamics and microbial community vary predictably with soil physicochemical variables directly related to mineralogical differences among soil parent materials. Specifically, the data suggest a gradient in the dominant SOC stabilization mechanism among sites, with chemical recalcitrance and metal-humus complexation the

dominant control in soils of the acidic rhyolite and granite sites, and mineral adsorption the dominant factor in the basic limestone and basalt sites. Knowledge of parent material dependent SOC dynamics allows for improved estimates of ecosystem SOC stocks and the potential response of SOC to climate change.

The third study included in this dissertation (Appendices C & D) focuses on dissolved organic matter (DOM) interactions with Fe and Al oxide surfaces (goethite and gibbsite). The research included in Appendix C examined these interactions through an incubation of forest floor material in the presence of 1) goethite surfaces 2) gibbsite surfaces and 3) quartz sand surfaces (as a control treatment) to evaluate changes in molecular and thermal properties of dissolved organic matter as a product of interaction with oxide surfaces. Forest floor material was incubated over a period of 154 days. Dissolved organic matter was harvested on days 5, 10, 20, 30, 60, 90, and 154, and examined by Thermogravimetry/Digital Thermal Analysis (TG/DTA) and Diffuse Reflectance Fourier Transform Infrared Spectroscopy (DRIFT). Results indicated significant differences in DOM quality among treatments, though the effect of oxide surfaces on DOM properties did not change significantly with increasing time of incubation. DOM from both the oxide treatments had significantly lower C contents than DOM from the control treatment. Interaction with goethite produced DOM of mid-to-high-range thermal lability which was depleted in both proteins and fatty acids. The average enthalpy of DOM from the goethite treatment was significantly higher than either the gibbsite or control treatment, suggesting that interaction with goethite surfaces increases the thermal stability of DOM. Interaction with gibbsite produced DOM rich in

thermally recalcitrant and carboxyl-rich compounds in comparison to the control treatment. These data indicate that interaction of DOM with oxide surfaces significantly changes the composition of DOM.

Research presented in Appendix D examines the consequences of these changes in DOM properties for microbial communities utilizing DOM as a growth substrate. Pyrosequencing analysis indicated that both bacterial and fungal community composition were significantly different among treatments. Variation in microbial community composition was correlated with DOM characteristics that exhibited significant variation among treatments including concentrations of organic C, P, orthophosphate, pH and Al. Respiration rates of communities exposed to gibbsite surfaces were slightly lower than the control treatment, suggesting a possible Al toxicity effect. Data indicated that changes in DOM physiochemical properties have important consequences for the biodegrader community.

## REFERENCES

- Baldock, J.A., Skjemstad, J.O., 2000. Temperature effects on the diversity of soil heterotrophs and the delta C-13 of soil-respired CO<sub>2</sub>. *Soil Biology and Biochemistry* 32, 699-706.
- Banfield, J.F. Barker, W.W., Welch, S.A., Tauton, A., 1999. Biological impact on mineral dissolution: application of the lichen model to understanding mineral weathering in the rhizosphere. *Proceedings of the National Academy of Sciences U.S.A.* 96, 3404-3411.
- Bottner, P., Austrui, F., Cortez, J., Billès, G., Coùteaux, M.M., 1998. Decomposition of <sup>14</sup>C and <sup>15</sup>N labeled plant material under controlled conditions in coniferous forest soils from a north-south climate sequence in Western Europe. *Soil Biology and Biochemistry* 30, 597-610.
- Bundt, M., Widmer, F., Pesaro, M., Zeyer, J., Blaser, P., 2001. Preferential flow paths: biological 'hot spots' in soils. *Soil Biology and Biochemistry* 33, 729-738.
- Burns, R.G., 1989. Microbial and enzymic activities in soil biofilms. In *Structure and Function of Biofilms*, W.G. Characklis and P.A. Wilderer (Eds.). John Wiley & Sons, London, pp. 333-350.
- Brodowski, S., John, B., Flessa, H., Amelung, W., 2006. Aggregate-occluded black carbon in soil. *European Journal of Soil Science* 57, 539-546.
- Campo, R.J, Wood, M., 2001. Residual effects of successive exposure of soybean *Bradyrhizobium* strains to aluminium on solid defined medium. *Pesq. Agropec. Bras., Basilia.* 36, 1399-1407.
- Certini, G., Campbell, C.D., Edwards, A.C., 2004. Rock fragments in soil support a different microbial community form the fine earth. *Soil Biology and Biochemistry* 36, 1119-1128.
- Chenu C, Stotzky G, 2002. Interactions between microorganisms and soil particles, An overview. *In: Interactions between soil particles and microorganisms. Eds: PM Huang, JM Bollag, N Senesi: 3-39. Wiley-VCH-Verlag, Weinheim.*
- Chorover J, 2008. Lecture notes, for: Soil and Water Chemistry.
- Denman, K. L., Brasseur, G., Chidthaisong, A., et al. 2007. Couplings between changes in the climate system and biogeochemistry. In *Climate Change 2007: the Physical Science Basis. Contribution of Working Group I to the Fourth Assessment Report of the*

*Intergovernmental Panel on Climate Change*, ed. S. Solomon, D. Qin, M. Manning et al. Cambridge: Cambridge University Press.

Drever, J. I., Stillings, L. L., 1997. The role of organic acids in mineral weathering. *Aquatic Colloid and Surface Chemistry* 120, 167-181.

Eusterhues K, Rumpe C, Kleber M, Kogel-Knabner I, 2003. Stabilisation of soil organic matter by interactions with minerals as revealed by mineral dissolution and oxidative degradation. *Organic Geochemistry* 34: 1591-1600.

Essington ME, 2004. Chapter 4: Organic Matter in Soil. In: *Soil and Water Chemistry: An Integrative Approach*. CRC Press: Boca Raton, FL, 129-180.

Essington M.E., Nelson J.B. and Holden W.L. (2005) Gibbsite and goethite solubility: The influence of 2-ketogluconate and citrate. *Soil Science Society of America Journal* 69, 996-1008.

Fierer, N., and R. B. Jackson. 2006. The diversity and biogeography of soil bacterial communities. *Proc. Natl. Acad. Sci. USA* 103:626-631.

Fisher, J., Quentmeier, A., Gansel, S., Sabados, V., Friedrich, C.G., 2002. Inducible aluminum resistance of *Acidiphilium cryptum* and aluminum tolerance of other acidophilic bacteria. *Arch Microbiol.* 178, 554-558.

Flis, S.E., Glenn, A.R., Dilworth, M.J., 1993. The interaction between aluminium and root nodule bacteria. *Soil Biol. Biochem.* 25, 403-417.

Gleeson, D.B. et al., 2006. Characterization of bacterial community structure on a weathered pegmatic granite. *Microbial Ecology* 51, 526-534.

Golchin A, Oades JM, Skjemstad JO, Clarke P, 1994. Study of free and occluded particulate organic matter in soils by solid state <sup>13</sup>C CP/MAS NMR spectroscopy and scanning electron microscopy. *Australian Journal of Soil Research* 32: 285-309.

Golchin, A., Oades, J.M., Skjemstad, J.O., Clarke, P. 1994b. Soil structure and carbon cycling. *Australian Journal of Soil Research* 32: 1043-1068.

Grayston, S.J., Vaughan, D., Jones, D., 1997. Rhizosphere carbon flow in trees, in comparison with annual plants: the importance of root exudation and its impact on microbial activity and nutrient availability. *Applied Soil Ecology* 5, 29-56.

Greenland, D. J., 1971. Interactions between humic and fulvic acids and clays. *Soil Science* 111, 34-41.

- Güsewell, S., Gessner, M.O., 2009. N:P ratios influence litter decomposition and colonization by fungi and bacteria in microcosms. *Functional Ecology* 23, 211-219.
- Hassink J, 1997. The capacity of soils to preserve organic C and N by their association with clay and silt particles. *Plant and Soil* 191: 77-87.
- Hersman, L., Maurice, P., Sposito, G., 1996. Iron acquisition from hydrous Fe(III)-oxides by an aerobic *Pseudomonas* sp. *Chemical Geology* 132, 25-31.
- Houghton, R. A., Hackler, J. L., Lawrence, K. T., 1999. The US carbon budget: contributions from land-use change. *Science* 285, 574-578.
- Illmer, P., Marschall, K., Schinner, F., 1995. Influence of available aluminum on soil-micro-organisms. *Letters in Applied Microbiology* 21 (6), 393-397.
- Illmer, P., Obertegger, U., Schinner, F., 2003. Microbiological properties in acidic forest soils with special consideration of KCl extractable Al. *Water Air and Soil Pollution* 148, 3-14.
- IPCC (2001) *Climate Change 2001: The Scientific Basis (Contribution of Working Group I to the Third Assessment Report of the Intergovernmental Panel on Climate Change)*. Cambridge: Cambridge University Press.
- Jandl, R., Sollins, P., 1997. Water-extractable soil carbon in relation to the belowground carbon cycle. *Biology & Fertility of Soils* 25, 196-201.
- Jandl, R., Sletten, R.S., 1999. Mineralization of forest soil carbon: interactions with metals. *J. Plant Nutr. Soil Sci.* 162, 623-629.
- Jenny, H., 1941. *Factors of Soil Formation: A system of quantitative pedology*. New York: Dover Publications, Inc.
- Jo, Jinki, Jang, Yo-Soon, Kim, Ki-Yong, Kim, Mi-Hye, Kim, In-Jung, Chung, Won-Il, 1997. Isolation of *ALUI-P* gene encoding a protein with aluminum tolerance activity from *Anthrobacter viscosus*. *Biochemical and Biophysical Research Communications* 239, 835-839.
- John, B., Yamashita, T., Ludwig, B., Flessa, H., 2005. Organic carbon storage in aggregate and density fractions of silty soils under different types of land use. *Geoderma* 128, 63-79.
- Kaiser K, Guggenberger G, 2000. The role of DOM sorption to mineral surfaces in the preservation of organic matter in soils. *Organic Geochemistry* 31, 711-725.

Kaiser K, Guggenberger G, 2007. Sorptive stabilization of organic matter by microporous goethite: Sorption into small pores vs. surface complexation. *European Journal of Soil Science* **58(1)**: 45-59.

Kalbitz, K., Schmerwitz, J., Schwesig, D., Matzner, E., 2003a. Biodegradation of soil-derived dissolved organic matter as related to its properties. *Geoderma* 113, 273-291.

Kalbitz K, Schwesig D, Rethemeyer J, Matzner E, 2005. Stabilization of dissolved organic matter by sorption to the mineral soil. *Soil Biology and Biochemistry* **37**: 1319-1331.

Kalbitz, K., Solinger, S., Park, J.-H., Michalzik, B., Matzner, E., 2000. Controls on the dynamics of dissolved organic matter in soils: A review. *Soil Science* 165, 277-304.

Killham K., Amato, M., Ladd, J.N., 1993. Effect of substrate location in soil and soil pore-water regime on carbon turnover. *Soil Biology and Biochemistry* 25, 57-62.

Kleber M, Sollins P, Sutton R, 2007. A conceptual model of organo-mineral interactions in soils: self-assembly of organic molecular fragments into zonal structures on mineral surfaces. *Biogeochemistry* **85**: 9-24.

Kodama, H., Schnitzer, M., 1977. Effect of fulvic acid on the crystallization of Fe(III) oxides. *Geoderma* 19, 279-291.

Kodama, H., Schnitzer, M., 1980. Effect of fulvic acid on the crystallization of aluminum hydroxides. *Geoderma* 24, 195-205.

Kögel-Knabner, I., Guggenberger, G., Kleber, M., Kandeler, E., Kalbitz, K., Scheu, S., Eusterhues, K., Leinweber, P., 2008. Organo-mineral associations in temperate soils: Integrating biology, mineralogy, and organic matter chemistry. *Journal of Plant Nutrition and Soil Science* 171, 61-82

Lovely, D.R., Coates, J.D., Blunt-Harris E.I., Phillips, E.J.P, Woodward, J.C., 1996. Humic substances as electron acceptors for microbial respiration. *Nature* 382, 445-448.

Lynch, J.M., Bragg, E., 1985. Microorganisms and soil aggregate stability. *Aust. J. Soil Res.*, 27: 411-423.

Maier, R. M., Pepper, I. L., Gerba, C. P., 2000. *Environmental Microbiology*. Academic Press: San Diego, CA.

Marin-Spiotta, E., Swanston C.W., Torn, M.S., Silver, W.L., Burton, S.D., 2008. Chemical and mineral control of soil carbon turnover in abandoned tropical pastures. *Geoderma* 143, 49-62.

Marschner B, Brodowski S, Dreves A, Gleixner G, Gude A, Grootes PM, Hamer U, Heim A, Jandl G, Ji R, Kaiser K, Kalbitz K, Kramer C, Leinweber P, Rethemeyer J, Schäffer A, Schmidt MWI, Schwark L, Wiesenberg GLB, 2008. How relevant is recalcitrance for the stabilization of organic matter in soils? *Journal of Plant Nutrition and Soil Science* **171**: 91-110.

Martin, J. P., Haider, K., 1986. Influence of mineral colloids on turnover rates of soil organic carbon. In: P. M. Huang and M. Schnitzer (Eds.). Interactions of soil minerals with natural organics and microbes, pp. 284-304. Soil Science Society of America: Madison, Wisconsin.

McNamara, C.J., Perry, T.D., Bearce, K.A., Hernandez-Duque, G., Mitchell, R., 2006. Epilithic and endolithic bacterial communities in limestone from a Maya archaeological site. *Microbial Ecology* **51**, 51-64.

Metting, F.B., 1993. Structure and physiological ecology of soil microbial communities. In: Metting, F.B. (Ed.), *Soil Microbial Ecology – Application in Agricultural and Environmental Management*. Marcel Dekker, New York, pp. 3-24.

Michalzik, B., Matzner, E., 1999. Fluxes and dynamics of dissolved organic nitrogen and carbon in a spruce (*Picea abies* Karst.) forest ecosystem. *European Journal of soil science* **50**, 579-590.

Mikutta R, Mikutta C, Kalbitz K, Scheel T, Kaiser K, Jahn R, 2007. Biodegradation of forest floor organic matter bound to minerals via different binding mechanisms. *Geochimica et Cosmochimica Acta* **71**: 2569-2590.

Miller, R.M., Jastrow, J.D., 1990. The Hierarchy of root and mycorrhizal fungal interactions with soil aggregation. *Soil Biology and Biochemistry* **22**:579-584.

Mulder, J., DeWit, H.A., Boonen, H.W.J., Bakken, L.R., 2001. Increased levels of aluminium in forest soils: Effects on the stores of soil organic carbon. *Water, Air, and Soil Pollution* **130**, 989-994.

Nierop, K.G.J., Jansen B., Verstraten, J.M., 2002. Dissolved organic matter, aluminum and iron interactions: Precipitation induced by metal/carbon ratio, pH and competition. *Sci. Total Environ.* **300**, 201–211.

Oades, J.M., 1988. The retention of organic-matter in soils. *Biogeochemistry* **5**, 35-70.

Ohm H, Hamer U, Marschner B, 2007. Priming effects in soil size fractions of a podzol Bs horizon after addition of fructose and alanine. *Journal of Plant Nutrition and Soil Science* **170**: 551-559.

- Paul, S., Veldkamp, E., Flessa, H., 2008. Soil organic carbon in density fractions of tropical soils under forest – pasture –secondary forest land-use changes. *European Journal of Soil Science* 59, 359-371.
- Rasmussen, C., Torn, M.S., Southard, R.J., 2005. Mineral assemblage and aggregates control C dynamics in a California conifer forest. *Soil Science Society of America Journal* 69:1711-1721.
- Reicosky, D.C., Dugas, W.A., Torbert, H.A., 1997. Tillage-induced soil carbon dioxide loss from different cropping systems. *Soil and Tillage Research* 41, 105-118.
- Rethemeyer, J., Kramer, C., Gleixner, G. et al., 2005. Transformation of organic matter in agricultural long-term field trials: Radiocarbon concentration versus soil depth. *Geoderma* 128, 94-105.
- Rousk, J., Brookes, P.C., Bååth, E., 2009. Contrasting soil pH effects on fungal and bacterial growth suggest functional redundancy in carbon mineralization. *Applied Environmental Microbiology* 75, 1589-1596.
- Sachse, A., Babenzien, D., Ginzel, G., Gelbrecht, J., Steinberg, C.E.W., 2001. Characterization of dissolved organic carbon (DOC) in a dystrophic lake and an adjacent fen. *Biogeochemistry* 54, 279-296.
- Saggar S, Parfitt RL, Salt G, Skinner MF (1998) Carbon and phosphorus transformations during decomposition of pine forest floor with different phosphorus status. *Biol Fertil Soils*. 27:197–204
- Scheel, T., Dörfler, C., Kalbitz, K., 2007. Precipitation of dissolved organic matter by aluminum stabilizes carbon in acidic forest soils. *Soil Science Society of America Journal* 71, 64-74.
- Six J, Conant RT, Paul EA, Paustian K, 2002. Stabilization mechanisms of soil organic matter: Implications for C-saturated soils. *Plant and Soil* 241: 155-176.
- Sollins P, Homann P, Caldwell BA, 1996. Stabilization and destabilization of soil organic matter: mechanisms and controls. *Geoderma* 74: 65-105.
- Stevenson, F. J., 1994. *Humus Chemistry: Genesis, Composition, Reactions*. John Wiley & Sons, Inc.: New York.
- Swanston, C.W., Torn, M.S., Hanson, P.J. et al., 2005. Initial characterization of processes of soil carbon stabilization using forest stand-level radiocarbon enrichment. *Geoderma* 128, 52-62.

- Tan, K.H., 1986. Degradation of soil minerals by organic acids. *In: Interactions of soil minerals with natural organics and microbes. (Eds. P.M. Huang and M. Schnitzer) Soil Science Society of America, Inc.: Madison, Wisconsin, pp. 1-25.*
- Tebrügge, F., Düring, R.A., 1999. Reducing tillage intensity – a review of results from a long-term study in Germany. *Soil and Tillage Research* 53, 15-28.
- Theng BKG, Tate KR, 1989. Interactions of clays with soil organic constituents. *Clay Research* 8: 1–10.
- Thomas R. S., Dakessian, R.N. Ames, M.S. Brown, Bethlenfalvay, G.J. 1993. Separation of vesicular-arbuscular mycorrhizal fungus and root effects on soil aggregation. *Soil Science Society of America Journal* 57: 77-81.
- Ver, L.M.B., Mackenzie, F.T., Lerman, A., 1999. Biogeochemical responses of the carbon cycle to natural and human perturbation: past, present, and future. *American Journal of Science* 299, 762-801.
- von Lützow M, Kogel-Knabner I, Ekschmitt K, Matzner E, Guggenberger G, Marschner B, Flessa H, 2006. Stabilization of organic matter in temperate soils: mechanisms and their relevance under different soil conditions - a review. *European Journal of Soil Science* 57: 426-445.
- Wagai, R., Mayer, L.M., Kitayama, K., Knicker, H., 2008. Climate and parent material controls on organic matter storage in surface soils: A three-pool, density-separation approach. *Geoderma* 147, 23-33.
- Wagai, R., Mayer, L. M., Kitayama, K. 2009. Nature of the "occluded" low-density fraction in soil organic matter studies: A critical review. *Soil Science and Plant Nutrition* 55: 13-25.
- Wagner, S., Cattle, S.R., Scholten, T. 2007. Soil-aggregate formation as influenced by clay content and organic-matter amendment. *Journal of plant nutrition and soil science* 170: 173-180.
- Wander, M.M., Bidart, M.G., 2000. Tillage practice influences on the physical protection, bioavailability and composition of particulate organic matter. *Biology and Fertility of Soils* 32, 360-367.
- Wattel-Koekkoek EJW, van Genuchten PPL, Buurman P, van Lagen B, 2001. Amount and composition of clay-associated soil organic matter in a range of kaolinitic and smectitic soils. *Geoderma* 99: 27-49.

Wood, M., 1995. A mechanisms of aluminum toxicity to soil bacteria and possible ecological implications. *Plant and Soil* 171, 63-69.

Yano, Y., McDowell, W. H., Kinner, N., 1998. Quantification of biodegradable dissolved organic carbon in soil solution with flow-through bioreactors. *Soil Science Society of America Journal* 62, 1556-1564.

Zech W. and Guggenberger G. (1996) Organic matter dynamics in forest soils of temperate and tropical ecosystems. In: *Humic Substances in Terrestrial Ecosystems*. (ed. A. Piccolo). Elsevier, Amsterdam. pp. 101–170.

Zsolnay A. (1996) Dissolved humus in soil waters. In *Humic substances in terrestrial ecosystems*. (ed. A. Piccolo). Elsevier, Amsterdam. pp. 225-264.

APPENDIX A

LITHOLOGIC CONTROLS ON REGOLITH WEATHERING AND MASS FLUX IN  
FORESTED ECOSYSTEMS OF THE SOUTHWESTERN USA

Katherine Heckman\* and Craig Rasmussen

\*Corresponding Author

Department of Soil, Water and Environmental Science; University of Arizona

1177 E. Fourth Street PO Box 210038

Tucson, AZ 85721-0038, USA

kheckman@email.arizona.edu

phone : +1 520 621 1646, fax : +1 520 621 1647

Prepared for submission to *Geoderma*

### Abstract

Parent material has a profound impact on the pedogenic processes of mineral weathering and chemical mass flux, including fluxes of inorganic C consumed during mineral weathering. However, there remains a relative paucity of lithosequence studies that directly examine parent material control on pedogenic processes. We offer a lithosequence of four parent materials (rhyolite, granite, basalt, limestone/volcanic cinders) under *Pinus ponderosa*, to explicitly quantify the contribution of parent material to the character of the resulting soil. We explored variation in pedogenesis and mass flux as a product of parent material through a combination of quantitative X-ray diffraction and elemental mass balance. Results indicated significant differences in profile characteristics, and chemical mass flux according to parent material. Calculations of mass flux were confounded by the addition of volcanic cinders in the limestone soils and addition of eolian materials in both the basalt and limestone soils. These variations in parent material were accounted for using a combination of refractory element indices and x-ray diffraction in the case of quartz additions. Total mass flux from the basalt soils during weathering of bedrock was balanced or exceeded by addition of eolian materials, leading to a total mass flux of  $+36 (\pm 97) \text{ kg m}^{-2}$ . Elemental mass balance calculations for the limestone soils were made in reference to a mixed parent material, including both the underlying limestone bedrock and the volcanic cinders deposited throughout the formation of the soil. Total mass flux from the limestone soils during weathering of both cinder material and underlying bedrock was also balanced or exceeded by addition of eolian materials, leading to a very small and highly variable total mass flux of  $-3 (\pm 97) \text{ kg}$

$\text{m}^{-2}$ . Rhyolite and granite soils exhibited large differences in degree of weathering and mass flux regardless of the nearly identical elemental and mineralogical compositions of the respective parent materials. Mass flux from granite soils was  $-203 (\pm 36) \text{ kg m}^{-2}$ , whereas mass flux from the rhyolite soils was much larger ( $-576 (\pm 39) \text{ kg m}^{-2}$ ), due differences in parent material grain size and bulk density. The data from this lithosequence demonstrates quantitatively the influence of parent material on inorganic C consumption during pedogenesis and that pedogenesis on different parent materials leads to the production of soils with significantly different abilities to sequester organic C.

## 1. Introduction

Parent material has been recognized as one of the fundamental factors of soil formation since the development of soil science as its own scientific discipline (Dokuchaev 1879, Jenny 1941). In a given ecosystem, soil weathering rates, profile depth, clay content and cation exchange capacity are all determined to a large degree by the type of parent material the soil develops from. However, despite the large role parent material plays in determining soil characteristics, there are relatively few pure lithosequence studies in the literature. Previous lithosequence studies have explored key differences among soils attributable to what are often small differences in parent material characteristics; including the influence of coarse fragment content (Schaeztl, 1991), carbonate content (Anderson et al. 1975), base cation content (Hoyum and Hajek, 1979), and porosity (Levine et al., 1989) on general morphological characteristics. These studies have indicated that differences in parent material lead to important differences in specific

soil parameters such as productivity, base cation content, and depth. Our examination offers a more broad perspective, focusing on the influence of parent material on a range of soil characteristics, including production and type of secondary minerals, soil morphology, and mass flux during weathering.

A lithosequence is also an informative tool to illustrate the role of lithology in the global carbon cycle, including both inorganic and organic forms of C. Mineral dissolution and transformation processes lead to the conversion of atmospheric CO<sub>2</sub> to bicarbonate salts which are in turn sequestered over geologic time scales in the form of carbonate rock (Berner 1983, MacKenzie & Lerman 2006). At the same time, mineral weathering leads to the production of surface area, organo-mineral complexes, and secondary minerals with structural and pH-dependent charge, properties which increase a soil's organic C sequestration capacity (Kögel-Knaber et al., 2008). The importance of lithology in determining atmospheric C consumption during pedogenesis is emphasized by several authors (Garrels & MacKenzie, 1971; Meybeck, 1986; Amiotte-Suchet & Probst, 1993; Bluth & Kump, 1994; Edmond et al., 1996), who also highlight the importance of parent material weatherability in determining rates of inorganic C consumption in soils. The influence of soil mineral assemblage on soil organic C content is also well documented, with previous studies highlighting clay content (Schimel et al. 1994, Percival et al. 2000), clay type (Wattel-Koekkoek et al. 2003), concentrations of Fe oxyhydroxides and allophanic materials (Torn et al., 1997; Rasmussen et al., 2006), and specific surface area and surface charge (Kahle et al. 2004) as some of the mineralogical parameters of primary importance in determining a soil's organic C content.

The object of this research was to give a quantitative description of pedogenesis across a lithosequence, utilizing quantitative mineralogy and elemental mass balance to illustrate differences in soil characteristics attributable to variation in parent material. The majority of data presented outlines the variation in mineral transformations and mass flux among the soils examined. We also offer a general discussion of the consequences of these processes for both inorganic and organic C cycling in soils.

## 2. Methods

### 2.1. Field sites

We sampled soils derived from four different parent materials (rhyolite, granite, basalt, limestone/volcanic cinder) from a regionally extensive and important *Pinus ponderosa* (ponderosa pine) forest ecosystem across Arizona, USA,. The limestone and basalt sites were located near Flagstaff, AZ on the Kaibab Limestone formation and late-Pleistocene aged basalt flows on the edge of the Colorado Plateau. Soils forming on the Colorado Plateau are known to have a long history of dust accumulation (Reheis et al., 2005; Reynolds et al., 2006), and both the limestone and basalt soils exhibited evidence of substantial eolian deposition. The limestone soil also contained mafic cinder material, deposited during the formation of local cinder cones. The addition of eolian materials and volcanic cinders were detected and accounted for through a combination of geochemical and mineralogical techniques (discussed in detail below). The granite site was located in the Santa Catalina Mountains north of Tucson, AZ on Precambrian aged granite. The

rhyolite site was located on the Mesozoic aged Turkey Creek Caldera in the Chiricahua Mountains in southeastern Arizona (Arizona Geological Survey, 2000).

Despite variation in the age of parent rock, the geomorphic surface age was assumed to be similar among sites. Soil mean residence times were assumed to be of the same order of magnitude, roughly 25,000-50,000 years with soil physicochemical properties in relative steady-state with mid- to late-Holocene climate conditions. Soils formed in the southwest United States have experienced substantial climate changes over the last glacial-interglacial transition. Cooler, wetter, winter rainfall dominated conditions were predominant during the last glacial, followed by pronounced heating and drying in the early-to-mid Holocene (Spaulding and Graumlich, 1986). However, climate conditions have been relatively stable in this region for the past ~8,000 years, with conditions similar to modern climate forcing. All sites were located within mesic soil temperature regimes and ustic soil moisture regimes, with similar slope, aspect and elevation. Overall, the vegetation and climatic characteristics were relatively constant among sites (see Heckman et al., 2009 for a detailed description of site characteristics), such that variation in soil physiochemical characteristics could be attributed to differences in parent material.

Three pedons were excavated to the saprolite-bedrock contact at each field site. Soil morphology was described in the field and soil samples collected by genetic horizon (Soil Survey Staff, 2004). Collected soil samples were air dried and sieved to <2 mm. All further analyses were performed on the <2 mm fraction of the soils. Parent material samples were collected either from the base of excavated pits or from exposed bedrock in

close proximity to sample locations. Parent material samples were ground and examined by X-ray diffraction and total elemental analysis.

## ***2.2 General soil characteristics***

Total organic C was determined by high temperature dry combustion with an elemental analyzer (Costech Analytical Technologies, Valencia, CA, USA) coupled to a continuous-flow mass spectrometer (Finnigan Delta PlusXL, San Jose, CA, USA) at the University of Arizona Stable Isotope Laboratory. Total carbon in the soils from the limestone site was measured both before and after acid fumigation (Harris et al, 2001) to quantify any contribution of carbonates to the total C content of these soils. Treated and untreated soils exhibited little to no variation in either C content or  $\delta^{13}\text{C}$ , therefore experimental results were assumed to be uninfluenced by detrital carbonates. Specific surface area was measured on bulk soils after organic matter removal using a Beckman Coulter SA 3100 Surface Area and Pore Size Analyzer (Fullerton, CA). Soils were degassed at 105°C overnight. Surface area was measured under  $\text{N}_2$  and modeled using the BET equation (Brunauer et al., 1938). Soil pH was measured in distilled water (1:1 weight to volume ratio). Exchangeable Al was determined from 1N KCl extracts, followed by colorimetric titration (Pansu & Gautheyou, 2006). Cation exchange capacity and was determined using the standard method of 1M  $\text{NH}_4\text{OAc}$  at pH 7.0 (CEC-7) (Soil Survey Staff, 2004).

Total elemental analysis was performed on the fine-earth fraction of each soil as well as the four parent materials. Soil was analyzed from each genetic horizon of all three

pits at each site. Total elemental composition was measured by Li-borate fusion with ICP-ES quantification at ACME Analytical Laboratories, Ltd. (Vancouver, British Columbia, Canada). Percent oxide weights were corrected for loss on ignition.

### ***2.3. Soil mineralogical characterization***

Prior to x-ray diffraction analysis, soils were pretreated with NaOCl adjusted to pH 9.5 to remove organics. After organic matter removal, sand, silt and clay size fractions were separated following Jackson (2005). Briefly, soils were dispersed using sodium hexametaphosphate, then sands were separated from silts and clays by sieving at 53  $\mu\text{m}$ . Clays and silts were suspended in dilute sodium carbonate and separated by centrifugation. Qualitative mineralogical analysis by x-ray diffraction was conducted on the clay (<2  $\mu\text{m}$ ), silt (2 - 53  $\mu\text{m}$ ), and very fine sand (53 – 100  $\mu\text{m}$ ) fractions for all genetic horizons at each site. Very fine sands and silts were analyzed as random powder mounts from 2-70 degrees two-theta. Clays were analyzed as oriented mounts on glass slides from 2-45 degrees two-theta with the standard treatments of K-saturation followed by heating to 350°C and 550°C, Mg-saturation, and Mg-saturation/glycerol solvation (Whittig and Allardice, 1986). X-ray diffraction analyses were conducted at the University of Arizona Center for Environmental Physics and Mineralogy using a PANalytical X'Pert PRO-MPD X-ray diffraction system (PANalytical, Almelo, AA, The Netherlands) producing Cu-K $\alpha$  radiation at an accelerating potential of 45 kV and current of 40 mA, fitted with a graphite monochromator and sealed Xenon detector.

Quantitative x-ray diffraction analysis of bulk soils were conducted after organic

matter removal, using the internal standard technique (Klug and Alexander, 1974; Brindley, 1980; Środoń et al., 2001). Zincite was used as the internal standard in all measurements. Samples were run as random powder mounts and measured from 5-65 degrees two-theta. After measurement, diffractograms were imported into RockJock (Eberl, 2003), a program for determining quantitative mineralogy from powder x-ray diffraction data. To improve the accuracy of RockJock's estimates of mineral composition, a set of mineral standards was collected and measured on the PANalytical X'Pert PRO-MPD X-ray diffraction system at the University of Arizona Center for Environmental Physics and Mineralogy. This set of mineral standards was incorporated into the RockJock program. Preparation of mineral standards and samples followed procedures outlined in the RockJock user's manual (Eberl, 2003). Measurement conditions for both samples and standards were as follows: 0.02° step size, 3 second dwell time per step, spinning at 1 revolution per second, 1° divergent anti-scatter slit, 10 mm divergent mask, 1° incident anti-scatter slit, 0.6mm fixed receiving slit.

Iron- and Al-oxyhydroxide and metal-humus content of bulk soil was measured using standard selective dissolution techniques using sodium dithionite, acid ammonium oxalate, and sodium pyrophosphate (Soil Survey Staff, 2004). Oxalate extracts Al ( $Al_o$ ), Fe ( $Fe_o$ ), and Si ( $Si_o$ ) from metal-humus complexes and short-range-order Fe oxyhydroxides and allophanic materials. Pyrophosphate extracts Al ( $Al_p$ ) and Fe ( $Fe_p$ ) from metal-humus complexes. Sodium dithionite extracts Fe ( $Fe_d$ ) from metal-humus complexes and crystalline and short-range-order Fe oxyhydroxides (Dahlgren, 1994).

Iron and aluminum concentrations of extracts were determined by ICP-MS (Perkin Elmer Elan DRC II, Waltham, MA).

#### **2.4. Elemental mass balance and chemical mass flux**

Time integrated elemental mass fluxes within the pedon and total mass loss from each pedon were calculated according to Brimhall et al. (1987) and Chadwick et al (1990). Following convention, we use the term *mass flux*, in units of  $\text{kg m}^{-2}$ , to refer to the loss or addition of mineral materials to/from a soil during pedogenesis. Though technically a flux term requires the use of a time unit (i.e.  $\text{kg m}^{-2}\text{yr}^{-1}$ ), the time unit is assumed in the case of mass flux during soil development. The *mass flux* term used in this study represents a time integrated mass flux, or the total mass loss/gain occurring over the entire time of pedogenesis. The fraction of element loss or gain in the soils, or mass transfer coefficient, was calculated in reference to parent material values using the immobile elements Zr and Ti as follows:

$$\tau_{j,w} = \left( \frac{C_{j,w} C_{Zr,p}}{C_{Zr,w} C_{j,p}} - 1 \right) \quad [\text{Eq 1}]$$

where  $\tau_{j,w}$  is the fraction of the mobile element  $j$  lost or gained from a particular soil horizon,  $C_{j,w}$  is the concentration of element  $j$  in the soil ( $w$ ) or parent material ( $p$ ),  $C_{Zr,p}$  is the concentration of the immobile element ( $Zr$  or  $Ti$ ) in the soil ( $w$ ) or parent material ( $p$ ). All concentrations are expressed on a weight percent basis. In this formulation only

parent material (rock) density is used and soil bulk density does not explicitly enter into the mass transfer coefficient calculations (Anderson et al., 2002; Porder et al., 2007). Because of the difficulty in accurately sampling bulk density of soils with high rock fragment content (Page-Dumroese et al., 1999), we believe the use of only rock density may produce more accurate results.

The time integrated mass flux for an individual horizon was calculated in reference to parent material density following Brimhall et al. (1992) and Chadwick et al (1990):

$$m_{j,flux} = \rho_{rock} [z_h (1 - \eta_h)] \cdot (\tau_{j,h} C_{j,p}) \quad [\text{Eq 2}]$$

where  $m_{j,flux}$  is mass loss per unit area ( $\text{kg m}^{-2}$ ) for the element  $j$ ,  $\rho_{rock}$  is the density of the parent material,  $z$  is the total depth of the soil profile,  $z_h$  is the thickness of horizon  $h$ ,  $\eta_h$  is the % rock fragment content of horizon  $h$  on a volumetric basis,  $m$  is the number of elements contributing to mass loss,  $\tau_j$  is the fraction of mass loss or gain of element  $j$  for the soil of horizon  $h$ , and  $C_{j,p}$  is the concentration of element  $j$  in the parent material. The total time integrated mass flux for each pedon ( $m_{j,flux,total}$ ) was calculated as the sum of mass loss or gain for each individual horizon in the pedon:

$$m_{j,flux,total} = \rho_{rock} \cdot \int_0^{z_{max}} \left[ (1 - \eta_h(z)) \cdot \sum_{j=1}^m \tau_j(z) \cdot C_{j,p} \right] \cdot dz \quad [\text{Eq 3}]$$

Mass balance calculations for the granite and rhyolite soils were performed using Zr as an immobile element, whereas Ti was used as the immobile reference element in the basalt and limestone soils due to differences in the relative abundance of the stable elements and the deposition of Zr in eolian materials (see section 2.5 below). The use of Zr for granite soils versus the use of Ti for basalt soils is further supported by the work of Neaman et al. (2006). In a study of element mobility following weathering of granite and basalt rock by exposure to organic ligands, Neaman et al. showed that when Zr is present in the form of zircons (as in granites) it exhibits lower mobility than Ti. Whereas when Zr is present in the form of Fe/Ti oxides (as in basalts), Ti is less mobile than Zr.

### ***2.5. Accounting for the influence of eolian dust and volcanic cinder deposits***

Basalt and limestone soils were strongly affected by the deposition of eolian materials, as evidenced by the presence of both primary and secondary minerals which were not present in the bedrock and could not have logically formed from bedrock primary minerals (e.g., quartz in basalt surface horizons, but not in the basalt bedrock). Evidence of eolian deposition was not found in the granite and rhyolite soils. The limestone and basalt sites were located near Flagstaff, AZ on the edge of the Colorado Plateau. Soils forming on the Colorado Plateau are known to have a long history of dust accumulation, so the presence of dust in these soils is not unusual. Dust sources on the Colorado Plateau have varied over time and have been both as local and as distant as the Mojave and Great Basin deserts (Reynolds et al., 2006, Goldstein et al., 2008).

Dust deposition can be a major limiting factor to the elemental mass balance approach outlined above because of varying mobile and immobile element concentrations in dust versus rock. The addition of substantial quantities of immobile elements to the soils in the form of dust can confound calculations of mass loss. However, geologic materials vary substantially both in concentrations of immobile elements and the ratio of Ti to Zr. This variation in immobile element ratios, along with variation in eolian dust mineral assemblage in comparison to bedrock mineral assemblage, provides an opportunity to quantitatively estimate dust contribution to soils. Previous studies have utilized dust traps (e.g. Ewing et al., 2006), magnetism (Reynolds et al., 2001, 2006) or isotopes of strontium (Capo et al., 1998) to estimate dust inputs to soils. Other techniques include estimating eolian contributions solely on differences in mineral assemblage or stable isotope concentration among bedrock and dust (e.g. Porder et al., 2007; Stiles and Stensvold, 2008). We use both the contrasting mineral assemblages and immobile element ratios between bedrock and dust to estimate dust contribution to the basalt and limestone soils.

Mineral phases in the basalt soils which could not be derived from the basalt parent material were classified as eolian materials. Eolian materials identified in the basalt soils included quartz, mica and illite, though abundance of mica and illite were low. Though the presence of feldspars in the eolian material is likely, and Al enrichment values in the soils support the addition of eolian feldspars (see section 3.3.3 below) the eolian feldspars could not be differentiated from feldspars derived from the basalt

bedrock. Using the data available, apparent mineralogical composition of the eolian dust included quartz, feldspar and mica/illite; a mineral assemblage common to granites.

The addition of eolian materials necessarily alters the elemental composition, including the concentration of the stable elements Ti and Zr. However, analysis indicated that if the majority of the eolian material was composed of quartz, then Ti could still be used to calculate mass fluxes from the soils in reference to the basalt bedrock. Specifically, the quartz structure does not allow substitution of either Ti or Zr, however zircon is often found in association with quartz in both igneous rocks and sedimentary rocks (Milnes & Fitzpatrick, 1989). The Zr:Ti of the basalt soils varied widely with depth, indicating addition of one of the elements. SiO<sub>2</sub> and Zr content were strongly and positively correlated in basalt soils ( $R^2 = 0.81$ ,  $P < 0.0001$ ), whereas SiO<sub>2</sub> and Ti were not ( $R^2 = 0.14$ ,  $P = 0.08$ ), indicating that Ti concentrations were likely unaffected by eolian additions. Therefore Ti was used as the immobile element in mass balance calculations for the basalt soils.

Soils derived from limestone exhibited substantial addition of mafic materials, in the form of volcanic cinders sourced from nearby cinder cones in the San Francisco volcanic field. The San Francisco volcanic field has been active for approximately ~3 million years, with the last eruption occurring ~1,000 years ago. Many cinder cones are found in the San Francisco volcanic field, with two located very close to the Limestone sample site: Elden Mountain and TV Hill. Qualitative XRD of the various particle size fractions indicated that cinders were found mostly in the fine to very coarse sand size fraction (100 - 2000 $\mu$ m) (Soil Survey Staff, 2004). Cinders were basaltic and contained

~5% magnetite (as determined by quantitative XRD) which allowed the grains to be removed from the sand fraction with a strong magnet. Cinders were collected from both A and Bt horizons of each pedon, rinsed and homogenized. Cinder grains removed from the sand fraction were angular with sharp corners, indicating that they were relatively unweathered. The cinders were examined through quantitative XRD and total elemental analysis. The limestone bedrock and basaltic cinders had strongly contrasting Ti:Zr ratios (12.5 and 112.7, respectively), allowing the use of a simple mixing model to determine the relative contribution of each parent material to the soils based on the Ti:Zr ratio of the soil in each pedon as follows:

$$f_{Cinders} = \left( \frac{\left( \frac{Ti}{Zr} \right)_{soil} - \left( \frac{Ti}{Zr} \right)_{bedrock}}{\left( \frac{Ti}{Zr} \right)_{bedrock} - \left( \frac{Ti}{Zr} \right)_{cinder}} \right) \times 100 \quad [\text{Eq 4}]$$

Where  $\left( \frac{Ti}{Zr} \right)$  is the ratio of titanium to zirconium content (in ppm) in either the *soil*, *bedrock*, or *cinders*, and  $f_{Cinders}$  is the percent by weight of the soil in a particular horizon derived from the basaltic cinder material deposited during the formation of nearby cinder cones. Calculations of  $\tau$  and  $m_{j,flux}$  for the limestone soils take into account the contributions of both parent materials, and estimates of mass flux were calculated in reference to the combined elemental and mineral values of the parent materials. Specifically, the percent contribution of each parent material (limestone bedrock and basaltic cinders) was calculated for each pedon sampled above the limestone bedrock using Equation 4. The parent material element compositions used as reference values for

$\tau$  and  $m_{j,flux}$  calculations for soils were calculated as a combination of both the bedrock and the cinders. For example, to calculate the Si content of the combined parent material for a pedon developed from limestone and cinder materials, the Si content of both the limestone and cinders would be taken into account:

$$[Si]_{PM} = (f_{LS} \times [Si]_{LS}) + (f_{Cinder} \times [Si]_{Cinder}) \quad [\text{Eq 5}]$$

Here,  $[Si]_{PM}$  is the Si concentration used as a reference to calculated relative gains or losses in Si concentration in soils in comparison to the mixed parent material;  $f_{LS}$  and  $f_{Cinder}$  are the fractions of soil derived from the limestone bedrock and cinders, respectively, where  $f_{LS} = 1 - f_{Cinder}$ ; and  $[Si]_{LS}$  and  $[Si]_{Cinder}$  are the concentrations of Si (or any element of interest) in the unweathered limestone bedrock and cinders, respectively.

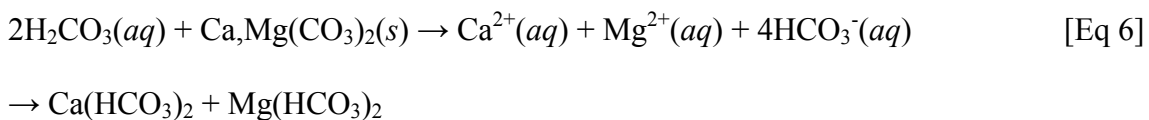
Given the proximity of the limestone and basalt sites, it is likely that the limestone and basalt soils share a common dust source. The similarity of the silt fractions (Figure 6b and 8b), and the presence of illite in both soils also may be indications of a common dust source. However, since the limestone parent material contained quartz and the mafic cinder material contained feldspars, eolian contributions are difficult to quantify.

Mineralogical examination of dust in the basalt soils indicated that the dust was likely granitic in character. Since granites and limestones have similar Ti/Zr ratios, contributions of eolian dust and limestone bedrock could not be separated in the soils from the limestone site. However, given the high similarity of Ti/Zr ratios of limestones and granites (i.e., 12.5 for the limestone at the site and an average of 12.3 for granites

(Milnes & Fitzpatrick, 1989)), the addition of eolian materials would not significantly affect calculations of cinder contributions to soils at the limestone site (Eq 4). Using the methods outlined above allows for estimation of mass fluxes during pedogenesis on soils significantly affected by eolian depositions. In both limestone and basalt soils, eolian additions are manifest as positive mass fluxes.

### ***2.6 Estimation of CO<sub>2</sub> consumption by mineral weathering***

Calculations of CO<sub>2</sub> consumption during soil development were made with the underlying assumption that base cations (Na, K, Ca, Mg) lost during soil development were charge balanced by dissolved bicarbonate in soil solution (e.g., Chadwick et al., 1994). One mole of base cation charge was assumed to consume one mole of bicarbonate, with the exception of the limestone soils since weathering of carbonates both releases and consumes CO<sub>2</sub>. Calculations for C consumption during weathering of the limestone bedrock assumed one mole of C was consumed for every 2 moles of cation charge, due to the fact that when Ca and Mg carbonates weather they release one mole of C upon dissolution and consume two when recombining with bicarbonate in the soil solution:



These calculations likely overestimate CO<sub>2</sub> consumption since base cations may form bonds with other anions in solution such as Cl<sup>-</sup> and SO<sub>4</sub><sup>-2</sup>, but provide a quantitative

proxy for cross-site comparison of the potential lithologic constraint on CO<sub>2</sub> consumption by mineral weathering

### **3. Results & discussion**

#### ***3.1 General soil characterization***

##### ***3.1.1 Clay content and CEC***

General morphological, physical and chemical properties varied substantially among parent materials (Table 1). Taxonomic classifications were assigned according to Keys to Soil Taxonomy (Soil Survey Staff, 2006) (Table 2). The soils sampled on limestone were shallow (~35 cm) and rocky (rock fragment content ~10-70% by volume), but exhibited presence of clay films and clay accumulation in the subsurface and hence classified as Lithic Argiustolls. The basalt soils presented well developed argillic horizons with clay contents on the order of 50% at the soil/saprolite boundary; these soils classified as Typic Paleustolls. The basalt soils were moderately deep (~60 cm), though with a high rock fragment content (~20-50%). Granite soils were shallow (~37 cm), rocky (rock fragment content ~5-50%), and classified as Typic Ustorthents due to lack of subsurface diagnostic horizon development. Rhyolite soils were classified as Typic Haplustepts. Rhyolite soils were deep (~1 m), but exhibited little evidence of clay translocation with cambic subsurface diagnostic horizons.

Clay content and CEC values varied across parent materials, both following a trend of Basalt>Limestone>Rhyolite>Granite. Clay content was the greatest in the subsurface of the basalt soils, reaching up to 50%, and lowest in the granite soils which

contained around 6% clay throughout the profiles. CEC followed variation in clay and organic matter content, with maximum values of  $32 \text{ cmol}_+ \text{ kg}^{-1}$  in the subsurface of the basalt soils and minimum values of  $7 \text{ cmol}_+ \text{ kg}^{-1}$  in the subsurface of the granite soils. Soils also varied in pH: granite and rhyolite soils were relatively acidic, whereas the basalt and limestone were relatively basic. The acidic soils had measurable levels of exchangeable Al.

### ***3.1.2 Selective dissolution***

Crystalline and short-range order Fe-oxhydroxides, as well as metal-humus complex content, varied across the lithosequence (Table 1) following variation in parent material elemental composition (Table 3). The limestone soils contained only small amounts of crystalline Fe oxyhydroxides, while short-range order Fe oxyhydroxide content of the limestone soil was approximately equal to that of the basalt soil. Though the limestone parent material did contain a small amount of Fe, weathering of the cinder material was the likely source of the majority of the Fe-oxhydroxides. In granite and rhyolite soils, Fe oxides were dominated by crystalline phases (goethite and hematite) with only small amounts of ferrihydrite, as evidenced by very low  $\text{Fe}_o:\text{Fe}_d$  in these soils. Basalt soils were rich in both crystalline and short range order Fe oxyhydroxides, in keeping with the mafic nature of the parent material. Basalt soils were still dominated by crystalline phases, whereas the limestone soils were dominated by ferrihydrite. The higher abundance of ferrihydrite in the limestone soils may be a consequence of differences in silica concentrations or degree of Ostwald ripening. Limestone soils

contained more silica than basalt soils and goethite/hematite formation is known to decrease significantly as Si concentrations in soil solution increase (Schwertmann et al., 1984). Ferrihydrite is also considered a “young” Fe oxide, since ferrihydrite is usually transformed into more crystalline goethite and hematite forms over time, a process sometimes referred to as Ostwald ripening (Cornell and Schwertmann, 2003). Some deposition of mafic cinder materials (no doubt the source of the majority of Fe oxides in the limestone soils) may have been rather recent (i.e., ~1,000 yr ago), such that Fe-oxide development may be in its nascent phases.

Abundance of Fe-humus complexes was approximately equal in the limestone, basalt and granite soils, even though Fe content of the basalt and cinder material (mafic cinder material found in the soils over limestone bedrock) was high. Al-humus complexes were not abundant in the basalt and limestone soils. Formation of Al-humus complexes may not have been favored by the circum neutral pH of these soils. Consistent with their more felsic nature, granite and rhyolite soils had low crystalline and short range order Fe oxyhydroxide contents. However, lower pH of these soils appeared to favor formation of metal-humus complexes, due to the higher solubility of Al at pH values less than 5.5 (Lindsay, 1979).

### ***3.1.3 Specific surface area***

Differences in primary mineral characteristics and their weathering patterns, specifically production of clays and oxyhydroxides also manifested as differences in specific surface area among soils. Basalt soils had the highest specific surface area of the

four soils examined (23-65 m<sup>2</sup> g<sup>-1</sup>), corresponding to its high clay and Fe-oxide content. Limestone and rhyolite soils had lower specific surface areas (~10-15 m<sup>2</sup> g<sup>-1</sup>), and granite soils had the lowest specific surface area (4-5 m<sup>2</sup> g<sup>-1</sup>). In all soils, variation in specific surface area followed variation in clay and Fe oxyhydroxide content (Table 1).

### ***3.1.4 Organic C content***

Organic C contents were significantly different among soils. Organic C contents were highest in rhyolite soils followed by basalt, granite and limestone soils. Detailed investigation of organic C cycling in these soils revealed a significant dependence of organic C on soil mineral assemblage, affecting both C content and microbial community composition and activity (Heckman et al. 2009). Metal-humus complex and Fe-oxyhydroxide content emerged as important controllers of organic C dynamics across all sites. Moreover, soil pH was significantly correlated with exchangeable Al<sup>3+</sup>, metal-humus complex content, bacterial community composition, and microbial biomass C/N ratios. Specifically, the data suggested that both sorption to mineral surfaces, formation of metal-humus complexes and chemical recalcitrance all played a role in organic C preservation in these soils, but that the relative importance of these preservation mechanisms varied according to soil mineral assemblage and soil pH. Results demonstrated that within a specific ecosystem, organic C dynamics and microbial community may be attributed to variation in parent material and soil mineral assemblage as discussed in detail below.

## **3.2 Mineralogical characterization**

### **3.2.1 Rhyolite**

Rhyolite parent material was fine-grained and had a relatively low bulk density ( $1506 \text{ kg m}^{-3}$ ). The rhyolite was composed of alkali feldspar (59%), cristobalite (26%), quartz (10%) biotite (5%), and trace amounts of zeolite. Though amorphous glass is often found in rhyolitic ash deposits, extraction of soils and parent material with acid ammonium oxalate and oxalic acid revealed no amorphous silica. The presence of cristobalite most likely indicates geothermal alteration of the original ash deposit (Henderson et al., 1972; Drees et al., 1989; Harvey, 1997). Though cristobalite may also precipitate as a secondary mineral during intense weathering and podsolization (Swindale, 1960), the presence of cristobalite in the parent material is more suggestive of hydrothermal alteration of the original ash deposit. Soil profiles were a meter deep, most likely due to the relatively low density and fine-grained texture of the parent mater. However, only slight mineralogical differences were observed among horizons. Changes in mineral composition with depth in the profile were mostly in the form of feldspar and cristobalite weathering, with losses greatest in the Bw1 and BCr horizons (Figure 1). Feldspar and cristobalite losses were accompanied by gains in kaolinite.

Quartz was the most abundant mineral in both sand and silt fractions. Biotite was more abundant in the sand fraction than in the silt fraction (Figure 2a,b). Clay contents were approximately 10% throughout the profile, varying little with depth (Figure 1). Some weathering of biotite to vermiculite was indicated by qualitative XRD of oriented clay mounts, however quantitative XRD indicated that vermiculite concentrations were

very low (estimated <3% of total soil weight). Quantitative XRD analysis indicated that kaolinite was the dominant secondary mineral formed in these soils.

Small amounts of a zeolite mineral (1-3% of soil by mass) were also noted and tentatively identified as clinoptilolite. The most prominent XRD peak of the zeolite is at 9Å and can be seen in both the silt and clay fractions and is barely visible in the sand fraction (Figure 2). Zeolite abundance is greatest in the surface horizons and slightly decreases with depth. The presence of zeolites in the BCr and Cr horizons of the rhyolite soils suggests the zeolites are inherited from the parent material rather than formed during pedogenesis. Increasing concentration from the Cr to A1 horizon may indicate selective preservation of the zeolites during soil development. Zeolites are commonly formed from acidic rocks through geothermal alteration or exposure to basic lake waters or rain, and zeolite formation is common in ash falls and pyroclastic deposits (Dixon & Weed 1989; Larsen and Crossey, 1996; Chipera et al., 2008). Formation of zeolites during exposure to meteoric waters requires supersaturation of Si in solution, conditions also associated with formation of the cristobalite found in the parent material. Precipitation of clinoptilolite, as opposed to other zeolite phases, is favored by low Na/K ratios in the parent material (Hawkins et al., 1978). Na/K ratios were indeed low in the rhyolitic ash (0.18), supporting the identification of the zeolite phase as clinoptilolite.

### **3.2.2 Granite**

Granite bedrock was coarse-grained and composed of quartz (33%), alkali feldspar (58%), and muscovite (9%). Soils were sandy and showed little weathering of

primary minerals or clay translocation which is typical for young soils developed from granite (Wilson, 2006). Mineral content of the soils mirrored the parent material composition for the most part with little variation in quartz and mica abundance throughout the profile (Figure 3). Mineralogy of the sand fraction was nearly identical to the parent material (Figure 4a), while the silt fraction exhibited some loss of feldspars relative to quartz content (Figure 4b).

Clay content averaged 5-6% throughout the granite profiles and varied little with depth. The clay fraction was composed of kaolinite, hydroxy-interlayered vermiculite, and muscovite in approximately equal parts (Figure 4c). Kaolinite and vermiculite are the most commonly encountered secondary phyllosilicates in granitic soils; kaolinites are derived from the weathering of feldspars, and vermiculites from the weathering of micas (Wilson, 2006). Interlayering of vermiculites with hydrous Al is common during weathering of muscovite, forming quickly under favorable pH conditions (Barnhisel and Bertsch, 1989; Dahlgren et al., 1997). Such hydroxy-interlayered phases are often considered an intermediate weathering product between muscovite and smectite in acidic forest soils (Douglas, 1989). Substantial amounts of gibbsite are often found in granitic soils, but gibbsite was not apparent in these soils. Interlayering of vermiculites with hydrous Al may remove enough Al from the soil solution such that precipitation of gibbsite is not favored, the so-called “anti-gibbsite effect” (Jackson, 1963a, 1963b).

### **3.2.3 Basalt**

Basalt bedrock was composed of alkali feldspar (anorthoclase) (50%), plagioclase (labradorite) (22%), augite (18%), olivine (5%), and magnetite (4%). The mineral assemblage of the soils reflected the relative weatherability of the parent material components. Soils exhibited an almost complete loss of labradorite, augite, and olivine throughout the profile. Losses of anorthoclase and magnetite were substantially lower, and varied with depth in the profile. Weathering of magnetite and anorthoclase increased with depth, and were greatest at the soil-saprolite boundary (Figure 5).

Of particular interest was the substantial portion of the fine earth fraction composed of quartz (~25%). Though basaltic rocks may contain quartz as an accessory mineral, if substantial amounts are found in basaltic soils they are usually of eolian origin (Wilson, 2006). Since bedrock at this site contained no quartz, the origin of the quartz in the soils is assumed to be eolian. The quartz was distributed among all size fractions, and was the dominant mineral in both the silt and very fine sand fractions (Figure 6a,b). Quartz content varied with depth, possibly indicating changing rates of eolian deposition over time. Eolian dust deposited in basalt soils likely contained substantial quantities of feldspars (see section 2.5 above), though quantities are impossible to estimate since eolian feldspars could not be differentiated from bedrock-derived feldspars. Thus, the trend of increasing alkali feldspar content going upwards in the profile is probably a combination of both selective preservation of the more resistant alkali feldspars and addition of alkali feldspars in the form of eolian dust.

Clay content in the basalt soils ranged from 20% in surface horizons to 50% at the soil-saprolite boundary. Clay types included kaolinite, smectite, vermiculite, and illite,

with kaolinite and smectite as the dominant phases (Figure 6c). Consistent with previous studies of basalt weathering in semiarid environments (Righi et al, 1999; Vingiani et al, 2004), relative abundance of kaolinite was greater in surface horizons, while smectite abundance was greatest in subsurface horizons. Neither hydrated nor dehydrated halloysite phases were identified. The lack of hydrated kaolin phases is likely a result of the generally hot and dry climate conditions and ustic soil moisture regime. Soils in ustic soil moisture regimes receive the majority of their precipitation in the summer when evapotranspiration demand is high, leading to low effective precipitation levels. Also, winter precipitation is mainly in the form of snow, much of which is lost to sublimation and surface runoff (Soil Survey Staff, 2006). This climate is thus characterized by brief periods of soil wetting in between extended periods of dry conditions. This cyclic wetting and drying drives secondary phyllosilicates to more crystalline forms, favoring the formation of kaolinite over halloysite (Allen and Hajek, 1989).

Vermiculite and illite were both present in small amounts in subsurface horizons, but only illite was found in surface horizons. Illites, or clay micas, are mostly inherited from parent material or formed through the weathering of coarser mica particles (Allen and Hajek, 1989). Though it has been suggested that illite may also form authigenically (Harder, 1974; Norrish and Pickering, 1983), or through the conversion of smectite to a 1 nm mineral in arid environments (Mahjoory, 1975). However, that is not likely the case in these soils. Soil temperature and moisture regimes at this site do not match conditions required for pedogenic formation of illites. Therefore, the presence of illite and vermiculite most likely indicates deposition of eolian micas. Though the presence of

micaceous phases in the silt and very fine sand fractions is barely discernable (Figure 6 a,b), the large enrichment of K in the soils supports the presence of micaceous phases (see section 3.3.3 below). The vermiculite phases were probably formed by alteration of the illites through stripping of interlayer K, a very common weathering pathway (Douglas, 1989).

### **3.2.4 Limestone**

The limestone bedrock was composed mostly of dolomite (95%) with smaller amounts of quartz (4%) and kaolinite (~1%). Development of the limestone soils was also affected by deposition of volcanic ash/cinders at the soil surface, and the addition of eolian material (Figure 7). Cinder material contributed from 20-60% of the material in the soils, with contributions varying both among pedons and with depth. The cinder material was basaltic in nature and was composed of plagioclase and alkali feldspar (72%), pyroxene (13%), olivine (10%) and magnetite (5%).

Soil mineral composition differed significantly from the underlying bedrock, both due to addition of allochthonous materials (see section 2.5 above) and selective preservation of quartz from the bedrock. Though the bedrock was composed mostly of dolomite, soils were dominated by quartz (~70% by weight). Dolomite is highly weatherable and undergoes dissolution upon exposure to soil solution leaching through the profile (Mackenzie & Lerman, 2006), leaving soils enriched in quartz silts and sands. The coarse sand fraction of the soils was composed mostly of basaltic cinders deposited from nearby cinder cones. Consequently, soils were composed of approximately 10% plagioclase feldspar, with small amounts of olivine, pyroxene, and magnetite. The fine

sand and silt fraction were dominated by quartz with small amounts of feldspar (Figure 8a,b). Feldspars were likely sourced both from weathering of the cinder material and eolian deposition, and quartz grains were both inherited from the underlying bedrock and deposited as eolian dust.

The addition of relatively weatherable mafic minerals from the basaltic cinders led to the formation of soils with higher clay content than would be expected otherwise. Clays included kaolinite, illite and hydroxy-interlayered vermiculite (Figure 8c). The clay fraction was dominated by kaolinite, both inherited from the limestone parent material and produced in situ through the weathering of plagioclase feldspars. Illites, likely derived from deposition of eolian micas, and hydroxy-interlayered vermiculite derived from weathering of illites were also present in the clay fraction.

### ***3.3 Total elemental analysis and chemical mass flux***

#### **3.3.1 Rhyolite soils**

Rhyolite parent material was felsic and fine-grained (Table 3). Whole pedon mass losses averaged  $-576 \text{ kg m}^{-2}$ , the largest mass flux of the four soils examined (Table 5). Elemental fluxes demonstrated little variation with depth, with the exception of Ca and Mg which were enriched by 65-85% and 12-14%, respectively, in surface horizons (Figure 1). Enrichment of base cations, especially Ca, in surface horizons is common in forest soils which experience periodic burnings (Wells, 1971; Wells et al., 1979; Waldrop et al. 1987). The majority of mass loss from the rhyolite soils was in the form of Si (-214

kg m<sup>-2</sup>), Al (-34 kg m<sup>-2</sup>) and K (-44 kg m<sup>-2</sup>), from the weathering of alkali feldspars, quartz, cristobalite and biotite (Table 4).

### 3.3.2 Granite soils

Elemental composition of the granite bedrock was nearly identical to that of the rhyolite parent material, with only slightly less K<sub>2</sub>O (Table 3). Elemental losses were less in the granite than in the other soils, with  $\tau$  values averaging ~0.3-0.4 (Figure 3).

Weathering and mass loss varied little with depth, with the exception of Ca concentrations, which was enriched by 30-60% in comparison to the parent material. Ca enrichments were greatest in the A1 horizon, and similar to the rhyolite soils were probably the product of burning. Whole pedon mass losses averaged -202 kg m<sup>-2</sup>, less than half the mass loss from the rhyolite soils. Similar to the rhyolite soils, the majority of the mass loss was in the form of Si (-73.2 kg m<sup>-2</sup>), Al (-13.9 kg m<sup>-2</sup>) and K (-9.6 kg m<sup>-2</sup>) due to feldspar, quartz and muscovite weathering.

Despite similarities in elemental and mineralogical composition, elemental fluxes were substantially less than the rhyolite soils. These differences likely manifest as a result of variation in parent material density and mineral grain size. As particle size decreases and specific surface area increases, solubility product generally increases such that smaller mineral grains may have dissolution rates several orders of magnitude greater than larger mineral grains (Holdren and Berner, 1979; White and Brantley, 1995; Lüttge, 2005). The granitic parent material had a density of 2364 kg m<sup>-3</sup>, and mineral grains in the parent material were distinct and measured up to several mm across. The rhyolitic

parent material was lower in density at  $1506 \text{ kg m}^{-3}$  and finer-grained than the granite. In the rhyolitic parent material individual grains were not distinguishable with the naked eye. Since the granite and rhyolite were of nearly identical elemental composition, differences in density may reflect differences in parent material porosity. The combined factors of lower density, greater porosity, and finer mineral grain size all contributed to greater mass loss in the rhyolite relative to the granite soils.

### 3.3.3 Basalt soils

The basalt bedrock elemental composition was typical of alkaline basalts (Table 3). Basalt soils had a large eolian component which included quartz, weathered mica/illite and most likely feldspar as well. Elemental fluxes for the basalt soils were calculated in reference to the underlying bedrock only, so that elemental additions due to eolian deposition are shown as mass additions (Table 4). The eolian quartz additions are shown in the % mineral plot (Figure 5) and are also reflected as large Si enrichments throughout the profile (25-50%), (Figure 5). Eolian additions had a large effect on estimates of mass flux. Total mass losses from basalt soils were small with a large variance,  $+36(\pm 95) \text{ kg m}^{-2}$ , due to the fact that mass addition through deposition of eolian dust was equal to or greater than mass loss through weathering of bedrock.

The majority of the mass loss from dissolution of the basalt bedrock was in the form of Fe ( $-11 \text{ kg m}^{-2}$ ), Mg ( $-48 \text{ kg m}^{-2}$ ), Ca ( $-68 \text{ kg m}^{-2}$ ) and Na ( $-16 \text{ kg m}^{-2}$ ), sourced mainly from the weathering of labradorite, augite, and olivine (Gíslason et al., 1994; Dessert et al., 2003). Si losses due to feldspar weathering were much less than Si additions due to

eolian quartz deposition. Losses of Al and Fe were highest in surface horizons and decreased with depth. Enrichment of Al at depth may be partially attributed to relocation of secondary phyllosilicates from overlying horizons; clay content was highest at depth. However, the positive overall Al flux may ( $+8 \pm 14 \text{ kg m}^{-2}$ ) suggest the addition of eolian feldspars. Losses of Ca, Mg, and Na were high (60-90%, or  $\sim 132 \text{ kg m}^{-2}$  in total) throughout the profile, while K was enriched by 100% or more ( $\sim +8 \text{ kg m}^{-2}$ ) due to the deposition of eolian micas (Figure 5) and possibly eolian alkali feldspars. Even though muscovite and illite account for a small percentage of soil weight (averaging 5%),  $\tau$  values of K were high due to the very low K content of the basalt parent material such that even a small elemental addition yields a large relative increase in the mass transfer coefficient.

### **3.3.4 Limestone soils**

Limestone soils were developed from three contrasting parent material sources: the underlying limestone bedrock, mafic cinders deposited during the eruption of local cinder cones, and eolian dust. Cinder material comprised 20-60% of the fine earth fraction by weight (depth-weighted average of 43%). Elemental fluxes were calculated in reference to a mixed parent material – both the mafic cinders and limestone bedrock. Eolian contributions could not be quantitatively estimated (see section 2.5 above) and eolian dust additions therefore manifest as mass additions in calculated mass fluxes from the limestone soils (Tables 4 & 5), consistent with calculations of eolian additions to basalt soils. Additions of eolian dust had a large impact on calculations of elemental

fluxes and total mass loss. As in the basalt soils, mass additions from eolian dust matched or exceeded mass losses through weathering of bedrock and cinder material, leading to an overall small total mass flux with high variance among pedons ( $-3 \pm 24 \text{ kg m}^{-2}$ ).

Limestone bedrock was composed mostly of CaO (55%), MgO (36%), and SiO<sub>2</sub> (7%). Concentrations of Al, Fe, Na, and K were all <1% by weight after accounting for a significant weight loss on ignition (45%). Cinder material was basaltic in nature (Table 3). Due to the fact that both materials contributed substantially to the formation of the soil, soil elemental fluxes were calculated in comparison to a mixture of both parent materials, in proportion to their contribution to the soil. In comparison to the mixed parent material (limestone bedrock and basaltic cinders), soils were significantly depleted in Mg ( $-52 \text{ kg m}^{-2}$ ) and Ca ( $-92 \text{ kg m}^{-2}$ ) (Figure 7, Table 4). The majority of Ca and Mg loss can be attributed to dissolution of dolomite from the limestone bedrock. However, some mass was also likely lost through weathering of the cinder material: Fe ( $-2 \text{ kg m}^{-2}$ ) and Na ( $-2 \text{ kg m}^{-2}$ ) and from weathering of olivine, augite and feldspar. Si, Al and K all showed substantial enrichment in the limestone soils. Si was highly enriched ( $+97 \text{ kg m}^{-2}$ ), with  $\tau$  values ranging from 1.7 to 2.4. The large enrichment of Si was due both through selective preservation of quartz during weathering of the limestone bedrock and deposition of eolian quartz and feldspar. Al enrichment was substantially smaller than Si enrichment, averaging only  $+7 \text{ kg m}^{-2}$  with  $\tau$  values averaging 0.3, and likely primarily due to deposition of eolian feldspars. As in the basalt soils,  $\tau$  values for K were extremely high (2.4-2.8) even though actual mass additions of K were relatively low ( $+4 \text{ kg m}^{-2}$ ).

The K is most likely sourced from the addition of eolian mica/illite and as in the basalt soils,  $\tau$  values for K were very high due to the very low K content of the parent material.

All four sites experience periodic burning which results in enrichment of base cations at the soil surface. Enrichment of Ca, and Mg to some degree, is very obvious in the felsic rhyolite and granite soils. However,  $\tau$  plots of the more basic basalt and limestone soils do not manifest similar surface horizon enrichment (Figures 5 & 7) despite clear evidence in the field that these sites have burned in the recent past. Absolute Ca and Mg concentrations were highest in surface horizons in both basalt and limestone soils. However, because  $\tau$  values are calculated in reference to the abundance of a particular element in the parent material, base cation enrichment in surface horizons was not obvious in the limestone and basalt soils due to the overall high base cation losses, i.e., enrichment of Ca & Mg due to fire were minor in comparison to the large depletion of these elements during weathering and soil formation.

### ***3.4 Inorganic C consumption and organic C stocks***

Inorganic C consumption during pedogenesis varied significantly among parent materials based on the assumption that all cation loss was charge balanced by bicarbonate (Table 5). Weathering of basalt consumed the most CO<sub>2</sub> (83 kg m<sup>-2</sup>), followed by weathering of limestone (51 kg m<sup>-2</sup>), rhyolite (26 kg m<sup>-2</sup>) and granite (6 kg m<sup>-2</sup>).

Elemental composition of parent material plays the central role in determining the flux of CO<sub>2</sub> consumed during weathering. Though carbonate-based parent materials such as limestones and dolostones are easily weathered, congruent dissolution of these

materials both consumes and releases CO<sub>2</sub>, and over geologic time scales, weathering of carbonates is C neutral (reference). It is only the weathering of silicates that has the potential to affect global atmospheric CO<sub>2</sub> concentrations. Furthermore, it is only the base cations released through silicate weathering which combine with bicarbonates in the soil solution and consume CO<sub>2</sub>.

Though total mass loss from the rhyolite soils was high (-576 kg m<sup>-2</sup>), the total amount of CO<sub>2</sub> consumed during weathering was modest relative to the other parent materials. After accounting for mass additions to basalt soils in the form of eolian quartz and mica/illite, total mass loss from basalt bedrock weathering during pedogenesis was around -356 kg m<sup>-2</sup> (this is likely an underestimation of mass loss since the mass of eolian feldspars added to the soil is not known. However, it is most probable that the mass of bedrock lost during formation of the basalt soils was less than that of the rhyolite soils), yet the total amount of CO<sub>2</sub> consumed during weathering was four times that of the rhyolite. This can be explained by examining the elemental composition of the parent materials (Table 3). Base cation content of the basalt parent material is over twice that of the rhyolite parent material when compared on a weight basis, and nearly four times when compared on the basis of moles of charge. Granitic soils had both low mass losses during formation and low base cation content leading to low CO<sub>2</sub> consumption values (6 kg m<sup>-2</sup>). Though over geologic time scales, weathering of limestone is a C neutral process, in the shorter term (decadal to century) ½ mole of CO<sub>2</sub> is consumed per mole of base cation charge released during dissolution of the limestone rock (see Eq. 6 above).

The high Mg and Ca content of the dolomite in the limestone bedrock yielded moderate CO<sub>2</sub> consumption values (51 kg m<sup>-2</sup>).

#### 4. Summary

The soils examined varied widely in their morphological and physiochemical characteristics, illustrating the strong influence of parent material on soil properties. Granitic soils were shallow with little morphological development. In contrast, rhyolite soils were moderately deep with a large flux of weathering and some morphological development. Though the rhyolite and granite parent materials were nearly identical in elemental and mineralogical composition, the rhyolite was fine-grained and less dense than the granite. Consequently the resulting soils were vastly different. In comparison to these felsic materials, the mafic nature of the basalt and limestone/cinder parent materials resulted in more clay-rich soils, with argillic horizons and an abundance of Fe-oxyhydroxides. These large differences in mass fluxes, secondary mineral production and degree of weathering have important consequences, not only for the morphology of the soils but also for the role they play in the global C cycle.

These soils illustrate how the pedogenic processes which lead to soil development and consumption of atmospheric CO<sub>2</sub> are also responsible for the development of soil properties important for the stabilization/sequestration of organic C. Weathering of bedrock minerals controls the long term consumption of atmospheric C (Berner *et al.* 1983). Specific bedrock type not only determines the rate of atmospheric C consumption as it weathers, but at the same time produces unique weathering products that have a

range of abilities to promote organic C stabilization in the soil over shorter decadal time scales. In turn, incorporation of organic matter into the soil exposes mineral surfaces to organic acids which promote mineral dissolution (Welch & Ullman 1993, Hausrath *et al.* 2009).

The felsic and coarse-grained granite bedrock experienced the smallest mass flux during pedogenesis and therefore the least production of secondary minerals. Being cation-poor, its small mass flux was associated with very little consumption of CO<sub>2</sub> during weathering. The lack of secondary mineral production and shallow depth also resulted in a low organic C content. Though the rhyolite parent material was more easily weathered than the granite, most of the mass loss was in the form of silica and aluminum, leading to low carbonate consumption during weathering. However, the larger degree of weathering did lead to the production of acidity, the liberation of Fe and Al cations, and the production of clays. Fe and Al form can form insoluble complexes with organics in solution (Nierop *et al.* 2002, Scheel *et al.* 2007), organics can sorb onto clay surfaces (Schimel *et al.* 1994, Percival *et al.* 2000), and acidity can reduce soil respiration rates (Anderson & Domsch 1993). All these factors combine to reduce the bioavailability of C and increase organic C stocks in soils.

Weathering of basalt has been recognized as an important consumer of inorganic C during mineral weathering (Dessert *et al.*, 2003; Gaillardet *et al.*, 1999). Even though the basalt parent material is not as easily weathered as the rhyolite material, its high base cation content leads to much higher IC fluxes during soil development. The mafic nature of basalt leads to an abundance of base cations and Si in solution which favors the

production of phyllosilicate clays as well as crystalline and short-range order Fe-oxyhydroxides. The high specific surface area produced during pedogenesis of the basalt soils favors sorption and preservation of organic C on mineral surfaces. The limestone bedrock is easily weatherable and rich in base cations, however the bedrock undergoes almost complete dissolution when weathering, leaving soils composed mostly of quartz sands. The basic pH of the soil does not encourage organo-metal complex formation, nor does it negatively affect soil respiration rates. Quartz sands are fairly unreactive surfaces and are effective for sorbing organic C. Consequently, though the bedrock is easily weathered, the parent material mineral assemblage does not allow for the formation of secondary mineral phases useful for the preservation of organic C. The impact of limestone weathering on inorganic C consumption is equally dubious. Over geologic time scales, the net CO<sub>2</sub> consumption due to limestone weathering is zero. Over shorter time scales, the production of bicarbonate salts from the dissolution of carbonates does result in some consumption of inorganic C. However, only half as much CO<sub>2</sub> is consumed from the weathering of limestones as is consumed from the weathering of silicates.

Overall, the data taken from this lithosequence illustrates the importance of lithology in determining rates of regolith mass flux, and the role of lithology both in the long-term sequestration of inorganic C and the shorter-term sequestration of organic C.

## 5. Figures & Tables

Figure 1. Rhyolite soils, from L to R: soil profile, % mineral composition (by weight) with depth, elemental  $\tau$  values. Data is presented by horizon as labeled in the profile photo on the left. The 2 lowest data points in the % mineral composition plot represent the mineral composition of soil saprolite (90 cm) and parent material (95 cm). Bars represent the standard deviation of 3 pedons.

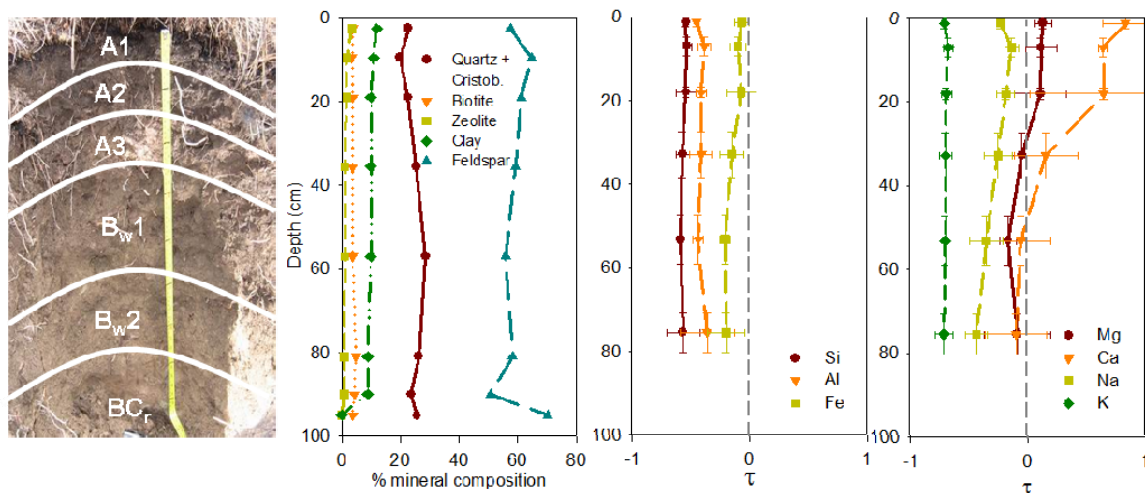


Figure 2. XRD patterns (CuK $\alpha$ ) of particle size classes of the RHYOLITE soils: a) very fine sands (53-100  $\mu\text{m}$ ); b) silts (2-53  $\mu\text{m}$ ); c) oriented clay mounts (<2  $\mu\text{m}$ ) -treatments from top to bottom for each horizon: saturation with MgCl<sub>2</sub> and glycerol, saturation with MgCl<sub>2</sub>, saturation with KCl.

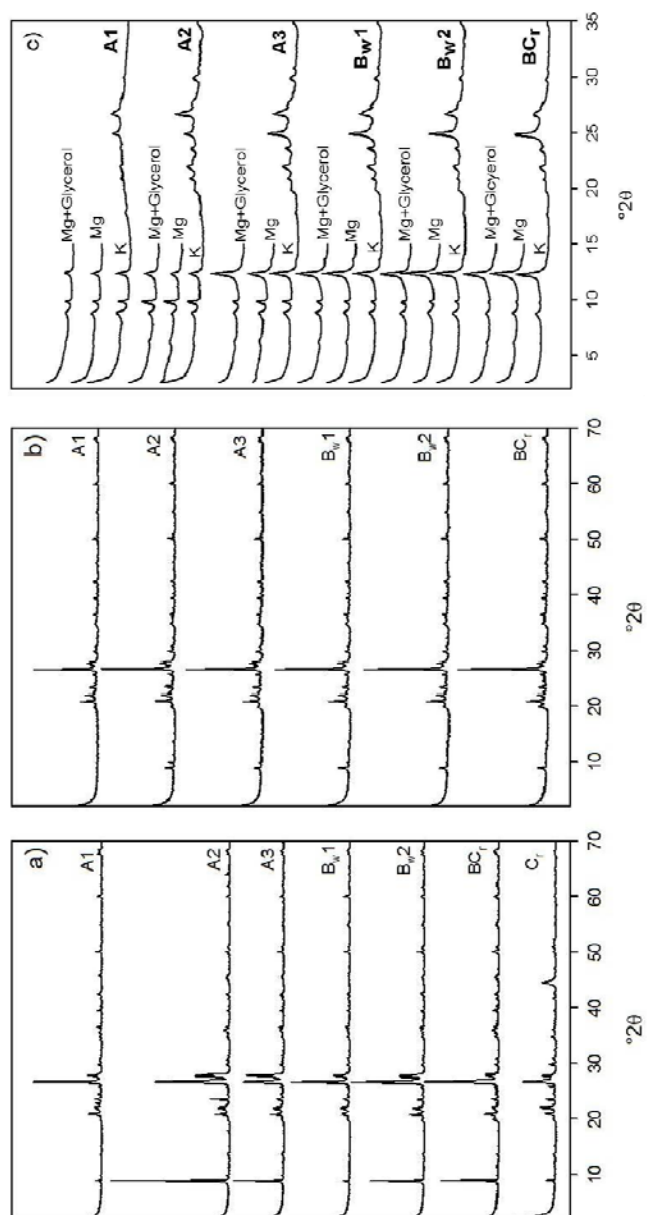


Figure 3. Granite soils, from L to R: soil profile, % mineral composition (by weight) with depth, elemental  $\tau$  values. Data is presented by horizon as labeled in the profile photo on the left. The lowest data point in the % mineral composition plot (37 cm) represents the mineral composition of the soil parent material. Bars represent the standard deviation of 3 pedons.

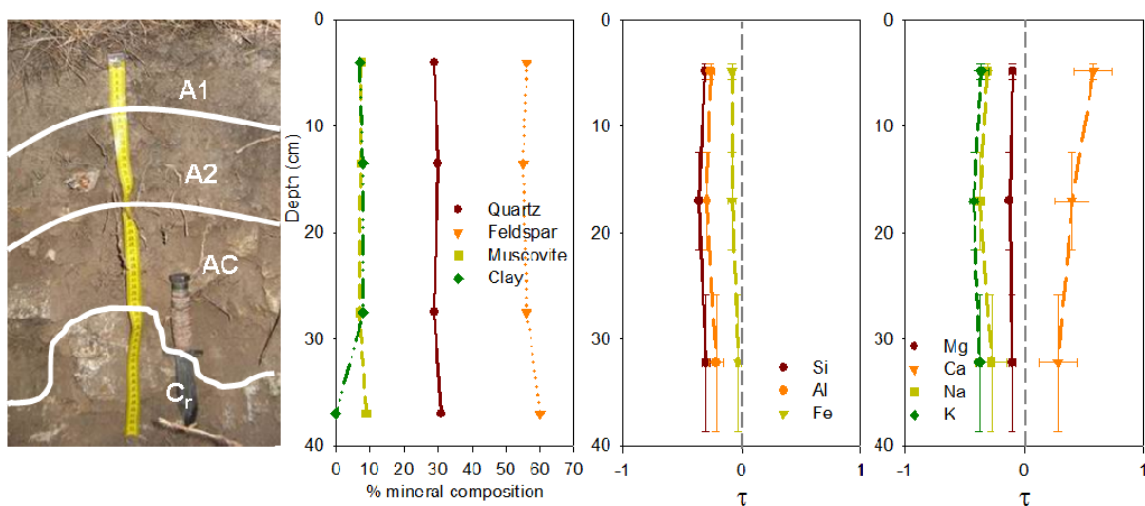


Figure 4. XRD patterns (CuK $\alpha$ ) of particle size classes of the GRANITE soils: a) very fine sands (53-100  $\mu\text{m}$ ); b) silts (2-53  $\mu\text{m}$ ); c) oriented clay mounts (<2  $\mu\text{m}$ ) -treatments from top to bottom for each horizon: saturation with MgCl<sub>2</sub> and glycerol, saturation with MgCl<sub>2</sub>, saturation with KCl.

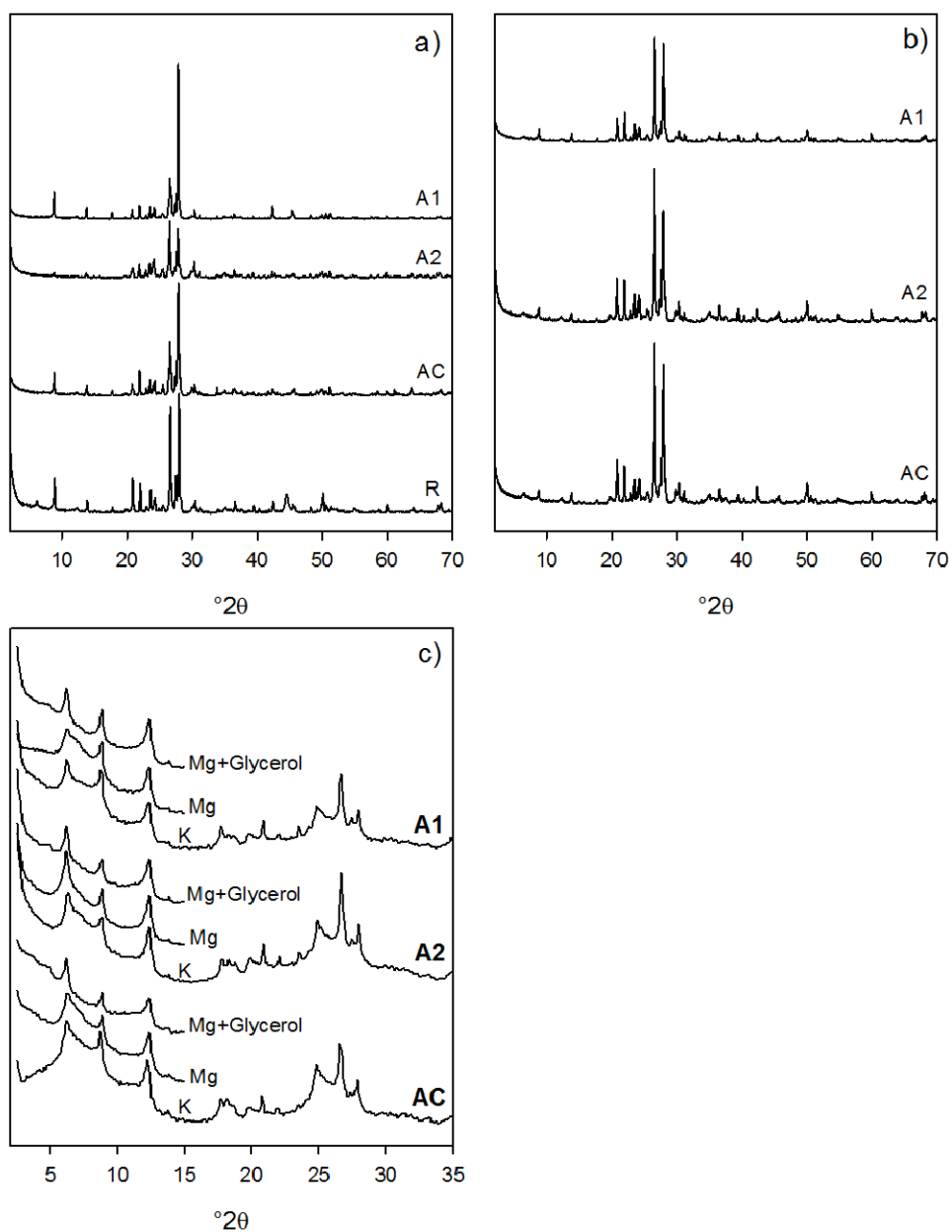


Figure 5. Basalt soils, from L to R: soil profile, % mineral composition (by weight) with depth, elemental  $\tau$  values. Data is presented by horizon as labeled in the profile photo on the left. The lowest data point in the % mineral composition plot (60 cm) represents the mineral composition of the soil parent material. Bars represent the standard deviation of 3 pedons.  $\tau$  values for K exceeded 100% ( $\tau = 1$ ), therefore the x axis of the base cation  $\tau$  plot was extended to 2.

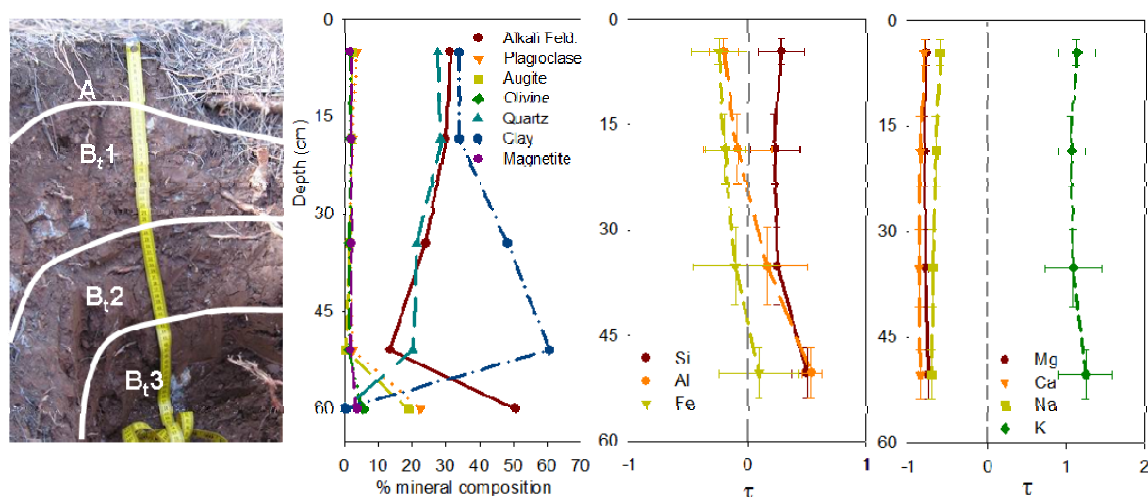


Figure 6. XRD patterns (CuK $\alpha$ ) of particle size classes of the BASALT soils: a) very fine sands (53-100  $\mu\text{m}$ ); b) silts (2-53  $\mu\text{m}$ ); c) oriented clay mounts (<2  $\mu\text{m}$ ) -treatments from top to bottom for each horizon: saturation with MgCl<sub>2</sub> and glycerol, saturation with MgCl<sub>2</sub>, saturation with KCl.

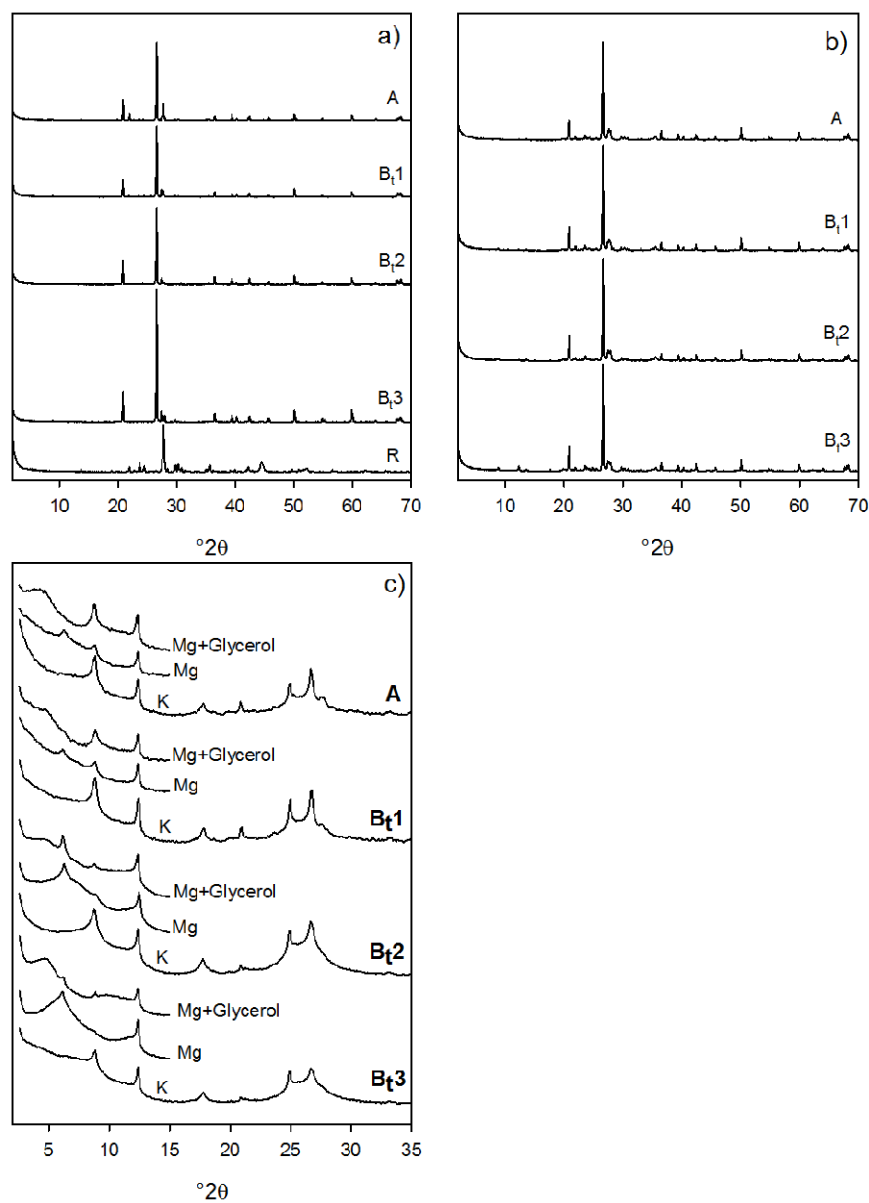


Figure 7. Limestone soils, from L to R: soil profile, % mineral composition (by weight) with depth, elemental  $\tau$  values. Data is presented by horizon as labeled in the profile photo on the left. The lowest data point in the % mineral composition plot (25 cm) represents the mineral composition of the soil parent material. Bars represent the standard deviation of 3 pedons.  $\tau$  values for Si and K exceeded 100% ( $\tau = 1$ ), therefore the x axis of the  $\tau$  plots were extended to 3 and 4, respectively.

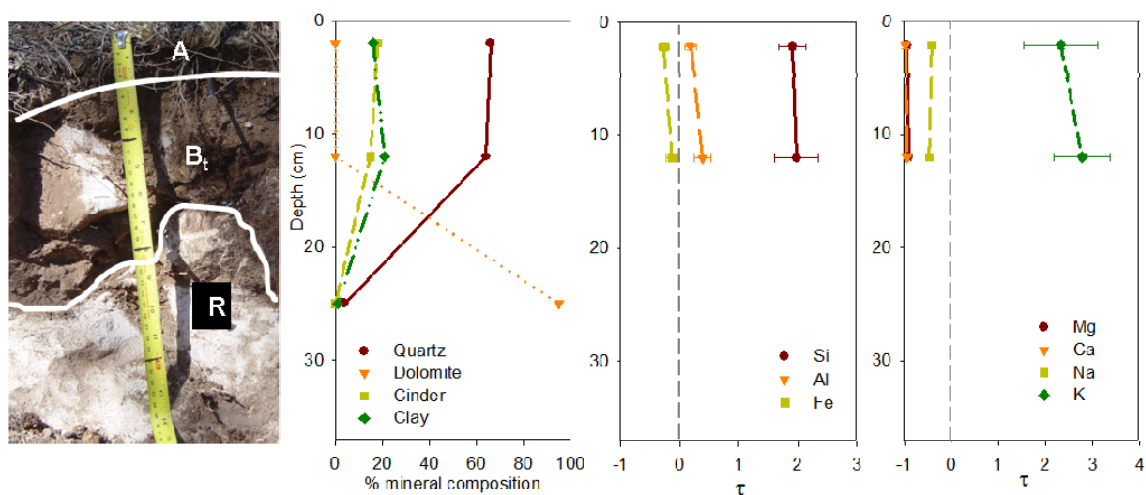


Figure 8. XRD patterns ( $\text{CuK}\alpha$ ) of particle size classes of the LIMESTONE soils: a) very fine sands (53-100  $\mu\text{m}$ ); b) silts (2-53  $\mu\text{m}$ ); c) oriented clay mounts (<2  $\mu\text{m}$ ) -treatments from top to bottom for each horizon: saturation with  $\text{MgCl}_2$  and glycerol, saturation with  $\text{MgCl}_2$ , saturation with  $\text{KCl}$ .

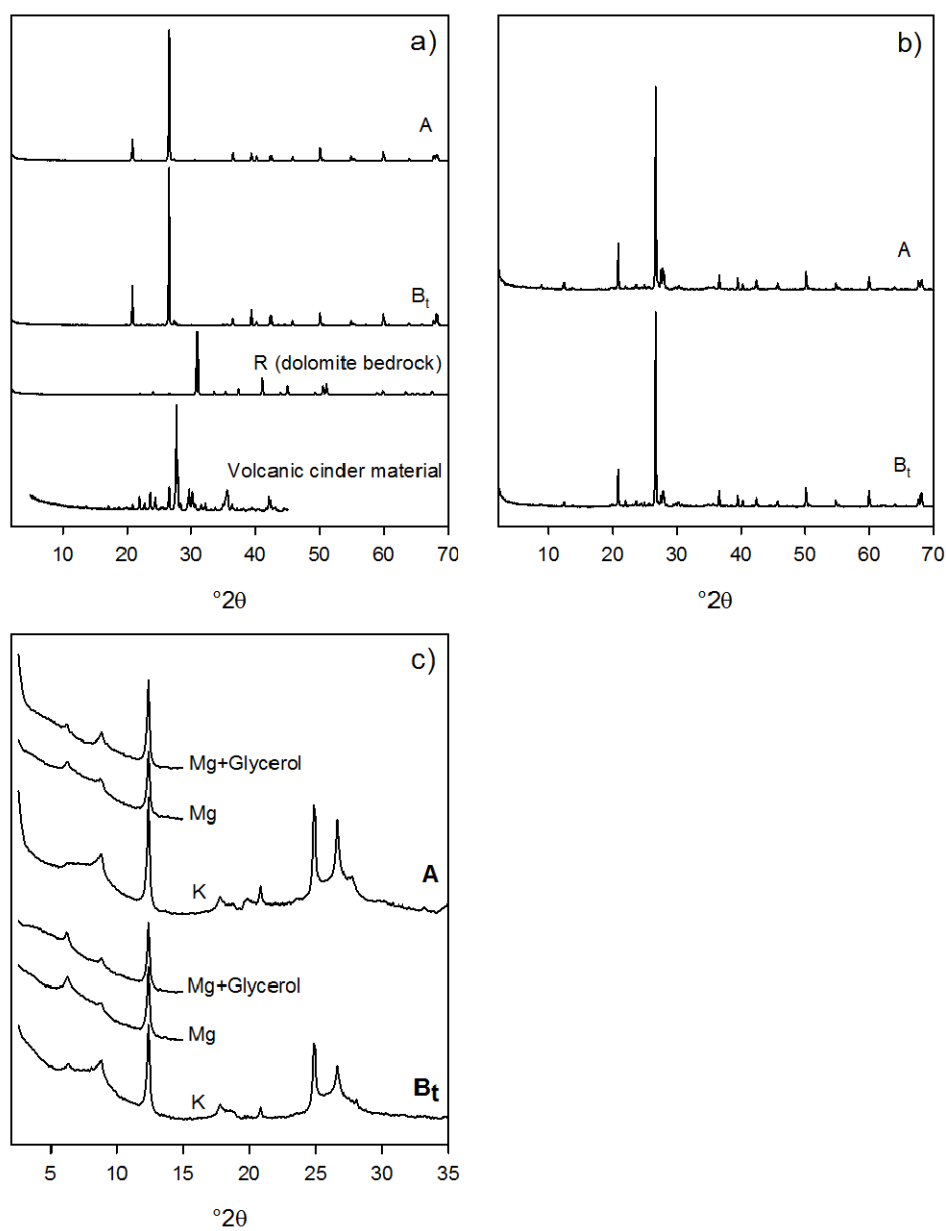


Table 1. Soil characterization data by horizon

Parent Material	Horizon	Depth (cm)	SOC* (%)	pH 1:1 H <sub>2</sub> O	Clay (%)	CEC <sup>^</sup> (cmol <sub>c</sub> kg <sup>-1</sup> )	Fe <sub>d</sub> - Fe <sub>o</sub>	Fe <sub>o</sub> -Fe <sub>p</sub> (g kg <sup>-1</sup> )	Fe <sub>p</sub>	Al <sub>p</sub>	SSA** (m <sup>2</sup> g <sup>-1</sup> )
Rhyolite	A1	0-5	8.4 (4.5)	5.8(0.4)	11 (1)	20 (3)	4.3 (0.7)	0.4 (0.1)	1.3 (0.1)	2.9 (0.8)	5.5
	A2	5-14	4.0 (1.1)	5.7(0.3)	10 (1)	16 (2)	4.6 (0.7)	0.2 (0.1)	1.4 (0.1)	2.9 (0.2)	10.9
	A3	14-24	1.7 (0.5)	5.4	10 (0)	12 (2)	4.5 (0.3)	0.2 (0.1)	1.1 (0.3)	2.3 (1.4)	11.0
	B <sub>w</sub> 1	24-47	1.0 (0.0)	5.3(0.2)	10 (1)	11 (1)	5.2 (0.6)	0.3 (0.2)	0.7 (0.2)	1.2 (0.4)	15.1
	B <sub>w</sub> 2	47-65	0.4 (0.1)	5.3(0.1)	9 (1)	9 (1)	5.0 (0.7)	0.4 (0.2)	0.4 (0.1)	0.6 (0.1)	15.4
	BC <sub>r</sub>	65-82	0.3 (0.0)	5.4(0.2)	9 (2)	11 (1)	4.1 (0.7)	1 (0.5)	0.3 (0.0)	0.6 (0.1)	16.8
	C <sub>r</sub>	82-					unconsolidated rhyolitic ash				
Granite	A1	0-10	2.8 (0.4)	5.8(0.2)	5 (1)	9 (1)	5.6 (0.5)	0.3 (0.1)	0.9 (0.0)	1.5 (0.1)	4.0
	A2	10-22	1.8 (0.4)	5.8(0.2)	6 (0)	8 (1)	6.6 (0.5)	0.4 (0)	0.9 (0.1)	1.4 (0.3)	4.4
	AC	22-37	1.0 (0.1)	5.6(0.2)	6 (0)	7 (0)	6.8 (0.2)	0 (0.2)	0.9 (0.2)	1.4 (0.3)	4.8
	C <sub>r</sub>						granitic saprolite				
Basalt	A	0-10	4.4 (0.3)	6.2(0.2)	19 (2)	27 (4)	13.8 (0.7)	5.6 (0.8)	1.1 (0.2)	1.1 (0.2)	23.4
	B <sub>t</sub> 1	10-27	1.5 (0.3)	6.2(0.1)	28 (6)	26 (4)	19.9 (0.7)	4.5 (0.3)	1.1 (0.3)	1.0 (0.4)	25.6
	B <sub>t</sub> 2	27-42	0.8 (0.2)	6.2	39 (3)	32 (2)	22.3 (1.6)	4.0 (0.4)	0.9 (0.3)	0.9 (0.2)	48.1
	B <sub>t</sub> 3	42-60	0.7 (0.0)	6.5	49 (3)	32 (1)	20.0 (1.0)	4.7 (0.9)	0.4 (0.2)	0.5 (0.2)	65.2
	R						fractured basalt				
Limestone	A	0-4	1.8 (0.5)	6.6(0.1)	9 (2)	14 (2)	1.8 (0.1)	3.9 (0.6)	0.9 (0.2)	0.9 (0.2)	8.0
	B <sub>t</sub>	4-20	1.5 (0.2)	7.1(0.2)	16 (3)	18 (3)	3.0 (1.7)	4.8 (0.2)	1.0 (0.1)	0.7 (0.1)	14.5
	R						consolidated dolomitic limestone				

\* Soil Organic Carbon d = dithionite extractable

<sup>^</sup> Cation Exchange Capacity at pH o = oxalate extractable

BDL = below detection level p = pyrophosphate extractable

\*\* Specific Surface Area () = standard error of three replicates

Table 2. Family level classification of lithosequence soils

---

<b>Rhyolite</b>	loamy, mixed, superactive, mesic Typic Haplustept
<b>Granite</b>	loamy-skeletal, mixed superactive, mesic Typic Ustorthent
<b>Basalt</b>	clayey-skeletal, mixed superactive, mesic Typic Paleustoll
<b>Limestone</b>	loamy, mixed, superactive, mesic Lithic Argiustoll

---

Soils classified according to U.S. Soil Taxonomy, 10th Edition, 2006.

Table 3. Elemental composition of parent materials

	Si	Al	Fe	Mg	Ca	Na	K
	% by weight corrected for loss on ignition						
Limestone	5	<1	<1	33	60	<1	<1
Cinders	42	16	16	9	12	4	1
Rhyolite	68	15	3	<1	1	2	11
Granite	67	16	3	<1	1	5	7
Basalt	41	15	15	11	14	4	1

Table 4. Fluxes of major elements during soil formation

	Si	Al	Fe	Mg	Ca	Na	K
	kg m <sup>-2</sup>						
<b>Rhyolite</b>	-213 (±13)	-34 (±3)	-3 (±0)	0 (±0)	1 (±0)	-3 (±0)	-44 (±4)
<b>Granite</b>	-73 (±13)	-14 (±3)	-1 (±0)	0 (±0)	1 (±0)	-5 (±1)	-10 (±1)
<b>Basalt</b>	72 (±31)	8 (±14)	-11 (±1)	-48 (±1)	-68 (±3)	-16 (±1)	8 (±1)
<b>Limestone</b>	97 (±39)	7 (±4)	-2 (±0)	-52 (±15)	-92 (±26)	-2 (±1)	4 (±2)

Values are the average of three pedons sampled at each field site ( $n = 3$ ). Values are whole pedon sums, corrected for rock fragment content. Numbers in parentheses are standard errors.

Table 5. Inorganic C fluxes, organic C preserved, organic C preserved, total mass loss and the immobile element used for calculations in each soil

	Inorganic C	Organic C	Total mass loss*	Immobile element
	kg m <sup>-2</sup>			
<b>Rhyolite</b>	26.2 (±2.3) <sup>BC</sup>	10.97 (±0.43) <sup>A</sup>	-576.04 (±38.56)	zirconium
<b>Granite</b>	5.5 (±0.9) <sup>C</sup>	5.34 (±0.43) <sup>BC</sup>	-202.53 (±35.53)	zirconium
<b>Basalt</b>	83.3 (±8.3) <sup>A</sup>	8.68 (±1.18) <sup>AB</sup>	-36.23 (±94.74)	titanium
<b>Limestone</b>	51 (±14.0) <sup>B</sup>	3.46 (±1.11) <sup>C</sup>	4.21 (±31.06)	titanium

Values are the average of three pedons sampled at each field site ( $n = 3$ ). Significance was determined using one-way ANOVA by parent material followed by Tukey's HSD post hoc test ( $\alpha = 0.05$ ). Within each column, means followed by different superscript letters are significantly different. Values are whole pedon sums, corrected for bulk density and rock fragment content. Numbers in parentheses are standard errors. \*calculated based on oxide weight

## 6. References

Allen, B.L., Hajek, B.F., 1989. Mineral Occurrence in Soil Environments. *In: Minerals in Soil Environments*, SSSA Book Series:1 (Eds. J.B Dixon and S.B. Weed) pp. 218-220.

Amiotte-Suchet, P., Probst, J. L., 1993. Flux de CO<sub>2</sub> atmosphérique consommé par altération chimique continentale. Influence de la nature de la roche. *C.R. Acad. Sci. Paris* 317, 615-622, Série II.

Anderson JU, Bailey OF, Rai D, 1975. Effects of parent material on genesis of Borolls and Boralfs in south-central New Mexico mountains. *Soil Science Society of America Proceedings* 39, 901-904..

Anderson, S.P., Dietrich, W.E., Brimhall, G.H., 2002. Weathering profiles, mass-balance analysis, and rates of solute loss: Linkages between weathering and erosion in a small, steep catchment. *Geological Society of America Bulletin* 114, 1143-1158.

Anderson, T-H, Domsch, K.H., 1993. The metabolic quotient for CO<sub>2</sub> ( $q_{CO_2}$ ) as a specific activity parameter to assess the effects of environmental conditions, such as pH, of the microbial biomass of forest soils. *Soil Biology & Biochemistry* 25 (3), 393-395.

Arizona Geological Survey, Digital Geologic Map of Arizona: A Digital Database Derived from the 1983 Printing of the Wilson, Moore, and Cooper 1:500,000-scale Map (2000) Douglas M. Hirschberg and G. Stephen Pitts, Open-File Report 00-409 Version 1.0, U.S. Department of the Interior, U.S. Geological Survey.

Barnhisel, R.E., Bertsch, P.M., 1989. Chlorites and hydroxyl-interlayered vermiculite and smectite. *In: Dixon, J.B., Weed, S.B. (Eds.), Minerals in Soil Environments* (2<sup>nd</sup> Ed.). SSSA Book Series, 1, Madison, WI, pp. 729-788.

Berner, R.A., Kothavala, Z., 2001. Geocarb III: A revised model of atmospheric CO<sub>2</sub> over phanerozoic time. *American Journal of Science* 301, 182-204.

Berner RA, Lasaga AC, Garrels RM, 1983. The carbonate-silicate geochemical cycle and its effect on the atmospheric carbon-dioxide over the past 100 million years. *American Journal of Science* 283(7): 641-683.

Bluth, G.J.S., Kump, L.R., 1994. Lithological and climatological controls of river chemistry. *Geochimica et Cosmochimica Acta* 58, 2341-2359.

Brimhall GH, Dietrich WE, 1987. Constitutive mass balance relations between chemical-composition, volume, density, porosity, and strain in metasomatic hydrochemical systems – results on weathering and pedogenesis. *Geochimica et Cosmochimica Acta* 51(3): 567-587.

Brimhall GH, Chadwick OA, Lewis CJ, et al. 1992. Deformational mass transport and invasive processes in soil evolution. *Science* 255, 695-702.

Brindley, G.W. 1980. Chapter 7: Quantitative X-ray mineral analysis of clays, p. 411-438, In G. W. Brindley and G. Brown, eds. *Crystal structures of clay minerals and their x-ray identification*. Mineralogical Society, London.

Brunauer, S., P.H. Emmett, and E. Teller. 1938. Adsorption of Gases in Multimolecular Layers. *J. Am. Chem. Soc.* 60:309-319.

Capo, R.C., Stewart, B.W., Chadwick, O.A., 1998. Strontium isotopes as tracers of ecosystem processes: theory and methods. *Geoderma* 82, 197-225.

Chadwick Oliver A, Brimhall George H, and Hendricks David M, 1990. From a black to a gray box – a mass balance interpretation of pedogenesis. *Geomorphology* 3: 369-390.

Chadwick, O.A., E.F. Kelly, D.M. Merritts, and R.G. Amundson. 1994. Carbon dioxide consumption during soil development. *Biogeochemistry* 24:115-127.

Chipera, S.J., Goff, F., Goff, C.J., Fittipaldo, M., 2008. Zeolitization of intracaldera sediments and rhyolitic rocks in the 1.25 Ma lake of Valles caldera, New Mexico, USA. *Journal of Volcanology and Geothermal Research* 178, 317-330.

Cornell, R.M., Schwertmann, U., 2003. *The Iron Oxides: Structure, Properties, Reactions, Occurrence and Uses*. VCH: Weinheim.

Dahlgren, R.A., 1994. Quantification of allophane and imogolite. In: Amonette, J.E., Zelazny, L.W. (Eds.), *Quantitative Methods in Soil Mineralogy*. SSSA Inc., Madison, WI, 430-451.

Dahlgren, R.A., Boettinger, J.L., Huntington, G.L., Amundson, R.G., 1997. Soil development along an elevational transect in the western Sierra Nevada, California.

Dessert, C., Dupré, B., Baillardet, J., François, L.M., Allégre, C.J., 2003. *Chemical Geology* 202, 257-273.

Drees, Wilding, Smeck, Senkayi, 1989. Silica in soils: Quartz and silica polymorphs. In: *Minerals in Soil Environments*, SSSA Book Series:1 (Eds. J.B Dixon and S.B. Weed) pp. 913-974.

Dixon JB, Weed SB, 1989. *Minerals in Soil Environments*, Second Edition. JB Dixon & SB Weed (Eds), Soil Science Society of America, Madison, Wis.

- Dokuchaev, V.V. 1879. Short Historical Description and Critical Analysis of the More Important Soil Classifications. *Trav. Soc. Nat. St. Petersburg* 10: 64-67. (In Russian)
- Douglas, L.A., 1989. Vermiculites. In: *Minerals in Soil Environments*, SSSA Book Series:1 (Eds. J.B Dixon and S.B. Weed) pp. 635-674.
- Eberl, D.D. 2003. User's guide to a program for determining quantitative mineralogy from powder X-ray diffractions data. U.S. Geological Survey Open File Report 03-78.
- Edmond, J.M. et al., 1994. Fluvial geochemistry and denudation rate of Guyana Shield. *Geochimica et Cosmochimica Acta* 59, 3301-3325.
- Ewing SA, Sutter B, Owen J, Nishiizumi K, Sharp W, Cliff SS, Perry K, Dietrich W, McKay CP, Amundson R, 2006. A threshold in soil formation at Earth's arid-hyperarid transition. *Geochimica et Cosmochimica Acta* 70(21), 5293-5322.
- Gaillardet, J., Dupré, B., Louvat, P., Allégre, C.J., 1999. Global silicate weathering and CO<sub>2</sub> consumption rates deduced from the chemistry of large rivers. *Chemical Geology* 159, 3-30.
- Garrels, R.M., Machkenzie, F.T., 1971. *Evolution of sedimentary Rocks*. Norton, New York.
- Gíslason, S.R., Arnórsson, S., Armannsson, H., 1994. Present chemical weathering of basalt in Iceland. *Mineralogical Magazine* 58A, 333-334.
- Glasmann, J.R., Simonson, G.H., 1984. Alteration of basalt in soils of western Oregon. *Soil Science Society of America Journal*. 49: 262-273.
- Goldstein, H.L., Reynolds, R.L., Reheis, M.C., Yount, J.C., Neff, J.C. 2008. Compositional trends in aeolian dust along a transect across the southwestern United States. *Journal of Geophysical Research* 113
- Harder, H., 1974. Illite mineral synthesis at surface temperatures. *Chemical Geology* 14, 241-253
- Harvey, C.C., 1997. Exploration and assessment of kaolin clays formed from acid volcanic rocks on the Coromandel Peninsula, North Island, New Zealand. *Applied Clay Science* 11, 381-392.
- Hausrath EM, Neaman A, Brantley SL, 2009. Elemental release rates from dissolving basalt and granite with and without organic ligands. *American Journal of Science* 309: 633-660.

Hawkins, D.B., Sheppard, R.A., Gude, A.J. III, 1978. Hydrothermal synthesis of clinoptilolite and comments of the assemblage phillipsite-clinoptilolite-mordenite. p. 337-343. In: L.B. Sand and F.A. Mumpton (ed.) natural zeolites: Occurrence, properties, use. Pergamon Press Inc., Elmsford, NY.

Heckman, K., Welty-Bernard, A., Rasmussen, C., Schwartz, E., 2009. Geologic controls of soil carbon cycling and microbial dynamics in temperate conifer forests. *Chemical Geology* 267, 12-23.

Henderson, J.H., Clayton, R.N., Jackson, M.L., Syers, J.K., Rex, R.W., Brown, J.L.,

Sachs, I.B., 1972. Cristobalite and quartz isolation from soils and sediments by hydrofluosilicic acid treatment and heavy liquid separation. *Soil Science Society of America Proceedings* 36, 830-835.

Holdren, G.R., Berner, R.A., 1979. Mechanism of feldspar weathering 1. Experimental studies. *Geochimica et Cosmochimica Acta* 43, 1161-1171.

Hoyum RA, Hajek BF, 1979. A lithosequence in coastal plain sediments in Alabama. *Soil Science Society of America Journal* 43, 151-156.

Jackson, M.L. 1963a. Aluminum bonding in soils: A unifying principle in soil science. *Soil Sci. Soc. Am. Proc.* 27:1-10.

Jackson, M.L. 1963b. Interlayering of expansible layer silicates in soils by chemical weathering. p. 29-46. In *Trans. 11th Natl. Conf. Clays Clay Miner.* Pergamon Press, New York.

Jackson ML, 2005. *Soil Chemical Analysis: Advanced Course, 2nd Edition.* Parallel Press: Madison, Wisconsin.

Jenny, Hans (1994) *Factors of Soil Formation. A System of Quantitative Pedology.* New York: Dover Press.

Kahle, M., Kleber, M., Jahn, R., 2004. Retention of dissolved organic matter by phyllosilicate and soil clay fractions in relation to mineral properties. *Organic Geochemistry* 35(3), 269-276.

Kögel-Knabner, I., Guggenberger, G., Kleber, M., Kandeler, E., Kalbitz, K., Scheu, S., Eusterhues, K., Leinweber, P., 2008. Organo-mineral associations in temperate soils: Integrating biology, mineralogy, and organic matter chemistry. *Journal of Plant Nutrition and Soil Science* 171, 61-82

- Klug, H.P., and L.E. Alexander. 1974. X-Ray Diffraction Procedures For Polycrystalline and Amorphous Materials John Wiley & Sons: New York.
- Larsen, D., Crossey, L.J., 1996. Depositional environments and paleolimnology of an ancient caldera lake: Oligocene Creede Formation, Colorado. *Geol. Soc. Amer. Bull.* 108, 526–544.
- Levine SJ, Hendricks DM, Schreiber JF Jr, 1989. Effect of bedrock porosity on soils formed from dolomitic limestone residuum and eolian deposition. *Soil Science Society of America Journal* 53, 856-862.
- Lindsay, W.L., 1979. *Chemical Equilibria in Soils*. Wiley: New York.
- Lüttge, A., 2005. Etch pit coalescence, surface area, and overall mineral dissolution rates. *American Mineralogist* 90, 1776-1783.
- Mackenzie FT, Lerman A 2006. *Carbon in the Geobiosphere - Earth's Outer Shell*. Springer: Dordrecht, The Netherlands.
- Mahjoory, R.A., 1975. Clay mineralogy, physical and chemical properties of some soils in arid regions of Iran. *Soil Science Society of America Proceedings* 39, 1157-1164.
- Meybeck, M., 1986. Composition des ruisseaux non pollués de France. *Sci. Geol. Bull.* 39, 3-77.
- Milnes, A.R., and R.W. Fitzpatrick. 1989. Titanium and zirconium minerals, p. 1131-1205, In J. B. Dixon and S. B. Weed, eds. *Minerals in soil environments*. Soil Science Society of America, Madison, WI.
- Neaman, A., Chorover, J., Brantley, S.L., 2006. Effects of organic ligands on granite dissolution in batch experiments at pH 6. *American Journal of Science*, 306, 451-473.
- Nierop KGJ, Jansen B, Verstraten JM, 2002. Dissolved organic matter, aluminum and iron interactions: precipitation induced by metal/carbon ratio, pH and competition. *Science of the Total Environment* 300: 201-211.
- Norris, K., Pickering, J.G., 1983. Clay minerals. p.281-308. In *Soils: An Australian viewpoint*, Division of Soils, CSIRO, Melbourne. Academic Press Ltd., London.
- Page-Dumroese, D.S., Jurgensen, M.F., Brown, R.E., Mroz, G.D., 1999. *Soil Science Society of America Journal* 63, 379-383.
- Pansu, M., Gautheyrou, J., 2006. Exchangeable Acidity. In: *Handbook of Soil Analysis*. Springer-Verlag, The Netherlands, 678-686.

Percival HJ, Parfitt RJ, Scott NA, 2000. Factors Controlling Soil Carbon Levels in New Zealand Grasslands: Is Clay Content Important? *Soil Science Society of America Journal* 64:1623-1630.

Porder, S., G.E. Hilley, and O.A. Chadwick. 2007. Chemical weathering, mass loss, and dust inputs across a climate by time matrix in the Hawaiian Islands. *Earth and Planetary Science Letters* 258:414-427.

Rasmussen, C., Southard, R.J., Horwath, W.R., 2006. Mineral control of organic carbon mineralization in a range of temperate conifer forest soils. *Global Change Biology* 12, 834-847.

Reheis, M. C., R. L. Reynolds, H. Goldstein, H. M. Roberts, J. C. Yount, Y. Axford, L. S. Cummings, and N. Shearin (2005), Late Quaternary eolian and alluvial response to paleoclimate, Canyonlands, southeastern Utah, *Geol. Soc. Am. Bull.*, 117, 1051– 1069.

Reynolds, R., J. Belnap, M. Reheis, P. Lamothe, 2001. Aeolian Dust in Colorado Plateau Soils: Nutrient Inputs and Recent Change in Source. *Proceedings of the National Academy of Sciences of the United States of America* 98, 7123-7127.

Reynolds, R. L., M. C. Reheis, J. C. Neff, H. Goldstein, and J. C. Yount (2006), Late Quaternary eolian dust in surficial deposits of a Colorado Plateau grassland: Controls on distribution and ecologic effects, *Catena*, 66, 251– 266.

Righi, D., Terribile, F. and Petit, S. (1999) Pedogenic formation of kaolinite-smectite mixed layers in a soil toposequence developed from basaltic parent material in Sardinia (Italy). *Clays and Clay Minerals*, 47, 505\_514.

Schaetzl, R.J., 1991. Factors affecting the formation of dark, thick epipedons beneath forest vegetation, Michigan, USA. *Journal of Soil Science* 42, 501-512.

Scheel, T., Dörfler, C., Kalbitz, K., 2007. Precipitation of dissolved organic matter by aluminum stabilizes carbon in acidic forest soils. *Soil Science Society of America Journal* 71, 64-74.

Schimel, D.S., Braswell, B.H., Holland, E.A., McKeown, R, Ojima, D.S., Painter, T.H., Parton, W.J., Townsend, A.R., 1994. Climatic, edaphic, and biotic controls over storage and turnover of carbon in soils. *Global Biogeochemical Cycles* 8(3), 279-293.

Schwertmann, U., Carlson, L., Fechter, H., 1984. Iron-oxide formation in artificial ground waters. *Swiss Journal of Hydrology* 46, 185-191.

- Środoń, J., V.A. Drits, D.K. McCarty, J.C.C. Hsieh, and D.D. Eberl. 2001. Quantitative X-ray diffraction analysis of clay-bearing rocks from random preparations. *Clays and Clay Minerals* 49:514-528.
- Stiles, C.A., and K.A. Stensvold. 2008. Loess contribution to soils forming on dolostone in the driftless area of Wisconsin. *Soil Science Society of America Journal* 72:650-659.
- Soil Survey Staff, National Soil Survey Laboratory, 2004. *Methods Manual: Soil Survey Investigations Report No. 42, Version 4.0*, United States Department of Agriculture, Natural Resources Conservation Service, National Soil Survey Center, Lincoln, NE.
- Soil Survey Staff, 2006. *Keys to Soil Taxonomy 10th Edition*. United States Department of Agriculture, Natural Resources Conservation Service.
- Spalding, W.G., Graumlich, L.J., 1986. The last pluvial climatic episodes in the deserts of southwestern North America. *Nature* 320, 441-444.
- Swindale, L.D., 1960. A mineralogical study of soil formation in four rhyolite-derived soils from New Zealand. *New Zealand Journal of Geology and Geophysics* 3, 141-183.
- Torn, M.S., Trumbore, S.E., Chadwick, O.A., Vitousek, P.M., Hendricks, D.M., 1997. Mineral control of soil organic carbon storage and turnover. *Nature* 389, 170-173.
- Vingiani, S, Righ, D, Petit, S, Terribile, F. Mixed-layer kaolinite-smectite minerals in a red-black soil sequence from basalt in Sardinia (Italy). *Clays and Clay Minerals*, Vol. 52, No. 4, 473–483, 2004.
- Waldrop, T.A., Van Lear, D.H., Lloyd, F.T., Harms, W.R., 1987. Long-term studies of prescribed burning in loblolly pine forests of the southeastern coastal plain. *USDA For. Serv. Gen. Tech. Rep. SE-GTR-45*. 23 pp.
- Wattel-Koekkoek, E.J.W., Buurman, P., van der Plicht, J., Wattel, E., van Breemen, N., 2003. Mean residence time of soil organic matter associated with kaolinite and smectite. *European Journal of Soil Science* 54(2), 269-278.
- Welch SA, Ullman WJ, 1993. The effect of organic acids on plagioclase dissolution rates and stoichiometry. *Geochimica et Cosmochimica Acta* 57( 12): 2725-2736.
- Wells, C.G., 1971. Effects of prescribed burning on soil chemical properties and nutrient availability. In: *Proceedings of the Prescribed Burning Symposium*. USDA For. Serv. SE For. Expt. Sta., Ashville, NC, pp. 86–98.

Wells, C.G., Campbell, R.E., DeBano, L.F., Lewis, C.E., Fredriksen, R.L., Franklin, E.C., Froelich, R.C., Dunn, P.H., 1979. Effects of fire on soil: a state-of- knowledge review. USDA For. Serv. Gen. Tech. Rep. WO-GTR-7, 34 pp.

Whittig, L.D., Allardice W.R., 1986. X-ray diffraction techniques. In: Kute, A. (Ed.), Methods of Soil Analysis. Part 1. Physical and mineralogical methods. 2<sup>nd</sup> ed. SSSA Book Ser. 5. SSSA, Madison, WI.

Wilson, M.J., 2006. Factors of soil formation: parent material. As exemplified by a comparison of granitic and basaltic soils. In: Soils: basic concepts and future challenges (Eds. R. Scalenghe and G. Certini). Cambridge University Press, New York. pp. 113-129.

White AF, Brantley SL, 1995. Chemical weathering rates of silicate minerals: an overview. Rev. Mineral. 31, 1-22.

APPENDIX B

GEOLOGIC CONTROLS OF SOIL CARBON CYCLING AND MICROBIAL  
DYNAMICS IN TEMPERATE CONIFER FORESTS

Katherine Heckman<sup>a\*</sup> Amy Welty-Bernard<sup>b</sup>, Craig Rasmussen<sup>a</sup>, and Egbert Schwartz<sup>b</sup>

\*Corresponding Author

<sup>a</sup>Department of Soil, Water and Environmental Science; University of Arizona

1177 E. Fourth Street PO Box 210038

Tucson, AZ 85721-0038, USA

kheckman@email.arizona.edu

phone : +1 520 621 1646, fax : +1 520 621 1647

<sup>b</sup>Department of Biological Sciences, Northern Arizona University

PO Box 5640

Flagstaff, AZ 86011-5640, USA

phone : +1 928 523 2381, fax : +1 928 523 7500

Published in *Chemical Geology*, Volume 267, No. 1-2, pp.12-23

### Abstract

Understanding soil carbon cycling is important for assessing ecosystem response to climate change. Temperate conifer forest soils contain a substantial portion of the global soil C pool and therefore are key components of the global carbon cycle. Despite the importance of temperate forest soil organic carbon (SOC) in the global carbon cycle, the mechanisms and dynamics of SOC accumulation and storage remain poorly understood. To address this knowledge gap, we sampled four soils over different bedrock types (rhyolite, granite, basalt, limestone) under *Pinus ponderosa* to explore the following questions: i) Within a specific ecosystem type, how do SOC contents vary among sites with differing mineralogy? ii) What physicochemical variables are most highly correlated with SOC content, soil microbial community composition and soil respiration? and iii) What mechanisms account for the influence of these variables on SOC cycling? Soil physiochemical and microbiological properties were characterized and compared on the basis of mineral assemblage, pH, organic carbon content, bacterial community composition, respiration rate, microbial biomass, specific metabolic activity ( $q\text{CO}_2$ ), and  $\delta^{13}\text{C}$  of respired  $\text{CO}_2$ . The selected field sites spanned a physicochemical gradient, ranging from acid (pH of 5.2) to basic (pH of 7.1) from rhyolite to granite to basalt to limestone. The acidic rhyolite and granite soils had measureable amounts of exchangeable  $\text{Al}^{3+}$  (up to  $3 \text{ cmol}_+ \text{ kg}^{-1}$ ). SOC content varied significantly among sites, ranging from 3.5 to  $11 \text{ kg C m}^{-2}$  in limestone and rhyolite soils, respectively. Soil bacterial communities were also significantly different among all sites. Metal-humus complex and Fe-oxyhydroxide content emerged as important controllers of SOC

dynamics across all sites, showing significant correlation with both SOC content (Al-humus:  $R^2=0.71$ ;  $P<0.01$ ; Fe-humus:  $R^2=0.75$ ;  $P<0.001$ ; crystalline FeOx:  $R^2=0.63$ ;  $P<0.01$ ) and bacterial community composition (Al-humus:  $R^2=0.35$ ;  $P<0.05$ ; Fe-humus:  $R^2=0.51$ ;  $P<0.01$ ; oxalate-extractable Fe:  $R^2=0.59$ ;  $P<0.01$ ). Moreover, soil pH was significantly correlated with exchangeable  $Al^{3+}$ , metal-humus complex content, bacterial community composition, and microbial biomass C/N ratios. Results indicated that within a specific ecosystem, SOC dynamics and microbial community vary predictably with soil physicochemical variables directly related to mineralogical differences among soil parent materials. Specifically, the data suggest a gradient in the dominant SOC stabilization mechanism among sites, with chemical recalcitrance and metal-humus complexation the dominant control in soils of the acidic rhyolite and granite sites, and mineral adsorption the dominant factor in the basic limestone and basalt sites. Knowledge of parent material dependent SOC dynamics allows for improved estimates of ecosystem SOC stocks and the potential response of SOC to climate change.

## 1. Introduction

Concerns over global warming have raised interest in quantifying controls of soil carbon storage (SOC) and fluxes across time and space. The global pool of soil organic carbon is estimated at 1920 petagrams of carbon, or roughly 1.25 times that of atmospheric and aboveground biomass stores combined (Ver et al., 1999). Despite the importance of soil carbon in the global carbon cycle, the mechanisms and dynamics of SOC accumulation and storage remain poorly understood. Recent work demonstrates

that, within a given ecosystem, mechanisms of SOC sequestration vary significantly among geologic parent materials due to the associated variation in soil mineral assemblage and soil physicochemical properties (e.g., Torn et al., 1997; Rasmussen et al., 2006; Zinn et al. 2007; Basile-Doelsch et al., 2007; Kögel-Knabner et al., 2008). However, current models of SOC dynamics, e.g., CENTURY (Kelly et al. 1997) or Denitrification-Decomposition Model (Li et al., 1992), generally do not incorporate the influence of mineralogy and soil profile chemical gradients such as organic acid concentration, metal-humus complex content, or horizonation on SOC stabilization (Hedges and Oades, 1997). Because soil mineral assemblage has a profound effect on both soil respiration and SOC content, SOC cycling cannot be accurately modeled without inclusion of mineralogical parameters. This study examines mineralogical control of SOC cycling, and specifically addresses the relationship between mineral assemblage, SOC content, and microbial dynamics in temperate conifer ecosystems.

Current understanding and conceptual models of SOC stabilization suggest organic carbon is stabilized within the soil matrix by a combination of physical and chemical mechanisms (Sollins et al., 1996; von Lützow et al., 2006). Carbon may be physically protected from decomposition by occlusion within soil aggregate structures (Reicosky et al., 1997; Tebrügge and Düring, 1999; Six et al., 2000; Six et al., 2002) and direct adsorption to mineral surfaces (Kleber et al., 2007; Mikutta et al., 2007). Both occlusion and adsorption limit SOC accessibility to microorganisms and thereby promote preservation of SOC. Chemical stabilization mechanisms include those related to the chemical nature of SOC and plant inputs (McClaugherty et al., 1985; Aber & Melillo,

1991; Trofymow et al., 2002; Valachovic et al., 2004) as well as the chemical environment within the soil matrix. For example, complexation of SOC with Fe- and Al- induces chemical and conformational changes that reduce SOC bio-availability (Baldock and Skjemstad, 2000; Nierop et al., 2002; Scheel et al., 2007), and favor precipitation of metal-humus complexes from solution. The molecular structure of these precipitates is more condensed and the orientation of functional groups is altered (Oades, 1988), thereby altering their susceptibility to enzyme attack. Soil organic carbon stabilization is also a function of adsorption to clay (Schimel et al., 1994; Percival et al., 2000), and non-crystalline materials such as Fe-oxyhydroxides and allophanic materials (Torn et al., 1997). The mean residence time of mineral associated SOC varies with mineral type (Wattel-Koekkoek et al., 2003), soil pH, microbial activity (Guggenberger and Kaiser, 2003), specific surface area and surface charge (Kahle et al., 2004).

Soil mineral assemblage may further control SOC stabilization via feedbacks between soil chemical properties and soil microbial community structure and activity. High soil acidity creates unfavorable conditions for many soil microorganisms, leading to lower levels of soil biomass and suppressing C mineralization rates (Motavalli et al., 1995; Han et al., 2007). Soil pH has also been suggested as a significant controller of soil microbial diversity (Fierer and Jackson, 2006). Aluminum chemistry and toxicity have also been implicated as significant controls over SOC stability and microbial communities in forest soils (Illmer et al., 1995, 2003; Scheel et al., 2007). The relative importance of each of these SOC preservation mechanisms varies depending on soil forming environment. Hence, soil mineral assemblage plays a dual role in determining

the organic carbon content of a soil. Soil mineral assemblage controls SOC content directly through its influence on surface chemistry and pH, and indirectly through its influence on microbial community structure and SOC accessibility.

The relative importance of chemical and physical stabilization mechanisms noted above vary with soil physicochemical properties directly controlled by soil parent material and pedogenic environment. Therefore, quantifying the specific relationships between soil physicochemical properties and SOC dynamics within a given ecosystem provides a means to constrain biogeochemical models given a range of soil parent materials. This study builds from previous work demonstrating significant empirical linkages between soil mineralogy and SOC dynamics in temperate conifer forests of the western U.S. (e.g., Rasmussen et al., 2006; Rasmussen et al., 2008) to address the following questions: i) Within a specific ecosystem type, how does SOC content vary among sites with differing mineralogy? ii) What physicochemical variables are most highly correlated with SOC content, soil microbial community composition and soil respiration across sites? and iii) What mechanisms account for the influence of these variables on SOC cycling?

## **2. Methods**

### *2.1. Field Sites*

To address the research questions, we focused this study within *Pinus ponderosa* (ponderosa pine) forests of Arizona, a regionally important temperate forest ecosystem. Ponderosa pine forests occupy approximately  $22 \times 10^6$  ha of the western United States,

with over  $1.6 \times 10^6$  ha in Arizona (USDA, 1993). Temperate conifer forests of the western U.S. and ponderosa pine forests in particular, represent a significant portion of regional SOC stocks (Schlesinger, 1997; Homann et al., 1998; Rasmussen, 2006). The substantial SOC stocks in these systems may be attributed to a combination of high rates of primary production and stabilization of SOC within the mineral soil matrix. We sampled four field sites dominated by ponderosa pine in the over story with soils derived from limestone, basalt, granite, and rhyolite. The range of parent materials encompasses a dramatic gradient of soil pH and soil mineral assemblage allowing for examination of how soil physiochemical properties moderate SOC dynamics and microbial community composition.

The limestone and basalt sites were located near Flagstaff, AZ on the Kaibab Limestone formation and late-Pleistocene aged basalt flows; the granite site was located in the Santa Catalina Mountains north of Tucson, AZ on Precambrian aged granite; and the rhyolite site was located on the Mesozoic aged Turkey Creek Caldera in the Chiricahua Mountains in southeastern Arizona (Arizona Geological Survey, 2000). Despite variation in the age of parent rock, the geomorphic surface age was assumed to be similar among sites, with soil properties in a relative steady-state with mid- to late-Holocene climate conditions. The overall vegetation and climatic characteristics were relatively constant among sites (Table 1), with the exception of  $C_4$  grasses in the inter-canopy spaces at the limestone and basalt sites. All sites exhibit bimodal precipitation with approximately 40% of total precipitation derived from winter cyclonic systems and the remaining 60% derived from convective summer thunderstorms. Winter precipitation

arrives as a mix of snow and rainfall. The rhyolitic soils receive slightly greater precipitation in the form of warm summer rainfall.

Three pedons were excavated to the saprolite-bedrock contact at each field site. We constrained pedon locations to similar slope (5-20%), aspect (ENE and WNW facing slopes), and canopy position (outside of tree canopy) as much as possible to minimize landscape and microclimate variability among field sites. Soil morphology was described in the field and soil samples collected by genetic horizon (Soil Survey Staff, 2004). Collected samples were air dried and sieved to <2 mm. All further analyses performed on the <2 mm fraction, with the exception of soils used for DNA extraction and microbial community analysis (TRFLP) (see section 2.3 below).

## *2.2. Soil physical and mineralogical characterization*

Bulk density was measured for each genetic horizon at the limestone and basalt sites using a hammer core (Blake and Hartge, 1986). Relatively high coarse fragment content at the granite and rhyolite sites limited the use of the hammer core. As such, bulk density data for these sites were compiled from the USDA NRCS Soil Survey Laboratory database (<http://ssldata.nrcs.usda.gov/>). Particle size distribution was determined by pipette (Jackson, 1985). Samples for particle size analysis were pretreated to remove organic matter with sodium hypochlorite at pH 9.5 and dispersed with dilute sodium hexametaphosphate. Limestone soils did not react with HCl, but were pretreated with sodium acetate at pH 5.0 to remove any detrital carbonates. Following particle size analysis, dispersed clay and silt fractions were further separated by repeated

centrifugation (150 G) with dilute  $\text{Na}_2\text{CO}_3$ . Soil pH was measured 1:1 (wt/wt) in  $\text{H}_2\text{O}$ , and 1:1 in 1M KCl (Soil Survey Staff, 2004).

Total organic C, N, and  $^{13}\text{C}$  were determined by high temperature dry combustion with an elemental analyzer (Costech Analytical Technologies, Valencia, CA, USA) coupled to a continuous-flow mass spectrometer (Finnigan Delta PlusXL, San Jose, CA, USA) at the University of Arizona Stable Isotope Laboratory. Soil carbon from the limestone site was measured both before and after acid fumigation (Harris et al, 2001) to quantify any contribution of carbonates to the total C content and  $\delta^{13}\text{C}$  signature of these soils. Treated and untreated soils showed little to no variation in either C content or  $\delta^{13}\text{C}$ , so experimental results were assumed to be uninfluenced by detrital carbonates.

Qualitative mineralogical analysis by x-ray diffraction was conducted on the clay (<2  $\mu\text{m}$ ), silt (2 - 53  $\mu\text{m}$ ), and very fine sand (53 – 105  $\mu\text{m}$ ) fractions for all genetic horizons at each site. X-ray diffraction analyses were conducted at the University of Arizona Center for Environmental Physics and Mineralogy using a PANalytical X'Pert PRO-MPD X-ray diffraction system (PANalytical, Almelo, AA, The Netherlands) producing Cu-K $\alpha$  radiation at an accelerating potential of 45 kV and current of 40 mA and fitted with a graphite monochromator and sealed Xenon detector. Very fine sands and silts were analyzed as random powder mounts from 2-70 degrees two-theta. Clays were analyzed as oriented mounts on glass slides from 2-45 degrees two-theta with the standard treatments of K-saturation followed by heating to 350°C and 550°C, Mg-saturation, and Mg-saturation/glycerol solvation (Whittig and Allardice, 1986).

Quantitative mineralogical analysis of bulk soil by selective dissolution using sodium dithionite, acid ammonium oxalate, and sodium pyrophosphate was performed (Soil Survey Staff, 2004). Oxalate extracts Al ( $Al_o$ ), Fe ( $Fe_o$ ), and Si ( $Si_o$ ) from metal-humus complexes and short-range-order Fe oxyhydroxides and allophanic materials. Pyrophosphate extracts Al ( $Al_p$ ) and Fe ( $Fe_p$ ) from metal-humus complexes. Sodium dithionite extracts Fe ( $Fe_d$ ) from metal-humus complexes and crystalline and short-range-order Fe oxyhydroxides (Dahlgren, 1994). Iron and aluminum concentrations were determined by ICP-MS (Perkin Elmer Elan DRC II, Waltham, MA). Exchangeable Al was determined from 1N KCl extracts, followed by colorimetric titration (Pansu & Gautheyou, 2006).

### *2.3. T-RFLP analysis of bacterial communities*

We used TRFLP (Terminal Restriction Fragment Length Polymorphism) to compare soil bacterial community composition among sample sites. The TRFLP method has been used extensively to detect changes in diversity and composition of soil microbiota (Liu et al., 1997; Tokunaga et al., 2003). Although it does not provide as much information as clone libraries, this method is well suited for analysis of large sample sets and can be used to look at complex communities (Liu et al., 1997). Soil samples used for microbial community analysis were sampled separately from bulk material used for characterization and incubation. Samples for TRFLP analyses were placed in sterile 50 ml Falcon tubes (BD Biosciences; Canaan, CT) and frozen on dry ice in the field at the time of collection. Samples were collected from the A horizon(s) at

each sample site (i.e., samples from the limestone site contained soil from only one A horizon, but samples from the rhyolite site contained a mixture of soil from the A1, A2, and A3 horizons). Microbial samples were collected from each pedon for a total of three replicates per site.

DNA was extracted from 50 grams of homogenized A horizon soil following Schwartz et al. (2007). The primers 27F modified with the fluorescent dye 6-FAM (5' 6FAM - AGA GTT TGA TCM TGG CTC AG 3') and 519R (5' CCG CGG CKG CTG GCA C 3') were used to amplify part of bacterial 16s rRNA genes. Each PCR reaction contained 10 ng genomic soil DNA, 0.2  $\mu$ M each primer, 200  $\mu$ M dNTP, 2.5 mM MgCl<sub>2</sub>, 2 units Platinum Taq polymerase, and 1X Taq buffer. The PCR conditions consisted of a 2 min. cycle at 94° C, followed by 25 cycles of 30 sec. at 94°C, 30 sec. at 53°C, and 1 min of 72°C, and a final extension step at 72°C for 10 min. The PCR product was purified with a MinElute PCR Purification kit (Qiagen, Valencia, CA) and then digested with 5 units of MspI incubated at 37°C for 3 h. The fragments were analyzed on an ABI 3730xl DNA Analyzer and sized using GeneMapper software (Applied Biosystems). Only fragments between 50 and 600 base pairs in length with intensities higher than 0.5 % of the total fluorescence were used in subsequent analysis. Fragments were binned together if they differed from one another in size by less than 1 bp.

#### *2.4. Soil incubation*

Soil from each site was incubated in the laboratory to quantify short-term SOC dynamics and microbial community activity. Soil material (30 g of air dry soil) from the

uppermost A horizon and one subsurface horizon from each pedon were incubated in the dark for 40 days at ambient temperature ( $\sim 26^{\circ}\text{C}$ ). Subsurface soil samples were selected to have comparable depths and SOC content across sites, though genetic horizon designation varied among sites. Soil samples were placed in specimen cups (Starplex Scientific Inc.), wetted to 60% of field capacity (Cassel and Nielsen, 1986) with deionized water, and tamped to a uniform bulk density ( $1.2\text{ g cm}^{-3}$ ). Specimen cups were placed in either  $950\text{ cm}^3$  or  $475\text{ cm}^3$  mason jars; surface soils were placed in the larger jars to prevent respired  $\text{CO}_2$  from rising above 2% between headspace sampling intervals. Mason jars were fitted with septa to allow for headspace sampling. Soil moisture was maintained by the addition of 3 ml of water to the bottom of each jar to maintain relative humidity within the jar atmosphere at 100%. The incubation conditions provide optimum temperature and moisture for microbial growth and do not mimic field conditions. However, incubation of soils under controlled laboratory conditions is a widely used and commonly accepted method (Zibilske, 1994), and allows for direct comparison of respiration rates among soils.

Headspace samples were collected every 2-3 days by removal of a 1 ml aliquot of headspace gas using a syringe. Headspace  $\text{CO}_2$  concentration was measured using an Infra-Red Gas Analyzer (Qubit  $\text{CO}_2$  Analyzer, Kingston, ON, Canada). Jars were ventilated after each headspace measurement. Headspace gas samples for  $^{13}\text{CO}_2$  analysis were collected coincident with  $\text{CO}_2$  concentration samples on incubation days 5, 15, 25, and 40. Twelve milliliters of headspace gas were collected by syringe and injected into evacuated 12.5 ml glass tubes fitted with septa (Labco Limited: High Wycombe,

Buckinghamshire, UK). Headspace samples for  $^{13}\text{CO}_2$  were analyzed at the University of California Davis Stable Isotope Lab using a PDZ Europa 20-20 isotope ratio mass spectrometer (Sercon Ltd., Cheshire, UK) and reported on a per mil basis relative to the Pee Dee Belemnite standard (Balesdent and Mariotti, 1996). Both  $\text{CO}_2$  and  $^{13}\text{CO}_2$  values were corrected for background atmospheric values; background values averaged 0.06%  $\text{CO}_2$  and -9.9‰, respectively, over the course of the incubation. The isotopic enrichment of respired  $\text{CO}_2$  ( $\delta^{13}\text{C}_{\text{CO}_2}$ ) was expressed relative to that of the SOC ( $\delta^{13}\text{C}_{\text{SOC}}$ ):

$\Delta^{13}\text{C} = (\delta^{13}\text{C}_{\text{CO}_2} - \delta^{13}\text{C}_{\text{SOC}})$ , where all values were expressed in ‰ notation and greater values of  $\Delta^{13}\text{C}$  indicate greater enrichment of respired  $\text{CO}_2$  relative to SOC.

### 2.5. Microbial Parameters

Microbial biomass was measured by chloroform fumigation extraction on days 5, 15 and 40 of the incubation (Voroney et al., 1993). Chloroform fumigation extraction serves as a standard proxy for soil microbial biomass and exhibits accuracy in soils with varying acidity and SOC content (Vance et al, 1987). Briefly, six replicates of each soil sample were incubated for 5, 15, or 40 days. After incubation, three replicates were extracted with 0.5 M  $\text{K}_2\text{SO}_4$  (1:5 soil mass:solution ratio, 1 hour extraction time). The other three replicates were fumigated with ethanol-free chloroform, stored in the dark under vacuum for 24 hours, and then extracted with 0.5 M  $\text{K}_2\text{SO}_4$ . Extracted solutions were analyzed for total organic carbon and total nitrogen content using a Shimadzu TOC-VCSH TOC/TN Analyzer (Shimadzu Corporation, Columbia, MD). The difference in C

and N between fumigated and non-fumigated samples was considered to be derived from microbial biomass.

The metabolic quotient ( $q\text{CO}_2$ ) or specific respiration rate (Pirt, 1975) was calculated using the microbial biomass C measured by chloroform fumigation extraction and the mean of basal  $\text{CO}_2$  production from the 5 days prior to biomass measurement. Biomass C was divided by the rate of  $\text{CO}_2$  production and expressed as  $\mu\text{g C}_{\text{respired}} \mu\text{g}^{-1} \text{C}_{\text{biomass}} \text{day}^{-1}$ .

## 2.6. Data and statistical analyses

Calculation of  $\text{CO}_2$  respired throughout the incubation followed Zibilske (1994). Percent  $\text{CO}_2$  was converted to a mass of C and expressed on a per gram soil basis ( $\text{mg C g}^{-1}$  soil) and normalized to soil C content ( $\text{mg C g}^{-1}$  soil C). Nonlinear regression was used to fit a first order decay model to C mineralization data. The model that gave the best fit consisted of two pools, one time-independent pool and a labile pool:

$-dC/dt = C_0 + C_L e^{-k_L t}$ , where  $-dC/dt$  is [ $\text{mg C g}^{-1}$  soil C  $\text{day}^{-1}$ ],  $C_0$  the decomposition rate of a pool of SOC that exhibits a constant rate over time,  $C_L$  the decomposition rate of labile SOC that exhibits first order decay, and  $k_L$  the decomposition rate constant ( $\text{day}^{-1}$ ) for the labile pool. The pool size ( $\text{mg C g}^{-1}$  soil C) for each soil C pool,  $C_{T0}$  and  $C_{TL}$ , respectively, was estimated by integrating the area under the curve for each pool:

$$C_{T0} = C_0 t, \text{ and } C_{TL} = C_L / k_L (1 - e^{-k_L t}).$$

Each pedon was treated as a replicate for each sample site, providing a total of three replicates per study site. Significant differences between soil physical, chemical and

biological properties across sites were determined by two-way ANOVA using sample site and horizon depth (surface or subsurface) as the main effects followed by Tukey-Kramer *post hoc* test at a 95% confidence limit. Regression techniques were used to assess correlations between soil physicochemical variables, SOC content, and biological assays of SOC dynamics for surface and subsurface soils. Multiple linear regression was used to evaluate correlation of microbial parameters to soil physicochemical properties, namely, dithionite, oxalate and pyrophosphate extractable Fe and Al, clay content, exchangeable Al, soil pH, soil  $\delta^{13}\text{C}$ , and “dummy” variables representing sample site. Dummy variables are numerical variables used to distinguish between treatment groups (Zar, 1999), in this case the treatment effect associated with the differing mineralogy of the sample sites. We used a binary response (0 or 1) dummy variable for each sample site. To avoid issues of colinearity, explanatory variables with correlation coefficients greater than 0.70 were not concurrently included in regression models (Zar, 1999).

Microbial community fingerprint patterns were examined graphically using the non-metric dimensional scaling (NMS) with PC-ORD version 5 software (B. McCune and M. J. Mefford, 2006). NMS axes summarize community relatedness among samples on the basis of distance measure and rank transformation. Ordination was based on Sørensen’s distance (Faith et al., 1987) with random starting configurations, 250 runs with real data, a maximum of 400 iterations per run, and a stability criterion of 0.00001. A Monte-Carlo permutation procedure with 250 random runs was used to assess axis significance. Examination of stress patterns suggested two dimensions were appropriate for the final ordination. A stress value greater than 20 indicates that the MDS plot is close

to random, less than 20 indicates a useful two-dimensional picture and less than 10 corresponds to an ideal ordination (Clarke, 1993).

A multiresponse permutation procedure (MRPP) using Sørensen's distance and rank transformation was used to test for significant differences in community composition between groups defined by sample site. MRPP is a nonparametric method for testing group differences (McCune and Grace, 2002), and is similar to multivariate analysis of variance (MANOVA). The MRPP statistic measures within-group homogeneity compared to that expected by chance. A statistic value of 1 indicates complete homogeneity in a group and values below 0 indicate less agreement within groups compared to random expectation.

Relationships between communities to physical and chemical soil properties were assessed through joint bi-plots with soil physicochemical data, namely dithionite, oxalate and pyrophosphate extractable Fe and Al, clay content, exchangeable Al, soil pH, soil  $\delta^{13}\text{C}$ , soil C and N content, and the average C:N of the microbial biomass during soil incubation. Because the TRFLP profiles were developed from the entire A horizon, the physicochemical data from multiple A horizons were averaged when necessary. The angle and length of the lines on the bi-plot indicate the direction and strength of the correlation among soil physicochemical variables and microbial community. Varimax rotation on the ordination axes was used to maximize variance explained by the most significant correlation vectors. Univariate relationships between the newly rotated ordination scores and environmental variables were examined with Pearson's correlation coefficient and regression analysis in JMP 7.0 (SAS Institute, Cary NC).

### 3. Results

#### 3.1. Soil data

The study sites captured a clear soil acidity gradient that corresponded with significant variation in soil physiochemical properties (Table 2). Soil acidity decreased across sites from rhyolite to granite to basalt to limestone. Soil pH ranged from 5.2 to 7.1 (1:1 in water) and from 3.7 to 5.6 (1:1 in KCl) in soils from the rhyolite and limestone sites, respectively. Soil pH was significantly correlated with Al-phases, i.e., low pH corresponded with greater exchangeable Al and Al-humus complexes (Fig. 1).

Exchangeable Al was measured in the more acidic horizons of the granite soils, but only found in significant amounts in rhyolite soil horizons, where subsurface pH values were below 5.0 in H<sub>2</sub>O and 4.0 in KCl (Figure 1a). Al-humus complexes were present in all soils and concentrations were inversely related to soil pH (Figure 1b). Similarly, the concentration of Fe-humus complexes exhibited a negative correlation with soil pH, with rhyolite soils having significantly greater Fe<sub>p</sub> than soils from the other sites (Table 2). Significant amounts of allophanic materials were not found in any of the soils.

Concentrations of oxalate and dithionite-extractable Fe (Fe<sub>o</sub> and Fe<sub>d</sub>) varied significantly among sites (Table 2). In contrast to Al phases, Fe-oxyhydroxides did not exhibit correlation with pH and were more of a reflection of the mineral assemblage of the geologic parent material. Soils from the basalt site were enriched in Fe-oxyhydroxides as demonstrated by significant amounts of crystalline (Fe<sub>d</sub>-Fe<sub>o</sub> of 10 kg m<sup>-2</sup>) and short-range-order (Fe<sub>o</sub> of 2.9 kg m<sup>-2</sup>) materials reflecting the mafic mineralogy of

the basalt parent material. Basalt soils also contained significantly greater clay content relative to the other parent materials (Table 2). The enrichment of Fe-oxyhydroxides and high clay content of the basalt soils suggests substantial mineral surface area and potential for SOC adsorption. Soils from the granite and rhyolite sites contained relatively few Fe-oxyhydroxides, reflecting the felsic nature of the parent materials. Soils from the limestone site had unexpectedly large Fe-oxyhydroxide contents, mostly in the form of short-range-order Fe hydroxides. Overall, data indicated that the acidic soils from the rhyolite site were enriched in metal-humus complexes, whereas the more neutral soils from the basalt site were enriched in Fe-oxyhydroxides and clays.

Crystalline mineralogy as determined by XRD varied among sites and was mainly a function of parent material. All soils contained a mix of kaolinite and an Al-hydroxy interlayered 2:1 phyllosilicate, though total clay content varied significantly among sites (Table 2). The main differences in mineral assemblage among sites were in the coarse fraction. Rhyolite soils were dominated by quartz and K-spar with smaller amounts of mica and a zeolite. Coarse fractions from the granite soils contained quartz, alkali feldspar, mica, and chlorite. Silt and sand fractions from the basalt site were dominated by quartz, plagioclase feldspar and small amounts of mica. Silt and sand fractions from the limestone site also contained mostly quartz, with smaller amounts of alkali feldspar. Neither the basalt nor the limestone bedrock contained significant amounts of quartz, indicating a substantial eolian input to the soils at these sites. Since these sites are geographically close to one another, it is possible that they share a common dust source.

Soil carbon content varied significantly among sample sites (Table 2). Rhyolite soils contained significantly greater SOC ( $11 \text{ kg m}^{-2}$ ) relative to the other sites, followed by the basalt ( $8.7 \text{ kg m}^{-2}$ ), granite ( $5.3 \text{ kg m}^{-2}$ ) and limestone ( $3.5 \text{ kg m}^{-2}$ ). Regression analyses indicated significant correlation between SOC content and soil mineral variables (Figure 2). Crystalline Fe-oxyhydroxide content, Fe-humus complexes, and Al-humus complexes accounted for the greatest amount of variation in SOC content across sample sites. Soil carbon increased linearly with crystalline Fe-oxyhydroxide content in limestone, granite, and rhyolite soils, but showed a nonlinear relationship when basalt soils were included (Figure 2c). Fe-humus and Al-humus exhibited positive correlation with SOC content. Fe-humus content showed a linear relationship, whereas Al-humus content showed an exponential rise to maximum relationship to SOC content.

### *3.2. T-RFLP analysis of bacterial communities*

Analysis of the TRFLP data indicated significant separation in community composition across sites that corresponded with variation in soil physiochemical properties (Figure 3). The final stress of the NMS ordination plot was less than 10 (stress = 8.8;  $p = 0.008$ ), indicating the data was fit well (Clarke, 1993). The communities separated into three groups by site along the primary axis (Figure 3). The primary ordination axis was significantly correlated with soil acidity (pH 1:1 in  $\text{H}_2\text{O}$ :  $r = 0.84$ ,  $p = 0.0006$ ; pH 1:1 in KCl:  $r = 0.93$ ,  $p < 0.0001$ ), exchangeable Al ( $r = -0.90$ ,  $p < 0.0001$ ), and amorphous Fe-oxyhydroxides ( $\text{Fe}_o\text{-Fe}_p$ :  $r = 0.77$ ,  $p = 0.004$ ;  $\text{Fe}_o$ :  $r = 0.73$ ,  $p = 0.008$ ), indicating these parameters accounted for the majority of variation in microbial

community composition among sites. The primary ordination axis was also correlated with Al-humus complex content (Al<sub>p</sub>:  $r = -0.59$ ,  $p = 0.04$ ), C:N of microbial biomass ( $r = -0.67$ ,  $p = 0.02$ ), and  $\delta^{13}\text{C}\%$  of soil ( $r = 0.68$ ,  $p = 0.01$ ). The rhyolite and granite sites further separated along the secondary axis. The secondary axis was most strongly correlated with Fe-humus complexes (Fe<sub>p</sub>:  $r = 0.72$ ,  $p = 0.009$ ) indicating separation in community composition between the acidic sites based on content of metal-humus complexes. According to the MRPP, microbial communities differed significantly among the four sites ( $A = 0.18$ ,  $p = 0.001$ ). All pairwise comparisons of sites were significantly different ( $A > 0.1$ ,  $p < 0.05$ ), except for bacterial communities between the basalt and limestone sites (Table 3).

### *3.3. Incubation Results*

A short-term incubation was performed to evaluate differences in microbial dynamics and utilization of labile SOC among sites. Microbial dynamics were quantified as SOC mineralization rates (Figure 4), soil microbial biomass and metabolic quotient (Figure 5), and  $\delta^{13}\text{C}$  of respired  $\text{CO}_2$  (Figure 6). The microbial dynamic variables were regressed against soil physicochemical variables to identify correlation among mineralogical and microbial parameters.

#### *3.3.1. Soil C Mineralization*

Cumulative SOC mineralized and mineralization rates varied by site and with soil depth (Table 4, Figure 4). Rhyolite soils exhibited the lowest cumulative SOC

mineralization, both on a 'per gram of soil' and 'per gram of SOC' basis across all sites and soil depths (Figure 4). The basalt and limestone soils tended to mineralize the greatest SOC, with substantially greater SOC mineralization in limestone surface soils relative to the other sites when normalized to SOC content (Fig. 3b). Nearly 9%, i.e., 90 mg C g<sup>-1</sup> soil C, of SOC was mineralized in limestone surface soils relative to less than 2% of SOC mineralized in the rhyolite soils. The short incubation time limited SOC mineralization to the most labile SOC pool. Carbon isotope analyses of the respired CO<sub>2</sub> (see *Section 3.3.3*) suggested much of the mineralized SOC was sourced from turnover of microbial biomass.

Decomposition model parameters showed variation among sites, but few significant differences (Table 4). Initial decomposition rates ( $C_0$  and  $C_L$ ), C pool sizes ( $C_{T0}$  and  $C_{TL}$ ), and cumulative CO<sub>2</sub> respired [mg C (g soil C)<sup>-1</sup>] were greater in the subsurface relative to surface soils for all parent materials, except the limestone site. The greatest limestone initial decomposition rates and pool sizes were observed in limestone surface soils, with values significantly greater than the other sites. In contrast, the rhyolite soils tended to exhibit the lowest values for all model parameters, although differences were only statistically significant in a few cases.

Regression analyses indicated significant correlation between mineralization model parameters and soil physicochemical and microbial variables despite the lack of significant differences among sites (Table 5). The average microbial biomass C:N and a dummy variable representing the limestone site explained 90% of the variation in total SOC mineralization in surface soils ( $P < 0.05$ ), i.e., SOC mineralization was negatively

correlated with biomass C:N and positively correlated with soils derived from limestone. The basal decomposition rate,  $C_0$ , demonstrated significant correlation with Fe-humus content and  $\delta^{13}\text{C}$  of SOC prior to incubation ( $R^2=0.88$ ,  $P<0.05$ ). The initial decomposition rate of the SOC pool that exhibited first order decay,  $C_L$ , showed significant positive correlation with soil pH ( $R^2 = 0.64$ ,  $p<0.05$ ), and the first order rate constant,  $k_L$ , exhibited significant correlation with soil pH and biomass C:N ( $R^2 = 0.57$ ,  $P<0.05$ ). Subsurface SOC mineralization model parameters exhibited no significant correlations with soil mineral variables, but were all significantly and negatively correlated to biomass C:N (Table 5).

### 3.3.2. Soil Microbial Biomass & Metabolic Quotient

Soil microbial biomass C ( $C_{\text{mic}}$ ) and biomass C:N exhibited variation over time and with soil depth (Figure 5a). In general, surface soils had greater  $C_{\text{mic}}$  and lower C:N than subsurface soils. With the exception of the rhyolite subsurface,  $C_{\text{mic}}$  increased up to day 15 of the incubation, with subsequent decline over time. Though differences in  $C_{\text{mic}}$  among sites were not statistically significant, variation in  $C_{\text{mic}}$  did exhibit significant correlation with soil physicochemical variables. Subsurface  $C_{\text{mic}}$  was negatively correlated with Al-humus content ( $R^2=0.43$ ,  $P=0.005$ ), whereas surface horizon  $C_{\text{mic}}$  was positively correlated with SOC content of the soil prior to incubation ( $R^2=0.55$ ,  $P=0.02$ ). Biomass C:N also varied among sites and soil depth (Figure 5b). Biomass C:N was greater in subsurface horizons and exhibited highly significant negative correlation with soil pH ( $R^2=0.75$ ,  $P=0.0003$ ). Surface biomass C:N did not correlate with soil pH;

however the relatively acidic rhyolite surface soils did have significantly greater biomass C:N relative to the other parent materials.

The  $q\text{CO}_2$  values were greatest at incubation day 5 in both surface and subsurface soils (Figure 5c), decreased from day 5 to day 15, and exhibited little change between days 15 and 40. Such a pattern is not unusual and was most likely the result of disturbance to microbial communities during sample preparation (Zibilske, 1994). The  $q\text{CO}_2$  of surface soils was significantly higher than  $q\text{CO}_2$  of subsurface soils across all parent materials. The average metabolic quotient of the rhyolite soils was the lowest of all four parent materials in both surface and subsurface horizons, although differences were not significant. The  $q\text{CO}_2$  values did not exhibit significant correlation with soil mineral variables, but did correspond with microbial biomass C:N ( $R^2=0.50$ ,  $P=0.0001$ ), suggesting microbial efficiency increased with increasing biomass C:N.

### 3.3.3. *Isotopic signature of respired CO<sub>2</sub>*

In general, the  $^{13}\text{C}$  enrichment of respired  $\text{CO}_2$  reflects the enrichment level of the utilized substrate. However, the fraction of SOC utilized by the microbial community may not have a  $\delta^{13}\text{C}$  which is representative of the SOC as a whole (Balesdent and Mariotti, 1996). Respired  $\text{CO}_2$  was enriched relative to SOC over the course the incubation, indicating utilization of a C source substantially enriched in comparison to bulk SOC. This may reflect utilization of labile forms of plant-derived organic matter such as starches and sugars, or recycling of bacterial and fungal biomass that tend to be  $^{13}\text{C}$ -enriched relative to their growth substrate (Santruckova, 2000; Henn & Chapela,

2000; 2002). Subsurface  $\Delta^{13}\text{C}$  decreased over time, with the greatest change from 6.0 to 1.5‰ noted in rhyolitic soils (Figure 6). Decreased  $\Delta^{13}\text{C}$  over time likely resulted from utilization of dead microbial biomass at the start of the incubation with transition to more recalcitrant  $^{13}\text{C}$ -depleted SOC components over time. The soils were air dried prior to incubation, such that upon re-wetting a large amount of dead and lysed microbial biomass would be available for consumption (Fierer and Schimel, 2003). The surface soil  $\Delta^{13}\text{C}$  isotopic signature of respired  $\text{CO}_2$  demonstrated little variation ranging from 3-4‰ for the duration of the incubation. The greater  $\Delta^{13}\text{C}$  from the limestone surface horizon was likely a function of SOC derived from  $\text{C}_4$  grasses, which were noted at the field site.

## 4. Discussion

### *4.1 Physical & chemical properties controlling SOC content*

Significant variation was observed in SOC content among sites and the data suggest these differences may be explained by soil physicochemical properties, especially pH, metal-humus complex content, and Fe-oxyhydroxide content. Soils from the rhyolite site were rich in both Al- and Fe-humus complexes and exchangeable  $\text{Al}^{3+}$ . Soils from the basalt site were rich in Fe-oxyhydroxides and clay. Soils from these sites had significantly higher SOC contents than soils from the granite and limestone sites.

The rhyolite site had the highest SOC content (Table 2). The felsic and aphanitic nature of the rhyolite parent material yields soils with high acidity. In turn, the low pH of these soils yields high concentrations of Fe- and Al-humus complexes and exchangeable  $\text{Al}^{3+}$ . Complexation of SOC with dissolved Fe- and Al- induces chemical and

conformational changes that reduce SOC bio-availability (Baldock and Skjemstad, 2000; Nierop et al, 2002; Scheel et al., 2007), and favor precipitation of metal-humus complexes from solution. Soil organic carbon may also be preserved through suppression of microbial activity by exchangeable  $Al^{3+}$  (Illmer et al, 1995, 2003).

Soils from the basalt site also contained high SOC content. Basalt soils were rich in clays and “free” or pedogenic Fe-oxyhydroxides, suggesting high surface area and strong aggregation may play a role in SOC stabilization in these soils. The basalt soils had significantly higher crystalline Fe-oxyhydroxide content than soils from the other sites, and the significant positive correlation noted between crystalline Fe-oxyhydroxides and SOC (Fig. 2c) suggests sorption to Fe-oxyhydroxide surfaces as the dominant mechanism of SOC stabilization in these soils. The relationship between SOC and dithionite-extractable Fe content was non-linear when basalt soils were included in the analysis (Figure 2c). This may be due to differences in the relative importance of sorption as a carbon sequestration mechanism among sites. In the more acidic rhyolite and granite soils, sorption to mineral surfaces may account for only a portion of SOC retention. In contrast, basalt and limestone soils have a more neutral pH, and sorption is likely the predominant mechanism of C retention in these soils. Laboratory studies using natural SOC have shown that Fe-oxyhydroxide phases at pH 4-7 can sorb a maximum of 0.22 g OC g Fe<sup>-1</sup> (Kaiser and Guggenberger, 2007), when the source of Fe is solely ferrihydrite. In natural settings, all pedogenic Fe is not likely to be in the form of ferrihydrite and this ratio is most likely lower. OC to Fe ratios were far above 0.22 g OC g Fe<sup>-1</sup> in the granite and rhyolite sites, suggesting that sorption to Fe-oxyhydroxide surfaces cannot account

for the majority of the SOC in these soils. In contrast, basalt horizons exhibit OC:Fe ratios close to this value, suggesting greater dependence of SOC content on Fe-oxyhydroxides.

Physical and chemical properties and low SOC content of the granite and limestone soils suggest these soils lack properties necessary for SOC preservation and sequestration. Circum-neutral pH, low clay content, and low metal-oxyhydroxide content likely contribute to the granite and limestone soils exhibiting relatively labile SOC and hence lower overall SOC content. Specifically, limestone soil pH was in the range favorable for microbial growth and metabolism (Paul and Clark, 1996), likely favoring SOC decomposition. In contrast, the low clay, quartz rich granitic soils contain relatively low charged surface area for sorptive stabilization of SOC, and few weatherable mafic minerals to source Al- and Fe- for humus complexation (Chenu and Stotsky, 2002). Similarly, Rasmussen et al. (2006) and Trumbore et al. (1996) found SOC in granitic soils demonstrated rapid turnover that was suggested to be controlled by lack of physical and chemical stabilization.

#### *4.2 Physical & chemical properties controlling microbial community dynamics*

Results of our study strongly suggest that soil mineral assemblage affects SOC content both directly and indirectly, directly through its influence on surface chemistry and indirectly through its influence on microbial communities. Metal-humus complexes, pedogenic Fe-oxyhydroxides, and pH were identified as key physiochemical variables accounting for variation in SOC content, microbial community composition and

microbial activity across sites, demonstrating that soil properties that suppress microbial growth and respiration are also associated with greater SOC content.

Soil pH was an important overarching control of SOC dynamics. pH and SOC content were not directly correlated, but decomposition models indicated larger labile SOC pools for the more basic soils (basalt and limestone) relative to the acid soils (granite and rhyolite). pH was significantly correlated with mineral and microbial variables, corresponding with known control of pH over microbial diversity, activity and biomass (Anderson and Domsch, 1993; Schnittler and Stephenson, 2000; Bååth and Anderson, 2003; Fierer and Jackson, 2006) as well as mineral dissolution and metal speciation (Rai and Kittrick, 1994). For example, Fe-oxyhydroxide solubility increases with decreasing pH below 6-7 (Lindsay, 1979; Wagai and Mayer, 2007), favoring complexation and precipitation of  $\text{Fe}^{3+}$  with SOC in acid soils. The activity of  $\text{Fe}^{3+}$  in solution maintained by Fe-oxyhydroxides decreases by 1000 times for each unit increase in pH (Lindsay, 1979). Therefore at higher soil pH, Fe is less soluble and sorptive reactions between negatively charged Fe-oxyhydroxide surfaces and SOC are favored over formation of metal-humus complexes (Tipping et al., 2002). Similarly, Al-oxyhydroxide solubility and concentration of  $\text{Al}^{3+}$  increase with soil acidity, particularly below pH 5.0 (Lindsay, 1979). The data from the various parent materials follow these basic trends with significant increase of Fe- and Al-humus complexes and exchangeable  $\text{Al}^{3+}$  with decreasing pH (Figure 1). The toxic effect of monmeric Al on plants and associated microbial communities in acidic soils is well established (Illmer et al., 1995, Pina and Cervantes, 1996; Williams, 1999; Marschner et al., 2000; Kochian, 2005).

Greater available Al and metal-humus complexation likely explains the significant correlations between soil pH, bacterial community composition and the C:N of microbial biomass and indicates pH control of bacterial to fungal ratios. Moreover, metal-humus complexes and poorly-crystalline Fe-oxyhydroxides were correlated with microbial community composition and SOC decomposition rates in surface soils.

No single physicochemical variable exhibited control of subsurface soil respiration rates across sites, rather respiration rates varied as a function of biomass C:N. The relative  $^{13}\text{C}$  enrichment of respired  $\text{CO}_2$  and correlation of respiration rate parameters with microbial biomass C:N suggest that microbial biomass is an important, perhaps even primary, substrate for subsurface microbial communities. The C:N ratio of the biomass is thus of significance both as an indicator of fungal: bacterial ratio and substrate quality, and likely explains the lack of correlation of mineralization parameters with soil physicochemical variables. In contrast, surface soils contained substantial amounts of energy-rich litter derived C such that microbial respiration was not constrained by a lack of labile C, but rather soil physicochemical properties such as pH and metal-humus complex, content were the dominant limiting factors.

Variation among sites in the observed metabolic quotient ( $q\text{CO}_2$ ) may also be explained by variation in biomass C:N among sites. Rhyolite soil microbial biomass exhibited markedly different patterns than the other soils, with slow growth and low respiration rates throughout the incubation, and high biomass C:N suggesting dominance by fungal rather than bacterial communities. These patterns corresponded with low  $q\text{CO}_2$  values, contradicting previous findings that demonstrated a marked increase in metabolic

quotient with decreasing soil pH (Anderson & Domsch, 1993). However,  $qCO_2$  varies with fungal-to-bacterial ratio (Probst et al, 2008), with highly negative relationships observed between increasing fungal-to-bacterial ratio and  $qCO_2$  due to a higher substrate use efficiency by fungi (Sakamoto & Oba, 1994). Furthermore, significant correlations between biomass C:N ratio and  $qCO_2$  may indicate a dependence of metabolic efficiency on community composition (Sakamoto & Oba, 1994; Blagodatskaya & Anderson, 1998; Han et al, 2007). Soil pH varies with mineral assemblage, and microbial community composition and respiration vary with pH (Bååth and Anderson, 2003; Bååth and Arnebrant, 1994). Thus soil mineral assemblage exerts indirect control over SOC dynamics and turnover through its influence on microbial communities.

## 5. Summary

Soil organic carbon content, microbial community composition, and soil physicochemical properties varied significantly among sites. Data indicated variance in carbon stabilization mechanisms among sites that followed variation in physicochemical properties: sorptive stabilization of carbon was likely of greater importance in basalt and limestone soils, whereas metal-humus complexation played a more significant role in granite and rhyolite derived soils. The variation in carbon stabilization mechanism may be directly related to parent material control over soil pH and mineral assemblage. Additionally, significant variation in microbial community composition and efficiency of microbial metabolism with soil physicochemical properties indicates parent material control over microbial processing of soil carbon. Parent material thereby exerts an

indirect control of soil carbon dynamics through controls of the soil microbial community. The data thus demonstrate that within a given ecosystem, soil parent material and related soil physicochemical properties must be considered in landscape and regional scale models of soil carbon dynamics.

#### **6. Acknowledgements:**

This work was supported by a grant from the National Science Foundation (DEB #0543130).

## 7. Figures and Tables

Figure 1: Regression analysis of soil pH to [a] depth-weighted average exchangeable Al content by horizon, [b] Al from metal-humus complexes. Exchangeable Al is expressed in units of centimoles of charge per kg of soil. Al-humus complex concentration is expressed as kg of pyrophosphate extractable Al ( $Al_p$ ) per square meter of soil. Soil samples were taken from sites with four different parent materials: rhyolite, granite, basalt, limestone, all found in *Pinus Ponderosa* forests. Soils exhibit a wide range of pH values and therefore differ in their Al chemistry.

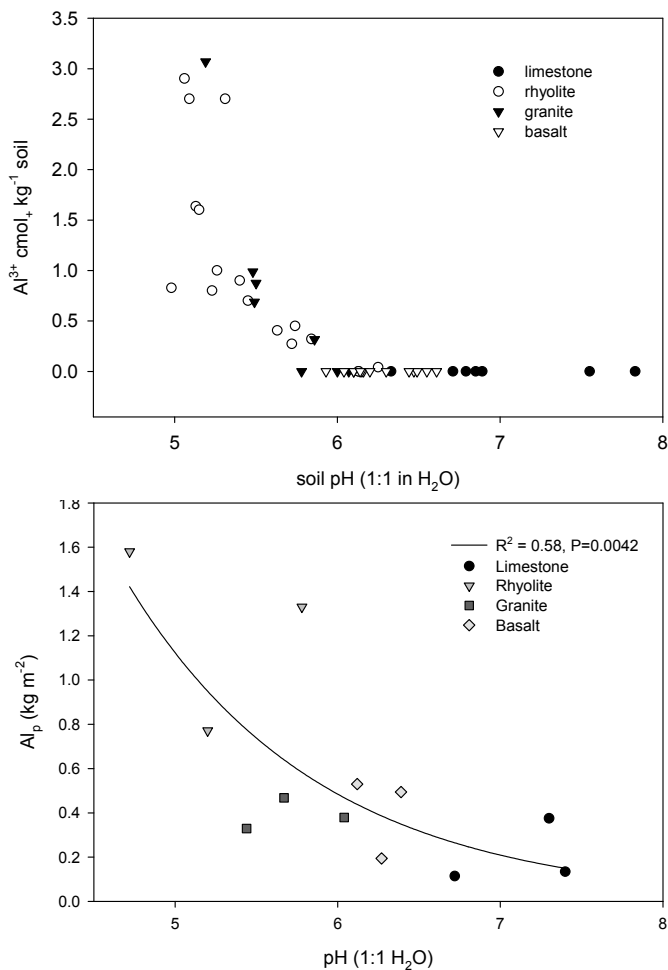


Figure 2: Soil organic carbon (SOC) content relative to soil mineral properties for a range of geologic parent materials (rhyolite, granite, basalt, limestone) in *Pinus Ponderosa* forests in Arizona: [a] Al-humus complexes (pyrophosphate extractable Al,  $Al_p$ ), [b] Fe-humus complexes (pyrophosphate extractable Fe,  $Fe_p$ ), and [c] crystalline Fe-oxyhydroxides (defined as the difference between dithionite and oxalate extractable Fe,  $Fe_d - Fe_o$ ). Curves represent the best fit linear and non-linear functions using least-squares regression. The linear function in [c] was fit excluding the basalt parent material samples; the non-linear function includes the basalt parent material samples, showing the strong dependence of C content on crystalline Fe content in basalt soils.

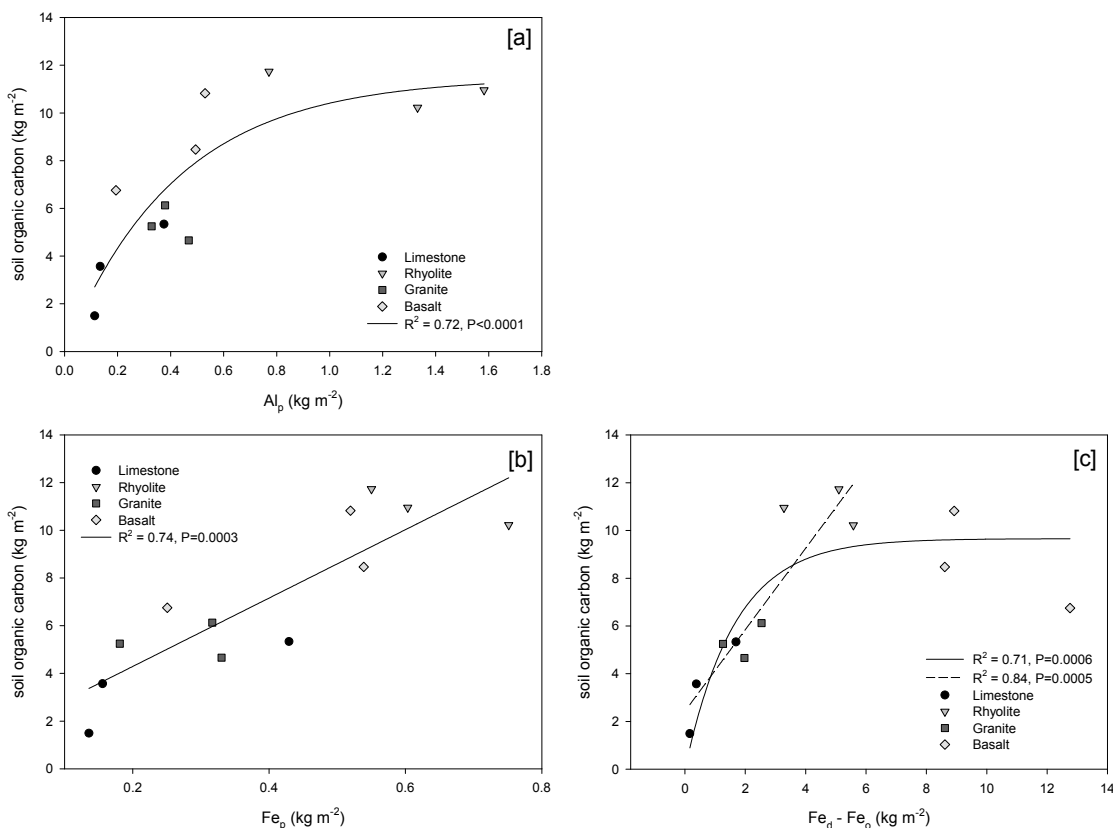


Figure 3. Non-metric multidimensional scaling ordination of TRFLP patterns. The plot was constructed using the 113 operational taxonomic units generated from the TRFLP profiles. Symbols code for sample site (basalt, rhyolite, limestone, and granite). Lines show correlation vectors of the measured environmental variables with the ordination:  $Fe_p$ ,  $Fe_o - Fe_p$ ,  $Fe_o$ ,  $\delta^{13}C\%$  of soil, respiration, C:N biomass (incubation),  $Al^{3+}$  (exchangeable aluminum), pH in  $H_2O$  (1:1 soil:water), pH KCl (1:1 soil:water). The final solution has two dimensions (stress = 8.8,  $p = 0.008$ ).

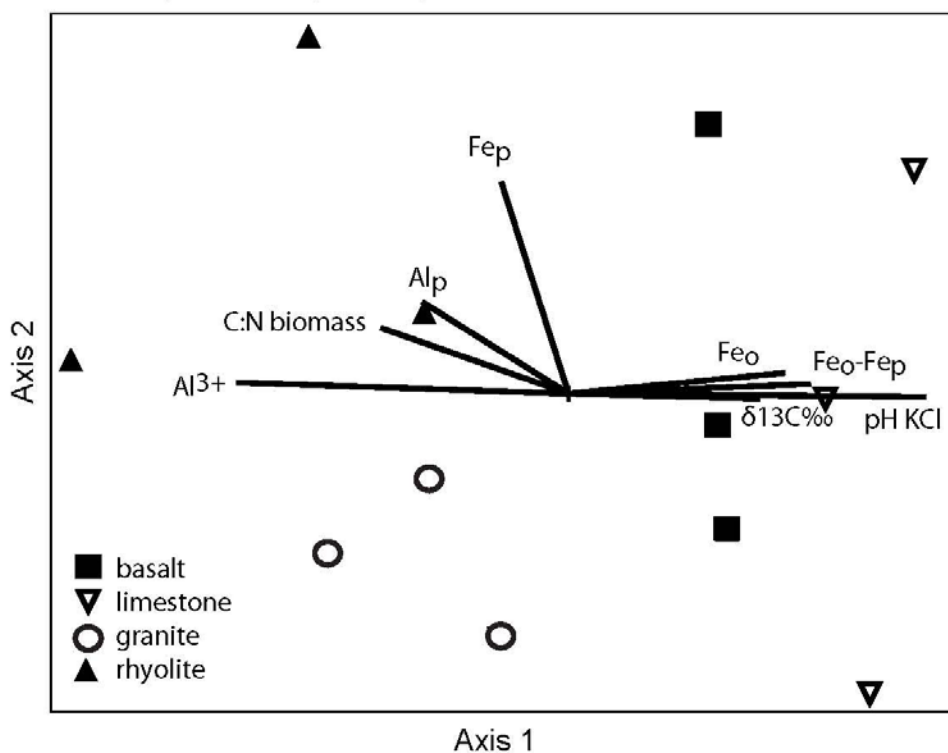


Figure 4: Cumulative C respired versus incubation day represented on a soil basis [ $\text{mg C}(\text{g soil})^{-1}$ ] and C activity basis [ $\text{mg C}(\text{g soil C})^{-1}$ ] for surface soils (a,b) and subsurface soils (c,d). Data is presented by soil parent material. Each data point is the average of three replicates, with bars representing standard error.

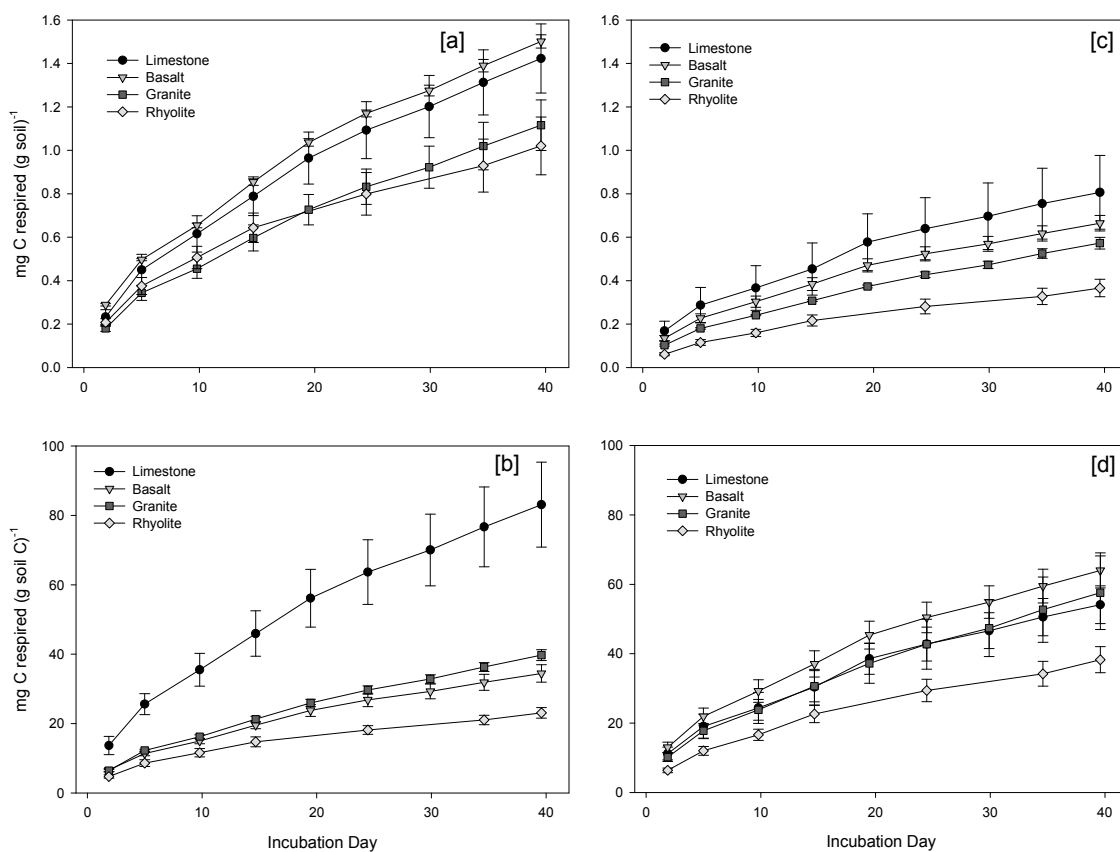


Figure 5: Changes in microbial biomass C [a], biomass C/N [b], and  $q\text{CO}_2$  [c] by parent material and soil depth (surface<sub>1</sub>/subsurface<sub>2</sub>) over time. Measurements were made after 5, 15, and 40 days of incubation. C/N ratios of biomass were much higher in subsurface than surface soils, while metabolic quotients were lower.

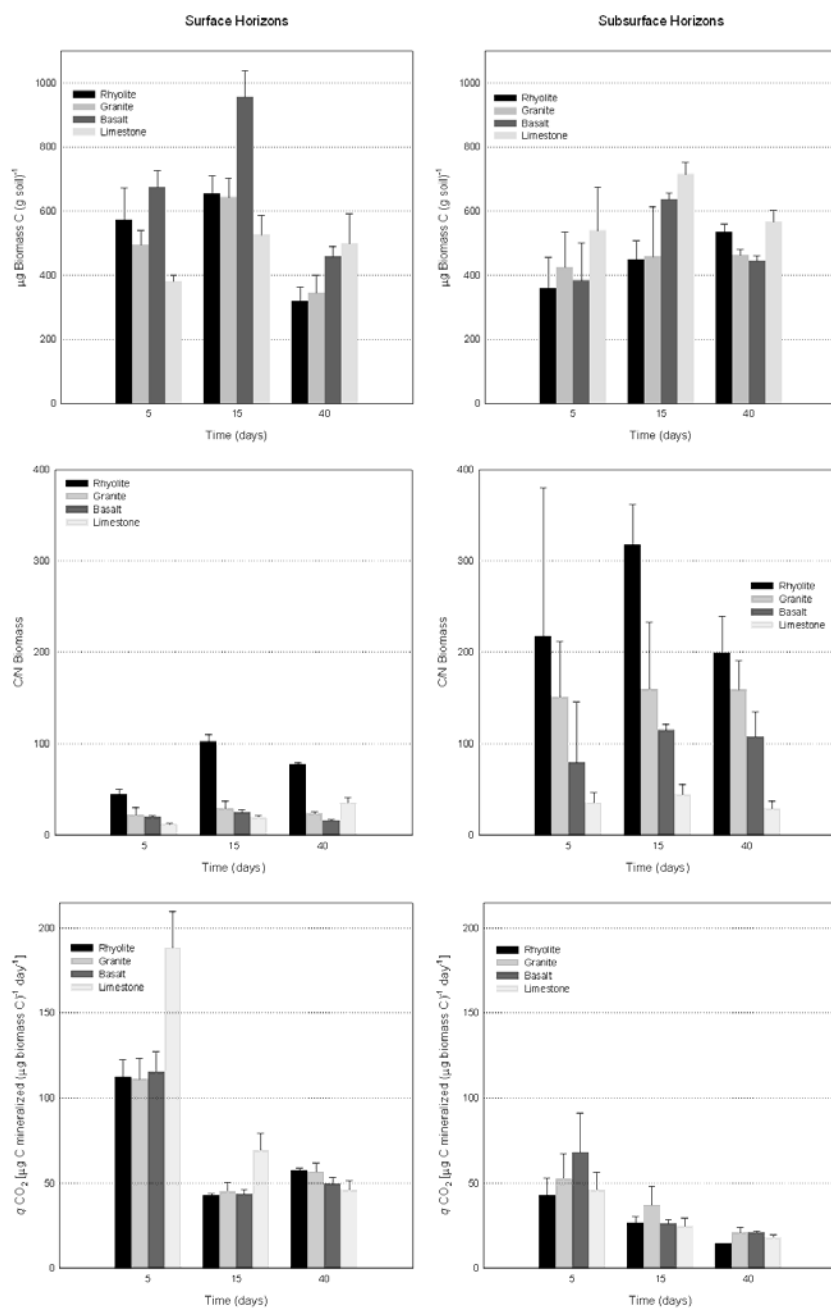


Figure 6: Change in  $\delta^{13}\text{C}$  of respired  $\text{CO}_2$  over time for surface and subsurface soils.

$\Delta^{13}\text{C}(\text{‰})$  is the enrichment of respired  $\text{CO}_2$  in relation to the  $\delta^{13}\text{C}$  of the soil. Larger values indicate greater enrichment of  $\text{CO}_2$  relative to the respective soil.  $\text{CO}_2$  respired from surface soils was  $\sim 4\text{‰}$  enriched relative to the soil over the course of the entire

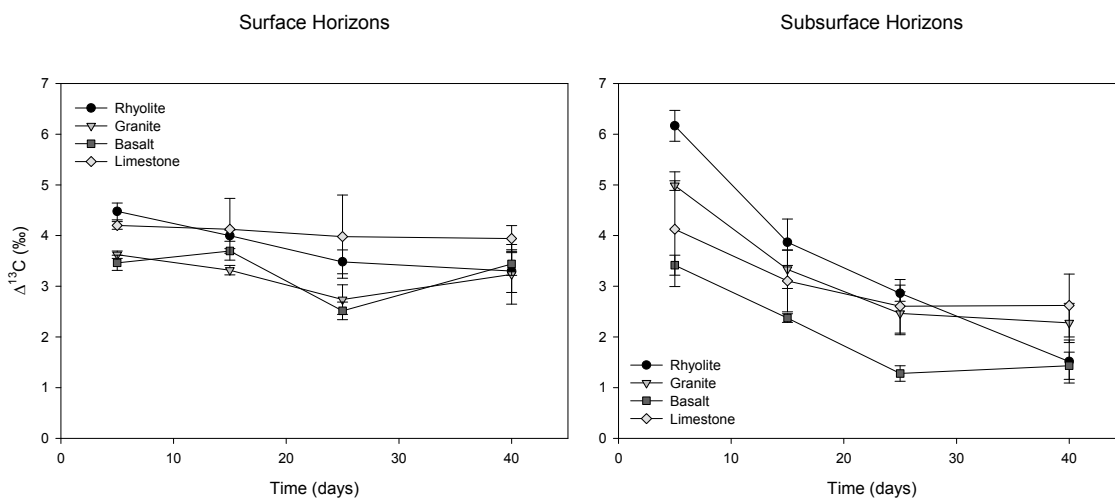


Table 1. Site data for the range of parent materials sampled in Pinus Ponderosa forests in Arizona

<b>Parent Material</b>	<b>Location (Latitude / Longitude)</b>	<b>Elevation (m)</b>	<b>MAP (mm)</b>	<b>MAT (°C)</b>	<b>Soil Classification</b>
<b>Rhyolite</b>	31°53'15" / 109°16'48"	2,591	815	12	loamy, mixed, superactive, mesic Typic Haplustept
<b>Granite</b>	32°25'8" / 110°44'7"	2,439	680	12	loamy-skeletal, mixed superactive, mesic Typic Ustorthent
<b>Basalt</b>	35°9'34" / 111°44'27"	2,195	675	9	clayey-skeletal, mixed superactive, mesic Typic Paleustoll
<b>Limestone</b>	35°5'4" / 111°36'35"	2,134	685	10	loamy, mixed, superactive, mesic Lithic Argiustoll

MAP - mean annual precipitation. Taken from the PRISM Climate dataset (4 km pixel resolution).

MAT - mean annual temperature. Taken from the PRISM climate dataset (4 km pixel resolution).

Soils classified according to U.S. Soil Taxonomy, 10th Edition, 2006.

Table 2. Analysis of variance of soil properties

Parent Material	pH 1:1 H <sub>2</sub> O (depth-weighted avg)	pH 1:1 KCl	Organic Carbon (kg m <sup>-2</sup> )	C:N	Clay	Fe <sub>d</sub> - Fe <sub>o</sub> (kg m <sup>-2</sup> )	Fe <sub>o</sub> (kg m <sup>-2</sup> )	Fe <sub>p</sub>	Al <sub>p</sub>	Exch'ble Al (cmol. m <sup>-2</sup> )
Rhyolite	5.2 (±0.2) <sup>C</sup>	3.7 (±0.1) <sup>C</sup>	11.0(±0.0) <sup>A</sup>	16.5 (±1.0) <sup>A</sup>	92.3 (±10.2) <sup>AB</sup>	4.7 (0.7) <sup>B</sup>	1.1 (±0.1) <sup>B</sup>	0.6 <sup>A</sup>	1.2 (±0.2) <sup>A</sup>	9.2 (±3.2) <sup>A</sup>
Granite	5.7 (±0.1) <sup>BC</sup>	4.2 (±0.1) <sup>BC</sup>	5.3(±0.0) <sup>B</sup>	19.2 (±3.5) <sup>A</sup>	16.4 (±3.1) <sup>B</sup>	1.9 (0.4) <sup>BC</sup>	0.4 <sup>C</sup>	0.3 <sup>B</sup>	0.4 <sup>B</sup>	1.3 (±0.7) <sup>B</sup>
Basalt	6.3 <sup>AB</sup>	4.9 <sup>AB</sup>	8.7 (±0.1) <sup>A</sup>	17.1 (±0.3) <sup>A</sup>	180.0 (±55.5) <sup>A</sup>	10.1 (1.3) <sup>A</sup>	2.9 (±0.1) <sup>A</sup>	0.4 (±0.1) <sup>B</sup>	0.4 (±0.1) <sup>B</sup>	0 <sup>B</sup>
Limestone	7.1 (±0.1) <sup>A</sup>	5.6 (±0.2) <sup>A</sup>	3.5 (±0.1) <sup>B</sup>	18.7 (±1.2) <sup>A</sup>	35.2 (±14.4) <sup>AB</sup>	0.7 (0.5) <sup>C</sup>	1.2 (±0.2) <sup>B</sup>	0.2 <sup>B</sup>	0.2 (±0.1) <sup>B</sup>	0 <sup>B</sup>

Values are the average of three pedons sampled at each field site (n=3). Significance was determined using one-way ANOVA by parent material followed by Tukey's HSD post hoc test (α=0.05). Within each column, means followed by different superscript letters are significantly different. Values are whole pedon sums, corrected for bulk density and rock fragment content

Table 3. Results of MRPP testing for significant differences between bacterial communities in soils from the four sites.

A values greater than 0.1 indicate significant differences between groups.

<b>pairwise comparison by site</b>	<b>A statistic</b>	<b>P</b>
basalt vs rhyolite	0.11	0.04
basalt vs limestone	-0.01	0.52
basalt vs granite	0.16	0.02
rhyolite vs limestone	0.18	0.02
rhyolite vs granite	0.14	0.02
limestone vs granite	0.24	0.02

Table 4. Cumulative soil CO<sub>2</sub> respired and decomposition model parameters for each parent material and depth

	Rate Model Parameters					Pool Sizes		$\delta^{13}\text{CO}_2$ ‰
	Cummulative CO <sub>2</sub> respired [mg C (g soil C) <sup>-1</sup> ]	C <sub>0</sub> [mg C (g soil C) <sup>-1</sup> ]	C <sub>L</sub> [mg C (g soil C) <sup>-1</sup> day <sup>-1</sup> ]	k <sub>L</sub> (day <sup>-1</sup> )	C <sub>T0</sub> [mg C (g soil C) <sup>-1</sup> ]	C <sub>TL</sub> [mg C (g soil C) <sup>-1</sup> ]		
<b>Surface</b>								
Rhyolite	22(±2) <sup>a</sup>	0.3 <sup>b</sup>	3.6(±0.4) <sup>b</sup>	0.262(±0.026) <sup>a</sup>	13(±1) <sup>b</sup>	14(±2) <sup>b</sup>	-20.8(±0.3) <sup>ab</sup>	
Granite	39(±1) <sup>a</sup>	0.8 <sup>b</sup>	4.7(±0.4) <sup>ab</sup>	0.299(±0.015) <sup>a</sup>	30(±1) <sup>b</sup>	16(±1) <sup>b</sup>	-21.2(±0.2) <sup>b</sup>	
Basalt	35(±2) <sup>a</sup>	0.6 <sup>b</sup>	5.8(±0.7) <sup>ab</sup>	0.366(±0.026) <sup>a</sup>	25(±2) <sup>b</sup>	16(±1) <sup>b</sup>	-20.7(±0.3) <sup>ab</sup>	
Limestone	83(±12) <sup>a</sup>	1.5(±0.3) <sup>a</sup>	10.4(±2.7) <sup>a</sup>	0.291(±0.057) <sup>a</sup>	61(±12) <sup>a</sup>	35(±3) <sup>a</sup>	-19.4(±0.1) <sup>a</sup>	
<b>Subsurface</b>								
Rhyolite	37(±4) <sup>a</sup>	0.6(±0.1) <sup>a</sup>	4.2(±0.5) <sup>b</sup>	0.225(±0.003) <sup>b</sup>	23(±2) <sup>a</sup>	19(±2) <sup>a</sup>	-20.1(±1.1) <sup>b</sup>	
Granite	59(±12) <sup>a</sup>	1.1(±0.3) <sup>a</sup>	8.9(±1.5) <sup>ab</sup>	0.377(±0.042) <sup>a</sup>	45(±10) <sup>a</sup>	23(±2) <sup>a</sup>	-20.5(±0.7) <sup>b</sup>	
Basalt	61(±4) <sup>a</sup>	1.1(±0.1) <sup>a</sup>	11.6(±1.4) <sup>a</sup>	0.373(±0.007) <sup>a</sup>	45(±3) <sup>a</sup>	31(±4) <sup>a</sup>	-19.9(±0.6) <sup>b</sup>	
Limestone	57(±5) <sup>a</sup>	0.9(±0.1) <sup>a</sup>	10.2(±1.1) <sup>a</sup>	0.381(±0.035) <sup>a</sup>	35(±3) <sup>a</sup>	35(±6) <sup>a</sup>	-18.3(±0.4) <sup>a</sup>	

Rate model parameters were estimated assuming two pool first-order decay equation parameters for CO<sub>2</sub> mineralization rate over time:

$$-dC/dt = C_0 + C_L e^{-k_L t}$$

C pool sizes were estimated by integrating the first-order decay equation:  $C_{TL} = (-C_L/k_L)(1 - e^{-k_L t})$ ;  $C_{T0} = C_0 + t$

Letters indicate significant differences ( $\alpha = 0.05$ , Tukey HSD)

Table 5. Regression analysis between cumulative soil CO<sub>2</sub> respired, decomposition model parameters, and soil mineral and microbial variables for surface and subsurface horizons

Depth	Model Parameter	Equation	R <sup>2</sup>
Surface	Cumulative CO <sub>2</sub> respired	= 95.7 - 1.4(Biomass C/N) + 35.1(LS*)	0.90
	C <sub>o</sub>	= 13.0 - 0.6(Fe <sub>p</sub> ) + 0.5(soil <sup>13</sup> C)	0.88
	ln(C <sub>L</sub> )	= 0.44(pH)	0.64
	k <sub>L</sub>	= 0.2 + 0.04(pH) - 0.005(Biomass C/N)	0.57
Subsurface	Cumulative CO <sub>2</sub> respired	= 74.6 - 0.7(Biomass C/N)	0.39
	C <sub>o</sub>	= 1.37 - 0.01(Biomass C/N)	0.37
	C <sub>L</sub>	= 15.3 - 0.2(Biomass C/N)	0.70
	k <sub>L</sub>	= 0.5 - 0.01(Biomass C/N)	0.79

Regression analysis calculated on pooled data for Rhyolite, Granite, Basalt & Limestone soils.

Values for CO<sub>2</sub> are in units of [mgC (g soil C)<sup>-1</sup>], values for soil mineral variables are in units of [g (kg soil)<sup>-1</sup>]

\*LS = limestone parent material

## 8. References

- Aber, J.D., Melillo, J.M., 1991. *Terrestrial Ecosystems*. Saunders College Publishings, Philadelphia.
- Anderson, T-H, Domsch, K.H., 1993. The metabolic quotient for CO<sub>2</sub> ( $q\text{CO}_2$ ) as a specific activity parameter to assess the effects of environmental conditions, such as pH, of the microbial biomass of forest soils. *Soil Biology & Biochemistry* 25 (3), 393-395.
- Arizona Geological Survey, Digital Geologic Map of Arizona: A Digital Database Derived from the 1983 Printing of the Wilson, Moore, and Cooper 1:500,000-scale Map (2000) Douglas M. Hirschberg and G. Stephen Pitts, Open-File Report 00-409 Version 1.0, U.S. Department of the Interior, U.S. Geological Survey.
- Bååth, E., Anderson, T.H., 2003. Comparison of soil fungal/bacterial ratios in a pH gradient using physiological and PLFA-based techniques. *Soil Biology & Biochemistry* 35, 955-963.
- Bååth, E., Arnebrant, K., 1994. Growth rate and response of bacterial communities to pH in limed and ash treated forest soils. *Soil Biology & Biochemistry* 26(8), 995-1001.
- Baldock, J.A., Skjemstad, J.O., 2000. Temperature effects on the diversity of soil heterotrophs and the delta C-13 of soil-respired CO<sub>2</sub>. *Soil Biology and Biochemistry* 32, 699-706.
- Balesdent, J., Mariotti, A., 1996. Measurement of soil organic matter turnover using <sup>13</sup>C natural abundance. In: Boutton, T., Ymasaki, S. (Eds.), *Mass Spectrometry of Soils*. Marcel Dekker Inc., New York, 83-112.
- Basile-Doelsch, I., Amundson, R., Stone, W.E.E., Borschneck, D., Bottero, J.Y., Moustier, S., Masin, F., Colin, F., 2007. Mineral control of carbon pools in a volcanic soil horizon. *Geoderma* 137, 477-489.
- Blagodastkaya E.V., Anderson, T-H, 1998. Interactive effects of pH and substrate quality on the fungal-to-bacterial ratio and  $q\text{CO}_2$  of microbial communities in forest soils. *Biology & Biochemistry* 30, 1269-1274.
- Blake, G.R., Hartage, K.H., 1986. Bulk density. In: Klute, A. (Ed.), *Methods of Soil Analysis, Part 1: Physical and Mineralogical Methods*, 2nd. SSSA Book Series 5. SSSA Inc., Madison, WI, 363-375.
- Cassel, D.K., Nielsen, D.R., 1986. Field capacity and available water capacity. In: Klute, A. (Ed.), *Methods of Soil Analysis. Part 1: Physical and mineralogical methods*, 2nd ed. SSSA Book Series 5. SSSA Inc., Madison, WI, 901-926

Chenu, C., Stotzky, G., 2002. Interactions between microorganisms and soil particles. An overview. In: Huang, P.M., Bollag, J.M., Senesi, N. (Eds.), *Interactions Between Soil Particles and Microorganisms*. Wiley-VCH-Verlag, Weinheim, 3-39

Clarke, K.R., 1993. Non-parametric multivariate analyses of changes in community structure. *Australian Journal of Ecology* 18, 117-143.

Dahlgren, R.A., 1994. Quantification of allophane and imogolite. In: Amonette, J.E., Zelazny, L.W. (Eds.), *Quantitative Methods in Soil Mineralogy*. SSSA Inc., Madison, WI, 430-451.

Faith, D.P., Minchin, P.R., Belbin, L., 1987. Compositional dissimilarity as a robust measure of ecological distance. *Vegetation* 69, 57-68.

Fierer, N., Jackson, R.B., 2006. The diversity and biogeography of soil bacterial communities. *PNAS* 103, 626-631.

Fierer, N., Schimel, J.P., 2003. A proposed mechanism for the pulse in carbon dioxide production commonly observed following the rapid rewetting of a dry soil. *Soil Science Society of America Journal* 67(3), 798-805.

Guggenberger G., Kaiser K., 2003. Dissolved organic matter in soil: challenging the paradigm of sorptive preservation. *Geoderma*, 113, 293-310.

Han, W., Kemmitt, S.J., Brookes, P.C., 2007. Soil microbial biomass and activity in Chinese tea gardens of varying stand age and productivity. *Soil Biology and Biochemistry* 39 (7), 1468-1478.

Harris, D., Horwath, W.R., van Kessel, C., 2001. Acid Fumigation of soils to remove carbonates prior to total organic carbon or carbon-13 isotopic analysis. *Soil Science Society of America Journal* 65, 1853-1856.

Hedges, J.I., Oades, J.M., 1997. Comparative organic geochemistries of soils and marine sediments. *Organic Geochemistry* 27 (7-8), 319-361.

Henn, M.R., Chapela, I.H., 2000. Differential C Isotope Discrimination by Fungi during Decomposition of C3- and C4-Derived Sucrose. *Applied and Environmental Microbiology* 66 (10), 4180-4186.

Henn, M.R., Chapela, I.H., 2002. Applied and Environmental Microbiology Growth - Dependent Stable Carbon Isotope Fractionation by Basidiomycete Fungi:  $^{13}\text{C}$  Pattern and Physiological Process 68 (10), 4956-4964

- Homann, P.S., Sollins, P., Fiorella, M., Thorson, T., Kern, J.S., 1998. Regional soil organic carbon storage estimates for western Oregon by multiple by multiple approaches. *Soil Science Society of America Journal* 62, 789-796.
- Illmer, P., Marschall, K., Schinner, F., 1995. Influence of available aluminum on soil-micro-organisms. *Letters in Applied Microbiology* 21 (6), 393-397.
- Illmer, P., Obertegger, U., Schinner, F., 2003. Microbiological properties in acidic forest soils with special consideration of KCl extractable Al. *Water Air and Soil Pollution* 148, 3-14.
- Jackson, M.L., 1985. *Soil Chemical Analysis: Advanced Course*, revised 2<sup>nd</sup> edn. Madison, WI.
- Kahle, M., Kleber, M., Jahn, R., 2004. Retention of dissolved organic matter by phyllosilicate and soil clay fractions in relation to mineral properties. *Organic Geochemistry* 35(3), 269-276.
- Kaiser, K., Guggenberger, G., 2007. Sorptive stabilization of organic matter by micro porous goethite: Sorption into small pores vs. surface complexation. *European Journal of Soil Science* 58(1), 45-59.
- Kelly, R.H., Parton, W.J., Crocker, G.J., Grace P.R., Klír, J., Körschens, M., Poulton, P.R., Richter, D.D., 1997. Simulating trends in soil organic carbon in long-term experiments using the century model. *Geoderma* 81, 75-90.
- Kleber, M., Sollins, P., Sutton, R., 2007. A conceptual model of organo-mineral interactions in soils: self-assembly of organic molecular fragments into zonal structures on mineral surfaces. *Biogeochemistry* 85(1), 9-24.
- Kochian L.V., Pineros M.A, Hoekenga O.W. 2005. The physiology, genetics and molecular biology of plant aluminum resistance and toxicity. *Plant and Soil* 274, 175-195.
- Kögel-Knabner, I., Guggenberger, G., Kleber, M., Kandeler, E., Kalbitz, K., Stefan, S., Eusterhues, K., Leinweber, P., 2008. Organo-mineral associations in temperate soils: Integrating biology, mineralogy, and organic matter chemistry. *J. Plant Nutr. Soil Sci.* 171, 61-82.
- Li, C., Frohling, S., Frohling, T.A., 1992. A model of nitrous oxide evolution from soil driven by rainfall events: 1. Model Structure and sensitivity. *Journal of Geophysical Research* 97, 9759-9776.
- Lindsay, W.L., 1979. *Chemical Equilibria in Soils*. Wiley: New York.

Liu, W.-T., Marsh, T.L., Cheng, H. Forney, L.J. , 1997. Characterization of microbial diversity of determining restriction fragment length polymorphisms of genes encoding 16S rRNA. *Applied and Environmental Microbiology* 63, 4516-4522.

Marschner P., Klam A., Jentschke G., Douglas L. Godbold D.L., 2000. Aluminum and lead tolerance in ectomycorrhizal fungi. *Journal of Plant Nutrition and Soil Science* 162, 281-286.

McClaugherty, C.A., Pastor, J., Aber, J.D., Melillo, J.M., 1985. Forest litter decomposition in relation to soil-nitrogen dynamics and litter quality. *Ecology* 66, 266-275.

McCune, B., Grace, J. B., 2002. *Analysis of ecological communities*. MjM Software, Glenden Beach, Oregon.

Mikutta, R., Mikutta, C., Kalbitz, K., Scheel, T., Kaiser, K., Jahn, R., 2007. Biodegradation of forest floor organic matter bound to minerals via different binding mechanisms. *Geochimica et Cosmochimica Acta* 71, 2569-2590.

Motavalli, P.P., Palm, C.A., Parton, W.J., Elliott, E.T., Frey, S.D., 1995. Soil pH and organic C dynamics in tropical forest soils: Evidence from Laboratory and simulation studies. *Soil Biology and Biochemistry* 27(12), 1589-1599.

Nierop, K.G.J., Jansen B., Verstraten, J.M., 2002. Dissolved organic matter, aluminum and iron interactions: Precipitation induced by metal/carbon ratio, pH and competition. *Sci. Total Environ.* 300, 201–211.

Oades, J.M., 1988. The retention of organic-matter in soils. *Biogeochemistry* 5, 35-70.

Pansu, M., Gautheyrou, J., 2006. Exchangeable Acidity. In: *Handbook of Soil Analysis*. Springer-Verlag, The Netherlands, 678-686.

Paul, E.A., Clark, F.E., 1996. *Soil Microbiology and Biochemistry*. Academic Press, California.

Pina, R. G. and Cervantes, C.: 1996, Microbial interactions with aluminum, *BioMetals* 9, 311–316.

Pirt, S.J., 1975. *Principles of Microbe and Cell Cultivation*. Blackwell, Oxford.

Probst, B., Schuler, C., Joergensen, R.G., 2008. Vineyard soils under organic and conventional management - microbial biomass and activity indices and their relation to soil chemical properties. *Biology & Fertility of Soils* 44, 443-450.

Rai, D., Kittrick, J.A., 1994. Mineral equilibria and the soil system. In: Dixon, J.B., Weed, S.B., (Eds.), *Methods of Soil Analysis Part 1: Minerals in Soil Environments*, Soil Science Society of America, Inc. Madison.

Rasmussen, C., Southard, R.J., Horwath, W.R., 2006. Mineral control of organic carbon mineralization in a range of temperate conifer forest soils. *Global Change Biology* 12, 834-847.

Rasmussen C., Southard R.J., Horwath W.R., 2008. Litter type and soil minerals control temperate forest soil carbon response to climate change. *Global Change Biology* 41(4), 533-542.

Reicosky, D.C., Dugas, W.A., Torbert, H.A., 1997. Tillage-induced soil carbon dioxide loss from different cropping systems. *Soil and Tillage Research* 41, 105-118.

Sakamoto, K., Oba, Y., 1994. Effect of fungal to bacterial biomass ratio on the relationship between CO<sub>2</sub> evolution and total soil microbial biomass. *Biology & Fertility of Soils* 17, 39-44.

Santruckova, H., Bird, M.I., Lloyd, J., 2000. Microbial processes and carbon-isotope fractionation in tropical and temperate grassland soils. *Functional Ecology* 14, 108-114.

Schlesinger, W., 1997. *Biogeochemistry*. Academic Press, San Diego, CA.

Scheel, T., Dörfler, C., Kalbitz, K., 2007. Precipitation of dissolved organic matter by aluminum stabilizes carbon in acidic forest soils. *Soil Science Society of America Journal* 71, 64-74.

Schimel, D.S., Braswell, B.H., Holland, E.A., McKeown, R., Ojima, D.S., Painter, T.H., Parton, W.J., Townsend, A.R., 1994. Climatic, edaphic, and biotic controls over storage and turnover of carbon in soils. *Global Biogeochemical Cycles* 8(3), 279-293.

Schnittler, M., Stephenson, S.L., 2000. Myxomycete Biodiversity in Four Different Forest Types in Costa Rica. *Mycologia* 92, 626-637.

Six, J., Feller, C., Denef, K., Ogle, S.M., de Moraes Sa, J.C., Albrecht, A., 2002. Soil organic matter, biota and aggregation in temperate and tropical soils – effects of no-tillage. *Agronomie* 22, 755-775.

Sollins, P., Homann, P., Caldwell, B.A., 1996. Stabilization and destabilization of soil organic matter: mechanisms and controls. *Geoderma* 74, 65-105.

Soil Survey Staff, National Soil Survey Laboratory, 2004. Methods Manual: Soil Survey Investigations Report No. 42, Version 4.0. United States Department of Agriculture, Natural Resources Conservation Service, National Soil Survey Center, Lincoln, NE.

Soil Survey Staff, 2007. National Soil Survey Characterization Data, Soil Survey Laboratory, National Soil Survey Center, USDA-NRCS - Lincoln, NE. November 01, 2007.

Tebrügge, F., Düring, R.A., 1999. Reducing tillage intensity – a review of results from a long-term study in Germany. *Soil and Tillage Research* 53, 15-28.

Tipping, E., Rey-Castro, C., Bryan, S.E., Hamilton-Taylor, J., 2002. Al(III) and Fe(III) binding by humic substances in freshwaters, and implications for trace metal speciation. *Geochimica et Cosmochimica Acta* 66(18), 3211-3224

Tokunaga, T.K., Wan, J.M., Hazen, T.C., Schwartz, E., Firestone, M.K., Sutton, S.R., Newville, M., Olson, K.R., Lanzirrotti, A., Rao, W., 2003. Distribution of chromium contamination and microbial activity in soil aggregates. *Journal of Environmental Quality* 32, 541-549.

Torn, M.S., Trumbore, S.E., Chadwick, O.A., Vitousek, P.M., Hendricks, D.M., 1997. Mineral control of soil organic carbon storage and turnover. *Nature* 389, 170-173.

Trofymow, J.A., Moore, T.R., Titus, B., et al., 2002. Rates of litter decomposition over 6 years in Canadian forests: influence of litter quality and climate. *Canadian Journal of Forest Research* 32, 789-804.

Trumbore, S.E., Chadwick, O.A., Amundson, R.A., et al., 1996. Rapid exchange between soil carbon and atmospheric carbon dioxide driven by temperature change. *Science* 272, 393-396.

US Department of Agriculture (USDA) Forest Service, 1993. Forest Type Groups of the United States. (USDA, Forest Service, Washington, DC) US Government Printing Office, Washington, DC.

Valachovic, Y.S., Caldwell, B.A., Cromack, K., 2004. Leaf litter chemistry controls on decomposition of Pacific Northwest trees and woody shrubs. *Canadian Journal of Forest Research - Revue Canadienne de Recherche Forestiere* 34(10), 2131-2147.

Vance, E.D., Brookes, P.C., Jenkinson, D. S., 1987. An extraction method for measuring soil microbial biomass C. *Soil Biology and Biochemistry* 19 (6), 703-707.

- Ver, L.M.B., Mackenzie, F.T., Lerman, A., 1999. Biogeochemical responses of the carbon cycle to natural and human perturbation: past, present, and future. *American Journal of Science* 299, 762-801.
- von Lützow, M., Kögel-Knabner, Ekschmitt, K., Matzner, E., Guggenberger, G., Marschner, B., Flessa, H., 2006. Stabilization of organic matter in temperate soils: mechanisms and their relevance under different soil conditions – a review. *European Journal of Soil Science* 57, 426-445.
- Voroney, R.P., Winter, J.P., Beyaert, R.P., 1993. Soil microbial biomass C and N. In: Carter, M.R. (Ed.), *Soil Sampling and Methods of Analysis*. Lewis, Boca Raton.
- Wattel-Koekkoek, E.J.W., Buurman, P., van der Plicht, J., Wattel, E., van Breemen, N., 2003. Mean residence time of soil organic matter associated with kaolinite and smectite. *European Journal of Soil Science* 54(2), 269-278.
- Whittig, L.D., Allardice W.R., 1986. X-ray diffraction techniques. In: Kute, A. (Ed.), *Methods of Soil Analysis. Part 1. Physical and mineralogical methods*. 2<sup>nd</sup> ed. SSSA Book Ser. 5. SSSA, Madison, WI.
- Williams, RJP, 1999, What is wrong with aluminum? *Journal of Inorganic Chemistry*, 76, 81-88.
- Zar, J.H., 1999. *Biostatistical Analysis*, Prentice Hall: Upper Saddle River, NJ.
- Zibilske, L.M., 1994. Carbon mineralization. In: Weaver, R.W., Angle, S., Bottomley, P. (Eds.), *Methods of Soil Analysis Part 2: Microbiological and Biochemical Properties*, Soil Science Society of America, Inc. Madison, WI, 835-864.
- Zinn Y.L., Lal R., Bigham J.M., Resck, D.V.S., 2007. Edaphic controls on soil organic carbon retention in the Brazilian Cerrado: Texture and mineralogy. *Soil Science Society of America Journal* 71(4), 1204-1214.

## APPENDIX C

CHANGES IN DISSOLVED ORGANIC MATTER DURING BIOGEOCHEMICAL  
INCUBATION OF FOREST FLOOR MATERIAL IN THE PRESENCE OF QUARTZ,  
GOETHITE AND GIBBSITE SURFACES

Katherine Heckman<sup>a\*</sup> Craig Rasmussen<sup>a</sup>, Jon Chorover<sup>a</sup>, Angelica Vazquez Ortega<sup>a</sup>, and  
Xiaodong Gao<sup>a</sup>

\*Corresponding Author

<sup>a</sup>Department of Soil, Water and Environmental Science; University of Arizona

1177 E. Fourth Street PO Box 210038

Tucson, AZ 85721-0038, USA

kheckman@email.arizona.edu

phone : +1 520 621 1646, fax : +1 520 621 1647

Prepared for submission to *Geochimica et Cosmochimica Acta*

**Abstract**

The release of dissolved organic matter (DOM) from forest floor material constitutes a significant flux of C to the mineral soil in temperate forest ecosystems, with estimates on the order of 120 to 500 kg C ha<sup>-1</sup> year<sup>-1</sup>. Interaction of DOM with minerals and metals results in sorptive fractionation and stabilization of OM within the soil profile. Iron and aluminum oxides, in particular, have a significant effect on the quantity and quality of DOM transported through forest soils due to their high surface area and the toxic effects of dissolved aluminum. We directly examined these interactions by incubating forest floor material, including native microbiota, for 154 days in the presence of 1) goethite ( $\alpha$ -FeOOH), 2) gibbsite ( $\gamma$ -Al(OH)<sub>3</sub>), and 3) quartz ( $\alpha$ -SiO<sub>2</sub>) sand (as a control). Changes in molecular and thermal properties of dissolved organic matter were evaluated. Dissolved organic matter was harvested on days 5, 10, 20, 30, 60, 90, and 154, and examined by thermogravimetry/digital thermal analysis (TG/DTA) and diffuse reflectance Fourier transform infrared (DRIFT) spectroscopy. Results indicated significant differences in DOM quality among treatments, though the way in which oxide surfaces effected DOM properties did not seem to change significantly with increasing incubation time. Dissolved organic C concentrations were significantly lower in DOM from the oxide treatments in comparison to the control treatment. Incubation with goethite produced DOM with mid-to-high-range thermal lability which was depleted in both proteins and fatty acids. The average enthalpy of DOM from the goethite treatment was significantly higher than either the gibbsite or control treatment, suggesting that

interaction with goethite surfaces increases the thermal stability of DOM. Incubation with gibbsite produced DOM rich in thermally recalcitrant and carboxyl-rich compounds in comparison to the control treatment. These data indicate that interaction of DOM with oxide surfaces significantly changes the composition of DOM and may play an important role in determining the biodegradability of DOM in forest soils.

## **1. Introduction**

The global pool of soil organic carbon is estimated at 1550 Gt, twice the size of the atmospheric C pool (760 Gt) (Lal, 2004). Concerns over global climate change have spurred interest in investigating the mechanisms controlling the stability of this large carbon pool, since increased rates of soil organic carbon mineralization would mean a substantial efflux of CO<sub>2</sub> to the atmosphere. Though dissolved organic matter (DOM) comprises only ~1% of the total soil organic carbon pool, DOM is the most mobile fraction of soil organic carbon (Zsolnay, 1996) and is thought to be the largest source of new C inputs to subsurface soils in temperate forest systems (Zech and Guggenberger, 1996; Kaiser and Guggenberger 2000; Michalzik et al. 2001 Rumpel and Kögel-Knabner, 2010).

Under favorable conditions, large portions of DOM are readily degradable. However, in soil environments, many factors influence DOM degradation rates. In the initial stages of biodegradation, relative structural recalcitrance plays a large role in determining the mean residence time of specific organics. Polycyclic and phenolic compounds such as lignin dimers and charred materials are generally preferentially

preserved relative to more labile substrate compounds such as proteins and polysaccharides (cf. von Lützow et al., 2006). Additionally, persistence of organic matter is increased by binding to oxides and secondary phyllosilicates as well as interaction with polyvalent metal cations ( $\text{Al}^{3+}$ ,  $\text{Fe}^{3+}$ ) to form organo-metal complexes. Such interactions with mineral surfaces have long been recognized as an important factor controlling soil organic matter content (Greenland, 1971; Martin and Haider, 1986; Theng and Tate, 1989; Baldock and Skjemstad, 2000). Sorption of soil organic matter to mineral surfaces has other important effects on the soil system, including changes in the surface properties of minerals and potential influence on soil microbial communities.

Goethite and gibbsite are ubiquitous in soils (Kampf et al., 2000) and have a significant impact on organic C cycling both due to their high specific surface areas and abundance of reactive hydroxyl groups. As DOM percolates through the soil profile, Fe and Al oxides interact with organics in solution both through surface sorption and the formation of organo-metal complexes from Fe and Al cations released during mineral dissolution. Hydroxyl and carboxyl functional groups of dissolved organics can form strong inner sphere complexes with goethite and gibbsite surfaces through ligand exchange reactions (Parfitt et al., 1977; Gu et al., 1994; Molis et al., 2000; Chorover and Amistadi, 2001), or can be more weakly sorbed through hydrophobic interactions and hydrogen bonding (Evanko and Dzombak, 1999; Stevenson, 1994). Formation of organo-metal complexes involves bonding of reactive organic functional groups with dissolved metal ions, which induces chemical and conformational changes in the organics and reduces their susceptibility to enzyme attack (Byler et al., 1987; Baldock and Skjemstad,

2000; Nierop et al, 2002; Scheel et al., 2007). Such interactions have been hypothesized to both decrease the bioavailability of DOM, and increase C mean residence times by slowing the decomposition process (Boudot et al., 1989; Veldkemp, 1994; Torn et al., 1997; Jones and Edwards, 1998; Eusterhues et al., 2003; Masiello et al., 2004). However, how the influence of oxide surfaces on DOM characteristics may change with increasing degree of biodegradation is not well known, especially in biologically active systems.

Sorption of organics to hydrous oxide surfaces has been well studied. Previous experiments using leaching columns and batch isotherm experiments have demonstrated preferential sorption of specific classes of organics to Fe- and Al-oxyhydroxides. These organics include high molecular weight compounds, compounds rich in N or P, compounds with reactive acidic groups, and aromatic compounds (McKnight et al., 1992; Stevenson, 1994; Gu et al., 1995; Meier et al., 1999; Stevenson and Cole, 1999; Chorover and Amistadi, 2001; Zhou et al., 2001). Though such batch and column studies have allowed us to identify characteristics and bonding mechanisms that affect short-term abiotic DOM fractionation and preferential adsorption, they have not captured the dynamics of ongoing sorption and desorption dynamics that occur throughout the longer term biodegradation process.

To address this knowledge gap, we conducted laboratory experiments to evaluate the influence of goethite and gibbsite surfaces on DOM quality and quantity over the course of long term (> 150 day) incubations in bioactive sediments. We employed DRIFT, TG/DTA, and other basic quantitative measures of DOM quality such as pH,

molar absorptivity, and concentrations of Fe and Al in DOM solutions to assess these effects.

## **2. Methods**

### **2.1. Characterization of minerals**

Minerals used in the incubation experiment were thoroughly characterized prior to use. Quartz sand was purchased from Fisher Scientific (Pittsburgh, PA). Prior to use, sand was submerged in 30% H<sub>2</sub>O<sub>2</sub> (1:1 weight to volume ratio) and shaken for 24 hours to remove any organic matter. Sand was rinsed three times with deionized water, then submerged in 1M HCl (1:1 weight to volume ratio) and shaken for 24 h to remove any exchangeable cations. The sand was then rinse with deionized water until the pH and EC of the rinse water matched that of the deionized water. Sand was then dried at 110 °C and stored in an acid-washed sterile container until use.

Goethite and gibbsite were purchased from Ward's Natural Science (Rochester, NY). Quartz, goethite and gibbsite were thoroughly characterized prior to use in the incubation. Phase purity was determined by X-ray diffraction. Minerals were analyzed as random powder mounts from 2-70° 2θ on a PANalytical X'Pert PRO-MPD X-ray diffraction system (PANalytical, Almelo, AA, The Netherlands) producing Cu-Kα radiation at an accelerating potential of 45 kV and current of 40 mA, and fitted with a graphite monochromator and sealed Xenon detector. Particle size was measured on a Beckman Coulter LS 13 320 Laser Diffraction Particle Size Analyzer (Beckman Coulter Inc, Fullerton, CA). Specific surface area was measured under N<sub>2</sub> on a Beckman Coulter

SA 3100 Gas Adsorption Surface Area Analyzer (Beckman Coulter Inc, Fullerton, CA), and calculated according to the BET theory (Brunauer et al., 1938). Particle size and specific surface area measurements were made on three subsamples of each mineral type.

All mineral samples were well homogenized prior to examination. There was little no variation among mineral subsamples for any of the parameters measured (standard error of experimental replicates was at zero or close to zero). All minerals were pure phases as determined by X-ray diffraction. Particle size and specific surface area varied among the minerals. Quartz particles had a mean diameter of 211  $\mu\text{m}$  and specific surface area of 0.03  $\text{m}^2 \text{g}^{-1}$ . Goethite particles had a mean diameter of 23  $\mu\text{m}$  and specific surface area of 3.51  $\text{m}^2 \text{g}^{-1}$ . Gibbsite particles had a mean diameter of 14  $\mu\text{m}$  and specific surface area of 1.32  $\text{m}^2 \text{g}^{-1}$ .

## 2.2. Experimental Design

Natural forest floor organic material was incubated in three mineral matrices: quartz sand mixed with goethite, quartz sand mixed with gibbsite, and quartz sand alone (as a control treatment). The matrices for each treatment were as follows: (i) Control treatment: 30 g quartz sand; (ii) Goethite treatment: 6 g goethite grains and 24 g quartz sand; and (iii) Gibbsite treatment: 6 g gibbsite grains and 24 g quartz sand. Mineral properties are described in detail above (see section 2.1).

Organic material used in the incubation experiment consisted of partially decomposed material collected from the full forest floor (Oi, Oe, Oa horizons) in an Arizona forest dominated by *Pinus ponderosa* in the overstory (see Heckman et al., 2009

for site details). Forest floor material was dried at 30°C, cut to pieces measuring ~1 cm in length and homogenized using a blender. Three grams of homogenized forest floor material was mixed with the respective quartz sand, gibbsite or goethite treatments in 125 ml glass jars (Fisherbrand, Fisher Scientific).

Microbial inoculum derived from field O horizon material was prepared following Wagai & Sollins (2002). Freshly collected forest floor material was mixed with deionized water at a mass to volume ratio of 1:5. The mixture was shaken vigorously for 30-min on reciprocal shaker followed by overnight shaking on a low frequency setting. After 12 hours of slow shaking, the mixture was vacuum filtered through a 5- $\mu$ m polycarbonate membrane filter. Vacuum line pressure was kept below 69 kPa (equivalent to 51.7 cm Hg or 20.4 in Hg) to prevent lysing of microbial cells. Filtrate was stored in a sterilized bottle overnight at 4 °C before use. A 1 ml aliquot of inoculum solution was added to each jar. Samples were homogenized, wetted to 60% of water holding capacity (Cassel and Nielsen, 1986) with deionized water, and tamped to a uniform bulk density. Sample cups were placed in 950 cm<sup>3</sup> mason jars. Soil moisture was maintained by the addition of 3 ml of water to the bottom of each jar to maintain 100% relative humidity within the jar atmosphere. Aerobic conditions in the sample jars were maintained by opening the jars and venting the samples periodically.

Samples were incubated at 25 °C, and sampled at seven time intervals: 5, 10, 20, 30, 60, 90 and 154 d. Each time interval was replicated three times per mineral treatment for a total of 63 samples. All 63 samples were prepared simultaneously and incubations were initiated at the same time. At the end of each time interval, the three replicates from

each treatment were destructively sampled. Samples were mixed with a spatula, and 12 g of homogenized material were removed and frozen to be used for microbial analysis at a later time. The remainder of the sample was mixed with deionized water in a 15:1 solution to solid mass ratio and shaken on a side-to-side shaker for 24 hours. Samples were vacuum filtered, first through a 1 micron glass fiber A/E filter, then through a 0.22 micron polymer filter (Millipore type GV). The filtrate was considered to contain the DOM fraction and was stored in sterilized bottles at 4 °C until analyses were completed.

## **2.3. DOM Analysis**

### *2.3.1 C, N, Fe, Al Concentrations & Molecular Weight*

Total organic C (non-purgeable) and total N of the DOM solutions were measured on a Shimadzu TOC-VCSH analyzer (Columbia, MD). Solution Fe and Al concentrations were determined by inductively coupled plasma mass spectrometry (ICP-MS) on a Perkin Elmer Elan DRC II ICP-MS (Waltham, MA). Concentrations of C, N, Fe, and Al were expressed relative to grams of litter C, with all values normalized to the C content of the solid state sample prior to incubation [ $\text{g C g}^{-1}$  litter C]. Apparent weight averaged molecular mass ( $MW_{AP}$ ) of the DOM solutions was measured by size exclusion high performance liquid chromatography on a Waters High Performance Liquid Chromatography system (Agilent Technologies, Palo Alto, CA). Solutions were diluted to a concentration of 50 mM of C L<sup>-1</sup> in a sodium phosphate solution buffered to pH 5.5.

### *2.3.2 Ultraviolet-Visible Spectroscopy*

Ultraviolet-visible spectra were obtained with a Shimadzu UV-Probe PC2501 UV-Vis spectrophotometer (Columbia, MD). Absorbances were recorded at 254 nm, 280 nm, and 365 nm. Prior to measurement, samples were diluted with sodium phosphate buffer (pH 5.5) both to standardize solution pH values among the treatment groups and ensure that all absorbance values were  $< 0.7$ . Absorbances at 280 nm were divided by the molar concentration of dissolved organic C in DOM extracts to give “molar absorptivity” or specific UV absorption (SUVA). Molar absorptivity at 280 nm is commonly accepted as an index of DOM aromaticity (Chin et al., 1994; Peuravuori and Pihlaja, 1997). The quotient of absorbance at 254 nm to absorbance at 365 nm ( $E_2/E_3$ ) is correlated with absorption from specific chromophores containing unbonded electrons and has been related to the molecular size of DOM (Peuravuori and Pihlaja, 1997; Guo and Chorover, 2003). Low  $E_2/E_3$  values are generally associated with higher molar mass constituents.

### *2.3.3 Infrared Spectroscopy*

DOM was lyophilized after all other analyses were completed. The freeze-dried DOM was mixed with KBr in a 1:20 ratio (DOM:KBr). Diffuse reflectance infrared Fourier transform (DRIFT) spectra were recorded using a Nicolet 560 Magna IR Spectrometer (Madison, WI). Samples were mixed with KBr, pressed gently into metal cups, and scanned over the  $4,000 - 400 \text{ cm}^{-1}$  range. Four hundred scans were averaged for each spectrum at a resolution of  $4 \text{ cm}^{-1}$  and normalized by using a pressed pure KBr pellet as background. An automatic baseline correction was applied to each spectrum to remove baseline distortions. Spectral analysis, including peak deconvolution and integration, was performed using the GRAMS Spectroscopy Software Suite (Thermo Scientific).

### 2.3.4 Thermal Analysis

Differential thermal analysis (DTA) and thermogravimetric (TG) analyses were conducted on lyophilized DOM samples using a Diamond series TG/DTA (PerkinElmer; Shelton, CT). A four point calibration using indium, tin, zinc, and silver standards was used to determine the conversion factor from electrical potential ( $\mu\text{V s}^{-1}$ ) to heat flow (mW). TG and DTA data were recorded simultaneously. The reference pan contained calcinated  $\alpha\text{-Al}_2\text{O}_3$  powder. Due to the limited sample size, DOM samples that were diluted with KBr for DRIFT analysis were also used for TG-DTA analysis (1:20 dilution ratio, DOM:KBr). KBr is thermally inert from room temperature to  $734^\circ\text{C}$ . To confirm that the presence of KBr would not cause artifacts in the data, several samples of DOM were run both with KBr and alumina. No differences were detected between the profiles, therefore KBr was assumed to have no effect on the thermal data. Sample mixtures were heated from  $50$  to  $650^\circ\text{C}$ , at a rate of  $20^\circ\text{C min}^{-1}$  with continuous air flow of  $50\text{ ml min}^{-1}$ . DTA peak integration was conducted using Origin 7.5 (OriginLab Corporation; MA). DTA profiles of mW versus time were integrated, yielding units of kJ per peak or per profile (total enthalpy of combustion). Enthalpy values (in kJ) were then divided by mass loss or total sample mass to give values of  $\text{kJ g}_{\text{mass loss}}^{-1}$  or  $\text{kJ g}_{\text{mass}}^{-1}$ .

## 2.4 Statistical methods

Each sample harvested at a specific destructive sampling period was treated as a replicate for a given treatment, providing three replicates for each treatment per sample time and a total of 21 replicates per treatment across all time periods. Significant

differences between DOM properties among treatments were determined by two-way ANOVA using mineral treatment (goethite, gibbsite or control/quartz) and time as the main effects followed by Tukey-Kramer *post hoc* test at a 95% confidence limit ( $n=21$  for each mineral treatment). Significant differences among DRIFT and TG/DTA peak areas were determined by one-way ANOVA by mineral type followed by Tukey-Kramer *post hoc* test at a 95% confidence limit. Only one spectrum (for both DRIFT & TG/DTA) per treatment per time period was analyzed for peak areas ( $n=7$  for each mineral treatment). Linear regression was used to assess trends in DRIFT and TG/DTA peak areas over time and to investigate correlations among measured DOM properties.

### **3. Results**

#### **3.1. Carbon and Nitrogen**

Dissolved organic carbon concentrations were significantly lower in oxide treatments relative to the control when averaged over time (control =  $20.3 \text{ mg g}_{\text{litter}} \text{ C}^{-1}$ , goethite =  $10.0 \text{ mg g}_{\text{litter}} \text{ C}^{-1}$ , gibbsite =  $9.6 \text{ mg g}_{\text{litter}} \text{ C}^{-1}$ ). However, this is mostly due to the two large spikes in C concentration at 20 and 60 d in the control treatment. In comparison, DOC concentrations of the oxide treatments did not exhibit large fluctuations as seen in the control treatment (Table 1). By day 154, there was little difference in DOC concentration among the control and oxide treatments, and DOC concentrations in all treatments decreased by approximately 50% over the course of the incubation.

C/N ratios were not significantly different among treatments and all treatments exhibited variation over time. However, C/N ratios did decrease from day 60 to day 154, and C/N ratios were an order of magnitude lower at the end of the incubation than at the beginning (~100 at day 5 versus ~21 at day 154).

### **3.2 pH & Metal:C ratios**

The pH of DOM solutions extracted from the forest floor material prior to exposure to oxide surfaces was 5.4. The pH values of both the control and oxide treatments increased over time, though all treatments exhibited large fluctuations early in the incubation. By day 30 of the incubation, pH levels of all treatments stabilized at a pH of 6 to 6.5. When averaged across time, the pH of the DOM was higher for the oxide treatments than for the control (6.05, 5.96, 5.78 for gibbsite, goethite and control treatments respectively), and pH of DOM from the gibbsite treatment was statistically significantly higher than that of control DOM. The change in pH was particularly interesting given that pH exerts an overarching control on the formation of metal-humus complexes. Solution pH strongly influences both the solubility of Fe- and Al-oxides and organic matter, affects the type of bonding favored between metals and organics, the rate and abundance of organo-metal complex formation, and the speciation of dissolved metals (Lindsay, 1979; Plankey and Patterson, 1987; Gu et al., 1994; Stevenson, 1994; Guan et al., 2006).

Metal:C ratios were relatively small throughout the incubation, but increased over time (Table 1). Among oxide treatments, Fe:C reached a maximum of 33 mmol Fe per

mol C at day 154 of the incubation in the goethite treatment, whereas Al:C reached a maximum of 9 mmol Al per mol of C at day 154 of the incubation in the gibbsite treatment. Low metal:C ratios are most likely due to the low solubility of both goethite and gibbsite at circum neutral pH values. The stability of gibbsite is at its maximum at pH values  $\sim 7.5$ , though at a pH of 6 to 6.5 it is still quite stable (Lindsay, 1979). Goethite is most stable at pH values of  $\sim 8$ , but still has low solubility at pH of 6 to 6.5 (Cornell and Schwertmann, 1996). Though the absolute metal concentrations were low, they were several orders of magnitude higher than those predicted for inorganic, monomeric Al and Fe based on solubility constants would suggest. Concentrations of Al in DOM from the gibbsite treatment were on the order of  $10^{-5}$  to  $10^{-6}$  mol L<sup>-1</sup>, however the equilibrium constant of gibbsite indicates Al concentrations on the order of  $10^{-10}$ . Solution Fe concentrations in DOM from the goethite treatment were  $10^{-4}$  to  $10^{-5}$  mol L<sup>-1</sup>, but the equilibrium constant of goethite suggests Fe concentrations on the order of  $10^{-18}$  (Lindsay, 1979).

Goethite exhibited much higher dissolution than the gibbsite. Equilibrium considerations suggest that Fe concentrations should be  $10^8$ -fold less than Al concentrations. Instead, Fe release from goethite was an order of magnitude greater than Al release from gibbsite. The differences in solubility may be controlled in part by variation in mineral specific surface area in that the specific surface area of goethite was nearly three times that of gibbsite ( $3.51$  and  $1.32$  m<sup>2</sup> g<sup>-1</sup> for goethite and gibbsite respectively). The XRD data also indicated gibbsite exhibited a greater degree of crystallinity than the goethite, which may also contribute to its lower apparent solubility

(Schwertmann, 1991). Also, it is likely that some reductive dissolution of Fe (III) may have occurred in anoxic areas of the incubating substrate.

### 3.3 Apparent molar mass of DOM

The apparent molar mass of DOM from the control treatment exhibited moderate fluctuation over time, whereas that of DOM from the goethite and gibbsite treatments steadily increased over the course of the incubation (Table 1). The apparent molar mass of DOM from all treatments increased slightly but significantly over time (time vs.  $M_{W,APP}$ :  $r^2 = 0.20$ ,  $p = 0.044$ ). When averaged across time, DOM from the control treatment had a significantly higher apparent molar mass than DOM from both the goethite and gibbsite treatments ( $p = 0.0022$ ).

$M_{W,APP}$  and metal:C ratios were significantly positively correlated in both the goethite ( $r^2 = 0.84$ ,  $p = 0.0035$ ) and gibbsite ( $r^2 = 0.76$ ,  $p = 0.0107$ ) treatments, but not in the control treatment ( $r^2 = 0.16$ ,  $p = 0.3792$ ). These correlations suggest that the  $M_{W,APP}$  measurements were strongly affected by the presence of dissolved metals and metal-humus complexes, and do not reflect the true  $M_{W,APP}$  of uncomplexed DOM components in the goethite and gibbsite treatments.

### 3.4 Ultraviolet-Visible Spectroscopy

$E_2/E_3$  ratios of gibbsite and control treatments were nearly equivalent (average  $E_2/E_3$  ratios were 6.1 and 6.2 for control and gibbsite, respectively) throughout the incubation and increased slightly from day 5 to day 154 (approximately 1 unit).  $E_2/E_3$

ratios of the goethite treatment were significantly lower ( $p < 0.0001$ ) than gibbsite and control values (average  $E_2/E_3$  ratio was 2.9) and showed no increase over time.  $E_2/E_3$  ratios are sometimes used as predictors of molar mass, and low  $E_2/E_3$  values are generally associated with high molecular weights (Peuravuori and Pihlaja, 1997; Guo and Chorover, 2003). In the current study however,  $E_2/E_3$  ratios were poorly correlated with apparent molecular weight ( $r^2 = 0.23$  for  $MW_{APP}$  versus  $E_2/E_3$ ), likely because of the effect of metal complexation on increasing apparent molar mass, as discussed above (see Section 3.3).

Molar absorptivity exhibited large fluctuations over time in all treatments (Table 1). Though molar absorptivity was not significantly different among treatments, it did increase significantly over time in all treatments (time vs. molar absorptivity:  $r^2 = 0.58$ ,  $p < 0.0001$ ).

### **3.5 DRIFT Spectroscopy**

All treatments yielded similar DRIFT spectra but with consistent, treatment dependent variation in relative peak areas (Figure 1). The gibbsite treatment spectra exhibited peaks from  $3450 - 3650 \text{ cm}^{-1}$  attributable to metal-OH stretching that were absent in the control and goethite treatment spectra. All other major peaks were present in all three treatments. Peaks were assigned as indicated in Table 2.

Peak deconvolution was necessary to separate the amide I band from the asymmetric carboxyl peak. A peak with a maximum  $\sim 1380 \text{ cm}^{-1}$  was present in all spectra, however in the gibbsite and goethite derived spectra only, this peak frequently

exhibited distortion in the form of narrowing and “pointiness” in some of the spectra. This peak is due to  $\text{-COO}^-$  stretching, and distortion of this peak is due to bonding of metals to carboxyl groups of organics (Fu and Quan, 2006; Gu et al., 1994), consistent with the elevated concentrations of Al and Fe observed in corresponding solutions.

Deconvolution of DRIFT spectra revealed differences in the structural characteristics of DOM among treatments (Table 3). Peak areas of the three treatments were calculated for six major bond types/regions: Amide I band ( $1650\text{ cm}^{-1}$ ), polysaccharides (calculated as the sum of peaks at  $1240$ ,  $1140$ ,  $1055$ ,  $950$  and  $900\text{ cm}^{-1}$ ), metal+ $\text{COO}^-$  bonds ( $1380\text{ cm}^{-1}$ ), esters ( $1730\text{ cm}^{-1}$ ),  $\nu_{\text{as}}\text{COO}^-$  (asymmetric carboxyl peak at  $1580\text{ cm}^{-1}$ ), and  $\nu$  metal-OH (metal-OH stretches at  $3500$  and  $3530\text{ cm}^{-1}$ ). In general, DOM from the goethite treatment was significantly different from the control in many respects, whereas DOM from the gibbsite treatment was rarely significantly different from either the control or the goethite treatment.

Amide I band areas were significantly lower in DOM from the goethite treatment than from the other treatments, indicating lower protein content in DOM from the goethite treatment. Assuming equivalent DOM production, the lower protein content indicates a preferential adsorption of proteins to goethite surfaces consistent with previous research (Omoike and Chorover, 2006). Similarly, the ratio of the amide I band area to the sum of the polysaccharide peak areas (Amide I:  $\Sigma$ Polysaccharide) were significantly higher in the controls than in the goethite treatment (control<sup>a</sup> > gibbsite<sup>ab</sup> > goethite<sup>b</sup>), also suggesting goethite surface preference for proteinaceous compounds. The “ $\nu\text{COO-metal}$ ” peak areas were significantly different among

treatments (goethite<sup>a</sup> > gibbsite<sup>ab</sup> > control<sup>b</sup>), indicating a greater abundance of carboxyl-metal bonds formed in the goethite treatment. The area of the ester peak, (~1730 cm<sup>-1</sup>) commonly associated with fatty acids, was also significantly higher in the control treatment than in the goethite treatment (control<sup>a</sup> > gibbsite<sup>ab</sup> > goethite<sup>b</sup>) potentially indicating preferential adsorption of fatty acids to the goethite surfaces.

Of particular interest were the time dependent dynamics of DOM carboxyl content and metal-carboxyl bonding among oxide treatments. Goethite-treatment DOM contained significantly greater “νCOO-metal” peak areas (goethite<sup>a</sup> > gibbsite<sup>ab</sup> > control<sup>b</sup>), indicating greater abundance of carboxyl-metal bonds that may be attributed to Fe- and Al-carboxyl complexation in the goethite and gibbsite treatments, respectively. Interestingly, spectral deconvolution indicated the gibbsite-derived DOM possessed relatively strong metal-OH peaks from 3450-3650 cm<sup>-1</sup> that were not present in the goethite or control samples. This suggests that Al in the gibbsite DOM was present as some form of Al(OH)<sub>x</sub>, whereas dissolved Fe in the goethite treatment was present in its elemental form. The asymmetric carboxyl stretch peak area (ν<sub>as</sub>COO<sup>-</sup>) was significantly higher in DOM from the gibbsite treatment than in the control (gibbsite<sup>a</sup> > control<sup>ab</sup> > goethite<sup>b</sup>). Increased carboxyl content is typically associated with increased humification and biodegradation (Stevenson 1994, Qualls *et al.* 2003). However, carboxyl groups interact strongly with oxide surfaces via ligand exchange, thereby removing carboxyls from solution. Therefore, lower carboxyl content in the goethite DOM indicates greater carboxylate bonding to oxide surfaces in association with the greater metal-carboxyl bonding noted above.

Several time dependent trends in the DRIFT spectra were shared by all treatments (Fig. 3). In general, the amide I peak area increased and the polysaccharide peak area showed a slight decrease over time, consistent with increasing protein:polysaccharide ratios in DOM. The carboxyl:polysaccharide ratio exhibited a general decline over time.

### 3.6 DOM Analysis: TG-DTA

All observable DTA peaks were exotherms, and all exotherms were associated with mass loss. In general, DTA spectra were composed of three peaks with maximums around 300°C (Exo<sub>1</sub>), 410°C (Exo<sub>2</sub>) and 550°C (Exo<sub>3</sub>), though goethite-derived DOM spectra showed a general merging of Exo<sub>2</sub> and Exo<sub>3</sub> peaks with increasing time of incubation (Figure 2). Because Exo<sub>2</sub> and Exo<sub>3</sub> peaks merged, mass loss and enthalpies were calculated for the sum of the Exo<sub>2</sub> and Exo<sub>3</sub> peaks in the goethite treatment. In all treatments, higher temperature peaks release more energy per unit mass than lower temperature peaks, which is consistent with previous research showing that more recalcitrant, higher-energy compounds are associated with higher combustion temperatures (c.f., Plante *et al.* 2009). Distribution of mass loss among the three peaks varied both among treatments and over time, but quantitative comparisons are difficult due to the merging of peaks in spectra from the goethite treatment. This merging of peaks could be the result of differences in the molecular composition of goethite-derived DOM relative to control or gibbsite-derived DOM. However, previous studies indicate that peak position and shape can also be affected by the presence of metal-humus complexes (Provenzano and Senesi, 1998). The presence of organo-Fe(III) complexes in DOM

solutions lowers the initiation temperature of DTA peaks, while organo-Al bonding tends to raise initiation temperatures (Schnitzer and Kodama, 1972; Tan, 1978; Lu et al., 1997). Though some organo-metal complexes were undoubtedly present in the DOM solutions, metal:C ratios were several orders of magnitude smaller than the ratios shown to effect initialization temperatures (Table 1). Also, when mass and energy losses from goethite-derived DOM Exo<sub>2</sub> and Exo<sub>3</sub> peaks were separated using basic peak decomposition, enthalpies of the two peaks were very similar, indicating that the compounds combusting in Exo<sub>2</sub> and Exo<sub>3</sub> were similar in composition. This indicates that merging of Exo<sub>2</sub> and Exo<sub>3</sub> peaks is more likely the result of actual changes in DOM composition rather than the presence of small amounts of organo-metal complexes.

In general, combustion in specific temperature ranges has been associated with the breakdown of specific compound types (Dell'Abate et al., 2003; Lopez-Capel et al., 2005; Manning et al., 2005; Plante et al., 2005; Lopez-Capel et al., 2006; Montecchio et al., 2006). However the assignment of specific compounds to certain temperature ranges in DTA profiles varies widely. Peaks at ~300°C can be produced by combustion of polysaccharides, decarboxylation of acidic groups and dehydration of hydroxylate aliphatic structures (Ciavatta et al., 1991; Dell'Abate et al., 2002). Peaks at ~400°C have been associated with the combustion of plant and microbially-derived aliphatic structures (Sheppard and Forgeron 1987; Schulten et al., 1999), but are sometimes assigned to aromatics (Ranalli et al., 2001; Dell'Abate et al., 2002; Strezov et al., 2004). Peaks around ~500-550°C have also been associated with combustion of aromatic structures and cleavage of C-C bonds (Stevenson, 1994; Monetecchio et al., 2006). However, other

studies assign combustion at temperatures over 500°C to polycondensed aromatics such as char or black C (Almendros et al., 1982; Lopez-Capel et al., 2005; De la Rosa et al., 2008). Though previous authors have shown good agreement between combustion at temperatures >500°C and the abundance of aromatics and polycondensed aromatics, DRIFT spectra of the DOM did not show the presence of significant amounts of aromatics (spectra lack the characteristic prominent peak at 1500 cm<sup>-1</sup> that is indicative of aromatics). This may indicate that mass losses at ~550°C were actually the product of cleavage of unsaturated C-C bonds sourced from non-aromatic compounds. Also, assignment of mass loss at certain temperatures cannot be definitively attributed to any particular structural quality, due to both the heterogeneity of natural organic substances and the fact that peak temperatures have been known to vary with a variety of experimental parameters (Cebulak and Langier-Kùzmiarowa, 1997).

DOM from the goethite treatment exhibited the highest enthalpy of combustion both based on total sample weight and mass loss during combustion. Average enthalpy of DOM, as measured in kJ per g of mass loss, was significantly higher in the goethite treatment than in either the control or the gibbsite treatment ( $p = 0.0198$ ), suggesting that exposure to goethite increases the thermal stability of DOM.

When calculated relative to the whole sample weight, DOM from all treatments had relatively low enthalpy values, averaging 9.4 kJ g<sup>-1</sup> across all treatments.

## **4. Discussion**

Interaction with goethite and gibbsite surfaces influenced both the quantity and quality of DOM derived from the biogeochemical incubation of forest floor material. Previous research has demonstrated that interaction with mineral surfaces results in systematic fractionation of DOM (by molecular size and type) into adsorbed and dissolved pools in both batch (Zhou et al., 2001; Chorover and Amistadi, 2001) and column (Guo and Chorover, 2001) experiments. Previous studies have also documented decreases in both DOM abundance and biodegradability as the result of exposure to mineral matrices (Kalbitz et al., 2000; Schwesig et al., 2003; Kalbitz et al., 2005). Consistent with this previous research, our data indicate that exposure to goethite and gibbsite surfaces reduced concentrations of dissolved organic C and also significantly changed its molecular composition and energetics.

### **4.1 Influence of goethite and gibbsite surfaces on DOM structural characteristics**

Goethite and gibbsite surfaces differed in their effect on DOM properties, with both structural composition and thermal stability varying with treatment. Though goethite-derived DOM and gibbsite-derived DOM varied in their structural and thermal characteristics, both displayed qualities indicating a more advanced degree of humification and greater biological recalcitrance in comparison to the control treatment.

In general, DOM from the goethite treatment was depleted in fatty acids and proteins in comparison to the control treatment, but also had a significantly lower abundance of carboxyls than the gibbsite treatment. Considering these data along with

information from the TG and DTA profiles indicating that the majority of mass and energy loss occurred over the temperature range of 400-550°C, DOM from the goethite treatment seemed to be dominated by aliphatics and carbohydrates of mid-to-high-range thermal stability. DOM from the goethite treatment exhibited higher average enthalpy than either the gibbsite or control treatments, suggesting that interaction with goethite surfaces significantly increases the thermal and, by extension, biological stability of DOM. Though the translation of thermal stability to biological recalcitrance has not been firmly established, indices of thermal stability have shown good agreement with other traditional indices of humification (Ciavatta et al., 1990, Plante et al., 2009). Therefore, enthalpy data may suggest that exposure to goethite surfaces increases the degree of humification of DOM. DOM from the control treatment exhibited a higher overall mass loss than DOM from the oxide treatments, though there was a statistically significant difference only between goethite DOM and control DOM ( $p = 0.0142$ ). Lower mass loss values for the goethite DOM may indicate a greater abundance of compounds with very high thermal stability.

DRIFT data indicated that molecular composition of DOM from the gibbsite treatments was structurally similar to DOM from the control treatments, aside from having a higher carboxyl content. Furthermore, the TG/DTA data suggested that DOM from the gibbsite treatment was dominated by high temperature/high enthalpy organics. The abundance of thermally stable components along with high carboxyl content may suggest a more advanced degree of humification for DOM from the gibbsite treatment in comparison to the control (Ciavatta et al., 1990; Stevenson, 1994; Qualls et al., 2003).

Ultraviolet-visible spectroscopic indices of DOM quality were less conclusive. Molar absorptivity indicated a general increase in aromaticity over time in all treatments, a phenomenon often observed as biodegradation progresses (Stevenson, 1994). However, aromaticity of DOM from the oxide treatments was not statistically different than control DOM. This may be due to preferential sorption of aromatic compounds by oxide surfaces as suggested by differences in apparent molar mass among treatments.

Interestingly, apparent molar mass data were significantly affected by the presence of dissolved metals in the DOM solutions, which is consistent with the emerging paradigm of DOM as comprising aggregated molecular entities inter-bonded by bridging cations as well as through H-bonding and hydrophobic interaction (Sutton and Sposito, 2005). Raw apparent molar mass data indicated that DOM from the control had a significantly higher apparent molar mass than DOM from both the gibbsite and goethite treatment. However, apparent molar mass was strongly correlated with Fe: C and Al: C ratios, suggesting that formation of metal-humus complexes strongly affected the apparent molar mass of DOM. After accounting for the influence of metal:C ratios on  $MW_{APP}$ , DOM from the goethite treatment still had significantly lower  $MW_{APP}$  than the control ( $p = 0.0024$ ) while DOM from the gibbsite treatment had intermediate  $MW_{APP}$  values. These data suggest the preferential sorption of high molecular weight compounds by goethite surfaces, which is consistent with previous research (Chorover and Amistadi, 2001; Omoike and Chorover, 2006; Hunt et al., 2007; Ohno et al., 2007). Contrary to previous research (Peuravuori and Pihlaja, 1997; Guo and Chorover, 2003),  $E_2/E_3$  ratios were not correlated with  $MW_{APP}$ , either before or after accounting for the influence of

dissolved metal concentrations on  $MW_{APP}$ . Differences in  $E_2/E_3$  ratios may therefore indicate differences in the abundance of conjugated bonds associated with chromophores, with goethite having a significantly higher abundance of chromophores than both the control and gibbsite treatments.

#### **4.2 Metal-humus complex formation and abundance**

Dissolved Fe and Al were present in DOM from all treatments, and DRIFT data indicated that these dissolved metals interacted with organics in solution. Concentrations of both Fe, in goethite-derived DOM, and Al, in gibbsite-derived DOM were several orders of magnitude larger than their solubility constants would suggest. This large increase in oxide solubility was likely due to the presence of low molecular weight organic acids that substantially increased the solubility of the oxides (Stevenson, 1967; Zunino and Martin, 1977; Robert and Berthelin, 1986; Tan, 1986; Pohlman and McColl, 1988; Essington et al., 2005). Metal:C ratios were smaller than the values found to induce precipitation of metal-humus complexes (Nierop et al., 2002), so any such complexes formed during the incubation most likely remained in the solution phase.

Just as goethite and gibbsite surfaces differed in their effects on DOM properties, solution state Al and Fe also differed in their interaction with DOM. The larger area of the  $1380\text{ cm}^{-1}$  peak in the DRIFT spectra indicated that dissolved Fe had a greater propensity for metal-ligand complexation reactions with dissolved organics than dissolved Al. Dissolved Al appeared to form bonds with both hydroxyls in solution and carboxyl groups of organics, and most likely formed metal-humus complexes both in the

form of Al-organic and Al(OH)<sub>x</sub>-organic complexes. FTIR spectra did not show evidence of hydroxy-Fe species, suggesting Fe-organic ligand bonding as the dominant process. Iron dissolved in the goethite treatment showed greater incorporation into metal-DOM complexes through binding with DOM carboxyls than was observed for Al resulting from the gibbsite treatment.

#### **4.3 Transition of DOM characteristics with increasing time of incubation**

Data did not indicate that the influence of oxide surfaces on DOM characteristics varied with increasing time of incubation, rather that oxide surfaces generally had a continuous and consistent effect on DOM properties throughout the degradation process. Previous work has indicated that sorption reactions among oxide surfaces and dissolved organics proceed rapidly, and that the strength of sorption increases over time (Kaiser et al., 2007). Once bonds are formed, desorption of organics displays a strong hysteresis effect indicating that organics are tightly sorbed to the oxide surface (Gu et al., 1994). Taking this into consideration, desorption of organics from mineral surfaces likely played little role in determining DOM composition throughout the incubation. Therefore, changes in DOM composition throughout the degradation process were most likely indicative of changes in microbial activity, microbial turnover, and the removal of organics from solution by sorption processes. Data indicated that goethite and gibbsite surfaces show a strong preference for certain compounds, affecting only the abundance of these specific organics and leading to a consistent effect over time. Data did suggest a general transition from plant-based compounds to microbially-sourced products in all

treatments (an enrichment in microbial products with increasing degree of degradation) a trend previously noted by Kalbitz et al. (2003).

Both DRIFT and TG/DTA data supported the idea of a transition from plant-based compounds to microbially-derived compounds in DOM solutions over time. Protein: polysaccharide ratios increased over time in all treatments, while the carboxyl: polysaccharide ratio exhibited a general decline. The increase in protein:polysaccharide may indicate enrichment of DOM in microbial byproducts and concomitant with consumption of plant-derived products over time. Polysaccharides derive from both plant and microbial sources, and the ratio of carboxyl groups to polysaccharides is likely affected both by the degree of decomposition of the plant-based organics and the abundance of biomolecules added to the DOM through biomass turnover. The negative carboxyl:polysaccharide trend thus supports the notion that the DOM transitioned from dominantly plant-based to dominantly microbially-based biomolecules over time. In addition, all treatments exhibited an increase in protein: carboxyl ratio which also indicates an increased dominance of DOM by microbially-derived biomolecules relative to more humified plant material.

DOM from all treatments had relatively low enthalpy values, averaging  $9.4 \text{ kJ g}^{-1}$  across all treatments. These values are slightly lower than values for bulk soil organic matter and humic acids found in the literature, which typically range from  $12\text{-}20 \text{ kJ g}^{-1}$  (Peuravuori et al., 1999; Rovira et al., 2008; Rasmussen and White, 2010), indicating that DOM has a relatively low enthalpy of combustion in comparison to soil organic matter as a whole. The low enthalpy of DOM is consistent with previous research indicating that

DOM is one of the more biologically labile fractions of soil organic matter (Zsolnay, 1996). The enthalpies of Exo<sub>1</sub>, Exo<sub>2</sub> and Exo<sub>3</sub> vary according to treatment (Table 4), indicating variation in the materials combusting at each temperature range. This is consistent with results from the DRIFT analysis which indicate both differences in the molecular composition of DOM among treatments and transition of DOM composition with increasing time of incubation.

## **5. Summary**

Results of this experiment illustrate that interaction with goethite and gibbsite surfaces causes changes in the molecular composition, lability and reactivity of DOM. These results not only support previous work indicating that the mineral matrix has a strong effect on DOM properties, but also indicate that specific mineral phases lead to significantly different effects on DOM properties. Such changes in DOM composition are important to soil C cycling as a whole, since DOM comprises the largest flux of nutrients to subsurface soils in temperate forested systems. Changes in the properties of DOM therefore have the potential to affect soil respiration rates and possibly microbial community composition and abundance. In addition, since introduction of labile DOM to subsurface soils often has a priming effect (i.e. increasing the biodegradation of old/stable C pools), changes in DOM properties may affect turnover rates of older/stable C pools in subsurface soils as well.

## **6. Acknowledgements**

This work was supported by a grant from the National Science Foundation (DEB 0543130). The authors wish to thank Dr. Mary Kay Amistadi and Selene Hernandez Ruiz for their generous assistance with HPLC and ICP-MS measurements and Dr. Mercer Meding for his expert guidance and assistance with TG/DTA measurements.

## 7. Figures & Tables

Figure 1. DRIFT spectra for each treatment at each sampling time during the incubation.

a) Control treatment: quartz sand and forest floor material, b) Goethite treatment: quartz sand mixed with goethite and forest floor material, c) Gibbsite: quartz sand mixed with gibbsite and forest floor material.

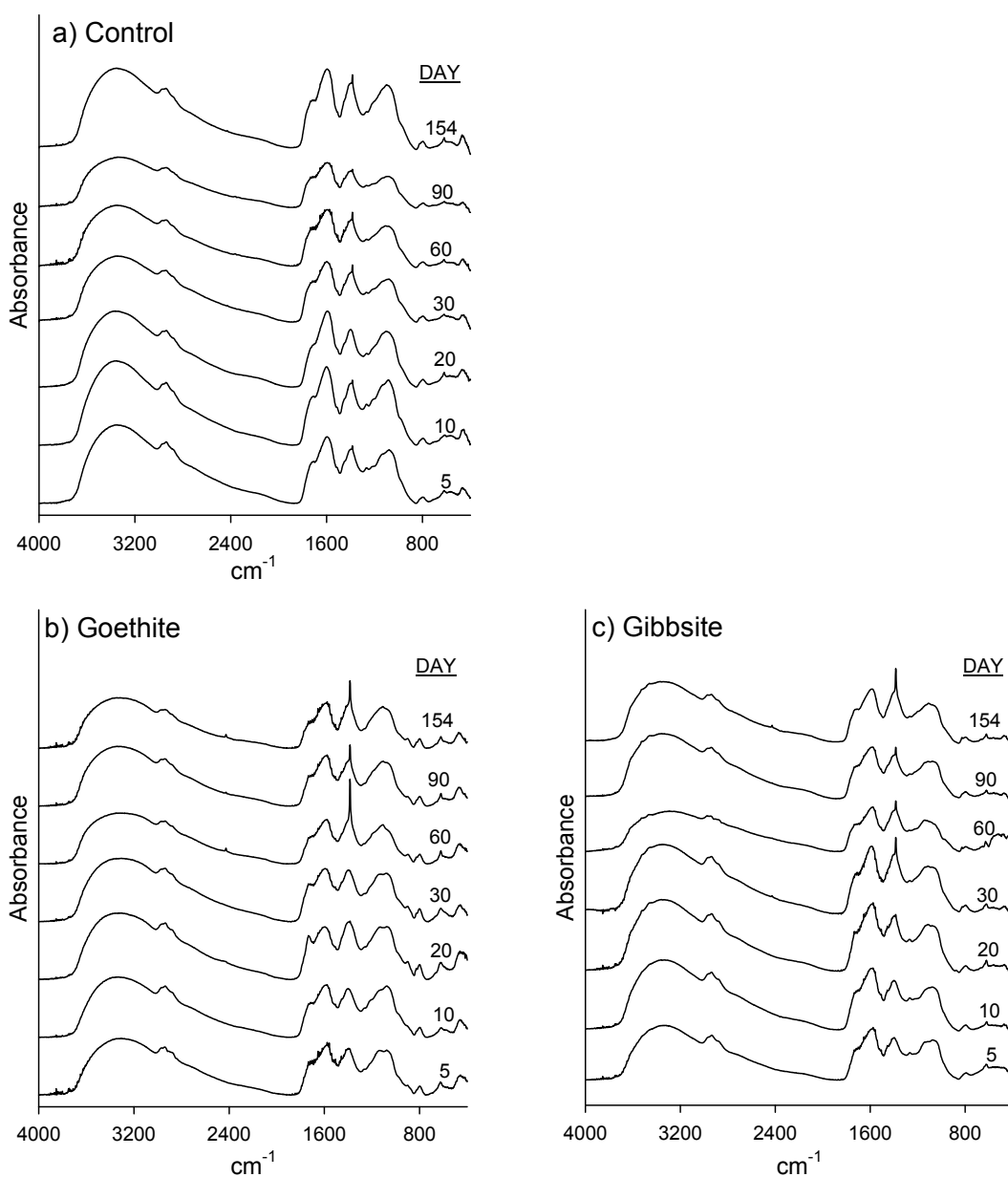


Figure 2: DTA plots for each treatment at each sampling time during the incubation. a) Control treatment: quartz sand and forest floor material, b) Goethite treatment: quartz sand mixed with goethite and forest floor material, c) Gibbsite: quartz sand mixed with gibbsite and forest floor material. Drop lines represent average peak maximums: 300°C, 410°C, and 550°C.

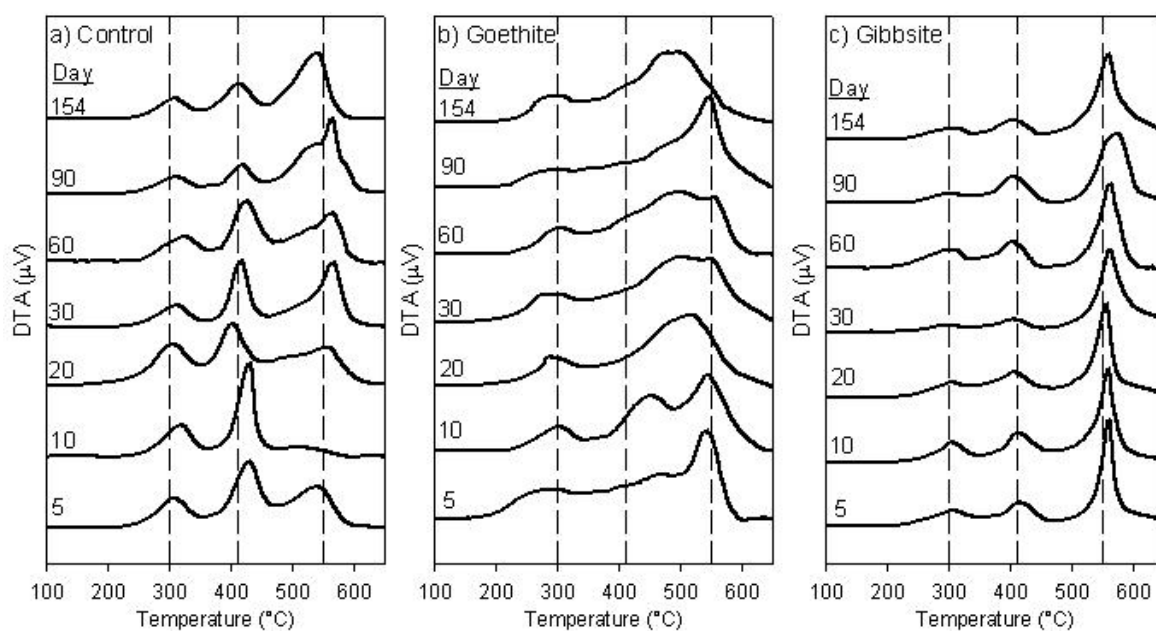


Figure 3. Analysis of DRIFT spectra. The ratio of the areas under the polysaccharide, amide 1, and the asymmetric carboxyl peak are plotted against time. a) The ratio of area under the Amide 1 band and polysaccharide peak are plotted against time of incubation, showing a general increase in amides over time in all treatment groups, b) The ratio of area under the Amide 1 band and the asymmetric carboxyl peak are plotted against time of incubation, showing an enrichment in amides in comparison to carboxyls with increasing time of incubation, c) The ratio of area under the asymmetric carboxyl peak and the area under the polysaccharide peak are plotted against time of incubation showing a slight decrease in carboxyl content in comparison to polysaccharide content with increasing time of incubation.

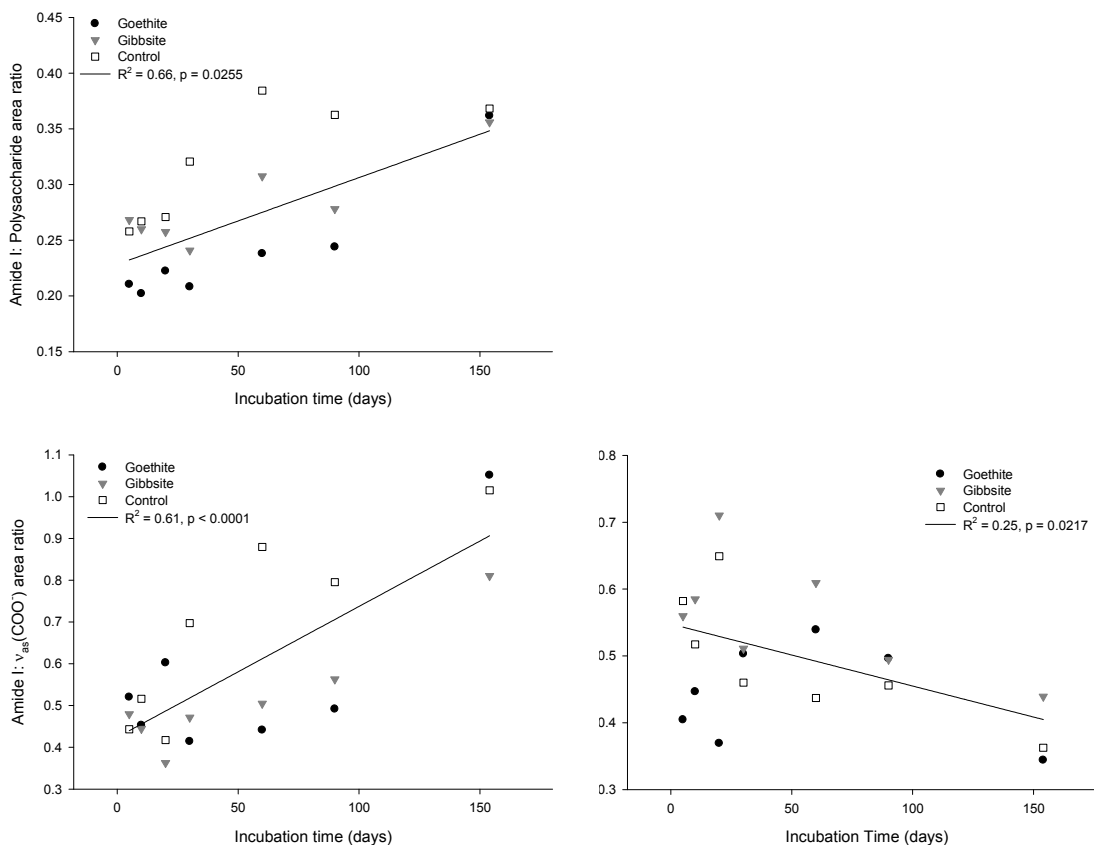


Table 1: Characteristics of dissolved organic matter solutions.

Treatment	Incubation length Days	DOC $\mu\text{mg g}^{-1}\text{ liter}^{-1}\text{ C}^{-1}$	C:N	E <sub>2</sub> /E <sub>3</sub>	Molar Absorptivity A mol <sup>-1</sup> C <sup>-1</sup>	pH	MW <sub>AP</sub> Daltons	Fe:C mmol <sub>Fe</sub> :mol <sub>boc</sub>	Al:C mmol <sub>Al</sub> :mol <sub>boc</sub>
Control	5	17.8 (3.5)	119.5 (23.9)	5.7 (0.2)	44.6 (8.8)	5.62 (0.03)	2957 (42)	0.09 (0.03)	0.91 (0.23)
	10	13.0 (1.7)	66.1 (14.2)	5.4 (0.1)	52.1 (8.7)	5.00 (0.07)	4951 (1815)	0.14 (0.02)	0.74 (0.11)
	20	41.1 (12.2)	221.7 (80.1)	6.9 (0.1)	15.4 (3.6)	5.75 (0.01)	2760 (194)	0.06 (0.01)	0.26 (0.06)
	30	8.1 (2.5)	42.5 (18.4)	5.5 (0.1)	87.1 (22.8)	5.62 (0.02)	4218 (681)	0.32 (0.08)	1.26 (0.33)
	60	46.7 (6.0)	88.1 (7.6)	6.1 (0.1)	88.1 (1.4)	6.06 (0.03)	2951 (12)	0.06 (0.01)	0.27 (0.03)
	90	10.1 (0.9)	61.4 (11.7)	5.9 (0.1)	63.7 (5.3)	6.13 (0.04)	2723 (27)	0.21 (0.01)	0.86 (0.10)
154	5.8 (0.2)	27.3 (13.2)	7.1 (0.6)	102.5 (0.9)	6.25 (0.02)	3904 (30)	0.44 (0.07)	2.47 (0.05)	
Average over time		<b>20.3<sup>A</sup></b>	<b>89.5<sup>A</sup></b>	<b>6.1<sup>A</sup></b>	<b>64.8<sup>A</sup></b>	<b>5.78<sup>B</sup></b>	<b>3495<sup>A</sup></b>	<b>0.19<sup>B</sup></b>	<b>0.97<sup>B</sup></b>
Goethite	5	15.2 (2.7)	128.4 (29.7)	2.8 (0.2)	32.4 (4.4)	5.95 (0.07)	1604 (105)	2.91 (0.7)	0.56 (0.32)
	10	9.6 (1.6)	60.2 (12.9)	3.3 (0.1)	39.8 (5.9)	5.71 (0.17)	1600 (123)	5.91 (1.17)	0.25 (0.07)
	20	14.4 (1.5)	32.0 (8.5)	3.3 (0.7)	26.5 (1.8)	5.41 (0.27)	1702 (295)	7.05 (1.7)	0.22 (0.07)
	30	11.3 (3.3)	80.5 (25.1)	2.6 (0.2)	29.5 (12.6)	5.92 (0.01)	2024 (292)	8.74 (1.61)	0.03 (0)
	60	7.2 (2.3)	219.5 (0.00)	2.5 (0.1)	77.3 (18.3)	6.10 (0.01)	2371 (8)	16.00 (3.98)	0.5 (0.12)
	90	8.3 (1.5)	57.1 (1.0)	3.1 (0.2)	47.7 (10.6)	6.27 (0.04)	2071 (95)	2.98 (0.75)	0.37 (0.08)
154	4.1 (0.4)	19.0 (2.0)	2.6 (0.1)	114.3 (17.4)	6.35 (0.02)	3016 (224)	32.75 (6.04)	1.62 (0.24)	
Average over time		<b>10.00<sup>B</sup></b>	<b>85.2<sup>A</sup></b>	<b>2.9<sup>B</sup></b>	<b>52.5<sup>A</sup></b>	<b>5.96<sup>A,B</sup></b>	<b>2056<sup>B</sup></b>	<b>10.91<sup>A</sup></b>	<b>0.51<sup>B</sup></b>
Gibbsite	5	11.5 (1.7)	65.5 (21.5)	5.6 (0.3)	46.5 (6.1)	6.17 (0.02)	1763 (27)	0.2 (0.03)	3.72 (0.43)
	10	10.5 (1.8)	80.2 (20.7)	5.6 (0.0)	44.5 (4.7)	5.92 (0.01)	2144 (27)	0.08 (0.01)	1.78 (0.17)
	20	16.9 (7.2)	54.5 (52.1)	7.6 (0.1)	34.0 (10.7)	5.20 (0.57)	2043 (204)	0.27 (0.18)	2.81 (0.98)
	30	7.0 (1.1)	47.6 (4.1)	5.6 (0.0)	57.4 (5.7)	5.95 (0.01)	2152 (79)	0.68 (0.47)	3.2 (0.11)
	60	11.7 (1.8)	83.9 (0.8)	6.1 (0.1)	40.2 (5.7)	6.15 (0.01)	2800 (22)	0.14 (0.02)	3.16 (0.45)
	90	5.5 (0.5)	42.1 (3.5)	5.9 (0.0)	78.8 (3.9)	6.40 (0.01)	2840 (492)	0.28 (0.01)	6.14 (0.13)
154	4.2 (0.1)	16.1 (12.0)	7.0 (0.8)	83.6 (2.4)	6.52 (0.04)	4835 (318)	3.40 (0.02)	8.88 (0.35)	
Average over time		<b>9.6<sup>B</sup></b>	<b>55.7<sup>A</sup></b>	<b>6.2<sup>A</sup></b>	<b>55.0<sup>A</sup></b>	<b>6.05<sup>A</sup></b>	<b>2654<sup>B</sup></b>	<b>0.28<sup>B</sup></b>	<b>4.24<sup>A</sup></b>

<sup>A</sup> specifically. Dissolved Organic Carbon, measured as milligrams of C in the dissolved organic C fraction, divided by the total grams of C in the solid sample prior to incubation. Values at each time point are the average of three replicates for each treatment (n=3). "Average over time" values are the average of all replicates across time (n=21). Significance was determined using two-way ANOVA with treatment and time as main effects, followed by Tukey's HSD *post hoc* test (α=0.05). Within each column, means followed by different superscript letters are significantly different.

Table 2. Peak assignments for DRIFT spectra of DOM samples

Peak position (cm <sup>-1</sup> )	Assignment	Reference
3530	Metal-OH stretch	4
3470	Metal-OH stretch	4
3380	phenolic OH stretch	1,2,3,5
2990	Aliphatic C-H stretch	4,6
2970-2950	Aliphatic CH <sub>2</sub> and CH <sub>3</sub> stretching	1,2
2910-2900	Aliphatic C-H stretching	4,5
1730	symmetric C=O stretch of esters	2
1655-1640	C=O stretch of amides	1,2,3,5
1580	asymmetric COO <sup>-</sup> stretch	1,2,3,6
1455-1445	CH <sub>2</sub> scissoring	4
1390-1400	symmetric COO <sup>-</sup> stretch	1,2,3,6
1385	COO-metal stretch	8,9
1270-1235	C-O stretch of polysaccharides, OH deformation of COOH	7
1200	C-O stretch of polysaccharides, OH deformation of COOH	7
~1140	C-O stretch of polysaccharides	7
1080	C-O stretch of polysaccharides	7
1055-1040	C-O stretch of polysaccharides	7
~950	C-O stretch of polysaccharides	7
~900	C-O stretch of polysaccharides	7

1) Gressel et al. 1995, 2) Swift 1996, 3) Baes & Bloom 1989, 4) Socrates 2001, 5) Senesi & Loffredo 1999  
6) Colthup 1950, 7) Stevenson 1994, 8) Fu & Quan 2006, 9) Gu et al. 1994

Table 3. Significant differences of DRIFT peak areas among treatments

	<b>Amide I</b>	<b>AmideI/<math>\Sigma</math>polysaccharide</b>	<b>Metal+COO<sup>-</sup></b>	<b>Esters</b>	<b>v<sub>as</sub>COO<sup>-</sup></b>	<b>vMetal-OH</b>
<b>peak max (cm<sup>-1</sup>)</b>	1650	1650/sum(1240,1140,1055,950,900)	1380	1730	1580	3500, 3530
<b>Control</b>	A	A	B	A	AB	B
<b>Goethite</b>	B	B	A	B	B	B
<b>Gibbsite</b>	AB	AB	AB	AB	A	A
<b>F statistic</b>	0.0018	0.0322	0.0159	0.0067	0.0213	<0.0001

Significance was determined using one-way ANOVA by treatment followed by Tukey's HSD *post hoc* test ( $\alpha=0.05$ ). Within each column, different letters indicate statistically significant differences among variables. ( $n=7$ ) for each treatment.

Table 4: Changes in distribution of mass and energy loss over the course of the incubation

Treatment	Incubation length Days	Enthalpy		Exo-ROT % mass loss	% of total mass loss per peak			Enthalpy (kJ g <sub>mass,loss</sub> <sup>-1</sup> )		
		kJ g <sub>mass,loss</sub> <sup>-1</sup>	kJ g <sub>mass</sub> <sup>-1</sup>		Exo <sub>1</sub>	Exo <sub>2</sub>	Exo <sub>3</sub>	Exo <sub>1</sub>	Exo <sub>2</sub>	Exo <sub>3</sub>
<b>Control</b>	5	21.7	11.4	52	49	34	18	9.9	25.7	46.3
	10	21.7	10.2	47	55	32	13	13.2	37.4	19.3
	20	23.2	12.0	52	50	29	21	13.4	19.5	51.8
	30	8.1	7.7	95	19	71	10	7.6	3.3	42.7
	60	14.3	7.4	52	50	25	25	5.8	21.4	24.4
	90	8.2	8.1	99	15	71	14	8.0	2.2	38.5
154	19.2	9.6	50	52	14	34	5.6	42.4	30.1	
Average over time		<b>16.6 (2.4)</b>	<b>9.5 (0.7)</b>	<b>64 (9)</b>	<b>41 (6)</b>	<b>39 (8)</b>	<b>19 (3)</b>	<b>9.1 (1.2)</b>	<b>21.7 (5.8)</b>	<b>36.1 (4.5)</b>
<b>Goethite</b>	5	32.0	15.0	46	47	53	53	21.9	42.3	42.3
	10	17.9	8.5	48	46	54	54	5.5	28.3	28.3
	20	23.8	11.4	47	48	52	52	15.4	32.4	32.4
	30	20.5	9.3	45	52	48	48	6.5	36.5	36.5
	60	20.7	8.3	39	48	52	52	5.7	36.2	36.2
	90	22.9	9.6	47	43	57	57	13.4	25.9	25.9
154	25.1	9.5	37	43	57	57	9.2	38.1	38.1	
Average over time		<b>23.2 (1.7)</b>	<b>10.2 (0.9)</b>	<b>44 (2)</b>	<b>47 (1.2)</b>	<b>46 (1)</b>	<b>46 (1)</b>	<b>11.1 (2.3)</b>	<b>34.2 (2.2)</b>	<b>34.2 (2.2)</b>
<b>Gibbsite</b>	5	17.0	9.4	55	48	25	28	6.1	13.9	38.2
	10	17.6	10.0	57	44	26	29	6.6	15.3	36.0
	20	20.5	11.0	54	44	25	31	8.1	17.4	40.8
	30	14.5	8.2	57	37	25	38	3.1	10.6	28.2
	60	15.4	8.0	52	42	24	33	4.8	7.4	34.7
	90	11.9	5.9	49	42	26	33	3.3	10.6	24.0
154	14.9	6.9	46	44	24	32	3.7	9.8	34.0	
Average over time		<b>16.0 (1.0)</b>	<b>8.5 (0.7)</b>	<b>52 (1)</b>	<b>43 (1)</b>	<b>25 (0)</b>	<b>32 (1)</b>	<b>5.1 (0.7)</b>	<b>12.2 (1.3)</b>	<b>33.7 (2.2)</b>

Numbers in parentheses the standard errors for the 7 sampling times.

## 8. References

- Almendros G., Polo A. and Vizcayno C. (1982) Application of thermal analysis to the study of several Spanish peats. *Journal of Thermal Analysis* **24**, 175-182.
- Baes A.U. and Bloom P.R. (1989) Diffuse Reflectance and Transmission Fourier Transform Infrared Spectroscopy of Humic and Fulvic Acids. *Soil Science of America Journal* **53**, 695-700.
- Baldock J.A. and Skjemstad J.O. (2000) Role of the soil matrix and minerals in protecting natural organic materials against biological attack. *Organic Geochemistry* **31**, 697-710.
- Boudot J.P., Bel Hadj B.A., Steiman R., Seigle-Murandi F. (1989) Biodegradation of synthetic organo-metallic complexes of iron and aluminum with selected metal:C ratios. *Biology and Biochemistry* **21**, 961-966.
- Brunauer S., Emmett P. H. and Teller E. (1938) Adsorption of gases in multimolecular layers. *Journal of the American Chemical Society* **60**, 309-319
- Byler D.M., Gerasimowicz W.V., Susi H. and Schnitzer M. (1987) FT-IR spectra of soil constituents: Fulvic acid and fulvic acid complex with ferric ions. *Applied Spectroscopy* **41**(8), 1428-1430.
- Cassel D.K. and Nielsen D.R. (1986) Field capacity and available water capacity. In *Methods of Soil Analysis. Part 1: Physical and mineralogical methods, 2nd ed.* SSSA Book Series 5. (ed. Klute A.). SSSA Inc., Madison, WI. pp. 901-926
- Chin Y.P., Aiden G. and O'Loughlin E. (1994) Molecular weight, polydispersity, and spectroscopic properties of aquatic humic substances. *Environmental Science and Technology* **28**, 1853-1858.
- Chorover J. and Amistadi M.K. (2001) Reaction of forest floor organic matter at goethite, birnessite and smectite surfaces. *Geochimica et Cosmochimica Acta* **65**(1), 95-109.
- Cebulak S. and Langier-Kùznarowa A. (1997) Application of oxyreactive thermal analysis to the examination of organic matter associated with rocks. *Journal of Thermal Analysis and Calorimetry* **50**(1-2), 175-190.
- Ciavatta C., Govi M., Antisari L.V. and Sequi P. (1990) Characterization of humified compounds by extraction and fractionation on solid ployvinylpyrrolidone. *Journal of Chromatography* **509** (1), 141-146.

Ciavatta C., Govi M., Antisari L. V. and Sequi P. (1991) Determination of organic carbon in aqueous extracts of soils and fertilizers. *Commun Soil Sci Plant Anal* **22**, 795–807.

Colthup N.B. (1950) Spectra-Structure Correlations in the Infra-Red Region. *Journal of the Optical Society of America* **40(6)**, 397-400.

Cornell R.M. and Schwertmann U. (1996) *The Iron Oxides*. VCH Inc., New York.

De la Rosa J.M., Knicker H., Lopez-Capel E., Manning D.A.C., Gonzalez-Perez J.A. and Gonzalez-Vila F.J. (2008) Direct detection of black carbon in soils by Py-GC/MS, carbon-13 NMR spectroscopy and thermogravimetric techniques. *Soil Science Society of America Journal* **72**, 258–267.

Dell'Abate M.T., Benedetti A., Trinchera A. and Dazzi C. (2002) Humic substances along the profile of two Typic Haploxerert. *Geoderma* **107**, 281–296.

Dell'Abate M.T., Benedetti A., and Brookes P.C. (2003) Hyphenated techniques of thermal analysis for characterization of soil humic substances. *Journal of Separation Science* **26**, 433–440.

Essington M.E., Nelson J.B. and Holden W.L. (2005) Gibbsite and goethite solubility: The influence of 2-ketogluconate and citrate. *Soil Science Society of America Journal* **69**, 996-1008.

Eusterhues K., Rumpel C., Kleber M. and Kögel-Knabner I. (2003) Stabilization of soil organic matter by interactions with minerals as revealed by mineral dissolution and oxidative degradation. *Organic Geochemistry* **34**, 1591-1600.

Evanko C.R. and Dzombak D.A. (1999) Surface complexation modeling of organic acid sorption to Goethite. *Journal of Colloid and Interface Science* **214**, 189-206.

Fu H. and Quan X. (2006) Complexes of fulvic acid on the surface of hematite, goethite, and akaganeite: FTIR observation. *Chemosphere* **63**, 403-410.

Greenland D.J. (1971) Interactions between humic and fulvic acids and clays. *Soil Science* **111**, 34.

Gressel N., McGrath A.E., McColl J.G. and Powers R.F. (1995) Spectroscopy of aqueous extracts of forest litter. I: Suitability of Methods. *Soil Science Society of America Journal* **59**, 1715-1723.

Gu B., Schmitt J., Chen Z., Liang L. and McCarthy J.F. (1994) Adsorption and desorption of natural organic matter on iron oxide: mechanisms and models. *Environmental Science and Technology* **28**, 38-46.

- Guan, X-H., Shang, C. and Chen, G-H (2006) ATR-FTIR investigation of the role of phenolic groups in the interaction of some NOM model compounds with aluminum hydroxide. *Chemosphere* **65**, 2074-2081.
- Guo M. and Chorover J. (2003) Transport and fractionation of dissolved organic matter in soil columns. *Soil Science* **168**, 108-118
- Heckman K., Welty-Bernard A., Rasmussen C., Schwartz E. (2009) Geologic controls of soil carbon cycling and microbial dynamics in temperate conifer forests. *Chemical Geology* **267**, 12-23.
- Hunt J.F., Ohno T., He Z., Honeycutt C.W. and Dail D.B. (2007) Influence of Decomposition on Chemical Properties of Plant- and Manure-Derived Dissolved Organic Matter and Sorption to Goethite. *Journal of Environmental Quality* **36**, 135-143.
- Jones D.L. and Edwards A.C. (1998) Influence of sorption on the biological utilization of two simple carbon substrates. *Soil Biology and Biochemistry* **30**, 1895-1902.
- Kaiser K., Guggenberger G. (2000) The role of DOM sorption to mineral surfaces in the preservation of organic matter in soils. *Organic Geochemistry* **31**, 711-725.
- Kaiser K., Mikutta R. and Guggenberger G. (2007) Increased stability of organic matter sorbed to ferrihydrite and goethite on aging. *Soil Science Society of America Journal* **71**, 711-719.
- Kalbitz K., Solinger S., Park J.-H., Michalzik B. and Matzner E. (2000) Controls on the dynamics of dissolved organic matter in soils: A review. *Soil Science* **165**, 277-304.
- Kalbitz K., Schwesig D., Schmerwitz J., Kaiser K., Haumaier L., Glaser B., Ellerbrock R. and Leinweber P. (2003) Changes in properties of soil-derived dissolved organic matter induced by biodegradation. *Soil Biology & Biochemistry* **35**, 1129-1142.
- Kalbitz K., Schwesig D., Rethemeyer J. and Matzner E. (2005) Stabilization of dissolved organic matter by sorption to the mineral soil. *Soil Biology & Biochemistry* **37**, 1319-1331.
- Kampf N., Scheinost A.L. and Schulze D.G. (2000) Oxide minerals.. In *Handbook of soil science*. (ed. M.E. Sumner). CRC Press, Boca Raton, FL. pp. 125-168
- Lal R. (2004) Soil carbon sequestration impacts on global climate change and food security. *Science* **304**, 1623-1627.
- Lindsay W.L. (1997) *Chemical Equilibria in Soils*. John Wiley & Sons, New York

- Lopez-Capel E., Sohi S.P., Gaunt J.L. and Manning D.A.C. (2005) Use of thermogravimetry differential scanning calorimetry to characterize modelable soil organic matter fractions. *Soil Science Society of America Journal* **69**, 136–140.
- Lopez-Capel E., Abbott G.D., Thomas K.M. and Manning, D.A.C. (2006) Coupling of thermal analysis with quadrupole mass spectrometry and isotope ratio mass spectrometry for simultaneous determination of evolved gases and their carbon isotopic composition. *Journal of Analytical and Applied Pyrolysis* **75**, 82–89.
- Lu X.G., Vassallo A.M. and Johnson W.D. (1997) Thermal stability of humic substances and their metal forms: an investigation using FTIR emission spectroscopy. *Journal of Analytical and Applied Pyrolysis* **43**, 103-113.
- Manning D.A.C., Lopez-Capel E. and Barker S. (2005) Seeing soil carbon: Use of thermal analysis in the characterization of soil C reservoirs of differing stability. *Mineral. Mag.* **6**, 425–435.
- Martin J. P. and Haider K. (1986) Influence of mineral colloids on turnover rates of soil organic carbon. *Soil Sci. Soc. Am. J.* **17**, 283-304.
- Masiello C.A., Chadwick O.A., Southon J., Torn M.S. and Harden J.W. (2004) Weathering controls on mechanisms of carbon storages in grassland soils. *Global Geochemical Cycles* **18**, GB4023, doi:10.1029/2004GB002219.
- McKnight D.M., Bencala K.E., Zellweger G.W., Aiken G.R., Feder G.L., and Thorn K.A. (1992) Sorption of dissolved organic-carbon by hydrous aluminum and iron-oxides occurring at the confluence of deer creek with the Snake River, Summit County, Colorado. *Environmental Science & Technology* **26**, 1388-1396.
- Meier M., Namjesnik-Dejanovic K., Maurice P.A., Chin Y.-P. and Aiken G.R. (1999) Fractionation of aquatic natural organic matter upon sorption to goethite and kaolinite. *Chemical Geology* **157**, 275-284.
- Michalzik B., Kalbitz K., Park J.H., Solinger S., Matzner E. (2001) Fluxes and concentrations of dissolved organic carbon and nitrogen – a synthesis for temperate forests. *Biogeochemistry* **52**, 173-205.
- Molis E., Barrès O., Marchand H., Sauzéat E., Humbert B. and Thomas F. (2000) Initial steps of ligand-promoted dissolution of gibbsite. *Colloids and Surfaces A: Physicochemical and Engineering Aspects* **163**, 283-292
- Montecchio D., Francioso O., Carletti P., Pizzeghello D., Chersich S., Previtali F. and Nardi S. (2006) Thermal analysis (TG-DTA) and DRIFT spectroscopy applied to

- investigate the evolution of humic acids in forest soil at different vegetation stages. *Journal of thermal analysis and calorimetry* **83**, 393-399.
- Nierop K.G.J.J., Jansen B. and Verstraten J.M. (2002) Dissolved organic matter, aluminum and iron interactions: precipitation induced by metal/carbon ratio, pH and competition. *The Science of the Total Environment* **300**, 201-211.
- Ohno T., Chorover J., Omoike A. and Hunt J. (2007) Molecular weight and humification index as predictors of adsorption for plant- and manure-derived dissolved organic matter to goethite. *European Journal of Soil Science* **58**, 125-132.
- Omoike A. and Chorover J. (2006) Adsorption to goethite of extracellular polymeric substances from *Bacillus subtilis*. *Geochimica et Cosmochimica Acta* **70**, 827-838.
- Parfitt R.L., Fraser A.R. and Farmer V.C. (1977) Adsorption on hydrous oxides. III. Fulvic acid and humic acid on goethite, gibbsite and imogolite. *European Journal of Soil Science* **28**, 289 – 296.
- Plankey, B.J. and Patterson, H.H. (1987) Kinetics of Aluminum-Fulvic Acid Complexation in Acidic Waters. *Environmental Science and Technology* **21**, 595-601.
- Plante A.F., Pernes M. and Chenu C. (2005) Changes in clay-associated organic matter quality in a C depletion sequence as measured by differential thermal analyses. *Geoderma* **129**, 186–199.
- Plante A.F., Fernández J.M. and Leifeld J. (2009) Application of thermal analysis techniques in soil science. *Geoderma* **153**, 1-10.
- Peuravuori J. and Pihlaja K. (1997) Molecular size distribution and spectroscopic properties of aquatic humic substances. *Analytica Chimica Acta* **337**, 133-149.
- Pohlman A.A. and McColl J.G. (1988) Soluble organics from forest litter and their role in metal dissolution. *Soil Science Society of America Journal* **52**, 265-271.
- Provenzano M.R. and Senesi N. (1998) Differential scanning calorimetry of river aquatic fulvic acids and their metal complexes. *Fresenius Environmental Bulletin* **7**, 423-428.
- Theng B.K.G. and Tate K.R. (1989) Interactions of clays with soil organic constituents. *Clay Res.* **8**, 1–10.
- Qualls R.G., Takiyama A., Wershaw R.L. (2003) Formation and loss of humic substances during decomposition in a pine forest floor. *Soil Science Society of America Journal* **67**, 899-909.

Ranalli G., Bottura G., Taddei P., Marchetti R. and Sorlini, C. (2001) Composting of solid and sludge residues from agricultural and food industries. Bioindicators of monitoring and compost maturity. *Journal of Environmental Science and Health. Part A Toxic/Hazardous Substances & Environmental Engineering* **36**, 415–436.

Rasmussen, C., and White, D.A., II (2010) Vegetation effects on soil organic carbon quality in an arid hyperthermic ecosystem. *Soil Science* **175**, DOI: 10.1097/SS.0b013e3181f38400.

Robert M. and Berthelin J. (1986) Role of Biological and Biochemical Factors in Soil Mineral Weathering. In *Interaction of Soil Minerals with Natural Organics and Microbes, Special Publication 17*. (eds. P.M. Huang and M. Schnitzer). Soil Science Society of America: Madison. pp. 1-27.

Rovira R., Kurz-Besson C., Couteaux M.M. and Vallejo V.R. (2008) Changes in letter properties during decomposition: a study by differential thermogravimetry and scanning calorimetry. *Soil Biology & Biochemistry* **40**, 172-185.

Rumpel C., Kögel-Knabner I. (2010) Deep soil organic matter – a key but poorly understood component of terrestrial C cycle. *Plant and Soil* (**in press**) DOI 10.1007/s11104-010- 0391-5.

Scheel T., Dörfler C. and Kalbitz K. (2007) Precipitation of dissolved organic matter by aluminum stabilizes carbon in acidic forest soils. *Soil Science Society of America Journal* **71**, 64-74.

Schnitzer M. and Kodama H. (1972) Differential thermal analysis of metal-fulvic acid salts and complexes. *Geoderma* **7**, 93-103.

Schulten H.R. and Leinweber P. (1999) Thermal stability and composition of mineral-bound organic matter in density fractions of soil. *European Journal of Soil Science* **50**, 237-248.

Schwertmann U. (1991) Solubility and dissolution of iron oxides. *Plant and Soil* **130**, 1-25.

Schwesig D., Kalbitz K. and Matzner E. (2003) Mineralization of dissolved organic carbon in mineral soil solution of two forest soils. *Journal of Plant Nutrition and Soil Science* **166**, 585-593.

Senesi N. and Elisabetta L. (1999) The chemistry of soil organic matter. In *Soil Physical Chemistry, second edition*. (ed. D. L. Sparks). CRD Press LLC, New York. Pp. 239-370.

Sheppard J.D. and Forgeron D.W. (1987) Differential thermogravimetry of peat fractions. *Fuel* **66**, 232-236.

Socrates G. (2001) *Infrared and Raman Characteristic Group Frequencies: Tables and Charts 3rd Edition*. John Wiley & Sons, Ltd, New York.

Stevenson F.J. (1967) Organic acids in soils. In *Soil Biochemistry*. (eds. A.D. McLaren and G.H. Peterson). Marcel Dekker, New York. pp. 119-146.

Stevenson FJ (1994) *Humus Chemistry—Genesis, Composition, Reactions, 2<sup>nd</sup> Ed*. Wiley, New York.

Stevenson FJ, Cole MA (1999) *Cycles of Soil: Carbon, Nitrogen, Phosphorous, Sulfur, Micronutrients, 2<sup>nd</sup> Ed*. John Wiley & Sons, Inc: New York.

Strezov V., Moghtaderi B. and Lucas J.A. (2004) Computational calorimetric investigation of the reactions during thermal conversion of wood biomass. *Biomass & Bioenergy* **27**, 459–465.

Swift R.S. (1996) Organic matter characterization. In: *Methods of Soil Analysis: Part 3, Chemical Methods, SSSA Book Series 5*. (eds. D.L. Sparks et al.). Soil Science Society of America, Madison, WI. pp. 1018–1020.

Tan K.H. (1978) Formation of metal-humic acid complexes by titration and their characterization by differential thermal analysis and infrared spectroscopy. *Soil Biology & Biochemistry* **10**, 123-129.

Tan K.H. (1986) Degradation of Soil Minerals by Organic Acids. In *Interaction of Soil Minerals with Natural Organics and Microbes, Special Publication 17*. (eds. P.M. Huang and M. Schnitzer). Soil Science Society of America, Inc., Madison, WI. pp. 1-27.

Torn M.S., Trumbore S.E., Chadwick O.A., Vitousek P.M. and Hendricks D.M. (1997) Mineral control of soil organic carbon storage and turnover. *Nature* **389**, 170-173.

Veldkemp E. (1994) Organic carbon turnover in three tropical soils under pasture after deforestation. *Soil Science Society of America Journal* **58**, 175–180.

von Lützw M., Kogel-Knabner I., Ekschmitt K., Matzner E., Guggenberger G., Marschner B., Flessa H. (2006) Stabilization of organic matter in temperate soils: mechanisms and their relevance under different soil conditions - a review. *European Journal of Soil Science* **57**, 426-445.

Wagai R. and Sollins P. (2002) Biodegradation and regeneration of water-soluble carbon in a forest soil: leaching column study. *Biology and Fertility of Soils* **35**, 18-26.

Zech W. and Guggenberger G. (1996) Organic matter dynamics in forest soils of temperate and tropical ecosystems. In: *Humic Substances in Terrestrial Ecosystems*. (ed. A. Piccolo). Elsevier, Amsterdam. pp. 101–170.

Zhou Q., Maurice P. A. and Cabaniss S. E. (2001) Size fractionation upon adsorption of fulvic acid on goethite: Equilibrium and kinetic studies. *Geochimica et Cosmochimica Acta* **65**, 803-812.

Zsolnay A. (1996) Dissolved humus in soil waters. In *Humic substances in terrestrial ecosystems*. (ed. A. Piccolo). Elsevier, Amsterdam. pp. 225-264.

Zunino H. and Martin J.P. (1977) Metal-binding organic macromolecules in soil: 1. Hypothesis interpreting the role of soil organic matter in the translocation of metal ions from rocks to biological systems. *Soil Science* **123**, 65-76.

## APPENDIX D

EXPOSURE TO GOETHITE AND GIBBSITE SURFACES ALTERS DOM  
NUTRIENT DYNAMICS AND MICROBIAL COMMUNITY COMPOSITION

Katherine Heckman<sup>a\*</sup>, Amy Welty-Bernard<sup>b</sup>, Craig Rasmussen<sup>a</sup>, Egbert Schwartz<sup>b</sup>,  
Jonathan Chorover<sup>a</sup>, Angelica Vazquez Ortega<sup>a</sup>

\*Corresponding Author

<sup>a</sup>Department of Soil, Water and Environmental Science; University of Arizona

1177 E. Fourth Street PO Box 210038

Tucson, AZ 85721-0038, USA

kheckman@email.arizona.edu

phone : +1 520 621 1646, fax : +1 520 621 1647

<sup>b</sup>Department of Biological Sciences, Northern Arizona University

PO Box 5640

Flagstaff, AZ 86011-5640, USA

phone : +1 928 523 2381, fax : +1 928 523 7500

Prepared for submission to *Geoderma*

### Abstract

Iron and aluminum oxides are ubiquitous in the soil environment and due to their high surface area have the potential to strongly affect dissolved organic matter (DOM) properties. We directly examined the effect of oxide surfaces on DOM nutrient dynamics and microbial community composition using an incubation of forest floor material in the presence of 1) goethite surfaces 2) gibbsite surfaces and 3) quartz sand surfaces (as a control treatment). Forest floor material was incubated over a period of 154 days. Dissolved organic matter was harvested on days 5, 10, 20, 30, 60, 90, and 154, and concentrations of P, N,  $\text{PO}_4^{3-}$ ,  $\text{NO}_2^-$ ,  $\text{NO}_3^-$ , and organic C were measured in the DOM solutions. Microbial community composition was examined through pyrosequencing on selected dates throughout the incubation. Results indicate that oxide surfaces have a strong effect on nutrient dynamics in DOM and the composition of the decomposer microbial community. Goethite and gibbsite surfaces showed a strong preference for sorption of P-containing compounds and high molecular weight compounds, but not for N-containing compounds. On average, organic C concentrations were significantly lower in DOM solutions from oxide treatments than from the control treatment. Microbial community composition varied both among treatments and with increasing time of incubation. Variation in bacterial and fungal community composition showed strong-to-moderate correlation with length of incubation, and several DOM physiochemical characteristics including apparent molecular weight, pH and electrical conductivity. Additionally, variation in bacterial community composition among treatments was correlated with P,  $\text{PO}_4^{3-}$ , organic C, and  $\text{NO}_3^-$  concentrations; while variation in fungal

communities was correlated with organic C concentrations, and Al concentrations to a lesser degree. Correlations among nutrient concentrations and community composition indicate that the influence of oxide surfaces on DOM quality has significant ramifications for both bacterial and fungal communities.

## **1. Introduction**

Concerns over global climate change have increased interest in clarifying the mechanisms regulating organic C storage in soils. Forest soils contain a substantial portion of the world's C stocks, and therefore mechanisms regulating the size and turnover rate of organic matter in forest soils are of particular importance. Though dissolved organic matter (DOM) comprises only ~1% of the total organic C in soils, DOM is the most mobile fraction of soil organic carbon (Zsolnay, 1996) and is the largest source of new C inputs to subsurface soils (Zech and Guggenberger, 1996). Previous research has also suggested that biodegradation of soil organic matter is mediated by the aqueous phase, (Kalbitz et al., 2003a) and that DOM may be the most important C source for soil microbes in general since C uptake mechanisms require an aqueous environment (Metting, 1993; Jandl and Sollins, 1997; Wagai and Sollins, 2002; Marschner & Kalbitz, 2003). Therefore, changes in the composition of DOM may have a profound influence on C mineralization rates and both size and activity of the decomposer community, especially in subsurface soils.

Sorption of organic C to mineral surfaces has been recognized as one of the most important stabilization mechanisms controlling organic C content in sediments (Keil et

al., 1994). Sorption of organics to mineral surfaces has been shown to reduce the bioavailability of microbial substrates and can greatly reduce C mineralization rates (cf. Sollins et al., 1996; Guggenberger and Kaiser, 2003). Due to their high specific surface area and abundance of reactive hydroxyl groups, Fe and Al oxides in particular have the potential to strongly affect DOM abundance and composition through sorption reactions.

Previous research has examined sorption of soil organic matter to oxide surfaces, with many studies focusing on goethite in particular. Goethite forms strong bonds with organics through ligand-exchange reactions which are often irreversible (Gu et al., 1994; Chorover and Amistadi, 2001; Fu and Quan, 2006, Kaiser et al., 2007). Goethite surfaces have been shown to preferentially sorb molecules of high molecular weight (Chorover and Amistadi, 2001, Ohno et al., 2007), N-containing compounds (Omoike and Chorover, 2006), and P-containing compounds (Ognalaga et al., 1994; Celi et al., 1999, and many others). Gibbsite surfaces have also been shown to form strong bonds with organics in soil (Guan et al., 2006), and their ability to sorb and retain P is at least equal to that of goethite (Shang et al., 1996; Stevenson & Cole, 1999). In addition, gibbsite also has the potential to influence microbial communities as a source of dissolved aluminum which can decrease microbial growth and respiration rates (Wood, 1995; Fischer, 2002; Schwesig et al., 2003).

These studies reveal a great deal about the interaction of organics with oxide surfaces, however the ultimate effect of these sorption reactions on nutrient cycling and their influence on microbial community composition remains unknown, especially with regards to how these effects may change over time and with increasing degree of

decomposition. To address this knowledge gap, we used a controlled laboratory incubation to evaluate the influence of goethite and gibbsite surfaces on DOM quality, organic C mineralization rates, and microbial community composition. The incubation was carried out over a period of 154 days to assess how these influences may change with increasing degree of decomposition. To examine changes in DOM quality after exposure to goethite and gibbsite surfaces, we measured concentrations of total N, nitrate, nitrite, total P, orthophosphate, and total organic C in DOM solutions derived from incubated forest floor material. To assess changes in microbial community activity, we measured respiration rates throughout the incubation. Changes in microbial community composition were assessed through pyrosequencing analysis.

## **2. Methods**

### ***2.1. Experimental Design***

To assess the influence of goethite and gibbsite surfaces on the characteristics of DOM throughout the degradation process, natural forest floor organic material was incubated in the presence of three matrix types: quartz sand mixed with goethite, quartz sand mixed with gibbsite, and quartz sand (as a control treatment). The matrices for each treatment were as follows: (i) Control treatment: 30 g quartz sand; (ii) Goethite treatment: 6 g goethite grains and 24 g quartz sand; and (iii) Gibbsite treatment: 6 g gibbsite grains and 24 g quartz sand. Detailed characterization of the minerals used in the incubation may be found in Heckman et al. (unpublished).

Organic material used in the incubation experiment consisted of partially decomposed forest floor material collected from (O<sub>i</sub>, O<sub>e</sub>, O<sub>a</sub> horizons) in an Arizona forest dominated by *Pinus ponderosa* in the overstory. Forest floor material was dried at 30°C, then cut to pieces measuring ~1 cm and homogenized using a blender. Three grams of homogenized forest floor material was mixed with the respective quartz sand, gibbsite or goethite treatments in 125 ml glass jars (Fisherbrand, Fisher Scientific). Microbial inoculum derived from field O horizon material was prepared following Wagai & Sollins (2002): Freshly collected forest floor material was mixed with deionized water at a weight to volume ratio of 1:5. The mixture was shaken vigorously for 30-min on reciprocal shaker followed by overnight shaking on a low frequency setting. After 12 hours of slow shaking, the mixture was vacuum filtered over a 5- $\mu$ m polycarbonate membrane filter. Vacuum line pressure was kept below 69 kPa (51.7 cmHg, 20.4 inHg) to prevent lysing of microbial cells. Filtrate was stored in a sterilized bottle overnight at 4°C before use. A 1 ml aliquot of inoculum solution was added to each jar. Samples were homogenized, wetted to 60% of water holding capacity (Cassel and Nielsen, 1986) with deionized water, and tamped to a uniform bulk density. Sample cups were placed in 950 cm<sup>3</sup> mason jars. Soil moisture was maintained by the addition of 3 ml of water to the bottom of each jar to maintain 100% relative humidity within the jar atmosphere. Aerobic conditions in the sample jars were maintained by opening the jars and venting the samples periodically.

Mason jars were fitted with septa to allow for headspace sampling. Headspace samples were collected every 2-3 days by removal of a 1 ml aliquot of headspace gas

using a syringe. Headspace CO<sub>2</sub> concentration was measured using an Infra-Red Gas Analyzer (Qubit CO<sub>2</sub> Analyzer, Kingston, ON, Canada). Jars were ventilated after each headspace measurement.

Samples were incubated over the course of 154 days to investigate how organo-mineral interactions might change as the degree of organic matter decomposition progressed. Samples were incubated at 25°C at seven time intervals: 5, 10, 20, 30, 60, 90 and 154 days. Each time interval was replicated three times for a total of 63 samples. All 63 samples were prepared at the same time. At the end of each time interval, 3 replicates from each treatment were destructively sampled. Samples were mixed with a spatula then 12 g of homogenized material was removed and frozen to be used for microbial analysis at a later time. The remainder of the sample was mixed with deionized water in a 15:1 solution to solid ratio and shaken on a side-to-side shaker for 24 hours. Samples were vacuum filtered, first over a 1 micron glass fiber A/E filter, then over a 0.22 micron polymer filter (Millipore type GV). The filtrate was considered the DOM fraction and was stored in sterilized bottles at 4°C until analyses were completed.

## ***2.2 DOM analysis***

Total organic carbon (non-purgeable) and total nitrogen of the DOM solutions were measured on a Shimadzu TOC-VCSH analyzer (Columbia, MD). Inorganic anions (NO<sub>3</sub><sup>-</sup>, NO<sub>2</sub><sup>-</sup>, PO<sub>4</sub><sup>3-</sup>) were measured by ion chromatography (Dionex Ion Chromatograph DX-500, Sunnyvale, CA) using the Ion Pac AS11 column with a guard column (AG11) and sodium hydroxide (50mM) as the mobile phase. Select samples were measured for

ammonium using the Berthelot reaction (Forster, 1995). Concentrations of ammonium were below detection level, therefore ammonium measurements were not carried out on the full sample set. Organic nitrogen was calculated by subtracting  $\text{NO}_3^-$  and  $\text{NO}_2^-$  from total nitrogen. Total phosphorus was measured by Inductively Coupled Plasma Mass Spectrometry (ICP-MS) on a Perkin Elmer Elan DRC II ICP-MS (Waltham, MA). Organic P was calculated by subtracting orthophosphate from total phosphorous.

### ***2.3 Microbial community analysis***

Shifts in bacterial and fungal community structure were evaluated over the course of the incubation (days 5, 19, 60, 90, and 154) using bacterial tag-encoded FLX amplicon pyrosequencing (bTEFAP), a universal bacterial identification method, and fungal tag-encoded FLX amplicon pyrosequencing (fTEFAP), a universal fungal identification method. The fTEFAP and bTEFAP methods were conducted by the Research and Testing Laboratory, Lubbock, Texas as described elsewhere (Acosta-Martinez et al., 2008). Briefly, DNA was extracted from approximately 0.5 g of soil using the Fast DNA Spin Kit for soil (QBIogene, Carlsbad, CA) following the manufacturer's instructions. The 16S universal Eubacterial primers 530F (50-GTG CCA GCM GCN GCG G) and 1100R (50-GGG TTN CGN TCG TTG) were used for amplifying the 600 bp region of bacterial 16S rRNA genes. For analysis of the fungal 18S rRNA gene, the primers 817f (5'-TTAGCATGGAATAATRRAATAGGA-3') and 1196r (5'-CTGGACCTGGTGAGTTTCC-3') were used (Rousk et al., 2010). All primers contained a 12 basepair barcode to identify the sample the sequence was

retrieved from. HotStarTaq Plus Master Mix Kit (Qiagen, Valencia, CA) was used for PCR under the following conditions: 94 °C for 3 min followed by 32 cycles of 94 °C for 30 s; 60 °C for 40 s and 72 °C for 1 min; and a final elongation step at 72 °C for 5 min. Equal volumes of the amplicon products were then pooled, and purified using Agencourt Ampure beads (Agencourt Bioscience Corporation, MA, USA). DNA amplicons were then sequenced using a 454 Genome Sequencer FLX System (Roche, Nutley, New Jersey).

#### **2.4 Statistical methods**

Calculation of CO<sub>2</sub> respired throughout the incubation followed Zibilske (1994). Percent CO<sub>2</sub> was converted to a mass of C and normalized to the C content of the sample prior to incubation (mg C g<sup>-1</sup> sample C). Nonlinear regression was used to fit a first order decay model to C mineralization data. The model that gave the best fit consisted of two pools which both exhibited first order decay, a faster-cycling “labile” pool and a slower-cycling “recalcitrant” pool:  $-dC/dt = C_L e^{-k_L t} + C_R e^{-k_R t}$ , where  $-dC/dt$  is [mg C g<sup>-1</sup> sample C day<sup>-1</sup>],  $C_L$  and  $C_R$  are the decomposition rates of the labile and recalcitrant pools of C, and  $k_L$  and  $k_R$  are the decomposition rate constants (day<sup>-1</sup>) for the C pools. The total pool size (mg C g<sup>-1</sup> sample C) for each soil C pool,  $C_{LT}$  and  $C_{RT}$ , respectively, was estimated by integrating the area under the curve for each pool:  $C_{TL} = C_L / k_L (1 - e^{-k_L t})$ , and  $C_{TR} = C_R / k_R (1 - e^{-k_R t})$ .

Each sample harvested at a specific destructive sampling period was treated as a replicate for a given treatment, providing three replicates for each treatment per sample time and a total of 21 replicates per treatment across all time periods. Significant differences between DOM properties among treatments were determined by two-way ANOVA using mineral treatment (goethite, gibbsite or control/quartz) and time as the main effects followed by Tukey-Kramer *post hoc* test at a 95% confidence limit ( $n=21$  for each mineral treatment).

To examine differences within and between communities, species frequencies were analyzed relative to time, mineral composition, and solution chemistry in the multivariate statistical software package PC-ORD version 5 software (B. McCune and M.J. Mefford, 2006). Pairwise community distances were estimated with the Sørensen (Bray-Curtis) index and ordinated with nonmetric multidimensional scaling (NMS). NMS is an iterative, best-fit technique that arranges samples in space so that the distance between each pair of samples is in rank order with their similarities in species composition. The optimal number of dimensions ( $k$ ) was selected based on Monte Carlo test of significance at each level of dimensionality comparing 250 runs with empirical data against 250 randomized runs with a step-down in dimensionality from 6 to 1 and a random seed starting value. For the bacterial communities, the  $k=1$  and  $k=2$  dimensional solutions produced the best solutions with stress values smaller than those in randomized runs ( $P = 0.004$ ). For ease of interpretation, the two-dimensional solution was selected and the data re-ordinated with  $k=2$  configuration using the seed generated from the  $k=2$  dimensional solution, a stability criterion at 0.0000001, 100 iterations to evaluate

stability. For the fungal communities, the k 2 dimensions produced the best solutions with a stress value smaller than those in randomized runs (P-0.004). The data was then re-ordinated following the same steps.

Relationships between communities and other variables measured during the incubation were assessed by overlays or joint biplots of those variables, which included mineral treatment, time, pH, EC, NPOC, TN, molecular weight,  $\text{NO}_2^-$ ,  $\text{NO}_3^-$ ,  $\text{PO}_4^{3-}$ , Al, Fe, and P. The angle and length of the lines on the biplots indicate the direction and strength of the correlation among variables and microbial community. Varimax rotation on the ordination axes was used to maximize variance explained by the most significant correlation vectors. Univariate relationships between the newly rotated ordination scores and environmental variables were examined with Pearson's correlation coefficient in JMP 7.0 (SAS Institute, Cary NC). A multiresponse permutation procedure (MRPP) using Sørensen's distance and rank transformation was used to examine statistical significance between samples. MRPP produces a test statistic A which ranges from -1 and 1. Objects that are more dissimilar between groups than within groups are indicated by statistic greater than 0.

### 3. Results

#### 3.1 *Phosphorous dynamics*

Average values of both orthophosphate and P were significantly lower in the oxide treatments than in the control (control<sup>A</sup>>goethite<sup>B</sup>=gibbsite<sup>B</sup>, Figure 1). Amounts of orthophosphate were below detection level in the oxide treatments for all sampling

periods except day 30 in the goethite treatment when very low levels of orthophosphate were measured in one of the replicates. Organic P concentrations in the oxide treatments were low throughout the incubation ( $\sim 0.2 - 0.4 \mu\text{mol g}^{-1} \text{C}$ ) until Day 154 where a dramatic increase in P was observed ( $\sim 1.2 \mu\text{mol g}^{-1} \text{C}$ ). Similarly, P concentrations in the control/forest floor treatment were higher than the oxide treatments ( $\sim 1.25 - 2.75 \mu\text{mol g}^{-1} \text{C}$ ), and also showed an increase in P content on Day 154 ( $\sim 3.0 \mu\text{mol g}^{-1} \text{C}$ ) (Table 2).

### ***3.2 Carbon Dynamics: DOC concentrations and respiration rates***

DOC concentrations were lower in oxide treatments than in the control when averaged over time (Table 1). However, this is mostly due to the two large spikes in C concentration at days 20 & 60 in the control treatment (Figure 3). By day 154, there was little difference in DOC concentration between the control and oxide treatments. DOC concentrations of the oxide treatments changed little over the course of the incubation, whereas DOC concentrations of the control showed large fluctuations. DOC concentrations decreased by approximately 50% over the course of the incubation in both the control and oxide treatments.

Respiration rates were similar among treatments (Table 2). Approximately 15% of the total substrate C was respired over the 154 day period in all treatments. The total amount of C respired by the gibbsite treatment was significantly lower than the amount of C respired by the control treatment (153 and 173 mg C, respectively). However, such small differences may not have much ecological significance. Respiration rate model parameters indicated that the labile pool of C ( $C_{LT}$ ) was actually larger in the gibbsite

treatment than in the control and goethite treatment, while the recalcitrant pool was smaller ( $C_{RT}$ ).

### ***3.3 Nitrogen Dynamics***

Total N concentrations were not significantly different among the treatments when averaged over time (16.7, 12.5, and 13.2  $\mu\text{mol N g}^{-1}$  litter C for control, goethite, and gibbsite, respectively). However, relative concentrations of nitrate, nitrite, and fluctuation patterns did show differences among the treatments (Figure 2), and concentrations of nitrate were significantly higher in the goethite treatment than in the control (2.82 and 1.25  $\mu\text{mol (g}_{\text{litterC}})^{-1}$ , respectively).

### ***3.4 C:N:P ratios of DOM***

The carbon to phosphorus (C:P) ratio is considered to provide an important indication of whether P will be mineralized or immobilized as the forest floor decomposes (Blair 1988). Saggiar et al. (1998) suggested a critical forest floor C:P ratio of 550 for net P mineralization. In the oxide treatments, C: P ratios of DOM were well above this critical value throughout the incubation until day 154 when C: P ratios declined sharply by an order of magnitude (Table 1), indicating that P was immobilized throughout the bulk of the incubation time and was likely a limiting nutrient in the oxide treatments. In general, C: P ratios of DOM from the control treatment were lower than in the oxide treatments and often dipped below the critical C: P ratio of 550, indicating that P limitation fluctuated through time in the control. The generally accepted critical C: N

value for N limitation is approximately 30. At C: N ratios above 30 net immobilization dominates, while at C:N ratios below 20 mineralization dominates. C: N ratios were above the critical 30:1 value until day 154 of the incubation in all treatments.

### ***3.5 Microbial community composition***

Analysis of the pyrosequencing data indicated that time was a dominant factor in structuring both bacterial and fungal communities, which corresponded to some extent with the variation in DOM physiochemical properties (Figures 5 and 6). NMS ordinations fit both bacterial and fungal datasets well (stress=4.3,  $P = 0.004$ , stress = 7.6,  $P = 0.004$ , respectively).

For the bacterial communities, the primary axis correlated primarily with length of incubation ( $r = 0.89$ ,  $P < 0.0001$ ) but showed moderate but significant correlations to other DOM qualities: pH ( $r = 0.48$ ,  $P = 0.0009$ ), EC ( $r = 0.43$ ,  $P = 0.0036$ ), and  $MW_{APP}$  ( $r = 0.57$ ,  $P < 0.0001$ ). Axis 2 also exhibited strong-to-moderate, significant positive correlations with  $PO_4$  ( $r = 0.79$ ,  $P < 0.0001$ ), total P ( $r = 0.60$ ,  $p < 0.0001$ ), and NPOC ( $r = 0.36$ ,  $P = 0.015$ ). According to the MRPP, bacterial communities differed significantly by incubation time ( $A=0.49$ ,  $P > 0.01$ ). All pairwise comparisons of the sites were significantly different except for days 60 and 90. Although MRPP did not indicate significant separation by mineral treatment, communities appeared to cluster visually by treatment.

For fungal communities, the primary axis again correlated primarily with length of incubation ( $r = 0.84$ ,  $P < 0.0001$ ) with moderate to weak correlations with  $MW_{APP}$  ( $r =$

0.51  $P = 0.0003$ ), pH ( $r = 0.46$ ,  $P = 0.0016$ ) and EC ( $r = -0.35$ ,  $P = 0.017$ ). Axis 2 exhibited a moderate negative correlation with NPOC ( $r = -0.48$ ,  $P = 0.0008$ ). According to the MRPP, fungal communities also differed significantly by incubation time ( $A=0.37$ ,  $P > 0.01$ ). Again, all pairwise comparisons of the sites were significantly different except for days 60 and 90. Although MRPP did not indicate significant separation by mineral treatment, communities from the goethite and gibbsite treatments appeared to cluster separately from the quartz control.

## 4. Discussion

### 4.1 *Influence of oxide surfaces on DOM quality*

The presence of goethite and gibbsite surfaces induced significant changes in the nutrient content and structural characteristics of the DOM solutions in comparison to the control treatment. The presence of goethite and gibbsite significantly reduced both the C and P content of the DOM solutions. Though N fluctuation patterns were different in the oxide treatments in comparison to the control, N concentrations were not significantly different among treatments when averaged over time. Goethite and gibbsite surfaces seemed to bind C, P and N with equal efficiency, even though their effect on DOM structural properties differed (effect of goethite and gibbsite surfaces on DOM structural characteristics is discussed in detail in Heckman et al., unpublished).

#### 4.1.1 *Phosphorous*

Though C, P and N concentrations of DOM were all affected by the presence of goethite and gibbsite, P concentrations were affected most strongly. Essentially all

orthophosphate and 75% of organic P were removed from solution in the oxide treatments, most likely through sorption of organic P on oxide and organic matter surfaces and preservation of orthophosphate through bonding with dissolved metals. It is well established that P may be removed from active cycling through sorption to oxide surfaces (Stevenson, 1994). Both inorganic P ( $\text{HPO}_4^{2-}$ ,  $\text{H}_2\text{PO}_4^-$ ) and organic P (biomolecules) may form strong bonds with oxide surfaces through ligand exchange with strength of phosphate fixation approximately equal for goethite and gibbsite (Stevenson & Cole, 1999). In addition to bonding with oxide surfaces, orthophosphate also forms bonds with humic substances through metal bridging, where orthophosphate is bound to Fe (III) and Al sorbed to humic functional groups (Gerke & Hermann, 1992). Bonding of P by metal bridging on organics can be up to 10 times that of P bonding to Fe oxide surfaces, implying that the presence of solution state metals may be more important in regulating P dynamics than the presence of the oxide surfaces themselves.

Solution pH also has a significant effect on the amount of P sorbed on both organics and oxide surfaces. As pH increases, the solubility of organics increases and the abundance of deprotonated hydroxyl and carboxyl groups increases. Consequently the accessibility and abundance of P-sorption sites increases. The results of Gerke and Hermann (1992) support this mechanistic explanation. In mixtures of fulvic acids, Fe, and P, they found that P adsorption increased from pH 5.2 to 6.2. They also showed a dependence of P sorption on the concentration of organically-bound Fe, with bound P consistently showing a 1:1 molar ratio with Fe. White and Thomas (1981) reported similar results for solution state Al, with P:Al ratios showing a dependence on the degree

of hydroxylation of the Al. pH values of the incubated oxide samples were in the range favorable for cation bridging of phosphates to organics, with pH values around 5.5-6.5 for the majority of the incubation. Such a mechanism of P sorption would affect both the phosphate and metal (Fe, Al) concentrations measured in the DOM solutions, since cation-bridging of P on organics would necessarily remove Fe and Al from solution. However, since measurements have only been made on the DOM solutions, the amount of solubilized Fe and Al removed from solution by cation bridging with organics and phosphate cannot be known.

#### **4.1.2 Carbon**

When averaged over time, C concentrations in the oxide treatments were half that of the control. Though differences in C concentration among the treatments may be partially attributed to differences in microbial degradation rates, it is likely that differences in C concentration are primarily the result of sorption of dissolved C to the oxide surfaces. Oxide surfaces form bonds with organics through ligand exchange reactions with phenolic OH and carboxyl groups (Parfitt et al., 1977; Gu et al., 1994; Molis et al., 2000). Once ligand exchange bonds are formed, they are difficult to reverse, and have been shown to persist and strengthen over time (Gu et al., 1994; Kaiser et al., 2007) Therefore, it is unlikely that organics bonded to the oxides would be released over the period of the incubation, and fluctuations in dissolved organic C throughout the incubations are more likely the result of microbial turnover and activity rather than desorption of organics from oxide surfaces. Differences in dissolved organic C concentrations among treatments are most pronounced on days 20 and 60 of the

incubation (Figure 3). We hypothesize that these large ‘flushes’ of C in the control treatment are representative of microbial biomass turnover events when large changes in community size or composition took place. Furthermore, we postulate that similar biomass turnover events were taking place in the oxide treatments, but that the solubilized C was sorbed by the oxide surfaces and consequently did not show up in the DOM extractions.

#### **4.1.3 Nitrogen**

Nitrogen concentrations were affected to a lesser degree than C and P concentrations. Perhaps the most striking quality of the nitrogen measurements over time (Figure 2) is the large spikes in N concentration. The control and oxide treatments both show one large spike in N content, at day 20 in the oxide treatments and at day 60 in the control. One explanation for the patterns of N concentrations may be microbial turnover and concomitant cell lysis. However, increases in N concentration were not accompanied by similar spikes in either C or P concentrations. The apparent decoupling of N and C dynamics in DOM solutions has been observed previously in many field studies. In experiments in spruce and pine forests, addition of N to soils did not cause observable changes in dissolved organic C yield (Stuanes and Kjønnass, 1998; Emmett et al., 1998), and no clear dependence of dissolved organic C flux on N availability could be found (Gunderson et al., 1998). This apparent decoupling of nutrient dynamics may imply that fluctuations in nutrients are more the product of predator/prey dynamics or shifts in nutrient limitations rather than strictly cell lysis.

#### **4.1.4 Nutrient ratios**

When concentrations of both N and P are low, either N or P will limit microbial growth and respiration depending on their ratio. Determining whether N or P is limiting is important since it can strongly influence microbial community composition. Güsewell et al. (2009) found that N-limited conditions favor bacteria, while P-limited conditions favor fungi. The shift from N to P limitation usually occurs at N:P substrate ratios of 1.7-45 depending on substrate type and microbial community composition. N:P ratios in the control treatment ranged from 5:1 to 41:1, indicating that growth was most likely N-limited throughout the incubation. In contrast, N:P ratios varied widely in the oxide treatments (Table 1). N:P ratios of the oxide treatments were high at the start of the incubation, but decreased with time of incubation, possibly indicating a shift from P-limitation to N-limitation as decomposition progressed. P limitation in the oxide treatments may offer a plausible explanation for the trend in nitrate concentrations. Throughout the incubation, nitrate concentrations were higher in the oxide treatments than the control (though only the goethite treatment was statistically significantly higher than the control at the  $\alpha = 0.05$  level). Nitrate and nitrite are typically only formed when N is not limiting, supporting the idea that microbial growth in the oxide treatments was primarily P limited while microbial growth in the control was more N limited.

Though there were significant differences in nutrient ratios among treatments, some general trends were apparent across all treatments. Over time, as decomposition of the forest floor material progressed, molar nutrient ratios (C:N and N:P) declined significantly. Changes in nutrient ratios together with changes noted in structural composition may indicate a shift from plant-based DOM to microbially-based DOM with

increasing degree of biodegradation. Though C: N ratios did not decrease steadily throughout the incubation, they did decrease from day 60 to day 154, and C: N ratios were an order of magnitude lower at the end of the incubation than at the beginning.

These decreases in C: N ratio over time would be consistent with a transition from plant-based to microbially-based DOM. Though C: N ratios at day 154 of the incubation were still relatively high (27, 19, and 16 for control, goethite and gibbsite treatments, respectively), they are not outlandishly high for soil biomass which is usually assumed to have C: N ratios ~8-12 (Paul and Clark, 1996; Wright and Coleman, 2000). Furthermore, N:P ratios also declined significantly throughout the incubation, and after 154 days of incubation were also drawing near the global stoichiometric average for forest microbial biomass of 9:1 (Cleveland and Liptzin, 2007). Such a transition from plant-derived molecules to microbially-produced products with increasing degree of decomposition is highly plausible. Especially considering that in natural systems, microbial metabolites have been found to comprise a significant portion of DOM (Kalbitz et al. 2000)

#### ***4.2 Alteration of DOM quality influences microbial community composition***

Microbial community composition varied both over time and among treatments (Figures 4 and 5). Variation in community composition was significantly correlated with variation in specific DOM properties, indicating that changes in DOM quality due to exposure to oxide surfaces have a significant effect on microbial communities.

Length of incubation had a strong effect on both bacterial and fungal communities and changes in both bacterial and fungal community composition with increasing time of

incubation were correlated with the same set of DOM parameters (day,  $M_{W_{APP}}$ , pH and EC). Regardless of treatment, communities grouped by sampling date along axis one. This was especially true for bacterial communities, and expressed less so for fungal communities. In fungal communities, sampling date maintained a strong influence on communities from the control treatment, but communities in the oxide treatments from days 60, 90 and 154 were grouped along axis 1 indicating that increasing time of incubation had less of an influence on fungal communities from the oxide treatments after 60 days of incubation. This strong influence of time may indicate that degree of substrate degradation is very important in determining both bacterial and fungal community composition. Apparent molecular weight also contributed to variation in community composition along axis 1 in both bacterial and fungal communities. Apparent molecular weight of organics in DOM solutions varied significantly over time ( $P=0.0002$ ), and was related to the abundance of metal-humus complexes (Heckman et al., unpublished). Correlation between  $M_{W_{APP}}$  and community composition could therefore indicate that the presence of metal-humus complexes influences community composition. Formation of metal-humus complexes induces chemical and conformational changes that reduce SOC bio-availability (Baldock and Skjemstad, 2000; Nierop et al, 2002; Scheel et al., 2007). Alternatively, correlations between community composition and  $M_{W_{APP}}$  could be an indication that substrate quality declined as degree of decomposition and  $M_{W_{APP}}$  increased over time. Electrical conductivity of DOM solutions (EC) was also correlated with changes in community composition over time, though a mechanistic explanation for this correlation is not immediately obvious. pH was also

significantly correlated with changes in both bacterial and fungal community composition over time, corresponding with known control of pH over microbial diversity, activity and biomass in both field and laboratory settings (Anderson and Domsch, 1993; Schnittler and Stephenson, 2000; Bååth and Anderson, 2003; Fierer and Jackson, 2006)

Both bacterial and fungal community composition varied among treatments, though DOM parameters correlated with variance in community composition were different for bacterial and fungal communities. Variation in bacterial community composition among treatments was correlated with P,  $\text{PO}_4^{3-}$ , organic C, and  $\text{NO}_3^-$  concentrations. Variation in fungal community composition among treatments was primarily correlated with organic C concentrations, and Al concentrations to a lesser degree. Correlations among nutrient concentrations and community composition indicate that the influence of oxide surfaces on DOM quality has significant ramifications for both bacterial and fungal communities. P availability strongly influenced bacterial communities, but was not associated with variance in fungal communities. This is consistent with previous research which has indicated that fungi are better able to cope with P limitation than bacteria (Smith, 2002; Güsewell and Gessner, 2009). Correlations among bacterial community composition and nitrate may indicate a greater abundance of nitrifying bacteria in the oxide treatments relative to the control treatment, consistent with the higher nitrate concentrations observed in DOM solutions from the oxide treatments. The significant correlation between fungal community composition and Al concentrations may indicate some degree of Al toxicity in the gibbsite treatments. Though Al is most toxic in its monomeric form,  $\text{Al}^{3+}$ , which is present only at pH values

less than 5.5, field studies have indicated that additions of Al alter microbial community composition regardless of pH (Joner et al., 2005). Al toxicity also effects soil microbial activity, often significantly reducing biomass and respiration rates in both laboratory and field experiments (Illmer et al., 1995, Pina and Cervantes, 1996; Williams, 1999; Marschner et al., 2000; Kochian, 2005). Increased levels of Al in the gibbsite treatment may explain the slightly suppressed respiration rates in the gibbsite treatment. The gibbsite treatment did have less N and P in the DOM extracts than the control, but N and P levels in the gibbsite treatment were similar to those in the goethite treatment indicating that substrate quality cannot explain variation in respiration rates. However, the toxic effects of dissolved Al are well documented (MacDonald and Martin 1998, Giesler et al 2004, Kochian 2005, Scheel et al 2007).

## **5. Summary**

Results clearly show that the presence of goethite and gibbsite has specific and significant consequences for the substrate quality of DOM. Results also indicate that these changes in DOM properties (reduced P and C availability, presence of dissolved metals) induce changes in both bacterial and fungal community composition. However, though exposure to oxide surfaces significantly altered substrate quality, the effect of these changes on respiration rates was minimal. This suggests that microbial communities were able to effectively adapt to changes in substrate characteristics in order to maintain maximum respiration rates.

## **6. Acknowledgements**

This work was funded by a grant from the National Science Foundation (DEB #0543130).

## 7. Figures & Tables

Figure 1. Changes in orthophosphate and organic P content of DOM solutions over time.

The P contents of the solutions were normalized to the respective C content of the solid sample prior to incubation.

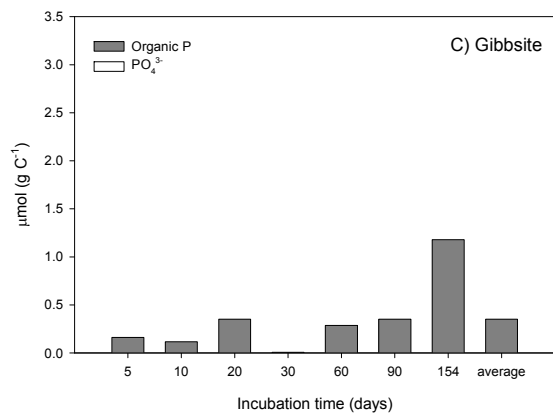
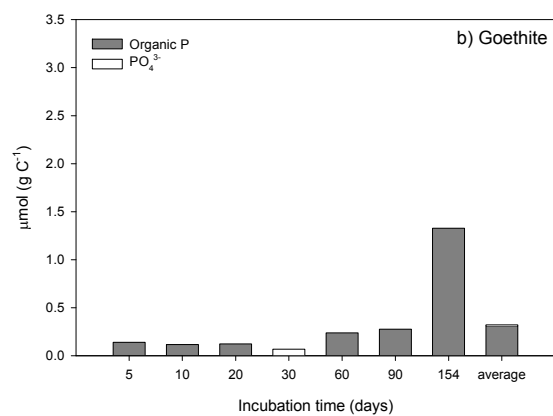
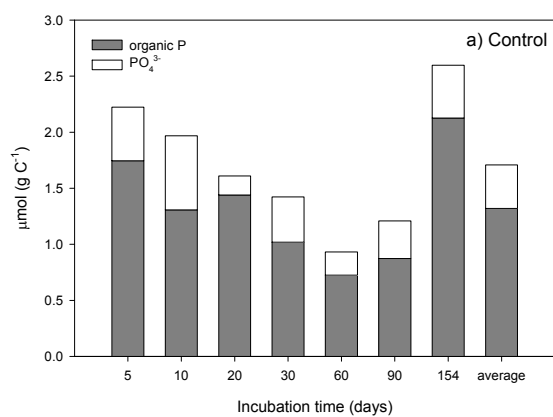


Figure 2. Changes in nitrate, nitrite and organic N + ammonium content of DOM solutions over time. The N contents of the solutions were normalized to the respective C content of the solid sample prior to incubation.

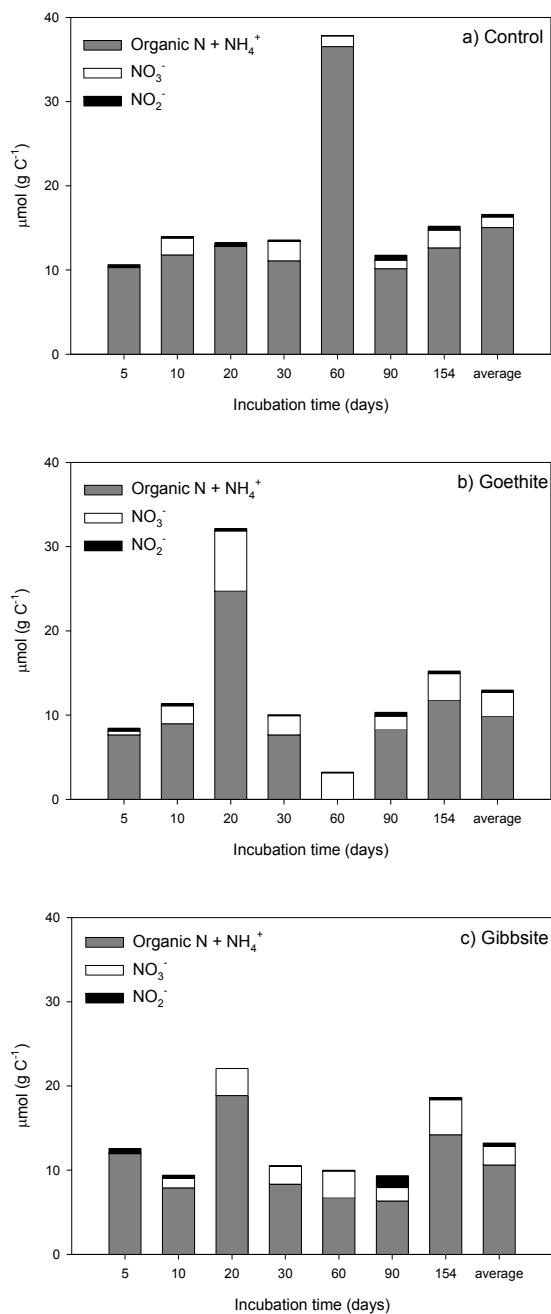


Figure 3. Changes in dissolved organic C (DOC) content of the dissolved organic matter (DOM) solutions over time. The DOC contents of the solutions were normalized to the respective C content of the solid sample prior to incubation.

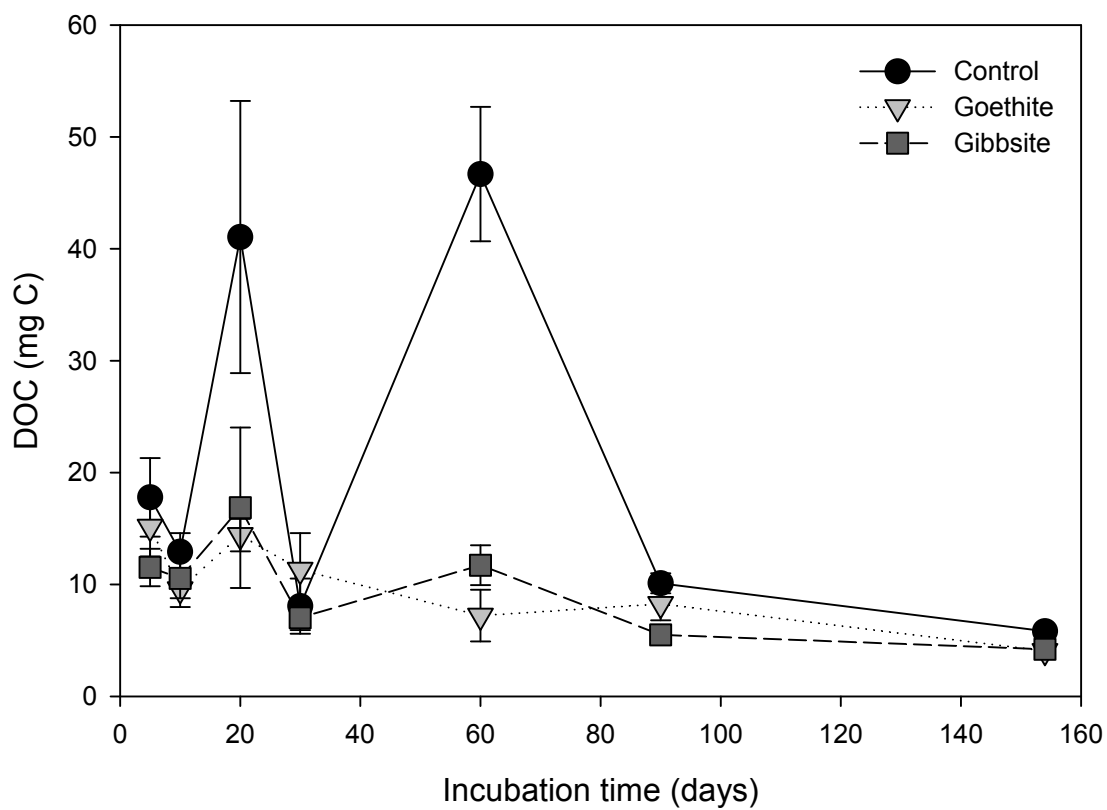


Figure 4. Non-metric multidimensional scaling ordination of bacterial pyrosequencing data. Symbols code for treatment (control  $\square$ , goethite  $\bullet$ , gibbsite  $\Delta$ ). Lines show correlation vectors of the measured environmental variables with the ordination: EC, NPOC, PO<sub>4</sub>, P, Mw, NO<sub>3</sub>, pH, day (length of incubation). The final solution has two dimensions (stress = 4.3,  $P = 0.004$ ).

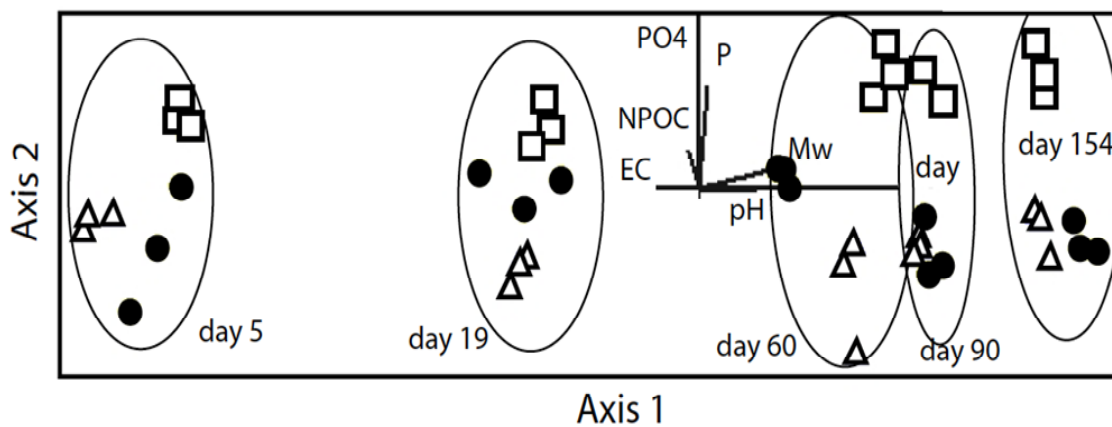


Figure 5. Non-metric multidimensional scaling ordination of fungal pyrosequencing data. Symbols code for treatment (control  $\square$ , goethite  $\bullet$ , gibbsite  $\Delta$ ). Lines show correlation vectors of the measured environmental variables with the ordination: EC, Al, NPOC, Mw, pH, day (length of incubation). The final solution has two dimensions (stress = 7.6,  $P = 0.004$ ).

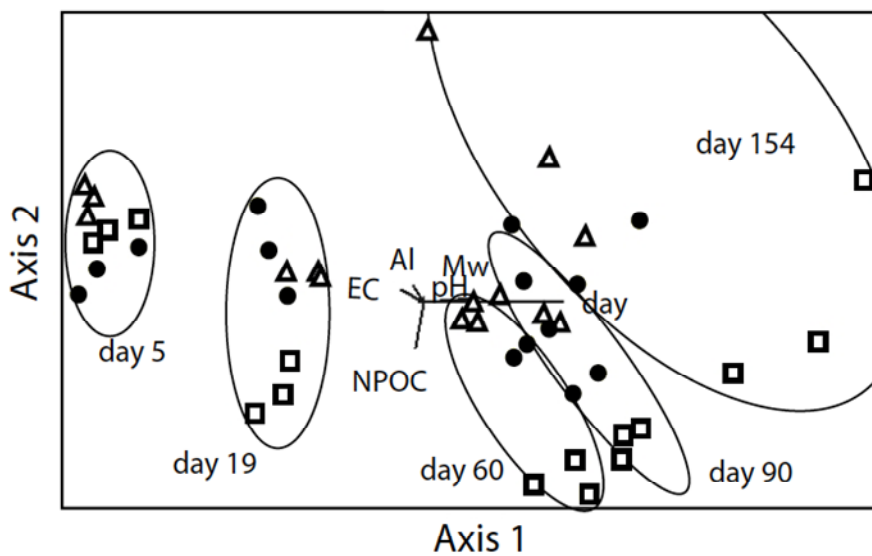


Table 1. Characteristics of dissolved organic matter solutions over time.

Treatment	Incubation length Days	Organic C $\mu\text{mol g}_{\text{litter C}}^{-1}$	Total N	$\text{NO}_3^-$	$\text{NO}_2^-$ $\mu\text{mol g}_{\text{litter C}}^{-1}$	Total P	$\text{PO}_4^{3-}$	C:N	C:N:P
Control	5	1.48 (0.29)	10.63 (0.82)	0.00	0.33 (0.18)	2.22 (0.31)	0.48 (0.03)	139 (24)	666:5:1
	10	1.08 (0.14)	13.96 (2.39)	1.99 (0.44)	0.18 (0.06)	1.97 (0.10)	0.66 (0.03)	77 (14)	546:7:1
	20	3.42 (1.01)	13.22 (2.10)	0.05	0.37 (0.13)	1.61 (0.14)	0.17 (0.03)	259 (80)	2,123:8:1
	30	0.67 (0.21)	13.55 (2.45)	2.31 (0.72)	0.15 (0.01)	1.42 (0.17)	0.4 (0.05)	50 (18)	472:10:1
	60	3.89 (0.50)	37.83 (1.57)	1.26 (0.17)	0.05	0.93 (0.16)	0.21 (0.03)	103 (8)	4,172:41:1
	90	0.84 (0.07)	11.76 (1.12)	1.02 (0.22)	0.59 (0.10)	1.21 (0.09)	0.34 (0.03)	72 (12)	696:10:1
	154	0.48 (0.01)	15.19 (0.66)	2.11 (0.15)	0.46 (0.14)	2.60 (0.39)	0.47 (0.05)	32 (13)	186:6:1
Average over time		<b>1.69 (0.32)<sup>A</sup></b>	<b>16.59 (5.39)<sup>A</sup></b>	<b>1.25 (0.24)<sup>B</sup></b>	<b>0.30 (0.09)<sup>A</sup></b>	<b>1.71 (0.14)<sup>A</sup></b>	<b>0.39 (0.03)<sup>A</sup></b>	<b>102 (21)<sup>A</sup></b>	<b>1,266:12:1</b>
Goethite	5	1.26 (0.22)	8.43 (0.96)	0.46 (0.46)	0.34 (0.18)	0.14 (0.02)	0.00	150 (30)	8,969:60:1
	10	0.80 (0.13)	11.36 (1.16)	2.13 (0.62)	0.27 (0.07)	0.12 (0.02)	0.00	70 (13)	6,839:97:1
	20	1.20 (0.12)	32.15 (6.53)	7.16 (0.62)	0.29 (0.19)	0.12 (0.02)	0.00	37 (9)	9,742:261:1
	30	0.94 (0.27)	6.69 (0.21)	2.29 (0.45)	0.11 (0.04)	0.03 (0.02)	0.07 (0.07)	94 (25)	34,619:369:1
	60	0.60 (0.19)	3.20 (0.50)	3.14 (0.50)	0.06 (0.01)	0.24 (0.01)	0.00	188	2,523:13:1
	90	0.69 (0.12)	10.32 (0.01)	1.45 (0.28)	0.45 (0.08)	0.28 (0.02)	0.00	67 (1)	2,480:37:1
	154	0.34 (0.03)	15.23 (1.27)	3.13 (0.35)	0.31 (0.11)	1.33 (0.27)	0.00	22 (2)	254:11:1
Average over time		<b>0.83 (0.09)<sup>B</sup></b>	<b>12.36 (5.70)<sup>A</sup></b>	<b>2.82 (0.47)<sup>A</sup></b>	<b>0.26 (0.10)<sup>A</sup></b>	<b>0.32 (0.10)<sup>B</sup></b>	<b>0.01 (0.01)<sup>B</sup></b>	<b>64 (16)<sup>A</sup></b>	<b>9,347:121:1</b>
Gibbsite	5	0.96 (0.14)	12.57 (2.98)	0.04 (0.04) <sup>A</sup>	0.56 (0.17)	0.16 (0.01)	0.00	76 (22)	5,924:78:1
	10	0.88 (0.15)	9.39 (0.79)	1.11 (0.52)	0.38 (0.10)	0.12 (0.01)	0.00	93 (21)	7,554:81:1
	20	1.40 (0.60)	22.07 (8.89)	3.20 (3.20)	0.00	0.35 (0.11)	0.00	64 (52)	4,004:63:1
	30	0.58 (0.09)	10.53 (0.68)	2.13 (0.15)	0.08 (0.02)	0.01	0.00	55 (4)	85,406:1539:1
	60	0.98 (0.15)	9.97 (4.97)	3.21 (0.49)	0.08 (0.02)	0.29	0.00	84 (1)	3,405:35:1
	90	0.46 (0.04)	9.34	1.59 (0.20)	1.41 (1.01)	0.35 (0.03)	0.00	49 (4)	1,304:27:1
	154	0.35 (0.01)	18.61 (0.89)	4.16 (0.28)	0.25 (0.05)	1.18 (0.65)	0.00	19 (12)	267:16:1
Average over time		<b>0.80 (0.11)<sup>B</sup></b>	<b>13.21 (4.38)<sup>A</sup></b>	<b>2.21 (0.70)<sup>AB</sup></b>	<b>0.40 (0.20)<sup>A</sup></b>	<b>0.35 (0.11)<sup>B</sup></b>	<b>0.00<sup>B</sup></b>	<b>61 (10)<sup>A</sup></b>	<b>15,414:263:1</b>

<sup>A</sup> specifically: measured as millimoles of the nutrient of interest in the dissolved organic matter fraction, normalized to the total grams of C in the solid sample prior to incubation. Values at each time point are the average of three replicates for each treatment ( $n=3$ ). <sup>B</sup> "Average over time" values are the average of all replicates across time ( $n=21$ ). Values in parenthesis are the standard error of replicates ( $n=3$  or  $n=21$ ), where parenthesis are not shown the standard error was zero.

Significance was determined using two-way ANOVA with treatment and time as main effects, followed by Tukey's HSD *post hoc* test ( $\alpha=0.05$ ). Within each column, means followed by different superscript letters are significantly different.

Table 2. Respiration rate data. Total C respired and respiration rate are the average of 3 replicates for each treatment.

Treatment	Total C Respired mg C	Respiration Rate mg C hour <sup>-1</sup>	C <sub>L</sub> g <sub>C( resp)</sub> g <sub>C( litter)</sub> <sup>-1</sup> day <sup>-1</sup>	k <sub>L</sub> day <sup>-1</sup>	C <sub>R</sub> g <sub>C( resp)</sub> g <sub>C( litter)</sub> <sup>-1</sup> day <sup>-1</sup>	k <sub>R</sub> day <sup>-1</sup>	C <sub>LT</sub> Pool sizes (mg C)	C <sub>RT</sub>
Control	172.8 (±5) <sup>A</sup>	0.0117 (±0.0003) <sup>A</sup>	0.285	0.0185	0.0656	0.00021	15.4	167.8
Goethite	163 (±7.9) <sup>AB</sup>	0.0111 (±0.0002) <sup>AB</sup>	0.247	0.0157	0.0651	0.00026	15.8	153.2
Gibbsite	152.5 (±5.9) <sup>B</sup>	0.0107 (±0.0002) <sup>B</sup>	0.227	0.0133	0.0639	0.00030	17.1	142.3

Respirate Rate parameters are fit according to the following function:  $y = C_L e^{-k_L t} + C_R e^{-k_R t}$   
 Significance was determined using one-way ANOVA by treatment, followed by Tukey's HSD *post hoc* test ( $\alpha=0.05$ ). Within each column, means followed by different superscript letters are significantly different.

## 8. References

- Acosta-Martinez, V, S. Dowd, Y. Sun, V. Allen. 2008 Tag-encoded pyrosequencing analysis of bacterial diversity in a single soil type as affected by management and land use. *Soil Biology & Biochemistry* 40: 2762–2770
- Anderson, T-H, Domsch, K.H., 1993. The metabolic quotient for CO<sub>2</sub> ( $qCO_2$ ) as a specific activity parameter to assess the effects of environmental conditions, such as pH, of the microbial biomass of forest soils. *Soil Biology & Biochemistry* 25 (3), 393-395.
- Bååth, E., Anderson, T.H., 2003. Comparison of soil fungal/bacterial ratios in a pH gradient using physiological and PLFA-based techniques. *Soil Biology & Biochemistry* 35, 955-963.
- Baldock, J.A., Skjemstad, J.O., 2000. Temperature effects on the diversity of soil heterotrophs and the delta C-13 of soil-respired CO<sub>2</sub>. *Soil Biology and Biochemistry* 32, 699-706.
- Blair JM (1988) Nitrogen, sulfur and phosphorus dynamics in decomposing deciduous leaf forest floor in the southern Appalachians. *Soil Biol Biochem* 20 : 693–701
- Cassel, D.K., Nielsen, D.R., 1986. Field capacity and available water capacity. In: Klute, A. (Ed.), *Methods of Soil Analysis. Part 1: Physical and mineralogical methods*, 2nd ed. SSSA Book Series 5. SSSA Inc., Madison, WI, 901-926
- Celi, L., S. La Macchia, F. Ajmone-Marsan, E. Barberis. 1999. Interaction of inositol hexaphosphate on clays: Adsorption and charging phenomena. *Soil Sci.* 164:574–585.
- Chorover, J., Amistadi, M. K., 2001. Reaction of forest floor organic matter at goethite, birnessite and smectite surfaces. *Geochimica et Cosmochimica Acta* 65, 95–109.
- Cleveland C.C., Liptzin D., 2007. C : N : P stoichiometry in soil: is there a “Redfield ratio” for the microbial biomass? *Biogeochemistry* 85, 235-252.
- Emmett, B.A., Reynolds, B., Silgram, M., Sparks, T. H., Woods, C., 1998. The consequences of chronic nitrogen additions on N cycling and soil water chemistry in a Sitka spruce stand, North Wales. *For. Ecol. Manage.* 101, 165-175.
- Fierer, N., Jackson, R.B., 2006. The diversity and biogeography of soil bacterial communities. *PNAS* 103, 626-631.
- Fischer J., Quintmeier A., Gansel S., Sabados V., Friedrich C.G., 2002. Inducible aluminum resistance of *Acidiphilium cryptum* and aluminum tolerance of other acidophilic bacteria. *Archives of Microbiology* 178, 554-558.

Forster, J.C., 1995. Soil nitrogen. In: Alef K and Nannipieri P (Eds.) *Methods in Applied Soil Microbiology and Biochemistry*. Academic Press, San Diego, pp. 79-87.

Fu H, Quan X, 2006. Complexes of fulvic acid on the surface of hematite, goethite, and akaganeite: FTIR observation. *Chemosphere* 63: 403-410.

Giesler, R., Satoh, F., Ilstedt, U. and Nordgren, A. 2004. Microbially Available Phosphorus in Boreal Forests: Effects of Aluminum and Iron Accumulation in the Humus Layer. *Ecosystems*. 7: 208-217.

Gerke, J, Hermann, Reinhold (1992) Adsorption of Orthophosphate to Humic-Fe-Complexes and to Amorphous Fe-Oxide. *Zeitschrift für Pflanzenernährung und Bodenkunde* 155(3): 233-236.

Gu B, Schmitt J, Chen Z, Liang L, McCarthy JF, 1994. Adsorption and desorption of natural organic matter on iron oxide: mechanisms and models. *Environmental Science and Technology* 28: 38-46.

Guan, X-H., Shang, C., Chen, G-H., 2006. ATR-FTIR investigation of the role of phenolic groups in the interaction of some NOM model compounds with aluminum oxide. *Chemosphere* 65, 2074-2081.

Guggenberger, G., Kaiser, K., 2003. Dissolved organic matter in soil: challenging the paradigm of sorptive preservation. *Geoderma* 113, 293-310.

Gunderson, P., Emmett, B.A., Kjønaas, O.J., Koopmans, C.J., Tietema, A., 1998. Impact of nitrogen deposition on nitrogen cycling in forests: A synthesis of NITREX data. *For. Ecol. Manage.* 101, 37-55.

Güsewell, S., Gessner, M.O., 2009. N:P ratios influence litter decomposition and colonization by fungi and bacteria in microcosms. *Functional Ecology* 23, 211-219.

Heckman, K., Rasmussen, C., Chorover, J., Vazquez Ortega, A., Gao, X., (unpublished). Changes in dissolved organic matter structural characteristics induced by exposure to goethite and gibbsite surfaces: DRIFT and TG/DTA analysis. *Geochimica et Cosmochimica Acta*, submitted.

Huang PM, 2008. Chapter 1: Soil Physical-Chemical-Biological Interfacial Interactions: An Overview. *In: Soil Mineral--Microbe--Organic Interactions: Theories and Applications*. Huang Q, Huang PM, Violante A (Eds). Springer-Verlag: Berlin Heidelberg.

- Illmer, P., Marschall, K., Schinner, F., 1995. Influence of available aluminum on soil-micro-organisms. *Letters in Applied Microbiology* 21 (6), 393-397.
- Jandl, R., Sollins, P., 1997. Water-extractable soil carbon in relation to the belowground carbon cycle. *Biology & Fertility of Soils* 25, 196-201.
- Joner, E.J., Eldhuset, T.D., Lange, H., Frostegård, A., 2005. Changes in the microbial community in a forest soil amended with aluminum in situ. *Plant and Soil* 275, 295-304.
- Kaiser, K., Mikutta, R., Guggenberger, G., 2007. Increased stability of organic matter sorbed to ferrihydrite and goethite on aging. *Soil Science Society of America Journal* 71, 711-719.
- Kalbitz K., Solinger S., Park J.-H., Michalzik B. and Matzner E. (2000) Controls on the dynamics of dissolved organic matter in soils: A review. *Soil Science* **165**, 277-304.
- Kalbitz, K., Schmerwitz, J., Schwesig, D., Matzner, E., 2003. Biodegradation of soil-derived dissolved organic matter as related to its properties. *Geoderma* 113, 273-291.
- Keil, R.G., Montluçon, D.B., Prahl, F.G., Hedges, J.I., 1994. Sorptive preservation of labile organic matter in marine sediments. *Nature* 370, 549-552.
- Kochian L.V., Pineros M.A, Hoekenga O.W. 2005. The physiology, genetics and molecular biology of plant aluminum resistance and toxicity. *Plant and Soil* 274, 175-195.
- MacDonald T.L, Martin, R.B. 1998. Aluminum in biological systems. *Trends Biochem. Sci.* 13:15-19
- Marschner P., Klam A., Jentschke G., Douglas L. Godbold D.L., 2000. Aluminum and lead tolerance in ectomycorrhizal fungi. *Journal of Plant Nutrition and Soil Science* 162, 281-286.
- Marschner, B., Kalbitz, K., 2003. Controls of bioavailability and biodegradability of dissolved organic matter in soils. *Geoderma* 113, 211-235.
- Metting, F.B., 1993. Structure and physiological ecology of soil microbial communities. In: Metting, F.B. (Ed.), *Soil Microbial Ecology – Application in Agricultural and Environmental Management*. Marcel Dekker, New York, pp. 3-24.
- Molis E., Barrès O., Marchand H., Sauzéat E., Humbert B. and Thomas F. (2000) Initial steps of ligand-promoted dissolution of gibbsite. *Colloids and Surfaces A: Physicochemical and Engineering Aspects* **163**, 283-292

- Nierop, K.G.J., Jansen B., Verstraten, J.M., 2002. Dissolved organic matter, aluminum and iron interactions: Precipitation induced by metal/carbon ratio, pH and competition. *Sci. Total Environ.* 300, 201–211.
- Ohno, T., Chorover, J., Omoike, A., Hunt, J., 2007. Molecular weight and humification index as predictors of adsorption for plant- and manure-derived dissolved organic matter to goethite. *European Journal of Soil Science*, 58, 125–132
- Ognalaga, M., E. Frossard, F. Thomas. 1994. Glucose-1-phosphate and myo-inositol hexaphosphate adsorption mechanisms on goethite. *Soil Sci. Soc. Am. J.* 58:332–337.
- Omoike, A., Chorover, J., 2006. Adsorption to goethite of extracellular polymeric substances from *Bacillus subtilis*. *Geochimica et Cosmochimica Acta* 70, 827-838.
- Parfitt R.L., Fraser A.R. and Farmer V.C. (1977) Adsorption on hydrous oxides. III. Fulvic acid and humic acid on goethite, gibbsite and imogolite. *European Journal of Soil Science* 28, 289 – 296.
- Paul EA, Clark FE (1996). *Soil microbiology and biochemistry*. Academic Press, San Diego.
- Pina, R. G. and Cervantes, C.: 1996, Microbial interactions with aluminum, *BioMetals* 9, 311–316.
- Rousk, J, E. Baath, P.C. Brookes, C.L. Lauber, C. Lozupone, JG Caporaso, R. Knight and N Fierer. 2010. Soil bacterial and fungal communities across a pH gradient in an arable soil. *The ISME Journal* 4:1340–135.
- Saggar S, Parfitt RL, Salt G, Skinner MF (1998) Carbon and phosphorus transformations during decomposition of pine forest floor with different phosphorus status. *Biol Fertil Soils.* 27:197–204
- Scheel, T., Dörfler, C., Kalbitz, K., 2007. Precipitation of dissolved organic matter by aluminum stabilizes carbon in acidic forest soils. *Soil Science Society of America Journal* 71, 64-74.
- Schnittler, M., Stephenson, S.L., 2000. Myxomycete Biodiversity in Four Different Forest Types in Costa Rica. *Mycologia* 92, 626-637.
- Schwesig, D., Kalbitz, K., Matzner, E., 2003. Effects of aluminium on the mineralization of dissolved organic carbon derived from forest floors. *European Journal of Soil Science* 54, 311 – 322.

- Shang, C., D. E. Caldwell, J. W. B. Stewart, H. Tiessen, P. M. Huang. 1996. Bioavailability of organic and inorganic phosphates adsorbed on short-range ordered aluminium precipitate. *Microb. Ecol.* 31: 29–39.
- Smith, V.H. (2002) Effects of resource supply ratios on the structure and function of microbial communities. *Antonie van Leeuwenhoek*, **81**, 99–106.
- Sollins, P., Homann, P, Caldwell, B.A., 1996. Stabilization and destabilization of soil organic matter: mechanisms and controls. *Geoderma* 74, 65-105.
- Stevenson FJ (1994) *Humus Chemistry—Genesis, Composition, Reactions*, 2<sup>nd</sup> Ed. Wiley, New York.
- Stevenson FJ, Cole MA (1999) *Cycles of Soil: Carbon, Nitrogen, Phosphorous, Sulfur, Micronutrients*, 2<sup>nd</sup> Ed. John Wiley & Sons, Inc: New York.
- Stuanes, A. O., Kjønnass, O. J., 1998. Soil solution chemistry during four years of NH<sub>4</sub>NO<sub>3</sub> addition to a forested catchment at Gårdsjön, Sweden. *For. Ecol. Manage.* 101, 215-226.
- Wagai, R. and P. Sollins (2002) Biodegradation and regeneration of water-soluble organic carbon in a forest soil: leaching column study. **Biology and Fertility of Soils** 35:18-26.
- White, R.E., Thomas, G.W. (1981) Hydrolysis of aluminum on weakly acidic organic exchanges: implications for phosphate adsorption. *Fert. Res.* 2: 159-167.
- Williams, RJP, 1999, What is wrong with aluminum? *Journal of Inorganic Chemistry*, 76, 81-88.
- Wood M., 1995. A mechanism of aluminum toxicity to soil bacteria and possible ecological implications. *Plant and Soil* 171, 63-69.
- Wright CJ, Coleman DC (2000) Cross-site comparison of soil microbial biomass, soil nutrient status, and nematode trophic groups. *Pedobiologia* 44, 2-23.
- Zech W. and Guggenberger G. (1996) Organic matter dynamics in forest soils of temperate and tropical ecosystems. In: *Humic Substances in Terrestrial Ecosystems*. (ed. A. Piccolo). Elsevier, Amsterdam. pp. 101–170.
- Zibilske, L.M., 1994. Carbon mineralization. In: Weaver, R.W., Angle, S., Bottomley, P. (Eds.), *Methods of Soil Analysis Part 2: Microbiological and Biochemical Properties*, Soil Science Society of America, Inc. Madison, WI, 835-864.

Zsolnay A. (1996) Dissolved humus in soil waters. In *Humic substances in terrestrial ecosystems*. (ed. A. Piccolo). Elsevier, Amsterdam. pp. 225-264.